# UNIVERSIDAD POLITÉCNICA DE VALENCIA

**DOCTORADO EN CIENCIA, TECNOLOGÍA Y GESTIÓN ALIMENTARIA**

UNIVERSITAT POLITÈCNICA DE VALÈNCIA

ITM

INSTITUTO DE TECNOLOGÍA DE MATERIALES

# TESIS DOCTORAL

"Films de PLA y PLA-PHB plastificados para su aplicación en envases de alimentos.
Caracterización y análisis de los procesos de degradación"


**Autor:**

Marina Patricia Arrieta

**Dirigida por:**

Dr. Juan López Martínez



**Fecha de presentación:**

Julio de 2014

UNIVERSITAT POLITÈCNICA DE VALÈNCIA

ITM INSTITUTO DE TECNOLOGÍA DE MATERIALES

# UNIVERSIDAD POLITÉCNICA DE VALENCIA

**DOCTORADO EN CIENCIA, TECNOLOGÍA Y GESTIÓN ALIMENTARIA**

# TESIS DOCTORAL

"Films de PLA y PLA-PHB plastificados para su aplicación en envases de alimentos.
Caracterización y análisis de los procesos de degradación"

**Marina Patricia Arrieta**

Dr. Juan López Martínez, Catedrático de Universidad del Departamento de Ingeniería Mecánica y de Materiales de la Universidad Politécnica de Valencia en calidad de Director de la Tesis Doctoral (modalidad Doctorado Internacional) presentada por Dña. Marina Patricia Arrieta, con el título "Films de PLA y PLA-PHB plastificados para su aplicación en envases de alimentos. Caracterización y análisis de los procesos de degradación".

CERTIFICA

Que la presente memoria, "Films de PLA y PLA-PHB plastificados para su aplicación en envases de alimentos. Caracterización y análisis de los procesos de degradación", para aspirar al grado de Doctor por la Universitat Politècnica de València constituye la tesis doctoral de Dña. Marina Patricia Arrieta (modalidad Doctorado Internacional) reúne las condiciones adecuadas para constituir su tesis doctoral.

Asimismo certifica que la citada tesis doctoral se ha realizado en el Instituto de Tecnología de Materiales de la Universitat Politècnica de València y en el European Center of Nanostructured Polymers (ECNP) and University of Perugia - UdR INSTM (Italia).

Y para que conste a los efectos oportunos, firma la presente en Alcoy a 11 de Abril de 2014.

Fdo. Juan López Martínez

A Manuel

*“Casi todo lo que realice será insignificante,*

*pero es muy importante que lo haga”*

*Mahatma Gandhi*

**Agradecimientos**

En primer lugar quiero expresar un profundo agradecimiento a mi Director, Profesor Juan López Martínez. Gracias Juan por toda la confianza que depositaste en mí durante estos tres años de formación pre-Doctoral porque eso me permitió disfrutar todos los días de mi trabajo y aprender con mucha ilusión. Gracias también por el soporte científico y técnico, por tu paciencia, genorosidad y por todo el apoyo personal. …

*¡Muchas Gracias!*

A la Conselleria d' Educació, Formació i Ocupació de la Generalitat Valenciana, por la beca otorgada (GRISOLIA/2011/007).

Al Ministerio de Economía y Competitividad por el soporte financiero de este trabajo (proyectos MAT2011-28468-C02-01 y MAT2011-28468-C02-02).

Al Instituto de Tecnología de Materiales de la Escuela Politécnica Superior de Alcoy de la Universitat Politècnica de València, donde se llevó a cabo el presente trabajo.

A la Universidad Católica de Córdoba (Argentina) por concederme una excedencia para realizar mi formación Doctoral.

Al Programa de Apoyo a la Investigación y Desarrollo de la Universitat Politècnica de València por la ayuda para "Estancias del PDI de la UPV en Centros de Investigación de Prestigio" (SP20120120).

A la Profesora María Consuelo Gonzáles del Departamento de Tecnología de Alimentos, Tutora del presente trabajo, por todo su apoyo y predisposición.

Al Profesor Rafael Balart y de manera extensiva a todo su grupo de investigación por la ayuda diaria brindada para el desarrollo de mi trabajo. A la Profesora Lourdes Sánchez Nácher por su lectura y ayuda con los últimos detalles. *¡Muchas gracias a tod@s!*

A los Profesores "Paco" Parres y "Santi" Ferrándiz por sus aportaciones y colaboraciones.

A la Profesora María Dolores Salvador y a su grupo de investigación por facilitarme sus equipos y apoyo cada vez que desarrollé parte de mi trabajo en el campus de Valencia.

Al Profesor Alfonso Jiménez de la Universidad de Alicante por permitirme utilizar sus instalaciones, por todo su apoyo y la gran aportación a este trabajo. También quiero agradecer a su grupo de investigación y especialmente a las Doctoras "Mecha" Peltzer y Nuria Burgos, por su ayuda, consejos y aportaciones a este trabajo y por todo lo que aprendí con ustedes.

Al Profesor Arturo Horta Zubiaga de la Universidad Nacional de Educación a Distancia (UNED) por sus consejos y las aportaciones en los inicios de este estudio.

Al Profesor José María Kenny de la Università degli Studi di Perugia (Italia) y a todo su grupo de investigación por la gran aportación a este trabajo. Especialmente a la Dra. Elena Fortunati por su gran colaboración y dedicación. *Grazie mille!*

Al Profesor Luis Barral Losada de la Universidad de A Coruña a su grupo de Investigación y al personal del Cetro de Investigaciones Tecnológicas de la Universidad de A Coruña. Especialmente a la Profesora María Victoria González Rodríguez y a la Dra. María del Mar Castro López por todo su apoyo. *¡Graciñas!*

Quiero agradecer especialmente al Profesor Emilio Rayón, por toda su ayuda en este trabajo. ¡Gracias Emilio! por transmitirme tu energía para investigar e innovar y por apoyarme tanto.

A mis compañeros: Mado, Vicent, Dani, Octavio, Isa, Jose, Alfredo y María. *¡Muchísimas Gracias!*... Chicos, sin ustedes esto no hubiera sido posible. Gracias por el día a día, por su tiempo, por enseñarme a manejar cada equipo, por la paciencia, por cada café, por cada gráfica de Origin, el valencià, las risas… y principalmente por el apoyo personal. Son unos compañeros excepcionales y unas excelentes personas de las cuales aprendí mucho. *¡Muchas Gracias! y ¡Moltes Gràcies!*

A mis amigos… A Phanie por las tardes de redacción. A los amigos de allí, a los de aquí y a los de más allá por el simple hecho de haber estado cada vez que necesité una charla o un abrazo para continuar. ¡Gracias a tod@s ustedes!

A mis hermanos, Pablo y Gaby, gracias por el apoyo, los consejos, las risas, la compañía "face-to-face" y "on-line". Este agradecimiento es extensivo también a Rocío y Carlos que son mis hermanos elegidos por mis hermanos… *¡¡¡Gracias por estar siempre!!!*

A mis padres, quienes me transmiten con el ejemplo la fortaleza para seguir estudiando y aprendiendo siempre. Perseguir los sueños y verle el lado positivo a todas las cosas. Gracias por acortar las distancias, por aceptar y apoyar mis emprendimientos siempre con una sonrisa. Sin su incondicional confianza, apoyo y amor, un doctorado no hubiera sido posible para mí, porque ustedes me dieron la educación más importante que es aquella que no se recibe en ninguna institución, sino en casa, y sin ella de nada sirve la educación primaria, secundaria, universitaria y post-universitaria. *¡¡¡Muchas, muchas, muchas… Gracias!!!*

Quiero agradecer de una manera muy especial a Manuel por el incondicional apoyo, la paciencia, por animarme… Manu, hiciste mi camino a la tesis mucho más fácil, adaptándote a todo y ayudándome a ser constante de una manera muy natural, positiva y feliz. Mil palabras no alcanzarían para expresar lo agradecida que estoy: *¡¡¡Muchísimas Gracias!!!*

Por último, quiero agradecer a todas aquellas personas que también colaboraron de una manera diferente, pero no secundaria, a la realización de este trabajo… a tod@s ellos: ¡Gracias!

**RESUMEN**

**"Films de PLA y PLA-PHB plastificados para su aplicación en envases de alimentos. Caracterización y análisis de los procesos de degradación"**

El principal objetivo de esta tesis doctoral fue el desarrollo y caracterización de films biodegradables de poli(ácido láctico) (PLA) con propiedades mejoradas para su aplicación en envasado de alimentos. Para modular las propiedades del PLA y mejorar su funcionalidad se estudió la incorporación de diferentes aditivos mediante mezclado en fundido como plastificantes (D-limoneno, poli(etilen glicol) (PEG) y citrato(acetil-tri-n-butilo) (ATBC)), otro biopolímero (poli(hidoxibutirato) (PHB)), nanocomponentes (nanocristales de celulosa (CNC)) y un antioxidante ((+)-catequina).

Se evaluó el efecto de plastificación del PLA mediante la adición de dos concentraciones de D-limoneno estudiando las propiedades estructurales, térmicas, mecánicas, de barrera a oxígeno de estos materiales. Se obtuvieron materiales flexibles debido a la reducción en la temperatura de transición vítrea. El aumento de la movilidad de las cadenas del PLA generó un aumenta en la permeabilidad al oxígeno y los materiales mostraron estabilidad térmica reducida.

La adición de un 25% en peso de PHB incrementó la cristalinidad y por consiguiente disminuyó la permeabilidad al oxígeno y la humectabilidad de la superficie del PLA. La adición de plastificantes a las mezclas de PLA-PHB mejoró la interacción entre los polímeros, incrementó la ductilidad y aceleró el proceso de degradación en compostaje, pero no mejoró la estabilidad térmica del material. Los mejores resultados se obtuvieron con ATBC.

Para mejorar la estabilidad térmica de los materiales se sintetizaron nanocristales de celulosa (CNC) a partir de celulosa microcristalina. La incorporación de un 5% en peso de nanocristales de celulosa condujo a una mejora significativa en la estabilidad térmica aumentando la ventana de proceso. En un siguiente paso se modificó la superficie de los CNC mediante un surfactante para evitar la aglomeración de los cristales. La funcionalización de los nanocristales (CNC-s) resultó en una homogénea dispersión de los mismos en la matriz de PLA-PHB obteniéndose materiales con propiedades mecánicas y de barrera al oxígeno mejoradas. Así mismo, CNC-s generó una reducción de la transmisión de la luz UV y aceleró la degradación en compostaje de los materiales

Por último, la adición de (+)-catequina como agente activo presentó una eficaz protección de los biopolímeros frente a su degradación oxidativa al mismo tiempo que la liberación en simulantes de alimentos grasos mostró una significativa actividad

antioxidante. Los materiales conservaron sus propiedades estructurales y mecánicas durante la exposición al simulante alimentario.

**RESUM**

**“Films de PLA i PLA- PHB plastificats per a la seua aplicació en envasos d'aliments. Caracterització i anàlisi dels processos de degradació "**

El principal objectiu d'aquesta tesi doctoral va ser el desenvolupament i caracterització de films biodegradables de poli(àcid làctic) (PLA) amb propietats millorades per a la seua aplicació en envasat d'aliments. Per modular les propietats del PLA i millorar la seua funcionalitat es va estudiar la incorporació de diferents additius mitjançant el mesclat en fos com plastificants (D-limonè, poli(etilen glicol) (PEG) i citrat (acetil-tri-n-butil) (ATBC)), un altre biopolímer (poly (hidoxibutirato) (PHB)), nanocompostos (nanocristalls de cel·lulosa (CNC)) i un antioxidant (catequina) .

Es va avaluar l'efecte de plastificació del PLA mitjançant l'addició de dos concentracions de D-limonè estudiant les propietats estructurals, tèrmiques, mecàniques, de barrera a oxigen d'aquests materials. Es van obtenir materials flexibles a causa de la reducció en la temperatura de transició vítria. L'augment de la mobilitat de les cadenes del PLA va generar un augment en la permeabilitat a l'oxigen i els materials van mostrar estabilitat tèrmica reduïda.

L'addició d'un 25% en pes de PHB va incrementar la cristal·linitat i per tant disminuir la permeabilitat a l'oxigen i la humectabilitat de la superfície del PLA. L'addició de plastificants a les mescles de PLA-PHB va millorar la interacció entre els polímers, incrementar la ductilitat i va accelerar el procés de degradació en compostatge, però no va millorar l'estabilitat tèrmica del material. Els millors resultats es van obtenir amb ATBC.

Per millorar l'estabilitat tèrmica dels materials es van sintetitzar nanocristalls de cel·lulosa (CNC) a partir de cel·lulosa microcristal·lina. La incorporació d'un 5% en pes de nanocristalls de cel·lulosa va conduir a una millora significativa en l'estabilitat tèrmica augmentant les opcions de procés. En un següent pas es va modificar la superfície dels CNC mitjançant un surfactant per evitar l'aglomeració dels nanocristalls. La funcionalització dels nanocristalls (CNC-s) va donar lloc una dispersió homogènia dels mateixos en la matriu de PLA-PHB obtenint materials amb propietats mecàniques i de barrera a l'oxigen millorades. Així mateix, els CNC-s van generar una reducció de la transmissió de la llum UV i accelerar la degradació en compostatge dels materials.

Finalment, l'addició de (+)-catequina com a agent actiu va presentar una eficaç protecció dels biopolímers davant la seva degradació oxidativa a la vegada que va mostrar una significativa activitat antioxidant en l'alliberament de simulants d'aliments grassos.

Els materials van conservar les seves propietats estructurals i mecàniques durant l'exposició al simulant alimentari.

**ABSTRACT**

**"Plasticized PLA-PHB films for food packaging applications. Characterization and analysis of degradation processes"**

The main objective of this thesis was the development and characterization of biodegradable films based on poly(lactic acid) (PLA) with improved properties for their application in food packaging. To modulate PLA properties and to improve its functionality the incorporation of different additives was studied through melt blend process, such as plasticizers (D-limonene, poly(ethylene glycol) (PEG) and acetyl(tributyl citrate) (ATBC)), another biopolymer (poly(hydoxybutyrate) (PHB)), nanocomponents (cellulose nanocrystals (CNC)) and one antioxidant ((+)-catechin).

PLA plasticization was evaluated through the addition of two different concentrations of D-limonene and the structural, thermal, mechanical and oxygen barrier properties of these materials were evaluated. Flexible materials were obtained due to the reduction of the glass transition temperature. The increase in PLA chain mobility generated an increase of oxygen permeability and material showed reduced thermal stability.

The addition of 25wt% of PHB increased the crystallinity and as a consequence the oxygen permeability decreased and the surface humidity of PLA. The plasticization of PLA-PHB blends improved the interaction between the polymers, increased the ductility and speeded up the degradation process in compost, but the thermal stability was not improved. The best results were obtained with ATBC.

To improve the thermal stability of materials cellulose nanocrystals (CNC) were synthesized from microcrystalline cellulose (MCC). The incorporation of 5 wt% of cellulose nanocrystals resulted in a significant improvement in thermal stability by increasing the process window. In the subsequent step, cellulose nanocrystal surface was modified by means of a surfactant to avoid nanocrystals agglomeration. The functionalization of nanocrystals (CNC-s) resulted in a homogeneous dispersion of them in the PLA-PHB matrix and the obtained materials showed improved mechanical and barrier properties. Likewise, CNC-s produced a decrease of the UV light transmission and also speeded up the degradation in composting of materials.

Finally, the addition of (+)-catechin as the active agent provided effective protection of biopolymers against their oxidative degradation while releasing into fatty food simulant showed significant antioxidant activity. The materials retained their structural and mechanical properties during exposure to food simulant.

# ÍNDICES

## ÍNDICE DE CONTENIDOS

**ÍNDICE DE FIGURAS**

**ÍNDICE DE TABLAS**

ECUACIONES

| | |
|---|---|
| $$m = \frac{(m_i - m_\infty)}{1 + (\frac{t}{t_0})^p} + m_\infty$$ | **$m_i$ =** masa inicial (asíntota inferior)<br>**$m_\infty$ =** masa final<br>**p=** coeficiente de Hill<br>**$t_0$ =** tiempo a la mitad de la máxima degradación |
| $$m = \frac{(m_i - m_\infty)}{1 + e^{\frac{(t-t_0)}{d_t}}} + m_\infty$$ | **$m_i$ =** masa inicial (asíntota inferior)<br>**$m_\infty$ =** masa final<br>**$t_0$ =** tiempo a la mitad de la máxima degradación<br>**$d_t$ =** parámetro que describe la forma de la curva |
| $$\chi_c = 100 \times \left[\frac{\Delta H_m - \Delta H_{cc}}{\Delta H_m^c}\right] \frac{1}{1 - m_f}$$ | **$X_c$ =** grado de cristalinidad<br>**$\Delta H_m$ =** entalpía de fusión<br>**$\Delta H_{cc}$ =** entalpía de cristalizacón<br>**$\Delta H^c_m$ =** entalpía de fusión teórica material 100% cristalino |
| $$\Delta E = \sqrt{\Delta a^{*2} + \Delta b^{*2} + \Delta L^2}$$ | **$\Delta E$ =** diferencia de color<br>**a* =** coordenada de saturación<br>**b* =** ángulo de tono<br>**L =** luminosidad |
| $$TSM = 100 \times \frac{m_0 - m_f}{m_0}$$ | **TSM =** masa total soluble<br>**$m_0$ =** masa seca inicial<br>**$m_f$ =** masa final |
| $$Transparency = \frac{A_{600}}{e}$$ | **$A_{600}$ =** absorbancia a 600 nm<br>***e*** **=** espesor |
| $$\delta = \frac{D\sum G}{M}$$ | **$\delta$ =** parámetro de solubilidad<br>**D =** densidad<br>**M =** masa molar por unidad repetitiva<br>**G =** constante de atracción molar |
| $$W_{dm} = \frac{m_1}{m_0} \times 100$$ | **$W_{dm}$ =** contenido de materia seca<br>**$m_0$ =** masa inicial antes del secado<br>**$m_1$ =** masa después del secado. |
| $$\frac{M_t}{M_{F,\infty}} = 1 - \sum_{n=0}^{\infty} \frac{8}{(2n+1)^2\pi^2} \, exp\left[\frac{-D\,(2n+1)^2\pi^2 t}{Lp^2}\right]$$ | **$M_t$ =** masa del migrante en el simulante a tiempo t<br>**MF, ∞ =** masa del migrante en el equilibrio.<br>**$L_p$ =** espesor<br>**D =** coeficiente de difusión |
| $$\frac{M_t}{M_p} = \frac{4}{L_p}\left(\frac{Dt}{\pi}\right)^{1/2}$$ | **$M_t$ =** masa del migrante en el simulante a tiempo t<br>**$M_P$ =** cantidad inicial de antioxidante en el film<br>**$L_p$** = espesor<br>**D** = coeficiente de difusión |

| | |
|---|---|
| $I\ (\%) = \left(\frac{Abs_{control} - Abs_{sample}}{Abs_{control}}\right) \times 100\%$ | **I (%)** = porcentaje de inhibición<br>**$Abs_{control}$** = absorbancia del control<br>**$Abs_{sample}$** = absorbancia del control |

**ABREVIATURAS Y TÉRMINOS**

***a*:** área de membrana

**a*:** saturación

**ATEC:** citrato de acetiltrietilo

**ATBC:** citrato de acetil-tri-n-butilo

**$A_w$**: actividad de agua

**b*:** ángulo de tono

**BCNC**: nanocristales de celulosa bacteriana

**BHT:** butil-hidroxitolueno

***c*:** coeficiente la concentración de saturación dentro del film

**CE:** celofán

**CNC:** nanocristales de celulosa

**CNC-s:** nanocristales de celulosa modificados superficialmente

**CNF:** celulosa nanofibrilada

**CoA**: coenzima A

**D:** densidad.

***D:*** coeficiente de difusión

**DPPH:** 2,2-difenil-1-picrilhidrazil

**DSC:** calorimetría diferencial de barrido

**dTG:** derivada de la masa frente a la temperatura

***e*:** espesor

***E*:** módulo elástico o de Young

**EFSA:** autoridad europea de seguridad alimentaria

***$E_r$***: módulo reducido

**FDA:** Food and Drug Administration (EEUU)

**FESEM:** microscopía electrónica de barrido de emisión de campo

**FTIR:** espectroscopía infrarroja de transformada de fourier

**G:** constantes de atracción molar

**GRAS:** generalmente reconocido como seguro

**H:** dureza

**HDPE:** poli(etileno) de alta densidad

**HPMC:** hidroxipropil metilcelulosa

**HPLC:** cromatografía líquida de alta resolución

**HV:** hidroxivalerato

***J*:** flujo de una sustancia

***L*:** luminosidad

**L/D:** relación longitud / diámetro

**LDPE:** poli(etileno) de baja densidad

***m*:** cantidad de permeante

**$M_n$:** masa molar promedio en número

**$M_w$:** masa molar promedio en peso

**MCM:** celulosa microcristalina

**OHB:** oligómero de 3-hidroxibutirato

**OIT:** tiempo de inducción a la oxidación

**OLA:** oligómeros de ácido láctico

**OTR:** velocidad de transmisión de oxígeno

***p*:** presión parcial en la atmósfera gaseosa

***P*:** coeficiente de permeabilidad

**PBAT:** poli(butileno adipato tereftalato)

**PBSA:** poli(ester alifáticos)

**PCL:** poli(caprolactona)

**PDA:** detector de red de diodos

**PDI:** índice de polidispersidad

**PE:** poli(etileno)

**PEA:** poli(ester amidas)

**PEG:** poli(etilenglicol)

**PET:** poli(etileno tereftalato)

**PHAs:** poli(hidroxialcanoatos)

**PHB:** poli(hidroxibutirato)

**PHV:** poli(hidroxivalerato)

**PHBV:** poli(hidroxibutirato-valerato)

**PLA:** poli(ácido láctico)

**PLLA:** poli(L-ácido láctico)

**PDLA:** poli(D-ácido láctico)

**PP:** poli(propileno)

**PS:** poli(estireno)

**PVC:** poli(cloruro de vinilo)

**Py-GC/MS:** pirólisis- cromatografía de gases/ espectrometría de masas.

**ROC:** copolimerización por apertura de anillo

**ROP:** polimerización por apertura de anillo

***S*:** coeficiente de solubilidad

**SEM:** microscopía electrónica de barrido

**sc-PLA:** estereocomplejos de PLA

**TBC:** citrato de tributilo

**TEC:** citrato de trietilo

**TGA:** termogravimetría

***t*:** tiempo

**T:** temperatura absoluta

$\mathbf{T_{\alpha=0,01}}$**:** temperatura de inicio de degradación

$\mathbf{T_{cc}}$**:** temperatura de cristalización en frio

**TBC:** citrato de tributilo

**TEC:** citrato de trietilo

$\mathbf{T_g}$**:** temperatura de transición vítrea

$\mathbf{T_m}$**:** temperatura de fusión

$\mathbf{T_{max}}$**:** velocidad máxima de degradación

***TS*:** resistencia a la tracción

**TSM:** masa total soluble

**UV:** ultravioleta

**V:** volúmen

$\mathbf{W_{PLA}}$**:** fracción en peso del PLA

**WVT:** permeabilidad al vapor de agua

**XRD:** difracción de rayos X

**α, α', β, γ:** modificaciones cristalinas de PLA

**Δc:** diferencia de concentración del permeante antes y después de atravesar el film

**Δ*E**:** diferencia de color

**Δ*E*/V:** densidad de energía cohesiva

**ΔG:** variación en la energía libre de Gibbs

**ΔH:** variación de la entalpía (calor de mezclado)

$\mathbf{\Delta H_{cc}}$**:** entalpía de cristalización en frío

$\mathbf{\Delta H_m}$**:** entalpía de fusión

$\mathbf{\Delta H_m^c}$**:** valor teórico de la entalpía de fusión

$\mathbf{\Delta H_{rel}}$: energía de relajación entálpica

**Δ*p*:** diferencia de presión parcial del permeante

**ΔS:** entropía de mezclado

$\boldsymbol{\varepsilon_{B\%}}$**:** elongación a la rotura

**δ:** parámetro de solubilidad

**∑G:** sumatorio de constantes de atracción molar

$\boldsymbol{\chi_c}$**:** grado de cristalinidad

# I. OBJETIVOS

## 1. OBJETIVO GENERAL

El objetivo general del presente trabajo es el desarrollo de films biodegradables en base a PLA mezclado en fundido con otro polímero biodegradable, PHB, y la evaluación de sus propiedades tras la incorporación de diferentes aditivos: (i) plastificantes, (ii) nanocristales de origen natural y (iii) antioxidantes, para su posible aplicación en envasado de alimentos.

## 2. OBJETIVOS ESPECÍFICOS

Para tal fin, se han planteado una serie de objetivos específicos que se describen a continuación:

- Estudio de la degradación térmica de PLA mediante pirólisis secuencial y determinación por cromatografía de gases acoplada a espectrometría de masas.

- Evaluación del efecto de la adición de un plastificante de origen natural (D-Limoneno) sobre las propiedades térmicas, estructurales, mecánicas, colorimétricas y de barrera del PLA.

- Aumento de cristalinidad de PLA mediante el mezclado en fundido con otro polímero biodegradable altamente cristalino (PHB) evaluando su efecto en las propiedades físicas del material.

- Evaluación del efecto de la incorporación de tres plastificantes (D-Limoneno, ATBC y PEG) sobre las propiedades físico-químicas de mezclas de PLA-PHB destinadas al envasado alimentario. Estudio de la degradación de los films plastificados en condiciones de compostaje.

- Síntesis de nanocristales de celulosa y modificación de su superficie con el objeto de incrementar su compatibilidad con las matrices poliméricas de PLA y PHB.

- Adición de los nanocristales de celulosa sintetizados a las mezclas de PLA-PHB y estudio de las condiciones de procesado de films y evaluación de la estabilidad térmica de las mezclas y la correcta incorporación de los nanocristales en las formulaciones obtenidas.

- Caracterización de las propiedades físico-químicas de interés en envasado alimentario de los nanocompuestos desarrollados y el estudio de su degradación en condiciones de compostaje.

- Caracterización de mezclas de PLA-PHB plastificadas con la incorporación de un antioxidante ((+)-catequina) y estudio de la liberación del componente activo en simulantes alimentarios. Evaluación de su actividad antioxidante y de la modificación de las propiedades térmicas, estructurales y nanomecánicas de los materiales después del estudio de migración.

Todos estos objetivos se desarrollarán a lo largo de la presente tesis doctoral y se presentan de forma esquemática en la Figura I. 1.

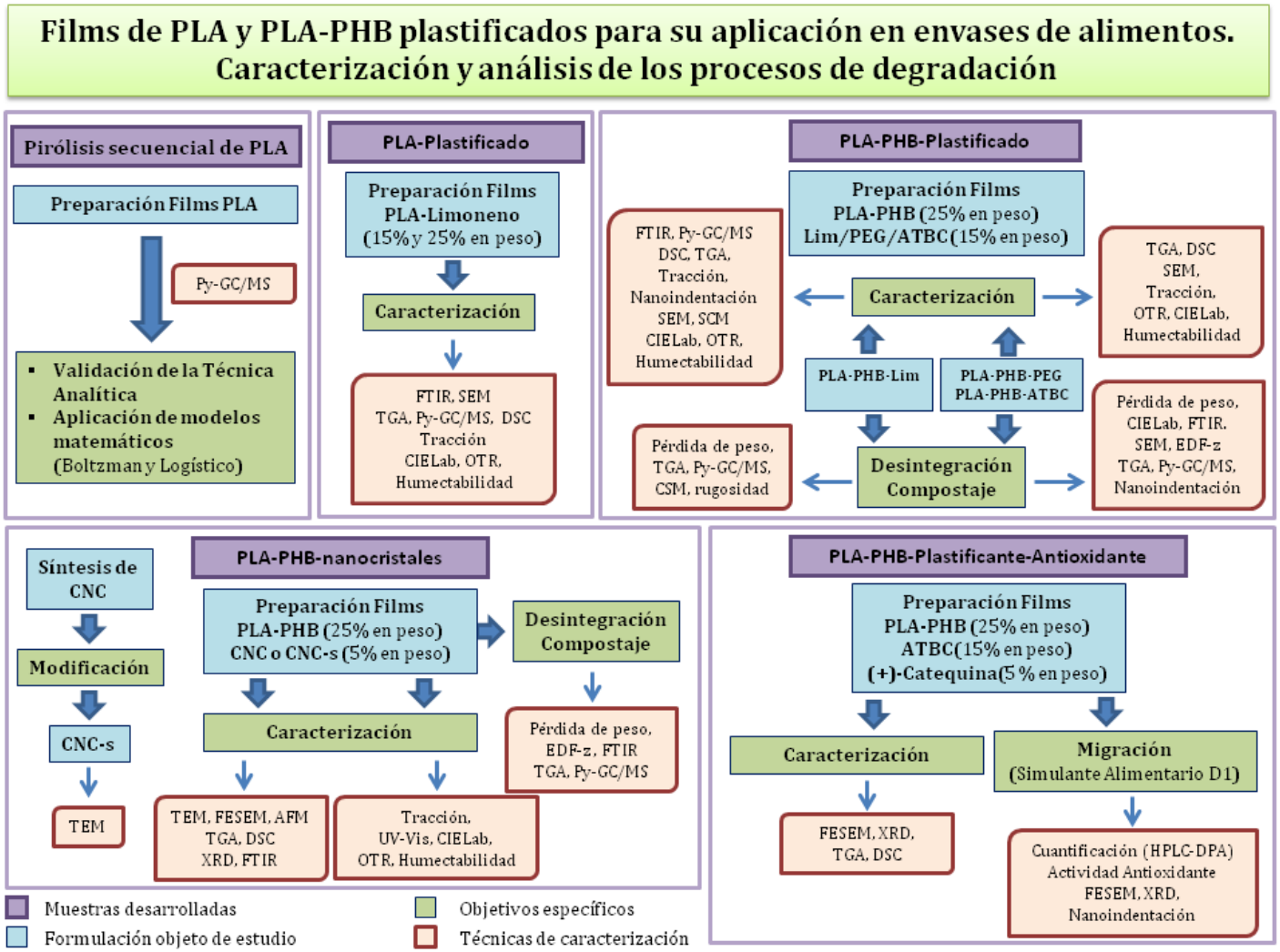


**Figura I. 1.** Esquema del trabajo realizado en la presente tesis doctoral

# II. INTRODUCCIÓN

## 1. POLÍMEROS EN APLICACIONES DE ENVASES ALIMENTARIOS

Los diferentes cambios del estilo de vida han influido directamente en el tipo de alimentos que consumimos y en los hábitos de consumo, lo que a su vez ha generado la necesidad en la industria alimentaria del desarrollo de nuevos envases y embalajes. Tal es así, que hoy en día prácticamente cualquier producto alimenticio que consumimos se comercializa envasado, no sólo para contener el alimento sino también para protegerlo durante toda la cadena de producción, es decir desde el lugar donde se han producido hasta el lugar de venta o consumo. De esta manera, los envases alimentarios cumplen funciones muy importantes para la conservación de los alimentos, los protegen de agentes externos previniendo la contaminación física, química y/o microbiológica, así como también de su posible adulteración. De esta manera, cumplen la función de barrera contra el medioambiente que los rodea, protegiendo los alimentos de la humedad y oxidación. Por otra parte, los envases también cumplen la función de información muy importante para el consumidor como son la información nutricional, fecha preferente de consumo o de caducidad y el modo de conservación de los alimentos que contienen. También pueden contener información del material del que está fabricado el envase, su reciclabilidad y donde debe ser desechado el envase una vez que ha cumplido su vida útil.

Los plásticos son, sin duda, los materiales que más se emplean en la industria de los envases alimentarios superando ampliamente a otros materiales como las cerámicas, el vidrio o el cartón, debido a que ofrecen aplicaciones prácticas de envasado. Estos plásticos de gran consumo utilizados en envases se denominan *comodities*, son materiales poliméricos derivados del petróleo como poli(etileno) (PE), poli(propileno) (PP), poli(cloruro de vinilo) (PVC), poli(etilentereftalato) (PET) y poli(estireno) (PS). La versatilidad que los materiales plásticos ofrecen, también permite la combinación de materiales plásticos con una menor proporción de algún otro material formando materiales compuestos o *composites*. Los materiales poliméricos derivados del petróleo que más se usan en envasado presentan numerosas ventajas, como son: su disponibilidad a gran escala, relativo bajo coste de producción, ligereza, gran versatilidad y relativamente buenas propiedades de barrera [1]. Por otra parte, los envases fabricados de materiales plásticos en la industria alimentaria se pueden producir en procesos integrados donde los envases se llenan y se sellan en la misma línea de producción, haciendo que el proceso sea más rápido, más seguro (en términos de seguridad alimentaria) y barato. Sin embargo, la utilización de los recursos fósiles para la producción de polímeros provocan un importante impacto medioambiental, como son el efecto invernadero, el calentamiento global [2] y el daño de la vida silvestre [3].

Por otra parte, la existencia de ciertas interacciones entre el material plástico del envase y el alimento que contiene genera ciertas restricciones de uso de algunos polímeros y sus aditivos para garantizar la protección del consumidor [4]. Sin embargo estas interacciones entre el envase y el alimento pueden ser beneficiosas para el desarrollo de envases activos.

## 1.1. Nuevas tendencias en envases poliméricos

La posibilidad de incorporar compuestos activos (antimicrobianos, antioxidantes, nutracéuticos, aromas, colorantes) en matrices poliméricas es una de las principales ventajas de los plásticos [5]. El desarrollo de envases activos es una tendencia actual en la tecnología del envasado de alimentos en que estos sistemas poliméricos activos aprovechan la interacción del envase con el alimento para la extensión de la vida útil [6, 7] o para mejorar las propiedades sensoriales del alimento, a la vez que mantiene la calidad del mismo [7]. La liberación de la sustancia es dependiente de la composición del polímero, la cristalinidad, la masa molar, la relación de superficie a volumen y el entorno a donde se libera [8]. Dentro del concepto de envasado activo los más importantes son aquellos sistemas capaces de eliminar oxígeno, etileno y dióxido de carbono, los reguladores de humedad, aquellos con actividad antimicrobiana o antioxidante, sistemas que liberan o absorben sabor y moléculas responsables de aromas [7]. El uso de antioxidantes tiene un interés especial en los materiales poliméricos destinados a envases alimentarios, debido a que muchas formulaciones de polímeros incluyen la adición de antioxidantes para evitar la degradación termo-oxidativa durante el proceso [4, 9]. Sin embargo, debe tenerse en cuenta su posible migración directa o la liberación de subproductos en los alimentos ya que pueden cambiar su calidad organoléptica e incluso inducir toxicidad potencial en algunos casos [9]. Por lo tanto, el desarrollo de formulaciones de polímeros con antioxidantes naturales no tóxicos ha cobrado especial interés en los últimos años.

## 1.2. Problemática actual de los polímeros convencionales en el envasado de alimentos

Los residuos representan un problema a nivel mundial cada vez mayor debido a que generan un impacto negativo en el medio ambiente por su acumulación y contaminación. Es por ello que las directivas de gestión de residuos establecen una estrategia de reducción de residuos estableciendo una jerarquía, en la cual se debe

primero prevenir la generación de residuos o bien reutilizar sin transformación previa, seguido del reciclado, otro tipo de valorización (como valorización energética por incineración) y como última opción la eliminación a un vertedero [10]. Sin embargo los vertederos continúan siendo una de las opciones más comunes de eliminación de residuos a nivel mundial.

Los envases alimentarios plásticos son utilizados durante un periodo de tiempo relativamente corto por lo que constituyen una fuente enorme de generación de residuos de difícil eliminación que persiste durante muchos años, representando uno de los problemas ecológicos más graves de la sociedad moderna [11]. Casi el 50 % de los plásticos de la Unión Europea se depositan en vertederos, y la mayoría de ellos son envases [12]. Del mismo modo, el uso extensivo y la expansión de los plásticos en la agricultura han generado un aumento de la acumulación de residuos plásticos en zonas rurales [13]. Con el crecimiento de la población, la globalización, la evolución de la industria y su continuo desarrollo, la eliminación de los residuos plásticos se convierte en una preocupación mundial cada vez mayor [14] debido al creciente interés en preservar los sistemas ecológicos [3]. Existen formas de revalorizar estos desechos, pero la valorización de los residuos plásticos presenta algunos inconvenientes. La incineración o la pirolisis de los residuos, permite disminuir el volumen de los desechos tratados hasta en un 90% y aprovechar la energía que se genera con la combustión de los residuos para recuperarla en forma de agua caliente, vapor o electricidad. Sin embargo, ésta valorización energética puede generar algunas emisiones tóxicas (por ejemplo, dioxinas) [2, 3]. Lo ideal sería que todos los productos plásticos fueran completamente reciclables a un coste razonable [12]. Parte de estos residuos plásticos pueden ser reciclados, pero otra parte de ellos son difíciles de reciclar por razones técnicas y/o financieras [13]. Los costes de recogida son bastante altos y el reciclado tiene un impacto negativo en la calidad de los materiales, tales como un aumento de la fragilidad [2]. La valorización de los materiales plásticos a través del reciclado implica algunas limitaciones relacionadas con las dificultades para encontrar salidas precisas y económicamente viables [3]. En este sentido, para materiales destinados a estar en contacto con alimentos, la normativa europea actual establece que determinados productos fabricados con plásticos reciclados pueden ser adecuados solamente para el contacto con alimentos específicos y en determinadas condiciones [15]. El potencial de reciclado de los plásticos sigue estando significativamente infrautilizado [12], porque no siempre los sistemas de gestión de residuos cuentan con un sistema de separación de residuos plásticos que permita su posterior reciclado, en particular aquellos de algunos países subdesarrollados. Así mismo, en países donde si existen los sistemas de separación muchas veces el consumidor no lo

utiliza adecuadamente, provocando que finalmente muchos de los residuos plásticos sean desechados junto con la basura orgánica. Esto genera que finalmente los residuos plásticos que no se reciclan ni se incineran se acumulen cada año [2]. Dependiendo del sistema de gestión de residuos utilizado estos residuos pueden finalizar en vertederos, donde son compactados y cubiertos por una capa de tierra diariamente, o bien ir a compostaje el cual es un proceso de estabilización rápida de la materia orgánica por la acción de microorganismos bajo ciertas condiciones controladas. Sin embargo, los residuos plásticos no pueden ser degradados por los microorganismos y se acumulan.

Esta problemática de la gestión de residuos plásticos, ha generado que los municipios y las distintas organizaciones (regionales y/o nacionales) encargadas de la gestión de residuos tomen conciencia acerca de los ahorros significativos que la recogida de los residuos compostables proveería [3]. Por otra parte, los datos correspondientes a las cantidades restantes de combustibles fósiles en el interior de la tierra cambian continuamente debido a los avances tecnológicos para la localización y extracción de hidrocarburos, pero finalmente el petróleo es una materia prima fósil, no renovable, que un día se agotará [2]. Aparte de estas consideraciones ecológicas, el precio del petróleo crudo es impredeciblemente fluctuante debido a la situación política-económica mundial.

En base a estas razones, resulta de gran interés reemplazar los plásticos convencionales por polímeros con menor impacto ambiental, especialmente para aplicaciones de envase y embalaje.

## 1.3. Polímeros biodegradables en aplicaciones de envases alimentarios

La actitud de la sociedad cada vez más proactiva hacia una reducción en el impacto ambiental producido por los envases alimentarios plásticos, ha centrado la atención de la industria e investigadores en el desarrollo de nuevos envases fabricados de forma que resulten sostenibles para el medioambiente, para lo cual se deben encontrar soluciones rentables y compatibles con la minimización y/o reutilización de residuos [14]. El proceso de fabricación de estos productos debe consumir el mínimo de energía, así como también el mínimo de materias primas no renovables. Para ahorrar recursos y minimizar residuos, debería optimizarse todo el sistema en el que los envases forman parte, incluyendo la prevención así como la reutilización y recuperación de los residuos [16].

Por otra parte, resulta ampliamente aceptado que el uso de materiales plásticos de larga duración para aplicaciones de corta duración, como es el caso de los envases alimentarios, no es del todo adecuada [3]. Existe cada vez más conciencia por parte de las industrias de la necesidad de promover nuevas técnicas de producción basadas en

recursos renovables [2] y por ello el uso de polímeros más sostenibles, como son los biopolímeros o los polímeros biodegradables, ha desplazado a los polímeros derivados del petróleo, representando una solución para resolver el consumo del mismo para la producción de plásticos y el problema de la acumulación de plástico en el medio ambiente, respectivamente.

Así, esta nueva generación de polímeros más sostenibles son aquellos que producen un menor impacto sobre el medioambiente: los bioplásticos y los plásticos biodegradables. Los bioplásticos son plásticos biobasados, que significa que tienen un origen natural renovable u origen "bio" debido a que provienen de las plantas, animales y/o microorganismos, es decir no son basados en el petróleo [17]. El Comité Europeo de Normalización (CEN) define el término "biobasado" como derivado de la biomasa y a un "producto biobasado" como aquel producto total o parcialmente derivado de la biomasa [17]. Es decir, bioplástico se refiere al origen del material y no a la gestión final de su ciclo de vida [12]. Así, las materias primas utilizadas en la producción de bioplásticos, provienen de la biomasa, principalmente de la agricultura y es por ello que también se los conoce como agropolímeros. Son producidos a partir de plantas ricas en carbohidratos, a partir del almidón (como patatas, trigo o maíz), de azúcares (como la remolacha o la caña de azúcar). La agroindustria también proporciona la materia prima a partir de la cual a través de biotecnología se producen distintos monómeros que permitirán la obtención de bioplásticos a gran escala.

Por su parte, los polímeros biodegradables son aquellos capaces de descomponerse en elementos químicos naturales por la acción de microorganismos: experimentan descomposición en moléculas simples que se encuentran en el medio ambiente como dióxido de carbono, metano, agua, compuestos inorgánicos o biomasa. Durante la descomposición el mecanismo predominante es la acción enzimática de los microorganismos, en un período determinado de tiempo e incluye la formación de compost que puede ser utilizado como acondicionador de terrenos [18, 19]. En la Figura II. 1 se muestran algunos polímeros biodegradables y sus distintos orígenes. Actualmente la mayoría de los plásticos biodegradables son también bioplásticos [12], pero los plásticos biodegradables también pueden estar fabricados de recursos basados en el petróleo, como por ejemplo la poli(caprolactona) (PCL). Así mismo, algunos bioplásticos no son biodegradables, como el biopolietileno producido a partir de bioetanol.

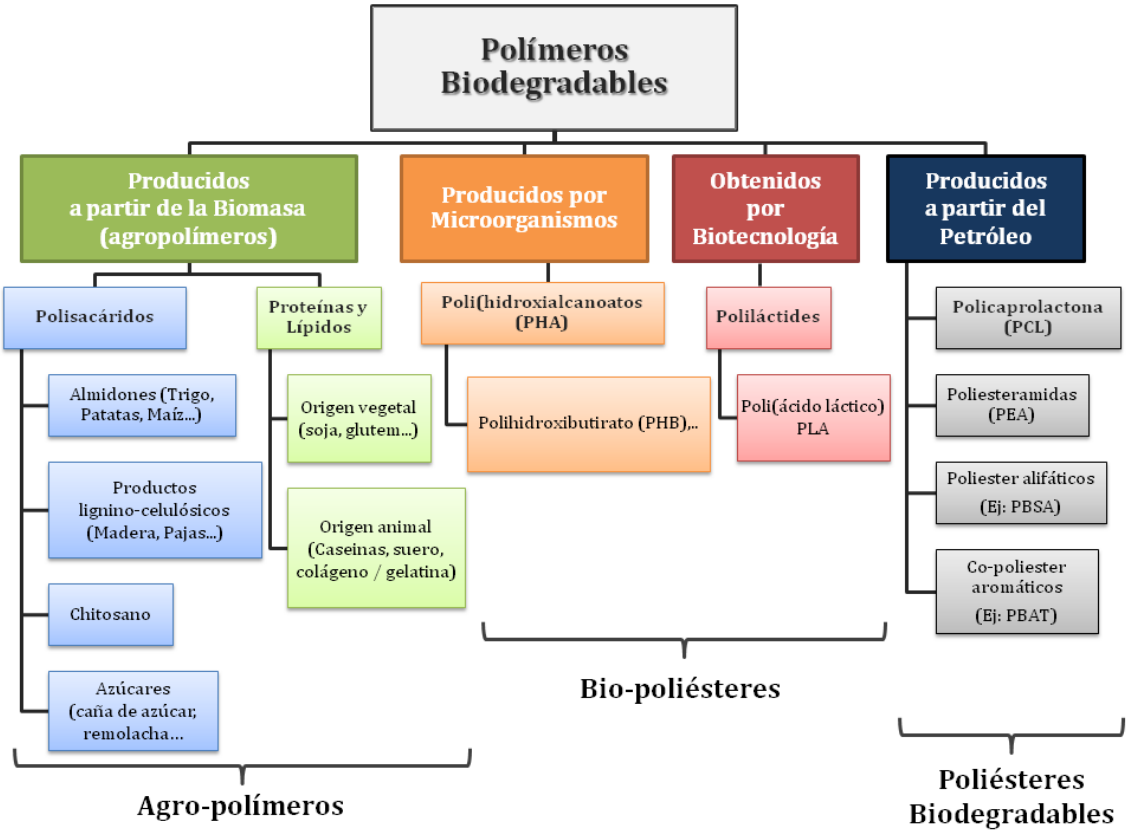


**Figura II.1.** Clasificación de polímeros biodegradables según su origen (Adaptada de Avérous 2004 [3]).

De entre todos estos polímeros sostenibles destacan los polímeros biobasados y biodegradables, ya que engloban los dos conceptos: son obtenidos a partir de recursos naturales renovables y presentan características biodegradables, lo que les permite ser reabsorbidos por la naturaleza completando así el ciclo de vida del material. El mercado de los biopolímeros y/o polímeros biodegradables termoplásticos es el que más se ha desarrollado. En la actualidad existen muchos materiales termoplásticos biodegradables que ofrecen una gran versatilidad en cuanto a propiedades mecánicas, térmicas, etc. La creciente demanda de estos materiales más sostenibles se refleja en el crecimiento substancial de las capacidades de producción de bioplásticos, la cual en el año 2012 ascendió a aproximadamente a 1.4 millones de toneladas y se espera que la capacidad de producción se multiplique para el año 2017 a más de 6 millones de toneladas Figura II.2 [20].

En este sentido, los biomateriales han cobrado especial interés en la industria del embalaje, porque presentan una serie de propiedades prometedoras en aplicaciones de envases alimentarios y representan una alternativa adecuada para reemplazar a los polímeros convencionales derivados del petróleo. Específicamente los biopolímeros

termoplásticos, presentan un excelente equilibrio de propiedades, además de ser procesables utilizando la misma maquinaria que se utiliza para procesar los plásticos convencionales, incluyendo la inyección por moldeo, extrusión, moldeo por soplado y termoconformado [21]. El poli(ácido láctico) (PLA) es uno de los biopolímeros comerciales más atractivos y se utiliza en la actualidad en muchas aplicaciones industriales.

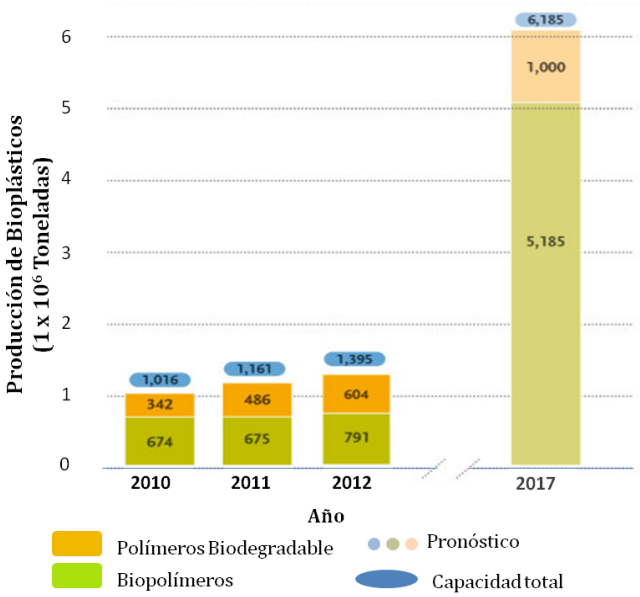


**Figura II.2.** Capacidad de producción de bioplásticos global (Fuente: European Bioplastics- Institute of Bioplastics and Biocomposites, 2013 [20])

## 2. POLI (ÁCIDO LÁCTICO) (PLA)

El PLA, es un polímero biodegradable cuyo monómero (ácido láctico) puede obtenerse de recursos renovables, productos agrícolas simples, como el maíz [7, 22, 23], celulosa [7], caña de azúcar y remolachas azucareras [23]. Presenta propiedades similares a algunos de los materiales plásticos de uso común, tales como el polietileno (PE) o el policloruro de vinilo (PVC), a un precio competitivo [24]. Se procesa en los equipos disponibles para el procesado de plásticos de uso común. El PLA es uno de los plásticos biodegradables que mayor crecimiento ha tenido en los últimos años. Se encuentra disponible en el mercado en aplicaciones plásticas prácticas como cubiertos, platos, tazas, tapas, pajitas de bebidas, bolsas, films [25], envases de fruta fresca o vegetales, botellas y helados [8].

Después de su uso, los productos de PLA pueden ser degradados en sistemas de compostaje o reciclados ya sea química o mecánicamente, por hidrólisis en ácido láctico o

reprocesando el material (triturado y transformación térmica), respectivamente [26]. Los envases de materiales biodegradables, tras su uso, en lugar de ser desechados con el resto de materiales plásticos, pueden ser tratados junto con los residuos orgánicos, incorporándose a la corriente de biomasa [27].

## 2.1. Estructura química del PLA

El PLA es un poliéster obtenido de la polimerización del ácido láctico, donde los monómeros de partida son producidos por fermentación o síntesis química [7]. El ácido láctico es una de las moléculas ópticamente activas más simples y existe como dos estereoisómeros: L(+) y D(-)[8, 28, 29] (Figura II.3).

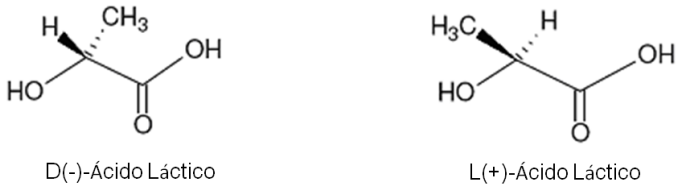


**Figura II.3.** Estructura química de los estereoisómeros del ácido láctico.

Los dos enantiómeros son producidos por hongos o por fermentación bacteriana (del género *Lactobacillus)* [30], siendo ésta última la forma más frecuente de obtención de ácido láctico a nivel industrial [8]. En la Figura II.4, se muestra la unidad repetitiva del PLA.

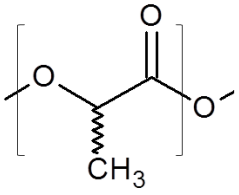


**Figura II.4.** Unidad repetitiva del PLA

El PLA sintetizado a partir de L-ácido láctico y D-ácido láctico son poli(L-ácido láctico) (PLLA) y poli(D-ácido láctico) (PDLA), respectivamente.

## 2.2. Síntesis de PLA

La producción de PLA comienza a partir de plantas ricas en carbohidratos, como es el caso del maíz donde el almidón se separa de los otros componentes del grano de maíz

(proteínas, grasas, fibras, cenizas y agua) y se convierte en dextrosa a través de una hidrólisis enzimática. En la Figura II. 5 se muestran las diversas etapas implicadas en la producción de PLA a partir del cultivo de maíz.

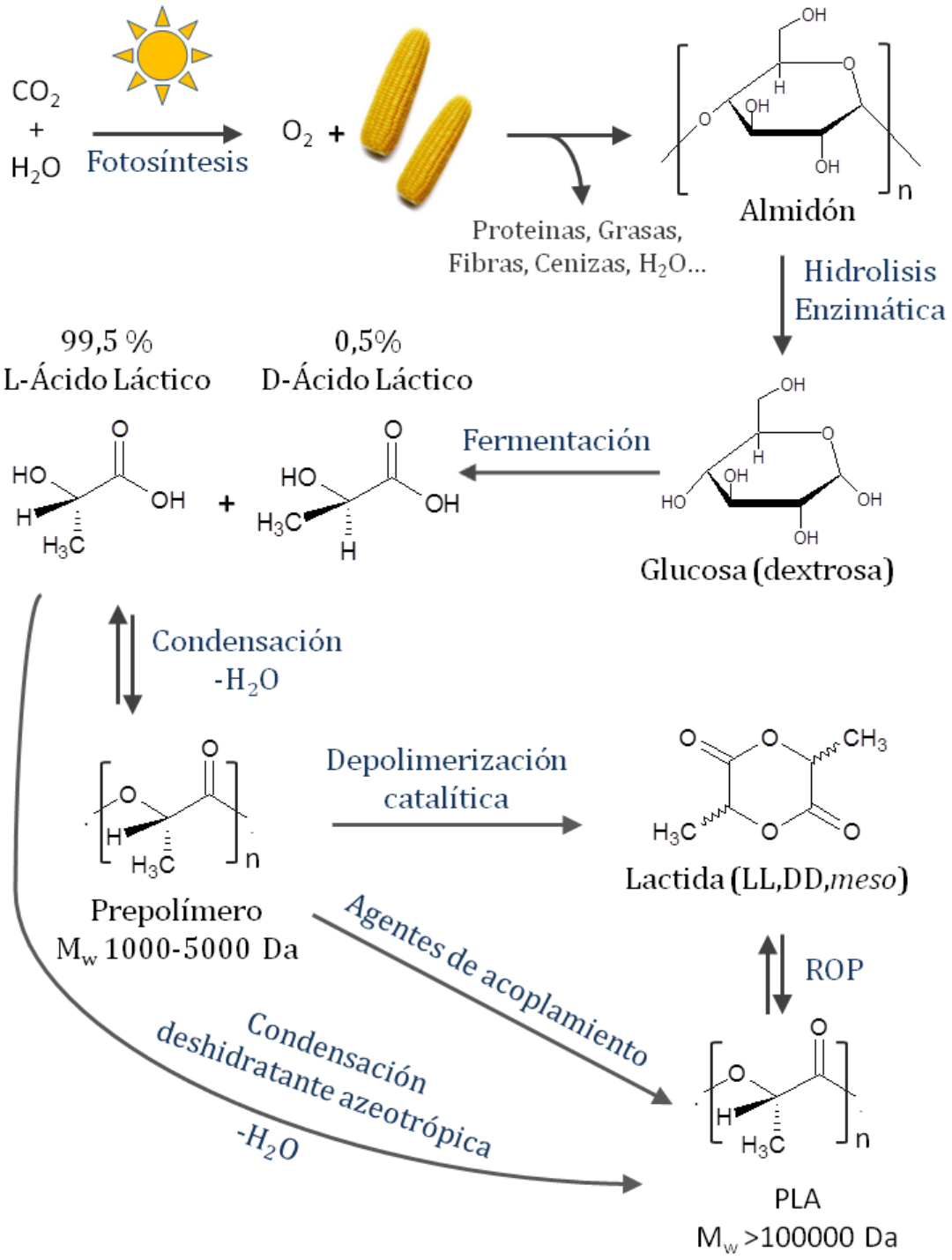


**Figura II.5.** Etapas implicadas en la producción de PLA.

El ácido láctico se puede obtener mediante síntesis química, que permite producir cantidades a gran escala de ácido láctico racémico pero es económicamente inviable [8]. Es

por ello que la mayor parte del ácido láctico se hace por la fermentación bacteriana de hidratos de carbono [8] a pH casi neutro [31]. A través de acidulación y una serie de pasos de purificación del caldo de fermentación se purifica sal de lactato para producir, a continuación, ácido láctico [31]. Los procesos de fermentación para la obtención de ácido láctico pueden ser heterofermentativos u homofermentativos. Los métodos heterofermentativos producen menor cantidad de ácido láctico y además generan niveles significativos de otros metabolitos tales como ácido acético, etanol, glicerol, manitol y dióxido de carbono. Por su parte, los métodos homofermentativos son los más utilizados por la industria debido a que producen mayores rendimientos de ácido láctico (1,8 moles de ácido láctico por mol de hexosa) y menores niveles de subproductos [8].

El PLA no puede ser sintetizado por polimerización directa del ácido láctico, porque cada reacción de polimerización genera una molécula de agua, que degrada la cadena de polímero formada a cadenas de baja masa molar [2]. El PLA se puede sintetizar a través de tres rutas principales (Figura II.5), (i) por polimerización directa por condensación del ácido láctico (2-hidroxi ácido propanoico) [8, 28, 31], (ii) por condensación azeotrópica deshidratante [8] o (iii) por polimerización de apertura del anillo de lactida [2, 8, 24, 28, 31].

La polimerización por condensación directa es la ruta menos costosa [8]. El ácido láctico se polimeriza directamente en presencia de un disolvente y un catalizador. La reacción se realiza mediante la aplicación de alto vacío y elevada temperatura para eliminar el agua que se genera durante la reacción de condensación [31]. El PLA obtenido puede estar compuesto o bien sólo por un estereoisómero o una combinación de D- y L-ácido láctico en varias proporciones o incluso ácido láctico en combinación con otros hidroxiácidos [29]. Sin embargo, es muy difícil obtener PLA de alta masa molar libre de disolvente por polimerización por condensación directa y se debe adicionar agentes de acoplamiento o adyuvantes que incrementan el costo del proceso además de hacerlo más complejo [8].

La síntesis por condensación deshidratante azeotrópica se realiza mediante una destilación a baja presión a 130 °C durante 2-3 horas y se elimina la mayor parte del agua que se genera durante la reacción de condensación. Posteriormente, se añade un catalizador y se recircula el disolvente a través de un tubo unido al recipiente de la reacción que contiene tamices moleculares a 130 °C durante 30-40 horas adicionales. Finalmente, se aísla el polímero o se disuelve y se precipita para una purificación adicional [8].

La síntesis de PLA mediante polimerización de apertura de anillo (Ring Opening Polymerization, ROP) es actualmente el método más usado para obtener PLA de alta masa

molar [8]. Los métodos ROP son los más comúnmente estudiados debido a que permiten un control de la síntesis química, y por lo tanto se puede variar las propiedades de los polímeros resultantes de una manera más controlada ampliando el ámbito de aplicación de estos materiales [29]. Para obtener PLA de alta masa molar, éste se produce a partir de los monómeros enantioméricos (D y L) por policondensación. En este primer paso el agua se elimina del proceso bajo condiciones suaves (y sin el uso de un disolvente) para producir un prepolímero de baja masa molar [31]. Posteriormente este prepolímero es catalíticamente depolimerizado en un dímero cíclico intermedio (lactida) [32], que es posteriormente purificado mediante destilación [31], el cual puede ser polimerizado mediante ROP en PLA de alta masa molar [2, 3, 21, 29]. Este mecanismo no genera agua adicional y, por lo tanto, mediante el control de la pureza de lactida [31], permite la producción de una amplia gama de pesos moleculares [2, 33]. De esta manera, se elimina el uso costoso y contaminante de disolventes.

Cuando el dímero es sintetizado a partir de una mezcla racémica de ácido láctico *rac*-lactida, se pueden obtener los tres estereoisómeros D-lactida, L-lactida (ambos con una temperatura de fusión de 97 °C) y *meso*-lactida (D,L-lactida) (con una temperatura de fusión de 52 °C) (Figura II.6).

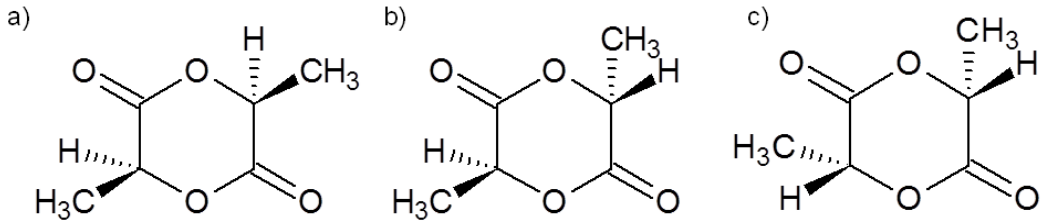


**Figura II.6.** Estructura química de los estereoisómeros de lactida:
**a)** *L,L*-lactida, **b)** *D,L*-lactida (*meso*-lactida) y **c)** *D,D*-lactida.

La polimerización por apertura de anillo, patentada por Cargill Inc. en 1992 es el método más frecuentemente utilizado para producir PLA [8]. En las dos últimas décadas, los avances en la tecnología de polimerización han reducido considerablemente el costo de producción y han contribuido a que el PLA sea económicamente competitivo con los polímeros provenientes del petróleo [28].

## 2.3. Procesado del PLA

El PLA puede ser procesado en los equipos convencionales de transformación industrial utilizados para los termoplásticos de uso común [34] como moldeo por

inyección, moldeo por soplado, termoconformado y formación de films [8, 21]. El PLA es susceptible de degradación térmica e hidrolítica [35]. La presencia de humedad durante el procesado puede provocar la hidrólisis de las cadenas poliméricas, reduciendo la masa molar del polímero [34]. Para evitar esta degradación el PLA debe ser secado antes de ser procesado a temperaturas inferiores a la temperatura de transición vítrea ($T_g$), la cual se encuentra entre 43 °C y 55 °C [7]. Por lo tanto, algunos parámetros del proceso como son la ausencia de humedad, la temperatura de trabajo y el tiempo de residencia deben ser optimizados y rigurosamente controlados durante el procesado y conformado del material [29].

La temperatura de procesado es función del tipo de polímero. Así, para el PLA amorfo la temperatura mínima de procesado la marca el valor de su $T_g$, aproximadamente 58°C [7], permitiendo un amplio rango de temperatura de trabajo. En cambio, para el PLA semicristalino la temperatura de proceso se encuentra en las proximidades de su temperatura de fusión ($T_m$) [36], la cual se puede encontrar en el rango de temperatura entre 130 °C a 180 °C [8].

## 2.4. Propiedades del PLA

Las propiedades del PLA se encuentran altamente influenciadas por la relación entre las dos formas isoméricas D y L que contienen [3, 8] y la masa molar [8]. La mayor parte del ácido láctico sintetizado por vía biotecnológica, a partir de recursos renovables, se encuentra como L-ácido láctico. Por lo tanto, generalmente el PLA contiene mayor proporción del enantiómero L [36].

### 2.4.1. Cristalinidad y transiciones térmicas

La temperatura de fusión y el grado de cristalinidad son dependientes de la masa molar, de la historia térmica del material y de la pureza del polímero [29]. La capacidad de controlar la estereoquímica permite un control sobre la velocidad de cristalización y, finalmente el grado de cristalinidad, las propiedades mecánicas y las temperaturas de transformación del material.

Para que la cristalización tenga lugar se necesita una pureza óptica de al menos 72-75 % (aproximadamente 30 unidades de ácido láctico isostático) [29]. El PLA enantioméricamente puro, indistintamente L o D, es semicristalino con un alto grado de cristalinidad, una temperatura de transición vítrea alrededor de 55 °C [29] y un

temperatura de fusión ($T_m$) alrededor de 180 °C [21, 29] con una entalpía de fusión de entre 40-50 J $g^{-1}$ [21].

Los cristales de los homopolímeros pueden desarrollarse en tres formas diferentes, dependiendo de las condiciones de formación (α, β y γ) [8, 37]. Los cristales de estructura α son cristales de una celda de forma pseudo-ortorrómbica que contiene dos cadenas antiparalelas (conformacón$10_3$ helicoidal) y presentan elevada estabilidad térmica [8, 38], con una temperatura de fusión de 185 °C [8].

La estructura β de poli(L-ácido láctico) se desarrolla tras el estiramiento mecánico de los cristales α [7]. Estos cristales están formados por una celda unitaria ortorrómbica que contiene seis cadenas antiparalelas (conformación $3_1$ helicoidal), presentando una temperatura de fusión de 175 °C [39]. Mientras que la estructura γ sólo se ha encontrado por cristalización epitaxial en sustrato hexametilbenceno [7, 38].

Cuando la cristalización se produce a temperaturas ($T_{cc}$) superiores a 120 °C, los homopolímeros cristalizan en homocristales de estructura α [37] que es más estable que la estructura β [8]. Sin embargo, si la cristalización ocurre a temperaturas inferiores a 100 °C se encuentran cristales con estructura tipo α', algo más desordenada y con menor estabilidad térmica que los cristales α [37]. Si la cristalización se produce entre 100 °C y 118 °C coexistirán ambas estructuras [40], ya que la velocidad de cristalización de PLA en este rango de temperaturas es muy alta [7].

El PLA de alta masa molar puede ser amorfo o semicristalino a temperatura ambiente, dependiendo de las cantidades de L, D y *meso*-lactida en la estructura. El PLA que contiene más del 93 % de L-ácido láctico es semicristalino, mientras que si contiene entre 50 y 93 % de L-ácido láctico es amorfo [8]. Así, el PLA amorfo de grado comercial contiene alrededor de un 4% de isómero D [31, 41]. A partir de la mezcla racémica de monómeros estereoisómericos D,L- lactida (50 % D y 50 % L) también se puede obtener PLA amorfo.

La introducción de defectos estereoquímicos en el poli(L-ácido láctico), es decir la incorporación de *meso*-lactida o D-lactida, reduce la temperatura de fusión, la velocidad de cristalización y el porcentaje de cristalinidad del polímero resultante [8, 21]; mientras que tiene poco efecto sobre el valor de $T_g$ [21]. De esta manera, el PLA puede mostrar polimorfismo cristalino que puede conducir a diferentes picos de fusión [3].

Por otra parte, mediante el mezclado en fundido de PLLA y PDLA se puede obtener una estructura estereoregular conocida como estereocomplejo de PLA (sc-PLA) [42] que consiste en estructuras cristalinas racémicas en las que las cadenas de PLLA y PDLA se empaquetan y se estabilizan mediante fuerzas de Van der Waals. Como resultado, los

estereocomplejos son materiales que presentan mejor estabilidad térmica, mayor resistencia mecánica y resistencia a la hidrólisis que el PLLA o PDLLA [42].

La cristalinidad del PLA se expresa como un porcentaje de la cristalinidad máxima teórica del PLA de alta masa molecular. Un valor de entalpía de fusión teórico del PLA 100 % cristalino comúnmente utilizado es 93 J $g^{-1}$ [29, 35, 43]. La cristalinidad influye en muchas propiedades de los polímeros como la dureza, módulo elástico, resistencia a la tracción y rigidez [7]. Por ejemplo, los estereocomplejos de PLA que son 100 % cristalinos (sc-PLA) tienen valores de entalpía mucho más altas (142 J $g^{-1}$) debido a su estructura cristalina diferente [35] y presentan una velocidad de cristalización mayor consiguiendo aumentar hasta 50 °C la temperatura de fusión ($T_m$ = 230 °C) con respecto a la de los homopolímeros puros (PLLA o PDLA) [8, 29, 39]. Además, sc-PLA forma otro tipo de cristales de estructura η mucho más estable térmicamente ($T_m$ = 230 °C) [38].

La temperatura de transición vítrea es dependiente de la proporción de PDLA y PLLA y se encuentra entre 50 °C y 80 °C [26]. Para el PLA amorfo la $T_g$ es uno de los parámetros más importantes, representando la temperatura máxima a la que el PLA conserva sus propiedades mecánicas debido a que por encima de la $T_g$ tienen lugar importantes cambios en la movilidad de las cadenas del polímero. Así, las propiedades del PLA amorfo dependerán en parte de cuán por debajo de $T_g$ se utiliza o se almacena el producto [8]. Las aplicaciones comerciales del PLA generalmente se utilizan en condiciones ambientales, temperatura inferior pero cercana a la $T_g$. Las cadenas termodinámicamente inestables tienden hacia un estado de equilibrio a través de reordenamientos segmentarios conocido como proceso de envejecimiento físico y puede tener desventajas importantes en la vida útil de los productos de PLA y sus aplicaciones comerciales [44]. Sin embargo, para el PLA semicristalino, tanto $T_g$ como $T_m$ son parámetros físicos importantes que permiten predecir el comportamiento del material. Es por ello que el valor de $T_m$ determina el proceso de transformación. La adición de D-lactida a la estructura del polímero puede conseguir una reducción en $T_m$ de entre 20 °C y 50 °C. Las aplicaciones comerciales de los productos de PLA amorfo se encuentran relacionadas con la temperatura a la que son utilizados.

A modo de resumen, en la Tabla II.1 se muestran los valores de temperatura de transición vítrea, temperatura de fusión, entalpía de fusión y cristalinidad del PLA enantioméricamente puro, PLA con distintos porcentajes de isómero D y esterocomplejos de PLA.

**Tabla II. 1.** Propiedades físicas ($T_g$, $T_m$, $\Delta H_m$ y $\chi_c$) de PLA con distintos grados de pureza

| | **PLA** (100 % L o D)[29] | **PLA** (98 % L)[26] | **PLA** (94 % L)[26] | **sc-PLA**[42] |
|---|---|---|---|---|
| $\mathbf{T_g}$ (°C) | 55 | 71 | 66 | 65-72 |
| $\mathbf{T_m}$ (°C) | 180 | 163 | 141 | 230 |
| $\mathbf{\Delta H_m}$ (J $g^{-1}$) | 93 | 38 | 22 | 102 |
| $\mathbf{\chi_c}$ (%) | 100 | 40 | 25 | 70 |

### 2.4.2. Estabilidad térmica

El PLA tiende a ser afectado por diferentes métodos de proceso y por el ambiente de almacenaje lo que puede causar diferentes tipos de reacciones de degradación, interacciones o inmiscibilidad entre mezclas de componentes [35]. Así, una de las principales limitaciones del PLA es su inestabilidad térmica para el procesado [45]. Durante el proceso de transformación, los enlaces éster de PLA tienden a degradarse y ocurre una disminución de la masa molar ocasionada por la degradación, lo que afecta a las propiedades finales del material, tales como la resistencia mecánica y la velocidad de degradación hidrolítica [46]. En este sentido, existen diferentes motivos que afectan la estabilidad térmica del PLA, la cual a su vez es dependiente de la masa molar inicial del polímero. La humedad puede provocar reacciones de termo-hidrólisis (Figura II.7) [45] que a su vez son catalizadas por los monómeros hidrolizados como ácidos láctico o lactida [8, 34]. La presencia de restos de catalizadores utilizados durante la síntesis pueden favorecer la depolimerización del PLA [8] formando lactida [47]. Además, el comportamiento de degradación depende fuertemente de la cristalinidad de las muestras [8], así como también del índice de polidispersidad (PDI). Cuando un material tiene un alto PDI contiene una cierta fracción de moléculas pequeñas que son volátiles, y cuanto mayor es el PDI menor es la estabilidad térmica del material [34].


**Figura II.7.** Escisión de la cadena de PLA debido al efecto del agua durante procesado térmico (adaptado de Carlson y coalaboradores 1998[45])

La degradación térmica del PLA es un proceso muy complejo debido a que varias reacciones ocurren simultáneamente [47, 48]. Kopinke y colaboradores (1996) estudiaron la degradación térmica del PLA mediante pirolisis combinada con cromatografía de gases

y espectrometría de masas, e indicaron que la degradación del PLA que tiene lugar a temperaturas superiores a 200 °C, incluye (i) procesos de transesterificación intramolecular (Figura II.8-a) que conducen a la formación de lactida y oligómeros cíclicos; (ii) mecanismos de *cis*-eliminación (Figura II.8-b) que dan lugar a la formación de ácido acrílico y oligómeros acíclicos y (iii) reacciones de fragmentación que conducen a la presencia de acetaldehído y $CO_2$ [48]. Al mismo tiempo, los oligómeros cíclicos se pueden combinar con poliésteres lineales a través de reacciones de inserción [46]. A temperatura superior a 300 °C pueden ocurrir también reacciones no selectivas radicalarias [48, 49].

De esta manera, la degradación térmica produce la escisión de la cadena polimérica, con la consiguiente formación de oligómeros, un aumento en los grupos terminales hidroxilo y carboxílicos, los cuales a su vez promueven la descomposición térmica. En consecuencia, se produce un descenso en la masa molar promedio y un aumento en la polidispersidad [45].

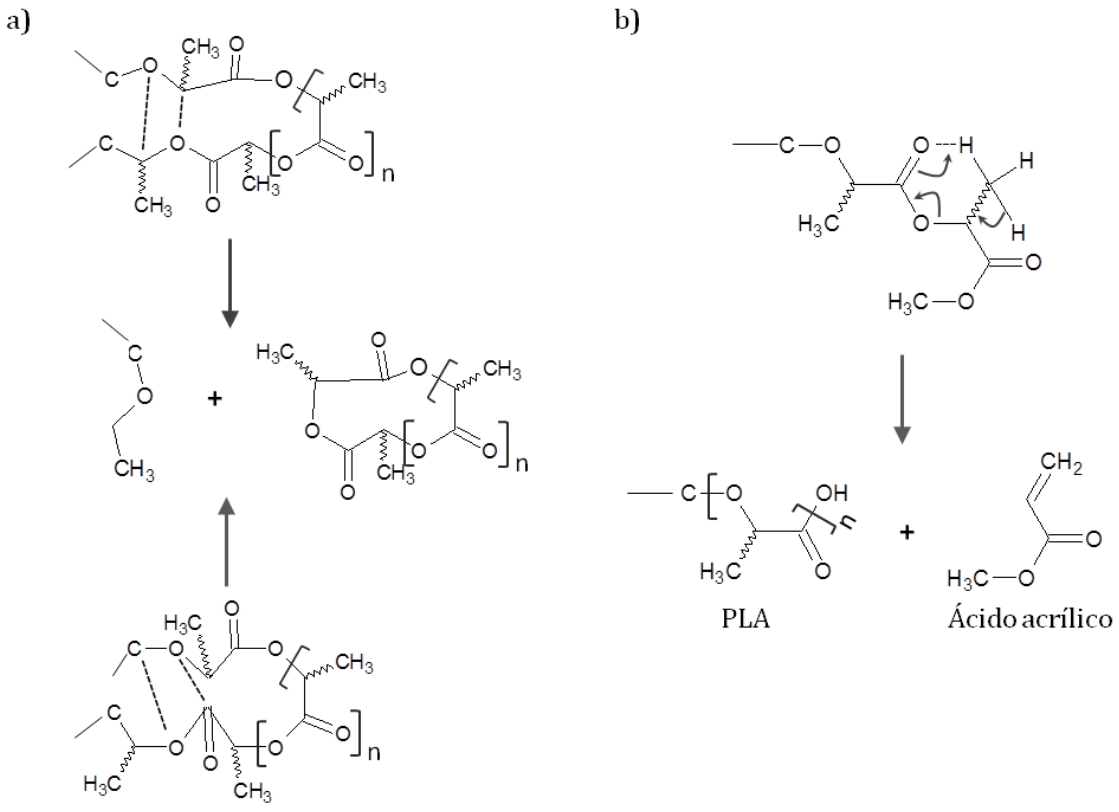


**Figura II.8.** Mecanismos de degradación térmica del PLA: a) transesterificación intramolecular, b)*cis*-eliminación (adaptado de Kopinke y colaboradores, 1996[48])

Además de la compresión de los distintos mecanismo de degradación térmica del PLA, la identificación de los productos de pirólisis del PLA cobra interés para estudiar

aspectos asociados con el grado de degradación del polímero sujeto a distintos procesos de degradación [50, 51]. Es por ello que en el presente trabajo se ha realizado un estudio preliminar de los productos obtenidos durante la pirolisis del PLA a elevadas temperaturas mediante la técnica de pirolisis combinada con cromatografía (cromatografía de gases y espectrometría de masas), para la mayor comprensión de resultados posteriores. En el apartado 2.4.6 del presente capítulo se desarrollará con más detalle el uso de la técnica de pirolisis acoplada a cromatografía de gases y espectrometría de masas (Py-GC/MS) como una medida indirecta y semicuantitativa de la asimilación de L-lactida por parte de los microorganismos.

### 2.4.3. Propiedades mecánicas

Las propiedades mecánicas del PLA dependen de la estereoquímica, del peso molecular y del porcentaje de cristalinidad [52]. Dependiendo de la proporción de D y L-ácido láctico se puede obtener PLA con una amplia gama de valores de rigidez [26], desde materiales blandos y elásticos a materiales de alta resistencia [29].

Cuando se desean propiedades mecánicas altas, se prefiere un PLA semicristalino [29] debido a que las regiones cristalinas ordenadas actúan como centros de alta densidad de enlaces covalentes [53]. El PLA semicristalino presenta mayor rigidez que el PLA amorfo, presentando valores de módulo elástico ($E$) de aproximadamente 3000 MPa, mientras que la resistencia a la tracción ($TS$) varía entre 50 y 70 MPa y su elongación a la rotura ($\varepsilon_{B\%}$) es aproximadamente de un 4% [29]. Así, presenta propiedades mecánicas superiores a PS, pero menores que al PET [7, 26]. Por su parte, las propiedades mecánicas del PLA amorfo indican que éste es un material algo más dúctil. Esta ductilidad dependerá ampliamente de si se encuentran por encima o por debajo de sus valores de $T_g$. Por su parte, sc-PLA presenta una rigidez superior en aproximadamente un 60% a la del PLLA [39], debido a que los cristales de los estéreo-complejos permiten la formación de enlaces intermoleculares cruzados [29].

El módulo elástico y la resistencia a la tracción aumentan con el aumento de la masa molar. Sin embargo, se ha visto que dicha tendencia se cumple cuando la masa molar promedio aumenta de 50 kDa a 100 kDa, aumentando los valores de $E$ y $TS$ en un factor de 2, mientras que aumentos mayores de la masa molar (por ejemplo: 300 kDa) no parecen influenciar estas propiedades [29].

Si bien la variación de la estereoquímica, la masa molar y la cristalinidad del PLA pueden mejorar su ductilidad y resistencia al impacto hasta cierto punto, esta mejora es generalmente insuficiente para satisfacer el requisito de la mayoría de las aplicaciones

prácticas [28]. La falta de ductilidad del PLA se puede corregir con la adición de plastificantes [22, 40, 54]. Por otra parte, las propiedades mecánicas finales de la pieza obtenida también dependen de la técnica y condiciones de procesado.

### 2.4.4. Interacción entorno-envase-alimento

Los envases de los alimentos son importantes para la protección del producto que contienen, conservarlo y extender su vida útil. Sin embargo, los materiales poliméricos pueden establecer interacciones tanto con el entorno como con el alimento, lo que puede dar lugar a una reducción de la calidad del producto, como alteraciones químicas, nutricionales y sensoriales del alimento que contienen, y como consecuencia una reducción de su vida útil.

Estas interacciones del envase con el entorno y el alimento involucran procesos de permeación, sorción, difusión y migración [55], los cuales se encuentran representados en la Figura II.9-a. Los procesos de permeación son aquellos que permiten el intercambio de sustancias a través del envase entre el entorno exterior y el entorno interior o espacio de cabeza [4], mientras que el fenómeno de difusión es la velocidad a la que estas sustancias atraviesan el polímero. El proceso de permeación es un proceso de difusión controlada donde un permeante es absorbido por, difunde a través de, y luego desorbe del polímero [55]. El proceso de sorción es la absorción de algunas sustancias procedentes del alimento (como el aroma, el sabor, olor o compuestos colorantes), que pueden ser retenidas por el material polimérico [4, 55]. Los fenómenos de migración involucran la transferencia de sustancias originalmente presente en el material de plástico del envase hacia el alimento [55].

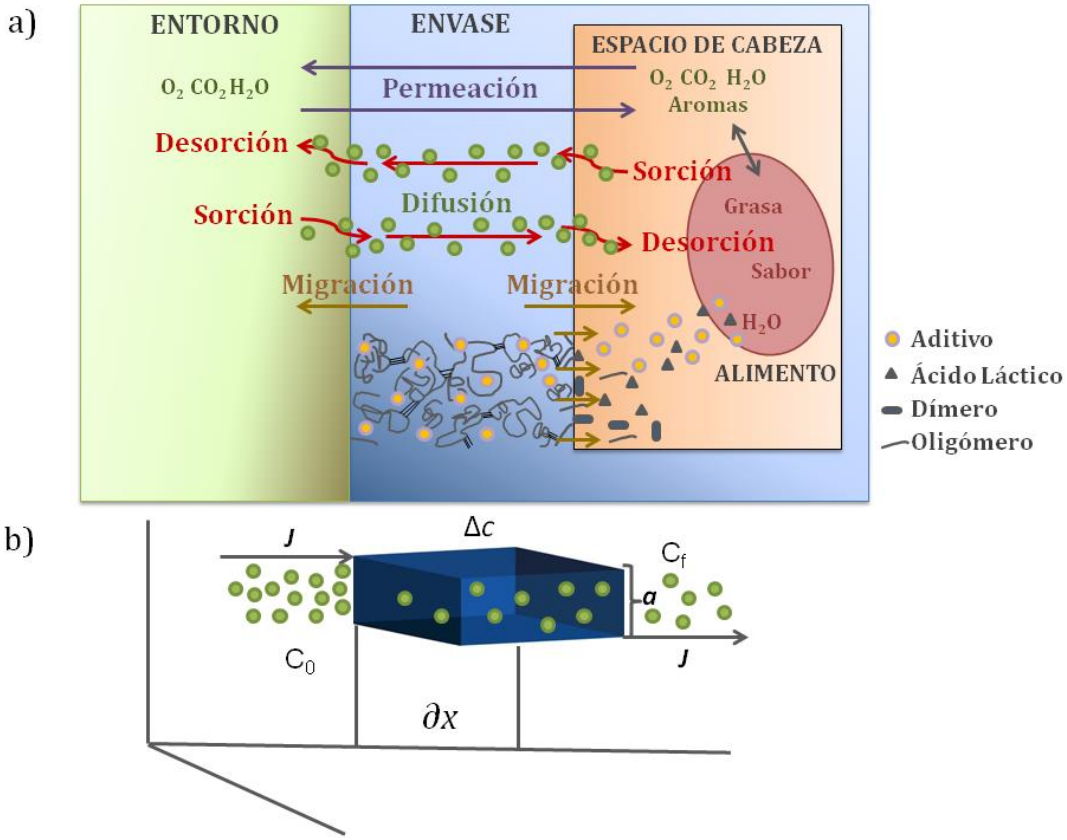


**Figura II.9.** Procesos de las posibles transferencias de masa involucrados en las interacciones entorno-PLA-alimento

### 2.4.4.1. Propiedades Barrera

En este sentido, los plásticos son relativamente permeables a las moléculas pequeñas (permeantes), tales como gases, vapor de agua, vapores orgánicos y líquidos [56], a diferencia de las cerámicas, vidrios y metales [55]. Por lo tanto, una de las propiedades más importantes cuando se trata de desarrollar un sistema para envasado de alimentos es la permeabilidad a los gases (especialmente dióxido de carbono y oxígeno) y al vapor de agua. El vapor de agua y oxígeno son dos de los principales permeantes estudiados en aplicaciones de envasado alimentario, ya que se pueden transferir, ya sea del medio interno o externo a través de la pared del envase polimérico, lo que provoca un cambio continuo en la calidad del producto y la vida útil [56]. Por otra parte, la permeabilidad química a través de las membranas poliméricas puede dar lugar a continuos cambios de la estructura del polímero [55].

El coeficiente de permeabilidad (*P*), permite determinar la capacidad que tiene una membrana polimérica para permitir el paso de un permeante a su través y tiene en cuenta

la solubilidad o coeficiente de absorción (*S*) y el coeficiente de difusión (*D*), los cuales se encuentran relacionados según la Ecuación II. 1.

$$P = S \cdot D \qquad \textbf{Ecuación II. 1}$$

*S* depende de la solubilidad de las moléculas de permeante en el material y *D* depende de la estructura del polímero y tiene en cuenta tanto el volumen libre de la matriz como su tortuosidad [57]. De esta manera, muchos polímeros muestran un incremento de la absorción de los gases con un incremento del volumen libre de la matriz polimérica [55], como por ejemplo el causado por la adición de plastificantes [40, 58], donde el aumento de la movilidad de las cadenas poliméricas permite el transporte de moléculas pequeñas a través de la matriz [59]. Dado que las regiones cristalinas son altamente ordenadas, en comparación con las regiones amorfas, el volumen libre es inferior o no existente y de esta manera las regiones cristalinas actúan como barreras impermeables para la difusión y la adsorción. Al mismo tiempo, las regiones cristalinas presentan una restricción de la cadena polimérica en la región amorfa que influye en el proceso de absorción en la fase amorfa limitando la eficacia de la trayectoria de difusión [55]. Así, la cristalización parcial del PLA reduce la permeabilidad a gases debido a que los cristales disminuyen el volumen de fase amorfa, a través de la cual los gases pueden permear con facilidad, al mismo tiempo que generan un camino más tortuoso, reduciendo el coeficiente de difusión [53].

Los gases tienen capacidad para penetrar en el material sólido, bien porque las moléculas del permeante interaccionan con el sólido y se disuelven en él, o bien porque penetran en los huecos microscópicos de la estructura sólida. La presencia de humedad y la temperatura influyen en el mecanismo de transporte de un gas a través del PLA. Auras (2007) observó un incremento de la difusión de oxígeno en PLA con el incremento de la actividad de agua atribuyendo este comportamiento al efecto de plastificación producido por el agua en la matriz de PLA. Con respecto a la permeabilidad al oxígeno, encontró que las muestras de PLA presentaron un aumento significativo (~3 veces) a la permeabilidad al oxígeno con el aumento de la temperatura de 5 °C a 40 °C. Sin embargo, las muestras de PLA ensayadas a altas actividades de agua ($A_w$ = 0.9) presentaron un menor aumento (~2 veces) de la permeabilidad al oxígeno con la temperatura, debido a la ocupación de parte del volumen libre por las moléculas de agua. Es por ello que el PLA muestra una reducción a la solubilidad del oxígeno con el aumento de contenido de agua [55].

El fenómeno de difusión (*D*), velocidad a la que las moléculas atraviesan el polímero, se encuentra gobernado por la primera Ley de Fick (Ecuación II. 2):

$$J = -D\frac{\partial c}{\partial x}$$ **Ecuación II. 2**

la cual establece que el flujo ($J$) de una sustancia (en dirección $x$) es proporcional al gradiente de su concentración ($c$) en la misma dirección. La penetración del permeante dará lugar a un desplazamiento neto de éste desde el lado más concentrado al menos concentrado. Termodinámicamente el potencial químico será mayor del lado más concentrado y tenderá a igualar dicho potencial igualando la concentración a ambos lados. El permeante se absorbe sobre la cara del film donde la concentración es mayor solubilizándose en la matriz polimérica, luego se reparte en el seno del film y se difunde dentro de él hasta llegar a la cara opuesta donde se desorbe para incorporarse en la atmósfera del otro lado, menos concentrada, estableciéndose un flujo neto (Figura II.9-b). Este equilibrio termodinámico está gobernado por la Ley de Henry [55], a ambos lados del film, Ecuación II. 3:

$$\Delta c = S \cdot \Delta p$$ **Ecuación II. 3**

la cual establece que el coeficiente de la concentración de saturación dentro del film ($\Delta c$), es proporcional a la presión parcial en la atmósfera gaseosa ($\Delta p$). El coeficiente de permeabilidad $P$ se puede expresar como la cantidad de permeante ($m$), que atraviesa el film (de espesor $e$), en la unidad de tiempo ($t$), por unidad de área superficial ($a$) cuando entre los dos lados de la membrana la diferencia de presión parcial del permeante ($\Delta p$) es la unidad (1 atm) (Ecuación II. 4) [55].

$$P = \frac{m \cdot e}{t \cdot a \cdot \Delta p}$$ **Ecuación II. 4**

Sin embargo, la relación directa entre el grado de cristalinidad del PLA y las propiedades de barrera es un tema de discusión [19]. En este sentido, Cocca y colaboradores (2012) indicaron recientemente que la permeabilidad al vapor de agua prácticamente no cambia con el aumento de la cristalinidad en films de PLA cristalizados (inmediatamente después de su preparación) a temperaturas inferiores a 110 °C. Sin embargo, obtuvieron una marcada disminución de la permeabilidad al vapor de agua con un aumento muy pequeño de la cristalinidad en las muestras cristalizadas a temperaturas entre 115 y 125 °C, correspondiente al rango de temperatura en el que la cristalización del PLA presenta un polimorfismo de cristales α y α' [60]. Con respecto a las propiedades de barrera al oxígeno del PLA, Guinault y colaboradores (2012) estudiaron la difusión de

oxígeno y el coeficiente de solubilidad en función del grado de cristalinidad en muestras de PLA con diferente cristalinidad, y encontraron que la permeabilidad se rige principalmente por el coeficiente de difusión. En films de PLA de cristalinidad inferior a 35%, el coeficiente de difusión aumentó con el aumento del grado de cristalinidad y atribuyeron este comportamiento no esperado a la creación de una fracción amorfa rígida con volumen libre más grande [61]. Las diferencias en el empaquetamiento molecular entre los cristales de forma α' y α influye también en la permeabilidad, donde la presencia de grandes fracciones de cristales α consiguen un empaquetamiento más estrecho de las cadenas de PLA que consiguen acoplarse fuertemente con las regiones amorfas y disminuir así la difusión a través del film [60].

El PLA presenta mejores propiedades de barrera al $CO_2$ que PS pero menores que PET [8], mejores propiedades de barrera al oxígeno que PS [26] y poli(etileno) de baja densidad (LDPE) [58], pero menores que PET [26, 58] y otros polímeros biodegradables como caseinatos [6] y gelatina [62].

#### 2.4.4.2. Migraciones

El PLA es aceptado como seguro en aplicaciones de envasado de alimentos y se encuentra clasificado como GRAS (de sus siglas en inglés: Generally Recognized As Safe) por la Food and Drug Administration (FDA) [63]. Así mismo, la normativa europea actual no incluye directrices específicas para ensayar los biopolímeros de manera diferente a los materiales poliméricos de uso común [64, 65]. Por lo tanto, sólo es necesario el control de la composición y los niveles de migración de este tipo de envases [66].

Los ensayos de migración se realizan mediante el contacto directo del material plástico hacia simulantes alimentarios seguido de una posterior cuantificación de los migrantes mediante el análisis químico en el caso de migración específica o un análisis gravimétrico en el caso de la migración global [67]. Desde los envases de PLA pueden migrar moléculas pequeñas hacia los alimentos como oligómeros, dímeros de ácido láctico, lactida y ácido láctico, por fenómenos de degradación hidrolítica [25]. En cualquier caso, el ácido láctico resulta el de especial interés porque dímeros y oligómeros en un sistema acuoso finalmente hidrolizan en ácido láctico [8] (Figura II.10), que es un ingrediente alimentario seguro y de uso común [25, 68], que también se encuentra naturalmente en algunos alimentos como en la carne de cerdo, carne de cordero, yogurt, quesos, chucrut, entre otros [25]. Tal es así, que el ácido láctico se encuentra en la lista autorizada de sustancias para entrar en contacto con alimentos sin límite de migración específica [69].

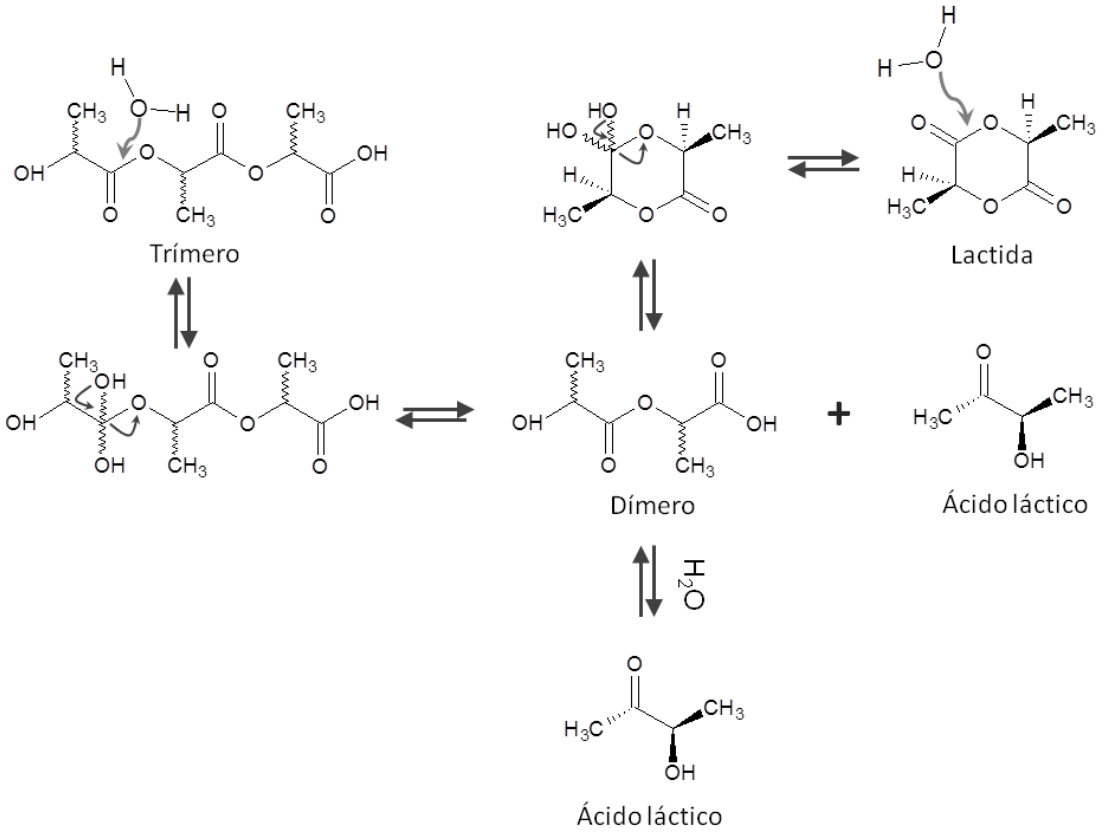


**Figura II.10.** Esquema de hidrólisis de PLA: trímero, dímero y lactida

Los procesos de transferencia de masa, pueden también ser empleados en beneficio del producto envasado con el objetivo de mejorar la calidad del producto [4] aprovechando su capacidad de interaccionar con el alimento mediante el desarrollo de envases activos. En este sentido, es sabido que el PLA se puede utilizar como matriz para la liberación sostenida de sustancias bioactivas [8], por lo cual se utiliza para aplicaciones biomédicas. La capacidad del PLA de liberar sustancias a partir de su matriz polimérica le confiere una ventaja adicional para su aplicación en envasado activo permitiendo interacciones entre algún aditivo del envase de PLA y el alimento o entre los aditivos del envase de PLA y la atmosfera interior del mismo [7].

### 2.4.4.3. Envase activo

Como se comentó anteriormente, una tendencia actual es la adición de aditivos con propiedades específicas, como antimicrobianas o antioxidantes, a las matrices poliméricas que al migrar del envase hacia el alimento interaccionaran con éste evitando el desarrollo microbiano o la oxidación de componentes del alimento, respectivamente. Una de las principales ventajas que ofrecen los envases activos, es que los materiales activos pueden

actuar como una fuente del aditivo que se libera a los alimentos a velocidades controladas [70] ofreciendo una ventaja con respecto a la adición directa del aditivo al alimento.

El efecto de la adición de sustancias activas a la matriz de PLA ha sido ampliamente estudiado en los últimos años, tanto componentes antimicrobianos [71, 72] como agentes antioxidantes [23, 73-76]. Jin y colaboradores (2009), incorporaron nisina a films de PLA y mezclas de PLA-pectina y demostraron inhibición de la actividad bacteriana de *Listeria monocitogenes* [71]. Fortunati y colaboradores (2012) mostraron actividad antibacteriana contra *Escherichia coli* y *Staphylococcus aureus* en films de PLA adicionados con nanopartículas de plata [72]. Manzanares López y colaboradores (2011) propusieron mezclas de PLA con α-tocoferol para el envasado de alimentos perecederos grasos debido a que demostraron un retraso de la inducción a la oxidación en aceite de soja debido a la liberación sostenida del agente antioxidante [73]. Hwang y colaboradores (2013) incorporaron resveratrol y α-tocoferol a PLA y mezclas de PLA-almidón y encontraron que ambos antioxidantes mejoran la estabilidad térmica de los materiales finales [23]. Por su parte, Iñiguez Franco y colaboradores (2012) incorporaron catequina y epicatequina al PLA y estudiaron la difusión de estos antioxidantes hacia diferentes simulantes alimentarios y observaron que el proceso de extrusión afectó a los antioxidantes añadidos, sin embargo, el contenido restante de antioxidante en las formulaciones finales demostró una efectiva actividad antioxidante [74].

### 2.4.5. Propiedades ópticas

Ver a través del film es uno de los requisitos más importantes para el envasado alimentario, ya que puede influir en la decisión del consumidor a la hora de elegir un alimento [77]. Por otra parte, la transmisión de la luz visible y ultravioleta son parámetros importantes en el diseño de los envases para conservar y proteger los productos hasta que llegan al consumidor [8]. Las longitudes de onda de interés en el envasado de alimentos se encuentran entre 200 y 2200 nm del espectro electromagnético: región ultravioleta (UV) (100-400 nm), espectro visible (400-700 nm) y la región del infrarrojo cercano (700-2200 nm). La luz UV a su vez se subdivide en tres regiones de longitud de onda distintas: UV-A (400-315 nm), UV-B (315-280 nm) y UV-C (280-100 nm). La luz UV-A, "luz negra", es el componente de menor energía mientras que la radiación UV-B es el componente de mayor energía de la luz UV natural [8]. La radiación UV-B es la que causa la degradación fotoquímica (fotólisis iniciada por fotooxidación) [78] de la mayoría de los plásticos y se encuentra parcialmente bloqueada por la capa de ozono [8]. La luz UV-C natural es

totalmente absorbida por la atmósfera y nunca alcanza la superficie de la tierra. Sin embargo, la luz UV-C es generalmente creada a partir de fuentes de luz artificial [8].

Auras y colaboradores (2005a) observaron que el PLA presenta mejores propiedades de barrera a la luz UV-C que LDPE, pero un poco inferiores que el PS, Celofán (CE), y PET [26]. Sin embargo, el PLA transmite más la luz UV-A y UV-B que PS, CE y PET [8]. Por lo tanto, para el envasado de algunos alimentos sensibles a la luz UV, la aplicación de envases de PLA transparentes puede requerir aditivos que sean capaces de absorber la luz UV y por lo tanto prevenir el daño a los alimentos envasados, lo que resulta en la retención de sabor y apariencia, la extensión de la vida útil y mejora de la calidad del producto [8].

Las propiedades ópticas del PLA dependen del grado de cristalinidad y por lo tanto un PLA amorfo presentará mayor transparencia que un PLA con mayor grado de cristalinidad [53]. Por otra parte, las propiedades ópticas de PLA resultan también importantes en las operaciones de teñido e impresión [40], su polaridad hace que tenga una energía superficial crítica elevada, lo que le proporciona una mayor facilidad para su impresión o teñido que PE y PP [53].

El color que presenta un envase alimentario es de fundamental importancia para los consumidores. Una coloración amarillenta de los envases alimentarios podría crear una percepción de que el envase es viejo [8] o bien considerar que el color amarillento proviene del alimento. La medida del color de PLA mediante el espacio colorimétrico CIELab ha demostrado que el PLA presenta apariencia similar a LDPE y PS [26]. El PLA presenta similar índice de amarillamiento (cambio de color de blanco o claro hacia amarillo) que PS y LDPE, mientras que el celofán y PET tienen valores más altos [8].

### 2.4.6. Degradación hidrolítica y enzimática

Una de las principales ventajas de los plásticos biodegradables es que son degradados fácilmente por los microorganismos presentes en el medio ambiente a diferencia de los plásticos convencionales los cuales son resistentes al ataque microbiano [7]. El carbono, hidrógeno y oxígeno en el PLA tienen su origen en agua y dióxido de carbono y si el envase de PLA, al finalizar su vida útil, es expuesto a degradación en condiciones de compostaje tendrá también su final en agua y dióxido de carbono, como consecuencia de la degradación biológica, completando así el ciclo de vida del PLA (Figura II.11).

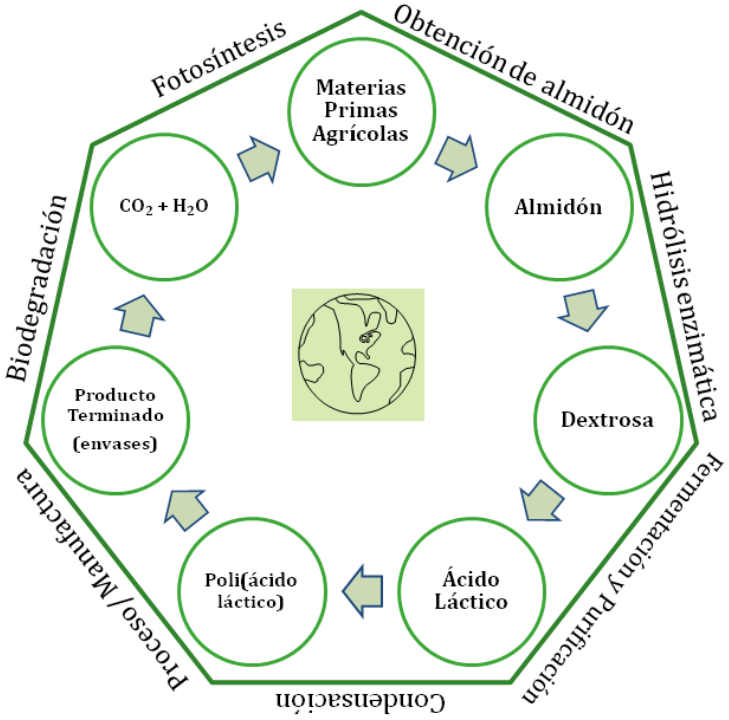


**Figura II.11.** Ciclo de vida del PLA

La degradación biológica de los plásticos puede ser aeróbica, en la naturaleza salvaje; anaerobia, en sedimentos y rellenos sanitarios; o una combinación de ambas parcialmente aeróbica y parcialmente anaeróbica, como es el caso de la degradación en suelo y en los medios de compostaje [78]. La degradación en compost, implica inicialmente procesos abióticos (degradación térmica y fotodegradación) y procesos bióticos, degradando el polímero en especies de baja masa molar. Sin embargo, los fragmentos de degradación resultantes deben ser utilizados completamente por los microorganismos, de lo contrario existe potenciales consecuencias ambientales y, en consiguiente, para la salud [18].

La degradación del PLA en condiciones de compostaje ocurre en dos etapas consecutivas, primero ocurre una degradación hidrolítica seguida de una degradación enzimática [19]. La desintegración del PLA comienza por la superficie que absorbe agua del medio, los grupos hidrolizables en la cadena principal son susceptible al ataque del agua, que comienza a erosionar el polímero [79]. Posteriormente, el agua difunde al seno del polímero produciendo escisiones no enzimática de cadenas del grupo éster al azar [19]. Así, las cadenas de alta masa molar hidrolizan a oligómeros de menor masa molar ($M_n$ de aproximadamente 40000) [21] y ácido láctico (Figura II.12) que pueden ser asimilados por los microorganismos tales como hongos y bacterias [19]. Además, ocurre un proceso de difusión de oligómeros solubles al seno del polímero [80]. La escisión y la

hidrólisis de los enlaces éster es autocatalizada por los grupos terminales ácidos carboxílicos [68].

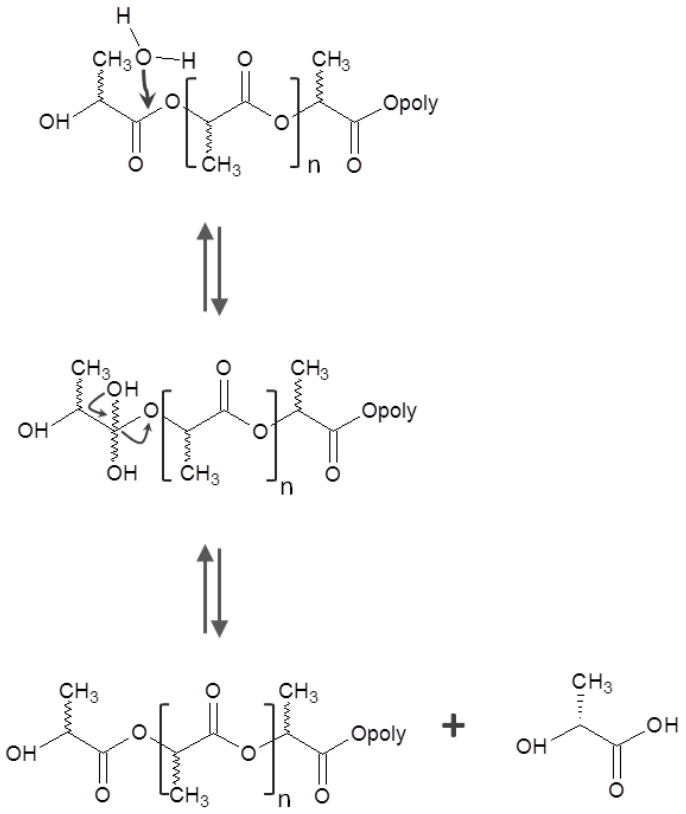

**Figura II.12.** Esquema de hidrólisis de PLA y pérdida de masa molar (Adaptado de Kale y colaboradores, 2006 [79])

Durante el proceso de hidrólisis, la integridad estructural del material se va afectando a medida que la masa molar disminuye [79], se observa una disminución en tamaño (reducción del espesor) y un aumento de la fragilidad del material [68]. La reacción de hidrólisis puede acelerarse debido a la presencia de ácidos o bases y se ve afectada tanto por la temperatura como por los niveles de humedad [21]. La velocidad de degradación hidrolítica del PLA y su consiguiente reducción de la masa molar es mayor en condiciones básicas que en medios ácidos [81]. Por otra parte, en el caso de medios de compostaje un pH ácido podría inhibir el desarrollo microbiano. La Figura II.13 muestra un esquema de la depolimeración del PLA en un medio básico. Durante la degradación del PLA en un medio alcalino en la cadena final puede ocurrir una transesterificación intramolecular, debida al ataque electrofílico del grupo terminal hidroxilo en el segundo grupo carbonilo, catalizado por una base, lo que conduce a una formación de anillo. El polímero se acorta por la hidrólisis de la lactida resultante, la cual en un siguiente paso se hidroliza en dos moléculas de ácido láctico. Al mismo tiempo, se produce una degradación

intramolecular al azar por el ataque alcalino en el carbono del grupo éster, seguido por la hidrólisis del enlace éster que genera nuevas moléculas de baja masa molar [82].

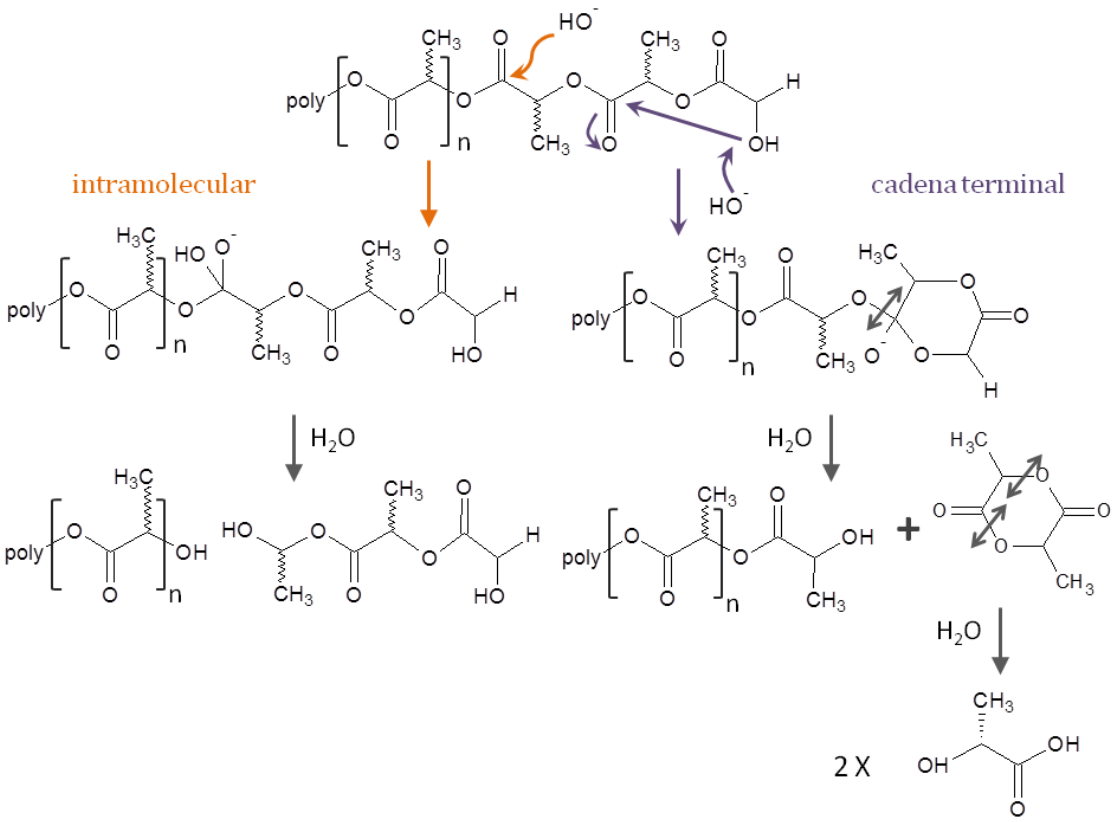


**Figura II.13.** Esquema de la hidrólisis de PLA en condiciones alcalinas (adaptado de Lucas y colaboradores 2008 [82]).

Independientemente del medio de hidrólisis, la escisión hidrolítica de las cadenas de PLA se produce principalmente en las zonas amorfas que se encuentran entre las regiones cristalinas [8]. A continuación del proceso de hidrólisis los microorganismos continúan el proceso de degradación del material mediante la conversión de estos componentes de menor masa molar en dióxido de carbono, agua, y humus [21].

Aunque el proceso de degradación del PLA en un medio de compostaje es un proceso simple de hidrólisis, cualquier factor que afecte a la reactividad así como también a la accesibilidad del agua y de los microorganismos a la matriz polimérica afectarán a la velocidad de degradación del polímero [8]. Estos factores pueden ser: la humedad, la temperatura, el pH, tipo de microorganismo presente, la disponibilidad de oxígeno y de nutrientes en el medio [83], el tamaño de partícula y su forma, la cristalinidad de la formulación final, el porcentaje de isómero, la concentración de ácido láctico residual, la masa molar, la distribución de masa molar, impurezas de metales del catalizador [8, 79] y

la presencia de grupos funcionales [84]. De esta manera, las condiciones adecuadas para la biodegradación de PLA en compost se alcanzan con temperatura por encima de 50 ºC y [33] una alta humedad relativa (40-50% de la capacidad máxima de retención de agua del suelo) [85] para promover la hidrólisis de las cadenas de PLA.

Las bacterias presentes en el suelo, aerobias y anaerobias, son los agentes implicados en el siguiente paso de la degradación de los polímeros biodegradables. Su acción degradativa es principalmente un resultado de la producción de enzimas y la consiguiente ruptura del sustrato con el fin de obtener nutrientes [85]. Las enzimas producidas por diferentes microorganismos tienen sitios activos con diferentes especificidades, con diferentes formas complementarias, cargas e hidrofilicidad/hidrofobicidad. En este sentido, los hongos *Aspergillus niger* y *Aspergillus flavus* presentes en el suelo y en cultivos, respectivamente, producen enzimas que digieren más rápidamente poliésteres derivados de monómeros de tamaño medio ($C_6$-$C_{12}$) que aquellos derivados de monómeros más largos o más cortos [84, 85]. Para que las enzimas puedan degradar un polímero biodegradable, la cadena de polímero debe ser capaz de encajar en el sitio activo de la enzima [85]. Por lo tanto, esta especificidad enzimática puede contribuir a diferentes tasas de degradación de poliésteres biodegradables en diferentes entornos de compostaje [84].

Khabbhaz y colaboradores (2000) estudiaron la degradación del PLLA en un medio biótico (cultivo mixto de microorganismos extraidos de compost) por la técnica de pirolisis a 500ºC acoplada a un cromatografo de gases y un espectrómetro de masas (Py/GC-MS) y compararon los resultados con muestras de PLLA degradadas en un medio abiótico [51]. Todas las muestras pirolizadas revelaron la presencia de dos picos con espectros de masas idénticos, correspondientes a la estructura química de lactida. Debido a que uno de estos picos representa a L-lactida o D-lactida (sin distinción) y el otro pico representa a *meso*-lactida [48], utilizaron la relación de áreas entre el pico correspondiente a meso-lactida y el pico correspondiente a L-lactida (*meso*-lactida : lactida) como una medida semicuantitativa de la asimilación de L-lactida por parte de los microorganismos. Observaron mayor cantidad de L-lactida o D-lactida en las muestras expuestas a la degradación biótica que en las muestras sin degradar y las expuestas al medio abiótico. Por su parte, la cantidad de *meso*-lactida resultó mayor en las muestras degradadas en medio biótico que en las muestras degradadas en medio abiótico. Se atribuyeron estos resultados a que los microorganismos prefieren la forma L-lactida en lugar de la forma D (D-lactida), lo que influye tanto en la formación como en las cantidades de *meso*–lactida y lactida (D o L lactida) durante la pirólisis [51].

Cada modificación sustancial en la formulación del material en base a PLA podría cambiar el patrón de producto de degradación obtenido mediante la introducción de nuevos compuestos solubles en agua o que afecten a la distribución de productos [35]. En este sentido, Lemmouchi et al. (2009) demostraron que la desintegración de PLA en condiciones de compostaje se ha mejorado por la presencia de plastificantes [86]. Por otra parte, se espera que la incorporación de polímeros cristalinos como parte de mezclas de materiales basados en PLA retarde el proceso de degradación del PLA en condiciones de compostaje, debido a que la degradación en compost ocurre principalmente en las zonas amorfas del polímero [8]. La incorporación de nanocargas a la matriz de PLA puede presentar diferentes comportamientos según la naturaleza de la carga. En este sentido, Fortunati y colaboradores (2014) encontraron que la adición de nanocristales de celulosa (CNC) acelera el proceso de degradación del PLA [87].

## 2.5. Aplicación del PLA en envases alimentarios

A pesar de las numerosas características positivas que presenta el PLA mencionadas anteriormente, el uso de PLA en aplicaciones de envase de alimentos se encuentra limitado debido principalmente a que presenta algunas restricciones en cuanto a sus propiedades térmicas, mecánicas y barrera [7].

### 2.5.1. Modificaciones del PLA para su aplicación en envases alimentarios

En el envasado de alimentos se debe garantizar la seguridad de un material evitando el deterioro de su estructura durante su servicio. Así, la degradación del PLA debe tenerse en cuenta [66]. En este sentido, los productos generados por la degradación térmica pueden ser una molécula de lactida, un anillo de oligómero o una mezcla de acetaldehído y $CO_2$, en función del lugar de la cadena donde ocurra la fragmentación. El acetaldehído resulta indeseable en aplicaciones destinadas para el envasado de alimentos ya que puede alterar las propiedades organolépticas del alimento [36].

La alta fragilidad del PLA limita tanto su capacidad de proceso como sus aplicaciones. Una manera de mejorar el comportamiento mecánico del PLA es mediante la adición de plastificantes [22] como poli(etilen glicol) (PEG) y citrato de acetil tri-n-butilo (ATBC) que resultan altamente recomendados para plastificar el PLA [57]. La Autoridad Europea de Seguridad Alimentaria (EFSA), informó que el uso de PEG [88] y ATBC [89] en materiales destinados a estar en contacto con alimentos no plantean un problema de seguridad para los consumidores. Sin embargo, la introducción de plastificantes a la

matriz de PLA genera un aumento de la permeabilidad a los gases de la matriz polimérica, lo que resulta perjudicial para el uso de envases alimentarios [22].

Para aplicaciones de envase alimentario tanto el PLA como el PLA plastificado no presentan propiedades de barrera suficiente a los gases (sobre todo dióxido de carbono y oxígeno), ni al vapor de agua [53], las cuales son propiedades fundamentales para esta aplicación debido a que el envase debe proteger al alimento, entre otras cosas de la oxidación y de la humedad. Por otra parte, como se comentó anteriormente, la presencia de agua tiene un efecto significativo en las propiedades barreras de los polímeros debido a que puede modificar la forma en que el gas o el vapor son absorbidos y difundidos a través de la matriz polimérica [90]. Es por ello que se han propuesto modificaciones para mejorar las propiedades de barrera del PLA, siendo las más estudiadas la preparación de multicapas y el aumento de la cristalinidad.

Para el desarrollo de envases de múltiples capas resulta imprescindible que los materiales utilizados, aparte del PLA, también sean biodegradables para mantener el carácter biodegradable del material final. Así, se han propuesto diferentes biomateriales que presentan mejores propiedades barreras al oxígeno como pueden ser las proteínas (gelatina [91], soja [92] o caseinatos [6]) y el gluten [93].

Otra vía para mejorar las propiedades barreras del PLA es mediante el aumento del grado de cristalinidad, lo que dificulta la difusión de los gases debido a que genera un camino más tortuoso a través de la estructura polimérica [90]. El aumento de la cristalinidad puede conseguirse desarrollando un material con un alto contenido de L-lactida, mezclando el PLA con otro polímero que sea cristalino o incorporando nanocompuestos.

Las mezclas de PLA con otro biopolímero resultan una estrategia atractiva para aumentar la cristalinidad del PLA debido a que es un proceso relativamente fácil y que se obtiene mediante la misma tecnología disponible en la industria para el procesado de PLA [94] y los plásticos de uso común. En este sentido, el poli(hidroxibutirato) PHB, es un biopoliéster cristalino, perteneciente a la familia de los poli(hidroxialcanoatos), biodegradable y presenta temperatura de fusión entre 173 °C y 180 °C [3, 95], próxima a la del PLA por lo que puede ser un candidato para mezclarlo con él en fundido.

Por otra parte resulta de fundamental importancia reducir la tasa de degradación térmica del PLA y mejorar su estabilidad térmica de manera que pueda tener aplicaciones más amplias, sin comprometer las propiedades del producto debido a la aparición del inicio de la degradación térmica [96]. De entre los muchos métodos que se pueden utilizar para reducir la degradación térmica de PLA, una alternativa prometedora es modificarlo mediante la adición de nanocargas. Los nanomateriales presentan propiedades mejoradas

respecto a los materiales originales debido a la incorporación de pequeñas cantidades de relleno, de escala nanométrica, en la matriz polimérica [33]. El uso de nanocargas de origen natural resulta especialmente interesante ya que engloba ambos conceptos respetuosos con el medio ambiente: origen renovable y biodegradable. En este sentido Fortunati y coaboradores (2010, 2012a), demostraron que la celulosa microcristalina (MCC), disponible comercialmente, resulta un aditivo muy efectivo para mejorar las propiedades de los polímeros [97] sin afectar la transparencia [72] y a partir de MCC se pueden obtener nanocristales de celulosa (CNC) [98]. La adición de CNC a la matriz de PLA ha demostrado mejorar efectivamente las propiedades del PLA, respecto a otros nanomateriales comúnmente utilizados como refuerzos y ofrece algunas propiedades adicionales como su biodegradabilidad, alta rigidez y baja densidad [98].

## 3. PLASTIFICACIÓN DEL PLA

El PLA es un material rígido y quebradizo para ser procesadas como film. Es por ello que comúnmente se incorporan aditivos al PLA tales como plastificantes, no sólo para facilitar la procesabilidad, sino también para obtener materiales más flexibles y dúctiles, mediante la disminución de la temperatura de transición vítrea [28]. Generalmente, los plastificantes son moléculas orgánicas pequeñas, relativamente no volátiles, que se añaden a los polímeros para reducir el número de contactos polímero-polímero relativo disminuyendo la rigidez de la estructura tridimensional, permitiendo de ese modo la deformación sin ruptura [99]. Sin embargo, la selección de un plastificante para ser aplicado en la industria del envasado alimentario biodegradable, requiere la consideración de varios criterios como compatibilidad, carácter biodegradable, permanencia del plastificante en el material durante el procesado [100], la resistencia a la migración, ausencia de toxicidad y baja volatilidad [28, 100], entre otros.

La eficiencia de plastificación de un plastificante, es evaluada generalmente en términos de la disminución de la $T_g$ y la mejora en las propiedades de tracción, las cuales dependen de su miscibilidad con la matriz polimérica y de a masa molar [28]. Por lo tanto, para conocer el efecto de plastificación es importante conocer la solubilidad que se va a presentar entre el PLA y los plastificantes, así como entre las mezclas de PLA-PHB y los plastificantes debido a que la correcta distribución del plastificante en el seno de la matriz polimérica estará determinada principalmente por el nivel de miscibilidad entre el plastificante y el polímero. Se puede suponer que la eficiencia del plastificante se relaciona principalmente con la estructura química de su molécula y su compatibilidad con la matriz polimérica. Desde un punto de vista molecular, el plastificante debe ser miscible con el

polímero y presentar fuerzas intermoleculares similares. En general, se ha observado que el plastificante más eficaz se asemeja mucho al polímero y se caracteriza por presentar parámetros de solubilidad similares a los de los polímeros [100]. El concepto de parámetro de solubilidad (δ) se basa en la energía libre de Gibbs, la ecuación de la energía libre de mezclado (Ecuación II. 5).

$$\Delta G = \Delta H - T\Delta S \qquad \textbf{Ecuación II. 5}$$

donde ΔG es la variación en la energía libre de Gibbs, ΔH la variación de la entalpía (calor de mezclado), T la temperatura absoluta y ΔS la entropía de mezclado.

Se requiere un valor negativo de ΔG para que se produzca la disolución [55]. Cuando las moléculas de polímero y del disolvente (plastificante) se mezclan para dar una disolución aumenta la entropía del sistema (ΔS), debido al desorden creado en el sistema. Por lo tanto, el signo del cambio de energía libre se encuentra determinado por ΔH, el cual representa el balance energético que resulta cuando el polímero y el disolvente pasan de su estado puro (polímero sólido o fundido y disolvente líquido) a la disolución (líquida); por tanto se requiere valores negativos o pequeños de calor de mezclado.

La compatibilidad de un plastificante depende de ambos, polímero y plastificante. Termodinámicamente, los polímeros amorfos pueden ser considerados como líquidos. Por eso la solubilidad del polímero en el plastificante o solvente puede ser tratada de la misma manera que la miscibilidad de dos líquidos [100]. Así, para que dos líquidos sean miscibles, sometiéndolos a calores de mezcla mínimos, deben presentar densidades de energía de cohesión similares. La densidad de energía de cohesión, es la energía requerida para la separación infinita de las moléculas de un líquido por centímetro cúbico evitando las fuerzas intermoleculares: energía de vaporización por unidad de volumen [101]. Generalmente se utiliza el parámetro de solubilidad, δ (Ecuación II. 6).

$$\delta = \sqrt{\frac{\Delta E}{V}} \qquad \textbf{Ecuación II. 6}$$

donde $\Delta E/\mathrm{V}$ representa la densidad de energía cohesiva (variación de energía molar de vaporización a presión cero por unidad de volumen V, del líquido) [55].

La afinidad relativa de un polímero y un plastificante se puede estimar usando los parámetros de solubilidad [8]. De esta manera, la cercanía de los parámetros de solubilidad entre plastificante y polímero se utiliza generalmente para evaluar la miscibilidad entre ellos, y proporciona una referencia para la selección de un plastificante

efectivo [28]. Para poder considerar la mezcla de los componentes compatibles, los parámetros de solubilidad del polímero y del plastificante deben ser del mismo orden.

Se han desarrollado varios métodos para la determinación del parámetro de solubilidad, sin embargo generalmente se calcula a partir de su fórmula estructural, debido a su simplicidad y a la validez de los resultados obtenidos. Considerando varios tipos de moléculas simples, Small elaboró una lista de constantes de atracción molar (G) para varias moléculas, las cuales son aditivas. Así, es posible calcular δ por adición de las constantes de atracción molar, considerando el aporte que cada uno de los grupos hace a la estructura global de la molécula (Ecuación II. 7).

$$\delta = \frac{D\sum G}{M_n} \qquad \textbf{Ecuación II. 7}$$

donde δ es el parámetro de solubilidad (cal $cm^{-3})^{1/2}$, D la densidad (g $cm^{-3}$), ∑G el sumatorio de constantes de atracción molar [(cal $cm^{-3})^{1/2}$ $mol^{-1}$] y $M_n$ es la masa molar promedio en número por unidad repetitiva (g $mol^{-1}$). Se debe tener en cuenta que las predicciones teóricas pueden ser relativas porque la solubilidad de un polímero en un plastificante se puede ver afectada por variaciones en la composición, la cristalinidad y la polaridad, entre otras [100].

Las moléculas pequeñas de plastificantes suelen resultar más eficientes que las más grandes, especialmente en la reducción de la $T_g$ de la matriz polimérica [28, 99]. Así, la miscibilidad de un polímero con plastificantes de la misma familia química disminuye con el aumento en la masa molar del mismo, porque una mezcla con plastificantes de baja masa molar tiene alta entropía de mezclado [28]. Se espera que un plastificante de menor masa molar resulte en una mayor disminución de la $T_g$ del PLA, sin embargo también puede migrar desde el material al alimento más fácilmente que plastificantes de mayor masa molar [99].

Se ha observado que se pueden alcanzar elevada ductilidad del PLA plastificándolo con poliadipatos comerciales en concentraciones de entre 10% y 20% en peso [58] sin dar lugar a separación de fases y migración del plastificante al finalizar el estudio de envejecimiento a 25 ºC durante tres meses [69]. Más recientemente, Burgos y Colaboradores (2013) estudiaron el envejecimiento de films de PLA plastificados con oligómeros de ácido láctico (OLA) usando concentraciones entre el 15 % y 25 % en peso sin observar separación de fases después de tres meses de almacenamiento a 25 ºC y 50 % de humedad relativa [40].

Varios monómeros y oligómeros han sido investigados como potenciales plastificantes para PLA. Entre ellos, poli(etilenglicol) (PEG) (Figura II.14-a) y ésteres de citrato son, quizás, los plastificantes más comúnmente investigados [28, 54, 57]. Existen varios ésteres de citrato comerciales como plastificantes para films destinados al contacto con alimentos, incluyendo citrato de trietilo (TEC), citrato de tributilo (TBC), citrato de acetiltrietilo (ATEC), y citrato de acetil-tri-n-butilo (ATBC) (Figura II.14-b) [28]. El desarrollo tecnológico de los bioplásticos, tales como PLA y PHB, aún no se ha traducido en un impacto significativo en el mercado y es por ello que la investigación de aditivos renovables y biodegradables constituye un motivo adicional para el desarrollo de nuevos plastificantes [99]. En este sentido, estudios recientes han propuesto el uso de D-limoneno como un nuevo monómero [102]. El D-limoneno (Figura II.14-c) es el monoterpeno más abundante en la naturaleza y el componente principal de los aceites esenciales de los cítricos [103, 104]. El uso de limoneno como aromatizante en productos alimenticios está permitido [5]. Por otra parte, se ha observado que el limoneno presenta propiedades antioxidantes y también se ha observado actividad antimicrobiana frente a algunos microorganismos como *Aspergillus penicilium* [5]. El limoneno ha sido tradicionalmente utilizado para estudiar la difusión de aromas en diferentes materiales poliméricos. Sin embargo, recientemente se ha adicionado aceite esencial de limón a matrices poliméricas como poli(etileno) de alta densidad (HDPE) destinado a envase de galletas y un análisis sensorial mostró una alta aceptación por parte de los jueces con respecto al aroma de limón y al sabor de las galletas [103]. Así mismo, se ha añadido aceite esencial de bergamota a matrices de polímeros biodegradables como hidroxipropil metilcelulosa (HPMC) [105] y quitosano [104]. Salazar y colaboradores (2012) estudiaron la absorción de diferentes compuestos aromáticos a través de la matriz de PLA y encontraron un efecto de plastificación de la matriz polimérica [106]. Por otra parte, el D-Limoneno es el residuo más importante en la industria de los cítricos, por lo que resulta interesante en términos medioambientales revalorizar este subproducto al usarlo como plastificante de polímeros.

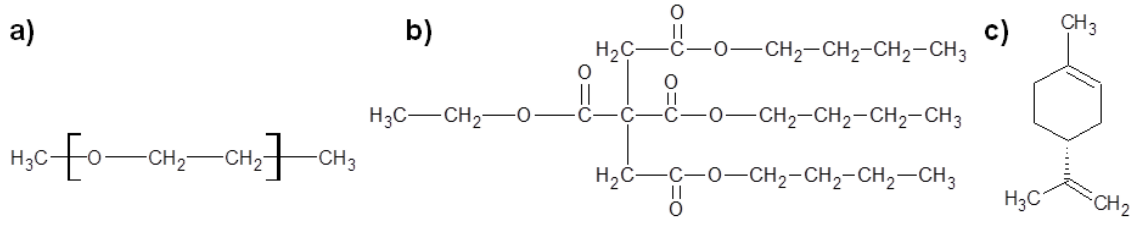


**Figura II.14.** Estructura química de los plastificantes: a) PEG, b) ATBC y c) D-Limoneno.

Se debe tener en cuenta que ATBC es un plastificante monomérico, mientras que PEG es un plastificante polimérico. Concretamente, en el caso de PLA plastificado con ATBC se encontró que éste resulta más efectivo en la mejora de la elongación cuando su presencia es de más de 10% en peso [28, 107]. Coltelli y colaboradores (2008) observaron que la plastificación de PLA con ATBC resultó en un aumento de la cristalinidad con concentraciones inferiores al 20% [108]. Lemmouchi y colaboradores (2009) reportaron que la combinación de PLA-ATBC en proporción 80:20 conduce a una mejora importante de las propiedades termo-mecánicas del PLA [86]. Así, en las mezclas de PLA con ésteres de citrato se produce separación de fases a partir de un 25% de ATBC [28]. Courgneau y colaboradores (2011) estudiaron PLA plastificado con PEG ($M_n$= 200g·mol$^{-1}$) y ATBC, y concluyeron que la adición de ATBC en contenidos mayores o igual al 13% en peso disminuye la $T_g$ del PLA y aumenta el alargamiento a la rotura, sin presentar separación de fases hasta un contenido de 17% en peso. Por el contrario, PEG muestra un límite de miscibilidad con PLA al presentar separación de fases a partir de un 9% en peso [57]. En los sistemas PLA-PEG, la miscibilidad se encuentra condicionada por la masa molar de PEG, donde su eficiencia de plastificación aumenta con la disminución de la masa molar [28, 109]. En este sentido, Martín y Avérous (2001) estudiaron sistemas PLA-PEG, de $M_w$ entre 400-1500 g·mol$^{-1}$, y encontraron que conforme disminuye la masa molar de PEG mejoran las propiedades mecánicas y disminuye la $T_g$ [54]. Kulinski y colaboradores (2005) observaron separación de fases macroscópica en mezclas de PLA con un 20% en peso de PEG 200 ($M_n$ = 200 g mol$^{-1}$) y en 30% en peso de PEG 400 (400 g mol$^{-1}$) [110]. En conclusión, se obtienen mejoras significativas en la ductilidad del material a concentraciones de plastificante por encima del 10% en peso, mientras que mejoras en las propiedades mecánicas se han obtenido para ≈20% en peso de plastificante. No obstante, en el presente trabajo el desarrollo de los sistemas plastificados tienen como finalidad la aplicación al sector de envasado de alimentos, por lo tanto la posible migración de plastificantes al alimento quiere evitarse. Así mismo, se pretende un equilibrio entre las propiedades mecánicas y barrera al oxígeno.

## 4. Copolímeros y mezclas de polímeros

La copolimerización y el mezclado con otros polímeros y/o aditivos son los dos medios más empleados para modificar las propiedades físicas del PLA.

Una práctica común en la síntesis de materiales, que se utiliza para mejorar las propiedades físicas de los polímeros, es la polimerización simultánea de dos o más monómeros diferentes [111] obteniéndose cópolimeros [112, 113], los cuales han

adquirido una importancia relevante, debido a que los procesos de copolimerización permiten combinar las características de los diferentes monómeros, resultando materiales con excelentes prestaciones [113].

Los copolímeros pueden ser: (i) de cadena lineal, (ii) de injerto y (iii) entrecruzados. En los copolímeros de cadena lineal los dos monómeros se distribuyen a lo largo de la misma cadena de una forma determinada (al azar, en secuencias o en bloques)[112]. En los copolímeros de injerto, sobre puntos específicos con alta reactividad de una cadena de polímero ya formada, se hace crecer una ramificación lateral de otro monómero [113]. En los copolímeros entrecruzados, uno de los monómeros tienen una funcionalidad mayor que dos dando lugar a estructuras ramificadas tridimensionales (geles) [112].

Mediante la manipulación de la arquitectura de la molécula, la secuencia de monómeros y la composición se pueden mejorar distintas características de los copolímeros, como las propiedades de tracción y de impacto [28]. Así mismo, la copolimerización permite mejorar las propiedades de barrera de un determinado polímero mezclándolo con otro que sea menos permeable. De esta manera, el copolímero puede presentar propiedades de ambos polímeros o intermedias entre ellos, aunque muchas veces el producto final presenta propiedades totalmente diferentes a las de los homopolímeros correspondientes [112], representando un poderoso medio para la obtención de materiales poliméricos con propiedades que resultan inalcanzables por los homopolímeros [28].

La composición es el factor más importante que determina las propiedades de un copolímero, es decir, la proporción relativa y la disposición de los comonómeros que lo constituyen. Por lo tanto, la composición final depende de la concentración de cada uno en la mezcla de alimentación y de su reactividad relativa [112].

La copolimerización del PLA puede llevarse a cabo ya sea a través de policondensación de ácido láctico con otros monómeros (o segmentos de polímero) o bien por copolimerización por apertura de anillo (ROC) de lactida con otros monómeros cíclicos (o segmentos de polímero). Siendo ésta última la copolimerización más utilizada para mejorar la tenacidad o flexibilidad del PLA, debido a que permite un control más preciso de la química y permite obtener copolímeros de mayor peso molecular [28].

Los copolímeros de PLA con otros monómeros, como ácido glicólico y caprolactona, son utilizados para aplicaciones biomédicas, debido a su excelente biocompatibilidad y como vehículo para la liberación sostenida de diversos fármacos [7]. En aplicaciones alimentarias estos sistemas resultan atractivos para la liberación sostenida de agentes activos. Sin embargo, a pesar de esta cualidad y de que se pueden

obtener un amplio espectro de propiedades mecánicas del PLA mediante su copolimerización con otros homopolímeros, la copolimerización es actualmente económicamente inviable a escala industrial para aplicaciones alimentarias [28].

Otro método de combinar las características de los materiales es a través de el proceso de mezclado mecánico en fundido o *blending*. En una mezcla, siempre que los polímeros lo permitan, se funden ambos polímeros conjuntamente y se mezclan. Al enfriar, se obtiene un material que combina las características de ambos y que presenta una única fase homogénea, si existe miscibilidad entre los componentes.

Cuando los polímeros que constituyen la mezcla son inmiscibles se forma un sistema bifásico, donde uno de ellos actúa como fase matriz y el otro como fase dispersa. Cuando la mezcla es inmiscible generalmente se trata de mezclas con malas propiedades mecánicas, ya que la adhesión entre las dos fases no es buena. Es por ello que la compatibilidad entre ambos polímeros y sus proporciones son factores de fundamentel importancia a la hora de preparar mezclas. Cuando los polímeros son compatibles también se debe seleccionar las cantidades adecuadas, ya que para obtener una compatibilidad óptima entre los dos polímeros es necesario que uno de ellos sea la fase mayoritaria que marque el comportamiento de la mezcla y la adición del otro polímero sea en menores cantidades [113].

El mezclado se utiliza con mayor frecuencia a nivel industrial por la versatilidad que presentan las mezclas obtenidas, ya que se puede conseguir un abanico de propiedades muy amplio y, además, es un método más rápido y económico. Las mezclas de polímeros son muy investigadas para el PLA con la finalidad de modificar algunas propiedades según la aplicación final del producto, como pueden ser las características de permeabilidad, propiedades térmicas y mecánicas [29]. Así, en la última década las mezclas de PLA con otros polímeros biodegradables han cobrado especial interés para aplicaciones de envases alimentarios biodegradables.

En el presente trabajo se propone mezclar el PLA con un 25 % en peso de PHB para incrementar la cristalinidad del PLA y ampliar su uso como films de envasado de alimentos. Esta modificación constituye uno de los puntos básicos del presente trabajo de investigación y en el apartado 6 del presente capítulo se desarrolla con más detalle.

## 5. POLI(HIDROXIALCANOATOS), PHAs

Los poli(hidroxialcanoatos) (PHAs) son poliésteres producidos por numerosas bacterias en la naturaleza [3, 114] como reserva de energía y carbono [3]. Los PHAs son polímeros isotácticos, de elevada masa molar, semicristalinos [111] y algo más versátiles

con respecto a sus propiedades que el PLA [2]. Los productos hechos de PHAs pueden ser compostados después de su utilización y se transforman en agua y $CO_2$ por un proceso de descomposición oxidativo mediado por la acción catabólica de diversos microorganismos [2]. Muchos PHAs además de biodegradables son biocompatibles, debido a que los productos de degradación son 3-hidroxiácidos, que se encuentran naturalmente en los animales. Procedente de la polimerización del monómero de 3-hidroxibutirato, el homopolímero de poli(3-hidroxibutirato) (PHB) es el PHA más simple [115] y más conocido [3, 116] y presenta propiedades similares al PP pero es algo más rígido y quebradizo [68]. Por esta razón, es también común encontrar el copolímero de PHB y poli(hidroxivalerato) (PHV), conocido como poli(hidroxibutirato-co-hidroxivalerato) (PHBV) [3], debido a que la copolimerización con hidroxivalerato (HV) permite ajustar las propiedades del material de PHB mediante la disminución de la cristalinidad y la temperatura de fusión [115], pero su precio es bastante elevado [68]. Sin embargo, el proceso de recuperación, es decir, los pasos de extracción y purificación, es decisivo para obtener un PHA de alta pureza y, a menudo explica por qué tales polímeros siguen siendo caros [33].

## 5.1. Poli (hidroxibutirato), PHB

El PHB es un polímero altamente cristalino, producido por una amplia variedad de bacterias [3, 11, 116]. Al obtenerse a partir de fuentes de carbono naturales renovables, como maíz [57], representa un material biodegradable prometedor para reemplazar a los plásticos sintéticos. Es utilizado en algunas aplicaciones prácticas como en la fabricación de envases plásticos biodegradables [83]. Sin embargo, no hay una gran fabricación de productos PHB, ya que tiene un mayor costo que los polímeros derivados del petróleo, es un plástico relativamente rígido y frágil y presenta una baja resistencia a la degradación térmica lo que limita su procesado [11, 116].

### 5.1.1. Estructura química del PHB

El PHB (Figura II.15) es el poliéster de cadena más corta dentro de la familia de los PHAs, es ópticamente activo y presenta un centro quiral [117]. Tanto el PHB como los poliésteres naturales presentan la misma configuración para el centro quiral, el cual se encuentra en la posición 3. Esta posición es muy importante, tanto para sus propiedades físicas como para las actividades de las enzimas implicadas en su biosíntesis y en su biodegradación [117].

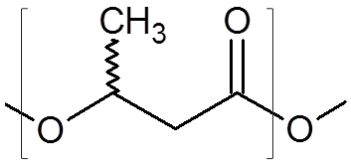


**Figura II.15.** Unidad repetitiva del PHB

### 5.1.2. Síntesis de PHB

El PHB es un producto polimérico de almacenamiento intracelular de una amplia variedad de bacterias [3, 11, 116], incluyendo bacterias Gram-positivas y Gram-negativas. Los gránulos intracelulares de PHB sirven como reserva de energía y de carbono [30, 117]. El polímero es producido por las bacterias en respuesta a una limitación de nutrientes en el medio [30, 117], con el objetivo de evitar la inanición si un elemento esencial deja de estar disponible [116, 117]. El PHB es ideal como un polímero de almacenamiento de carbono ya que es insoluble en agua, químicamente y osmóticamente inerte, y puede ser fácilmente reconvertido a ácido acético mediante una serie de reacciones enzimáticas dentro de la célula [117]. El PHB se produce a partir de acetil Coenzima A (CoA), derivada del ácido acético [117] mediante biosintésis en tres pasos catalizada por tres enzimas: 3-cetiolasa, acetil-CoA reductasa y PHA sintasa. La acetil-CoA es dimerizada (por la enzima 3-cetiolasa) en acetoacetil-CoA que posteriormente es convertida en el monómero R-3-Hidroxibutiril-CoA (por la acetoacetil-CoA reductasa), para finalmente producir PHB (por PHA sintasa) [116]. Este ciclo se activa debido a una deficiencia en nutrientes (generalmente fósforo, nitrógeno u oxígeno) que necesita la célula para promover la metabolización de acetil-CoA a través del ciclo del ácido tricarboxílico [117]. Cuando el nutriente limitante se repone, el PHB intracelular se degrada y el carbono resultante es utilizado por la bacteria para el crecimiento [116]. De esta manera, el PHB es un polímero natural que puede ser producido por síntesis bacteriana controlada [95]. Sin embargo, la síntesis de PHB en bacterias nativas o recombinantes a través de fermentación es un proceso bastante costoso [116].

La agricultura representa una alternativa prometedora para la producción de PHB a gran escala y a bajo costo. La síntesis del homopolímero PHB fue realizada por primera vez en plantas utilizando *Arabidopsis thaliana* como vector, en 1992. A través de ingeniería genética, los genes de las enzimas implicadas en la síntesis de PHB que se encuentran los tres juntos en un operón, se clonan y posteriormente se introduce el operón en una bacteria, como *Escherichia coli*. De esta manera, las bacterias genéticamente manipuladas que contienen el operón pueden expresar las tres enzimas y sintetizar PHB en grandes

cantidades a partir de una amplia gama de compuestos orgánicos [117]. Después de la fermentación, el PHB puede obtenerse a partir de la biomasa por extracción con disolventes orgánicos [3].

### 5.1.3. Procesado del PHB

En la actualidad, no existe una gran producción comercial de productos de PHB, ya que tiene un mayor costo que los polímeros derivados del petróleo [11]. El PHB dispone de un alto grado de cristalinidad, lo que le confiere una procesabilidad restringida [2]. Sin embargo, su baja resistencia térmica parece ser el problema más serio relacionado con su procesado [11]. Puesto que el punto de fusión del PHB ocurre alrededor de 170-180 °C [3, 11], la temperatura de proceso debería ser al menos 10 °C superior [11]. La diferencia entre la temperatura de descomposición (alrededor de 270 °C) y la temperatura de fusión proporciona una ventana pequeña de procesado para la tecnología de extrusión en estado fundido [2]. Además, entre 180 °C y 200 °C puede ocurrir una escisión de la cadena polimérica, lo que resulta en una disminución de la masa molar [11]. Por estos motivos la temperatura de proceso de PHB debe ser rigurosamente controlada.

### 5.1.4. Propiedades de PHB

El PHB es un biopoliéster que presenta un alto grado de cristalinidad (80%) [2, 3]. Debido a su alta cristalinidad, el PHB es rígido y quebradizo, lo que resulta en propiedades mecánicas muy pobres con un alargamiento mínimo a la rotura, limitando su campo de aplicación [11, 118]. El PHB presenta una coloración amarillenta y presenta menor transparencia que el PLA.

Se ha sugerido que el mecanismo de degradación térmica del PHB se produce casi exclusivamente mediante *cis*-eliminación, una escisión de la cadena al azar no radicalaria [47]. La *cis*-eliminación es siempre dominante en ésteres que tienen un enlace C-H activado, como es el caso del PHB, debido a que los hidrógenos de metileno se activan por la proximidad del grupo carboxilo incrementando su acidez [49] lo que implica un estado de transición de anillo de seis miembros y finalmente da lugar a la formación de ácido crotónico y oligómeros de PHB (Figura II.16)[47, 119].

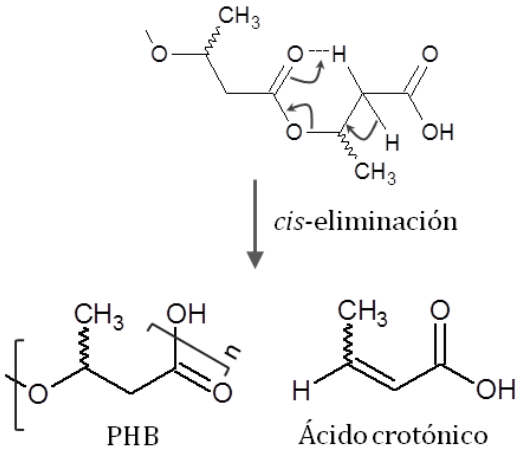


**Figura II.16.** Mecanismo de degradación térmica de PHB mediante *cis*-eliminación (Adaptado de Aoyagi y colaboradores (2002)[47])

El PHB presenta una variedad de propiedades apropiadas para el envasado alimentario, tales como biodegradabilidad, actividad óptica y buenas propiedades de barrera [120]. Por ejemplo, el PHB presenta mejores propiedades de barrera que el PET [121]. Al comparar el PHB con el polipropileno (PP), el PHB presenta algunas desventajas como son, su mayor rigidez y fragilidad (debido a su mayor cristalinidad), tiene una menor resistencia a los disolventes y una elongación a la rotura muy baja. Sin embargo, PHB presenta mayor resistencia a la luz ultra violeta (UV), mayor exclusión de oxígeno y, sobre todo, es biodegradable [2], siendo degradado por numerosos microorganismos (bacterias, hongos y algas) en diferentes ecosistemas [83].

Para facilitar la transformación, el PHB puede ser plastificado, como por ejemplo con esteres de citrato [3, 11]. También se puede modificar las propiedades del PHB mediante la interrupción de la matriz polimérica incorporando PHV [2] para dar lugar al PHBV.

Durante la degradación del PHB en condiciones de compostaje, causada por microorganismos, en primer lugar se observa la erosión de la superficie del polímero y posteriormente difunde gradualmente al interior [122]. El PHB presenta una velocidad de degradación en compostaje inferior a la del PLA, el cual es inicialmente hidrolizado.

## 6. Mezclas de PLA-PHB

Las mezclas de PLA-PHB han sido estudiadas por numerosos investigadores en los últimos años [94, 95, 123-127], tanto para mejorar las propiedades del PLA, como para mejorar las propiedades del PHB. Sin embargo, la miscibilidad entre estos dos

biopolímeros es bastante discutible. La miscibilidad entre el PLA y el PHB es dependiente de distintos factores como son: (i) la masa molar, (ii) la temperatura utilizada durante el proceso de mezclado y (iii) la proporción de cada biopolímero en la mezcla. Algunos estudios han indicado que el PLA muestra miscibilidad limitada o parcial con PHB de baja masa molar [94, 128]. Sin embargo, se considera que la temperatura tiene una mayor influencia y otros trabajos han demostrado que las mezclas de PLA-PHB son totalmente miscibles en estado fundido [127, 129]. En este sentido, Zhang y colaboradores (1996) encontraron que las mezclas de PLA-PHB preparadas a alta temperatura exhibieron mayor miscibilidad que las mismas mezclas preparadas con disolvente a temperatura ambiente [130]. Este efecto, de mayor miscibilidad entre el PLA y el PHB en su estado fundido, podría deberse a que ocurre una reacción de transesterificación entre el PLA y las cadenas de PHB a la temperatura de proceso [95, 130]. Además, la miscibilidad entre PLA y de PHB es fuertemente dependiente de su relación en la mezcla. En este sentido, Ni y colaboradores (2009) mezclaron oligómeros de 3-hidroxibutirato (OHB) con PLA y consiguieron mejorar la capacidad de cristalización del PLA, con cantidades de OHB inferiores a un 40% [125]. Estos mismos autores demostraron que cantidades superiores de OHB generaban una separación de fases, indicada por la presencia de dos $T_g$ [125]. Chang y Woo (2012), estudiaron el comportamiento de la cinética de cristalización de PHB mezclándolo con L-PLA y D-PLA (50:50), como agentes de nucleación biodegradables, y reportaron una mejora de la densidad de nucleación del PHB con un 10% en peso de cristalitos de D,L-PLA [124]. Por otra parte, se ha visto que la rigidez del PHB puede mejorarse significativamente mediante la mezcla con PLA [123]. Furukawa y colaboradores (2005) estudiaron mezclas de PLA-PHB preparadas por moldeo con disolvente en cloroformo con relaciones de mezcla 20/80, 40/60, 60/40, y 80/20 (PLA / PHB % en peso) e informaron que el PHB cristalizó como muy pequeñas esferulitas que pueden actuar como sitios de nucleación del PLA en la mezcla 20/80 [126]. Del mismo modo, Zhang y Thomas (2011) estudiaron mezclas de PLA-PHB en diferentes proporciones 100/0, 75/25, 50/50, 25/75 y 0/100 (PLA / PHB % en peso) mezcladas en el estado fundido y seguido de un proceso de moldeo por compresión para obtener films y encontraron que mezclando PLA-PHB en una proporción de 75/25 se consigue una óptima miscibilidad y una mejora de las propiedades de tracción con respecto al PLA puro, y atribuyeron este resultado al efecto de refuerzo que provocan los cristales de PHB en la matriz de PLA [95]. Más recientemente, Bartczak y colaboradores (2013) estudiaron la modificación de PLA mediante la adición de hasta un 20 % en peso de PHB y concluyeron que el PHB puede ser considerado como un efectivo modificador del PLA ya que aumenta su resistencia al impacto [94].

Como conclusión, la adición de un 25 % en peso de PHB a la matriz de PLA permite obtener un material en el cual el PHB cristaliza como pequeñas esferulitas que pueden actuar como agentes de nucleación capaces de recristalizar al PLA. Además, durante el mezclado en estado fundido ocurren reacciones de transesterificación entre el PLA y algunas cadenas de PHB favoreciendo la misciblidad entre ambos polímeros. Es por ello, que en la presente tesis doctoral se utilizaron dichas proporciones para preparar las mezclas de PLA-PHB con el principal objetivo de aumentar la cristalinidad del PLA y mejorar así sus propiedades de barrera, las cuales son de fundamental importancia en aplicaciones alimentarias.

## 7. NANOCOMPUESTOS

En las últimas décadas, ha habido un notable desarrollo en el campo de la nanotecnología en el sector de los plásticos debido a que permite modular las propiedades físico-químicas de los polímeros y mejorar su rendimiento mediante el desarrollo de nanocomposites. Un nanocomposite polimérico, es un material compuesto por dos o más fases en el cual el componente mayoritario es el polímero que forma una matriz continua en cuyo seno se dispersan pequeñas partículas. Dichas partículas tienen al menos una de las dimensiones en el orden de los nanómetros [7], conocidas como nanocargas o nanorefuerzos, y no suelen superar el 10 % en peso % en peso en total. Es preciso que la nanocarga y el polímero sean compatibles para poder obtener una dispersión homogénea de la nanocarga en la matriz polimérica. De esta manera, la interfase entre la matriz y la fase dispersa adquiere propiedades nuevas, que son intermedias a las correspondientes a ambas fases.

Los nanocompuestos cobran especial importancia en el envasado de alimentos debido a que se pueden obtener materiales con propiedades específicas mejoradas; como son las propiedades barrera, resistencia mecánica y estabilidad térmica [131], con respecto al polímero puro y a los composites convencionales. Los refuerzos para la matriz polimérica seleccionada pueden ser orgánicos o inorgánicos y con diferentes geometrías. Existen tres tipos de nanocompuestos dependientes de su aspecto, geometría y de lasdimensiones de las partículas nanométricas dispersas [132]; (i) nanopartículas isodimensionales (las 3 dimensiones son nanométricas)[7], como son las nanopartículas de sílice esféricas [132], (ii) nanotubos o nanocristales (*whiskers*) (con dos dimensiones nanométricas) las cuales forman una estructura alargada como los nanotubos de carbono, sepiolita y los nanocristales de celulosa [133], y (iii) nanopartículas en forma de láminas (con una dimensión en nanómetros) [7], como son las nanoarcillas (montmorillonita,

saponita). Éstas últimas a su vez se pueden presentar en tres formas: microcompuestos de fases separadas, nanocompuestos intercalados o nanocompuestos exfoliados [131].

Las nanocargas pueden ser clasificadas también según su origen (natural, semisintético o sintético) [134]. En este sentido, el uso de materia prima lignocelulósica para la obtención de nanocargas destinadas a reforzar materiales biopoliméricos ha cobrado especial interés en las últimas décadas, debido a que proporciona beneficios ambientales positivos con respecto a su eliminación final y al origen renovable, en comparación con cargas inorgánicas [135].

Para formulaciones de nanocompuestos de matriz biopolimérica donde interesa conservar las características de material biobasado y biodegradable se prefiere reforzar la matriz polimérica con nanocargas de origen renovable obteniendo un bio-nanocompuesto y se pretende que también sea biodegradable. Así, los bio-nanocompuestos son nanocompuestos en los cuales tanto la nanocarga como la matriz provienen de fuentes renovables.

## 7.1. Bio-nanocompuestos

Los bio-nanocompuestos representan una oportunidad de desarrollo de materiales sostenibles con un alto rendimiento, capaces de sustituir los materiales utilizados para envase y embalaje de plásticos convencionales, los cuales son a base de petróleo y en consecuencia no son biodegradables [80], para aplicaciones de requerimientos específicos. En particular para la aplicación de envases alimentarios, los bio-nanocompuestos muestran una gran promesa en la provisión de excelentes propiedades de barrera [80, 136], debido a que las cargas son capaces de retrasar la difusión de las moléculas haciendo que el camino sea más tortuoso [80].

De entre todos los bio-nanocompuestos los derivados de los polisacáridos se encuentran entre los más estudiados para su aplicación en envases [133] debido, entre otras cosas, a que se ha observado una correcta dispersión de las nanocargas mezclando los componentes en su estado fundido lo que permite adaptar el proceso a escala industrial [132]. Las nanocargas de origen ligninocelulósico se pueden obtener a partir de una amplia variedad de plantas, por lo que se pueden producir en todo el mundo a un menor costo que las nanocargas sintéticas y además se pueden obtener a partir de productos agrícolas no alimentarios [135].

## 7.2. Nanocristales de Celulosa

La estructura de las plantas se resume básicamente en fibras cristalinas de celulosa y una fase amorfa constituida por hemicelulosa y lignina [137]. Durante milenios, estos materiales lignocelulósicos naturales básicos se han utilizado en forma de fibras de madera y fibras de plantas por numerosas industrias para productos forestales, papel, textiles, etc. [138]. La celulosa es considerada como el polímero natural más abundante en la naturaleza [139-141]. Es una sustancia fibrosa dura, insoluble en agua, que juega un papel esencial en el mantenimiento de la estructura de las paredes celulares de las plantas [142]. En la Figura II.17 se muestra la estructura química de la celulosa con la unidad repetitiva de la celobiosa. La celulosa es un β-glucano, compuesto por moléculas de D-glucosa unidas en posición 1-4 (β) [139, 143]. Las cadenas poliméricas se conectan a través de fuerzas de van der Waals y enlaces de hidrógeno (intra e inter moleculares)[134] formando estructuras fibrosas [144] ordenadas jerárquicamente que dan lugar a nanofibras elementales (2-5 nm) [134]. Esta estructura hace que la celulosa sea un polímero relativamente estable, que no se disuelve fácilmente en disolventes acuosos típicos, no posee punto de fusión y presenta una alta rigidez axial [140]. Las microfibrillas están compuestas por las diferentes microestructuras jerárquicas de tamaño nanométrico con alta resistencia estructural y rigidez, siendo la parte cristalina conocida como nanocristales [144]. Cada monómero de celulosa tiene tres grupos hidroxilo con la capacidad para formar puentes de hidrógeno. Por lo tanto, estos grupos hidroxilos determinan la dirección en que se ordenan las estructuras cristalinas y también rigen las propiedades físicas más importantes de la celulosa [139], en particular, su (i) estructura microfibrilada multi-escala, (ii) la organización jerárquica (regiones cristalinas versus regiones amorfas), y (iii) la naturaleza altamente cohesiva (con una temperatura de transición vítrea superior a su temperatura de degradación)[141].

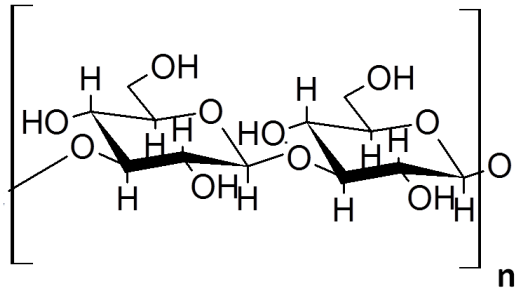


**Figura II.17.** Estructura química de la celulosa y unidad repetitiva de la celobiosa

La celulosa que se encuentra en la naturaleza se conoce como celulosa I o celulosa nativa y se produce en dos alomorfismos, $I_\alpha$ y $I_\beta$ [141, 142]. Las cadenas de celulosa se agregan en estructuras cristalinas repetidas para formar microfibrillas en la pared celular de las plantas, que a su vez se agregan en fibras macroscópicas más grandes. El alto rendimiento mecánico que confieren los materiales naturales extraídos de la agricultura es conferido por estas estructuras celulósicas jerárquicas [145]. Así mismo, esta estructura jerárquica es la que esencialmente se desensambla con el fin de generar las nanofibras de celulosa a partir de las plantas [140]. Las nanofibras de celulosa son mecánicamente más rígidas y por lo tanto adecuadas para el refuerzo de nanocompuestos. Es por ello que la segunda generación de materiales a base de celulosa se centra en la escala nanométrica y se encuentran representados por los nanocristales de celulosa (CNC)[138]. La celulosa nativa I es la principal fuente de nanocelulosa [141]. Los CNC son nanopartículas cristalinas en forma de varilla alargadas con un diámetro que oscila de 2 a 20 nm [144], obtenidos bajo condiciones controladas, que conducen a la formación de cristales individuales de alta pureza [141], que ofrecen nuevas características incluyendo una alta biodegradabilidad y una mayor uniformidad [138] y otras ventajas adicionales como son: baja densidad, superficie relativamente reactiva que es útil para injertar grupos específicos, fácil procesabilidad, alta resistencia y módulo específico [135]. Así, debido a que en general los bioplásticos presentan propiedades mecánicas bajas lo que dificulta su explotación práctica, los materiales celulósicos procedentes de recursos renovables han ganado especial importancia como potenciales elementos de refuerzo de biomateriales termoplásticos [137]. En este sentido, Fortunati y colaboradores (2012b, 2012c, 2013) han incorporado exitosamente nanocristales de celulosa (CNC) en la matriz de PLA [98, 146, 147]. Así mismo, Patricio y colaboradores (2013) han incorporado CNC a matrices de PHB [148], mostrando en ambos biopolímeros un incremento de las propiedades mecánicas superior que otros materiales de refuerzo. Por otra parte, la incorporación de CNC permite la reducción de la cantidad de biopolímero en la formulación final.

### 7.2.1. Síntesis de nanocristales de celulosa

Los nanocristales de celulosa (CNC) pueden obtenerse a partir de fibras celulósicas extraídas prácticamente de cualquier fuente de celulosa renovables como por ejemplo: a partir de algodón [149], cáñamo, sisal, palma, pulpa de madera blanda y pulpa de madera dura [142], lino [150] y celulosa bacteriana [151], entre otros. Por lo tanto, los CNC pueden obtenerse también a partir de celulosa microcristalina (MCC), que presenta

dimensiones en el orden de 10 a 50 µm. La MCC es un material disponible comercialmente, comúnmente utilizado para aplicaciones en la industria farmacéutica y alimentaria.

Dependiendo de la fuente de la que se obtienen, los nanocristales ofrecen una amplia variedad de relaciones de aspecto en cuanto a su longitud y diámetro (longitud / diámetro, L/D), desde nanopartículas con una relación L/D de 1 a aproximadamente 100.

Se pueden obtener distintos tipos de nanocargas de celulosa: (i) nanocristales de celulosa (cellulose nanocristals, CNC) a través de la disociación transversal de las partes amorfas presentes a lo largo de su eje produciendo nanopartículas en forma de varillas, libres de defectos (zonas amorfas) [134]; (ii) celulosa nanofibrilada (cellulose nanofibrillated, CNF) la cual se obtiene a partir de la delaminación lateral de haces de fibrillas elementales [134] mediante la combinación de tratamiento mecánico y un tratamiento químico o enzimático [138]; y (iii) nanocristales de celulosa bacteriana (bacterial cellulose nanocristals, BCNC) que se obtienen por bio-síntesis mediada por bacterias [134] de la familia *Gluconoacetobacter xylinius* a partir de glucosa [138].

La obtención de CNC a partir de materiales a base de celulosa ocurre en dos etapas. La primera es un pre-tratamiento del material de origen, en el caso de madera y plantas implica la eliminación completa o parcial de materiales de la matriz (hemicelulosas, lignina, etc.) y el aislamiento de las fibras celulósicas [138]. El segundo es un tratamiento químico controlado de las fibras celulósicas obtenidas que permita eliminar las regiones amorfas del polímero de celulosa [138] obteniendo una suspensión de CNC que presenta un comportamiento coloidal [135].

El principal proceso para la obtención de regiones cristalinas celulósicas a partir de las fibras, en su forma de nanocristales, se basa en una fuerte hidrólisis ácida [139, 141, 152] en condiciones estrictamente controladas de temperatura, agitación y tiempo [141]. Las regiones amorfas de la celulosa que rodean las microfibrillas son preferentemente hidrolizadas, mientras que las regiones cristalinas las cuales tienen mayor resistencia al ataque ácido permanecen intactas [135, 142]. Esto es debido a que la cinética de hidrólisis es más rápida en los dominios amorfos que en los cristalinos [135]. Los CNC obtenidos tienen morfología y cristalinidad similar a la celulosa de las fibras originarias [134]. Sin embargo, las condiciones de hidrólisis y el tipo de ácido utilizado afectan a las propiedades de los nanocristales finales [144].

Si bien los protocolos de extracción de CNC deben adaptarse a cada fuente de celulosa, la obtención de CNC mediante el uso de ácido sulfúrico ($H_2SO_4$) durante la hidrólisis ácida conduce a suspensiones acuosas más estables que las preparadas por otros ácidos [135, 140, 144] como por ejemplo ácido clorhídrico (HCl), el cual posee una capacidad de dispersión limitada en medios acuosos y las suspensiones coloidales de CNC

tienden a flocular [134, 142], debido a que los CNC no poseen la superficie funcionalizada (cargada iónicamente) [140]. En cambio, cuando se utiliza $H_2SO_4$ para la hidrólisis, los grupos sulfatos reaccionan con los grupos hidroxilo superficiales de celulosa lo que generan una superficie funcionalizada cargada negativamente, los grupos sulfatos se repelen lo que permite dispersiones homogéneas en agua [134, 142, 152, 153] y es por ello que es el ácido comúnmente utilizado para la síntesis de CNC. Sin embargo, la introducción de estos grupos sulfato cargados, compromete la termoestabilidad de los nanocristales, especialmente durante el proceso de obtención de nanocompuestos, donde la temperatura es elevada [98] y se encuentran en ausencia de disolvente [134].

La concentración de $H_2SO_4$ utilizada también es un factor a tener en cuenta. Una concentración baja puede generar una hidrólisis parcial o insuficiente, lo que da lugar a partículas de mayor tamaño con menor área de superficie y por lo tanto una carga superficial inferior que favorecen la interacción partícula-partícula [152]. Mientras que, una concentración de $H_2SO_4$ mayor a 65 % en peso puede disolver la celulosa [154]. En este sentido, utilizando una concentración de $H_2SO_4$ de 64 % en peso se pueden obtener CNC con elevada cristalinidad [138].

Existen otros factores que influyen en las propiedades de los CNC resultantes como el tiempo y la temperatura de hidrólisis [135]. La temperatura puede variar desde temperatura ambiente hasta 70 °C y el tiempo de hidrólisis puede variar entre 30 min y 24 horas dependiendo de la temperatura utilizada [142]. En principio, se puede obtener nanocristales más cortos si el tiempo de reacción es más largo [144], sin embargo tiempos de digestión altos pueden conducir a la carbonización y el oscurecimiento del producto [136]. Así mismo, el tiempo de reacción es también fuertemente dependiente de la fuente de obtención de CNC. Se ha sugerido que 45 °C es una temperatura óptima de reacción para la concentración de $H_2SO_4$ de 64 % en peso [143, 152].

Para mejorar la dispersión de los nanocristales la hidrólisis puede ser asistida por ultrasonidos [138], o bien la suspensión obtenida es posteriormente sometida a ultrasonidos controlando la temperatura para evitar sobrecalentamiento, que puede causar desulfatación de los grupos sulfato en la celulosa [152].

La Figura II.18 muestra un esquema de la obtención de CNC mediante hidrólisis ácida (a 45 °C durante 30 min) a partir de MCC siguiendo el procedimiento indicado por Fortunati y colaboradores (2012b) [98]. Después de la hidrólisis, para neutralizar la suspensión resultante se diluye con agua, se lava sucesivas veces y se dializa con agua ultrapura [98, 141, 142]. A la suspensión de celulosa se añade una resina de intercambio iónico para asegurar que todos los materiales iónicos se eliminan excepto los iones $H^+$ asociados con los grupos sulfato en las superficies de CNC [98]. Posteriormente, la

suspensión se somete a ultrasonidos con la finalidad de obtener nanocristales de dimensiones coloidales [143]. La suspensión se lleva a pH 9 con la finalidad de mejorar la estabilidad térmica de los CNC [98]. Finalmente, la suspensión es liofilizada para obtener los CNC en polvo y poder procesarlo con la tecnología de proceso de los termoplásticos comunes.

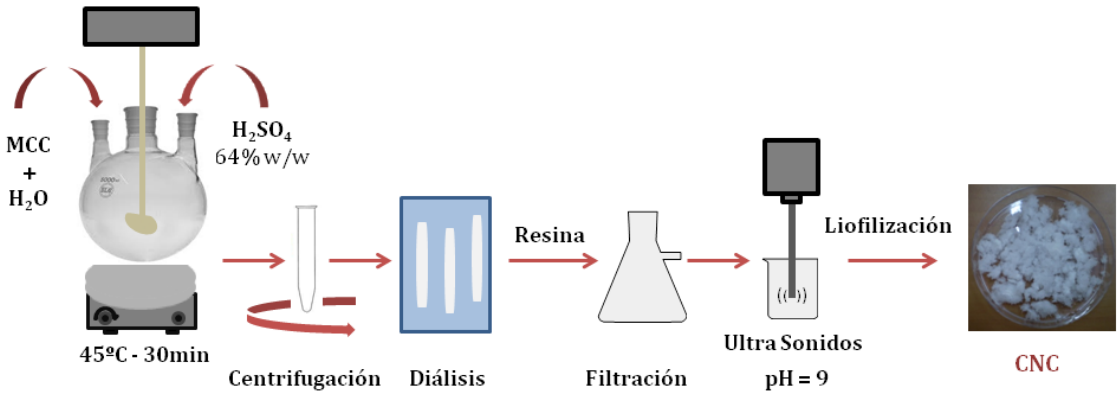


**Figura II.18.** Esquema de obtención de CNC a partir de MCC

Sin embargo, el principal problema asociado con la fabricación de nanocompuestos de celulosa eficaces está relacionada con su dispersión homogénea dentro de una matriz polimérica [140]. Por lo tanto los CNC, a pesar de todas las propiedades atractivas que presentan, se utilizan sólo en un grado limitado en la práctica industrial debido a las dificultades asociadas con las interacciones de su superficie. La naturaleza polar e hidrofílica inherente de los polisacáridos convierte a los medios acuosos en los ideales para las suspensiones de nanopartículas [87]. Esto se encuentra en contraposición con las características no polares de la mayoría de los termoplásticos, que no pueden ser disueltos en medios acuosos, dificultando la utilización de CNC como refuerzos de termoplásticos ya que dan como resultando materiales compuestos ineficientes [135]. Por otra parte, durante el secado de los nanocristales de celulosa se puede producir una aglomeración irreversible como resultado de fuertes enlaces de hidrógeno establecidos a través del gran número de grupos hidroxilo presentes en su superficie [134]. Por lo tanto, la liofilización, representa una etapa crítica para la obtención de CNC con dispersión uniforme [98, 155].

## 8. INCORPORACIÓN DE NANOCRISTALES DE CELULOSA EN LA MATRIZ DE PLA

El mayor desafío en la incorporación de nanocristales de celulosa en la matriz de PLA es la obtención de una buena dispersión de las nanopartículas en la matriz [134]. La

dispersión homogénea de CNC en la matriz de PLA no es fácil de lograr [156] debido a su carácter hidrofílico [151]. Una estrategia para favorecer la dispersión de los CNC en la matriz de PLA, y por consiguiente las propiedades de la formulación final, es la modificación de la superficie de los CNC. Así mismo, la modificación de superficie puede mejorar otros aspectos específicos, tales como proporcionar una mayor adhesión y reducir la sensibilidad a la humedad [157]. Una manera, efectiva de favorecer la dispersión de los CNC en la matriz de PLA es mediante una modificación superficial como puede ser un tratamiento con silanos, para mejorar la dispersión de los CNC en solventes orgánicos y así poder mezclarlos con la matriz de PLA en solución [149]. Otra estrategia, es el uso de agentes tensioactivos, como por ejemplo ésteres de fosfato aniónicos [87, 98, 149, 152, 155], que modifican la superficie de los CNC (denominados CNC-s) permitiendo una mejor dispersión de los mismos [98]. La cantidad de tensioactivo debe controlarse, ya que un exceso puede producir una degradación significativa de la matriz de PLA en la temperatura de proceso [134].

En la Figura II.19 se muestran las suspensiones típicas de CNC (Figura II.19-a) y CNC-s (Figura II.19-b) obtenidas a partir de la hidrólisis ácida de MCC. Una suspensión de CNC es turbia y blanca, mientras que una suspensión de CNC-s es una suspensión translúcida, debido a que gran parte de las partículas de celulosa en la suspensión se encuentran por debajo del límite de la dispersión de la luz [155]. Las Figura II.19-c y Figura II.19-d muestran nanocristales de celulosa observados por microscopía electrónica de transmisión (TEM). Se puede observar la presencia de algunos CNC agregados (Figura II.19-c), mientras que los CNC-s se encuentran perfectamente individualizados (Figura II.19-d). Los CNC y CNC-s presentan dimensiones de nanocristales de celulosa en el rango de 100 a 300 nm de longitud y entre 5 a 10 nm de ancho [98, 149, 155, 158]. Además, la modificación superficial producida por el surfactante obstaculiza la unión de puente de hidrógeno entre los CNC-s durante la liofilización evitando su aglomeración durante este proceso [155]. Esta metodología permite obtener CNC-s funcionalizados los cuales presentan una buena dispersión en la matriz de PLA.

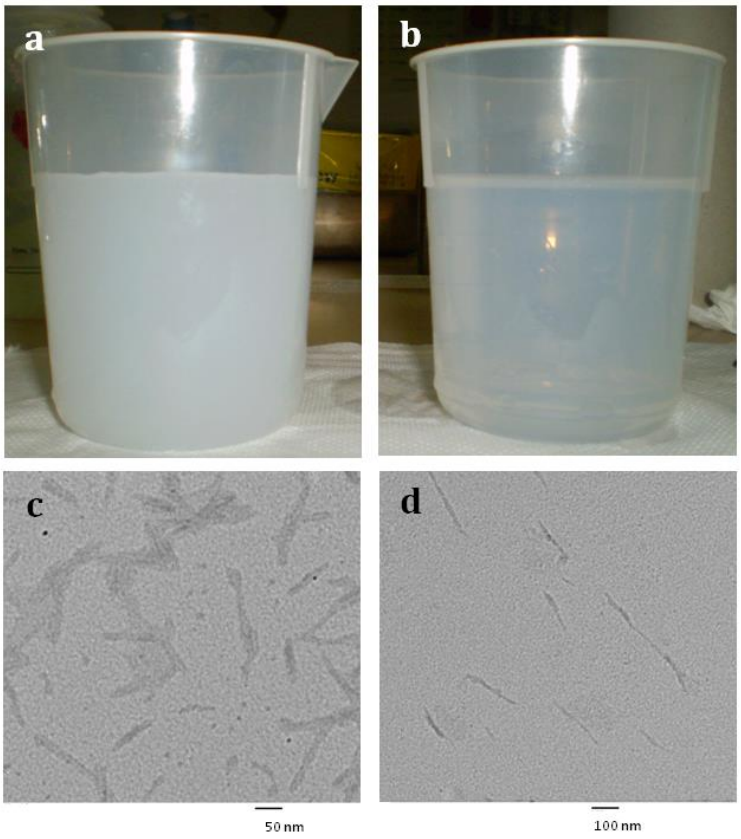


**Figura II.19.** Suspensiones de nanocristales de celulosa obtenidas por hidrolisis ácida: **a)** sin modificación superficial (CNC) y **b)** modificada con un surfactante (CNC-s). Imágenes TEM de suspensiones de: **c)** CNC (15.000 X) y **d)** CNC-s (10.000 X)

## 8.1. Propiedades de bio-nanocompuestos de PLA/CNC

Los CNC tienen origen renovable, pudiendo obtenerse a partir de numerosas fuentes disponibles en todo el mundo, y son biodegradables. Sin embargo, su origen bio y biodegradabilidad no son las únicas características positivas de los CNC como aditivos del PLA. Los CNC presentan una serie de propiedades intrínsecas atractivas para ser utilizados como nanorefuerzos de PLA como son sus dimensiones de nanoescala, área superficial, morfología única, baja densidad, alta resistencia específica y módulo de elasticidad, así como muy bajo coeficiente de expansión térmica [159].

La incorporación de CNC a la matriz de PLA produce un aumento de la cristalinidad de la formulación final, la cual se encuentra favorecida por la correcta dispersión de los CNC en la matriz de PLA, como es el caso de la modificación superficial de los nanocristales [98, 149]. Fortunati y colaboradores (2012b), desarrollaron film de PLA reforzados con CNC-s y encontraron que la nucleación de los CNC-s produce también una mejora de las propiedades mecánicas y térmicas con respecto al PLA puro y al PLA reforzado con CNC

(sin modificación superficial) [98]. Así mismo, la incorporación de CNC en la matriz de PLA genera una disminución a la transmisión de vapor de agua [136] y mejora las propiedades de barrera al oxígeno [136, 146] manteniendo una transparencia satisfactoria [19]. El PLA reforzado con CNC-s muestra efectos más pronunciados en cuanto a la mejora de las propiedades barrera al oxígeno [146], lo que resulta de especial interés en aplicaciones de envasado de alimentos.

## 9. INCORPORACIÓN DE ANTIOXIDANTES A LAS MATRICES POLIMÉRICAS

Para los alimentos sensibles a la oxidación resulta necesario retrasar este proceso y así extender su vida útil. Una manera de evitar la adición directa del antioxidante al alimento y permitir su comercialización como alimento libre de aditivos, es envasarlos en envases activos con propiedades antioxidantes.

Los antioxidantes son compuestos químicos capaces de reducir la oxidación de un sustrato al interceptar y reaccionar con los radicales libres a una velocidad mayor que el sustrato oxidable. Los antioxidantes se agregan a la matriz polimérica con un doble objetivo, proteger en una primera instancia al polímero durante el procesado y para extender la vida útil del alimento durante el servicio del material. En ambos casos los antioxidantes actúan mediante los mismos mecanismos de acción, el cual está condicionado por la estructura química del antioxidante seleccionado.

Los antioxidantes se dividen en antioxidantes primarios y antioxidantes secundarios. Los antioxidantes primarios (captadores de radicales) interrumpen la reacción de oxidación por combinación con los radicales libres que actúan en la propagación (R· y ROO·), ya sea como donantes de electrones e hidrógeno reduciendo ROO· a ROOH y aceptores de electrones para oxidar o atrapar R· en ausencia de oxigeno. Los más importantes son fenoles con impedimentos estéricos, donde el grupo reactivo es el OH (Figura II.20-a) y las aminas aromáticas secundarias donde el grupo NH dona un hidrogeno al radical carbono, oxigeno o al ROO· (Figura II.20-b), dando lugar a productos estables que pierde la capacidad de abstraer un nuevo hidrógeno.

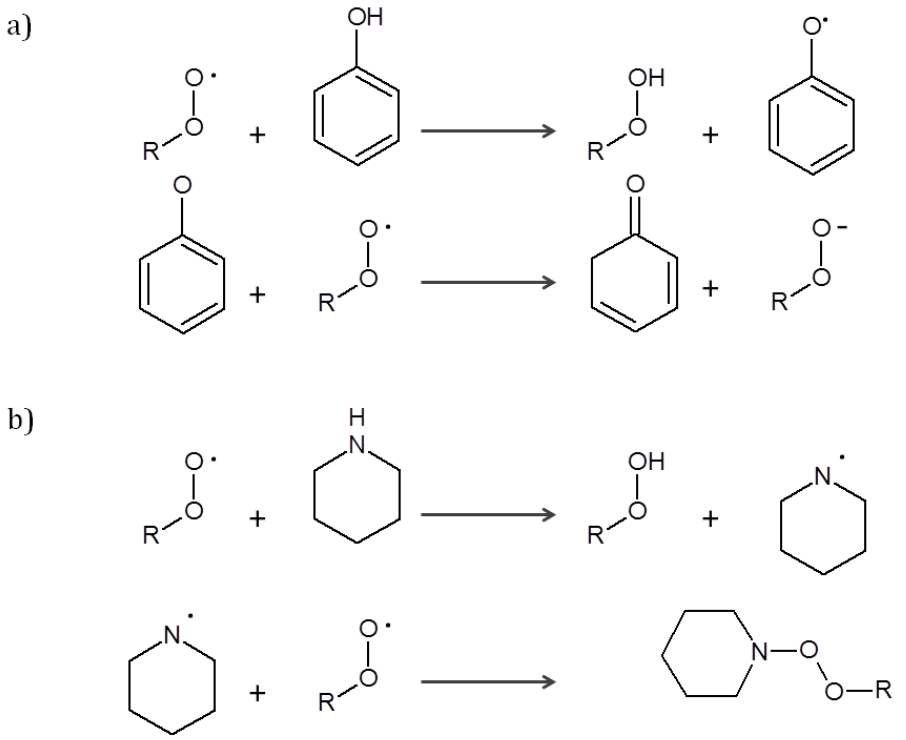


**Figura II.20.** Mecanismo de oxidación mediado por oxidantes primarios **a)** antioxidante fenólico y **b)** antioxidante amínico

Los antioxidantes secundarios actúan previniendo la introducción de grupos hidroperóxidos reduciéndolos a compuestos no radicalarios. En la Figura II.21 se muestra como ejemplo un antioxidante secundario, tris(2,4-di-tert-butilfenil) fosfito, añadido comúnmente para la protección del polímero durante el proceso.

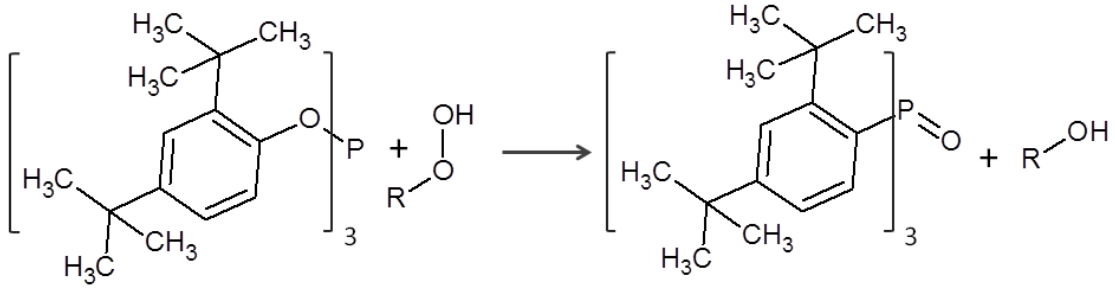

**Figura II.21.** Descomposición del grupo hidroperóxido por oxidación de tris(2,4-di-tert-butilfenil) fosfito.

Como se comentó anteriormente, el fenómeno de migración desde la matriz de PLA puede ser tomado como una ventaja a la hora de desarrollar envases antioxidantes. Para desarrollar un envase antioxidante, se requiere adicionar una sustancia antioxidante que

resista la temperatura de proceso y que posteriormente pueda ser liberado desde la matriz polimérica.

De esta manera, es necesario que el agente activo se intercambie entre el alimento y el envase con una cinética adecuada para que proteja al alimento eficientemente. Por otra parte, en la industria de los envases de alimentos, los aditivos sintéticos están siendo reemplazados por los conservantes naturales [6, 160-165]. Uno de los tipos de antioxidantes naturales más comunes son los compuestos fenólicos [162], son extraídos de fuentes de origen natural y tienen la capacidad de actuar de forma efectiva frente a los procesos de degradación oxidativa.

Los flavonoides, especialmente el grupo de las catequinas, han cobrado especial interés en aplicaciones de envasado activo de alimentos debido, no sólo por su efectividad frente a los procesos de degradación oxidativa de los alimentos, sino también por sus múltiples efectos biológicos [161, 162] y sus potenciales beneficios para la salud [161] por sus propiedades antiinflamatorias, antialérgicas, antivirales y anticancerígenas [166]. Las catequinas están presentes en el vino [166], el té, el cacao, en frutas (bayas, cítricos, manzanas, peras) y verduras [167, 168]. Sin embargo, sólo se encuentran en concentraciones elevadas en el té [167]. Así, la (+)-catequina y la (-)-epicatequina (Figura II.22), son los principales constituyentes activos del extracto de té verde [166, 169], el cual es muy conocido por las propiedades saludables que presenta, lo que le confiere a estos componentes una aceptación positiva por parte de los consumidores. Por otra parte, para su aplicación en la tecnología de envasado activo, la adición de (+)-catequina a la matriz polimérica presenta ventaja frente a otros antioxidantes naturales como los aceites esenciales, ya que es un compuesto que no es volátil, reduciéndose la pérdida de aditivo durante el procesado con el polímero [161]. Puede ocurrir la epimerización, es decir, la conversión de (+)-catequina a (-)-epicatequina bajo condiciones de calor [162]. Ambas, poseen actividad antioxidante similar debido a la semejanza de sus estructuras químicas [74].

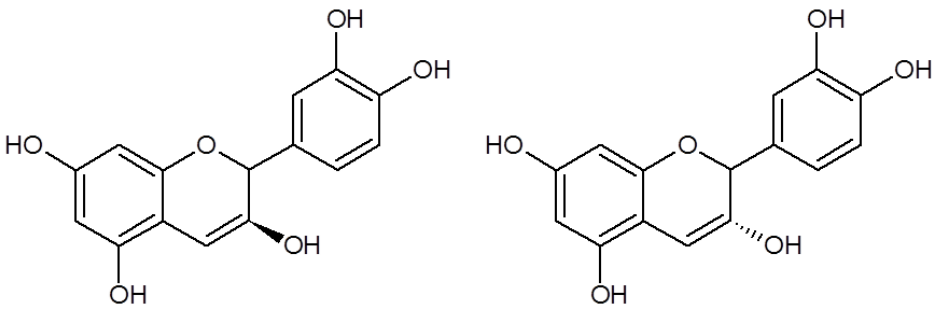


**Figura II.22.** Molécula de (+)-catequina y (-)-epicatequina

La estrategia del diseño de un sistema de envasado activo debe estar focalizada en obtener una capacidad de liberación efectiva del antioxidante desde la matriz del polímero. Debido a que se espera que el agente activo muestre una mayor afinidad por la matriz de polímero que por los productos alimenticios, se debe aumentar la movilidad de las cadenas del polímero para permitir la liberación del antioxidante hacia el alimento. Castro López y colaboradores (2012), reportaron que una forma efectiva para mejorar la liberación de la sustancias activas de la matriz polimérica es mediante la adición de plastificantes [170].

**REFERENCIAS**

[1] Tharanathan RN. Biodegradable films and composite coatings: Past, present and future. Trends in Food Science and Technology. 2003;14(3):71-78.

[2] Koller M, Salerno A, Dias M, Reiterer A, Braunegg G. Modern Biotechnological Polymer Synthesis: A Review. Food Technology and Biotechnology. 2010;48(3):255-269.

[3] Averous L. Biodegradable multiphase systems based on plasticized starch: A review. Journal of Macromolecular Science-Polymer Reviews. 2004;C44(3):231-274.

[4] Castro López MdM. Estudio del comportamiento de antioxidantes naturales adicionados a poliolefinas en aplicaciones industriales: Univerisidad de A Coruña; 2013.

[5] Sánchez-González L, Vargas M, González-Martínez C, Chiralt A, Cháfer M. Use of Essential Oils in Bioactive Edible Coatings: A Review. Food Engineering Reviews. 2011;3(1):1-16.

[6] Arrieta MP, Peltzer MA, López J, Garrigós MDC, Valente AJM, Jiménez A. Functional properties of sodium and calcium caseinate antimicrobial active films containing carvacrol. Journal of Food Engineering. 2014;121(1):94-101.

[7] Jamshidian M, Tehrany EA, Imran M, Jacquot M, Desobry S. Poly-Lactic Acid: Production, Applications, Nanocomposites, and Release Studies. Comprehensive Reviews in Food Science and Food Safety. 2010;9(5):552-571.

[8] Auras R, Harte B, Selke S. An Overview of Polylactides as Packaging Materials. Macromolecular Bioscience. 2004a; 4(9):864.

[9] Peltzer M, Navarro R, López J, Jiménez A. Evaluation of the melt stabilization performance of hydroxytyrosol (3,4-dihydroxy-phenylethanol) in polypropylene. Polymer Degradation and Stability. 2010;95(9):1636-1641.

[10] European Parliament and the Council of the European Union. on waste and repealing certain Directives. Official Journal of the European Union. 2008;Directive 2008/98/EC.

[11] Erceg M, Kovacic T, Klaric I. Thermal degradation of poly(3-hydroxybutyrate) plasticized with acetyl tributyl citrate. Polymer Degradation and Stability. 2005;90(2):313-318.

[12] European Commision. Green Paper. On an European Strategy on Plastic Waste in the Environment. 2013;123:1-20.

[13] Briassoulis D, Dejean C. Critical Review of Norms and Standards for Biodegradable Agricultural Plastics Part I (TM). Biodegradation in Soil. Journal of Polymers and the Environment. 2010;18(3):384-400.

[14] Guo X, Xiang D, Duan G, Mou P. A review of mechanochemistry applications in waste management. Waste Management. 2010;30(1):4-10.

[15] Commision E. EC Nº 282/2008 on recycled plastic materials and articles intended to come into contact with foods and amending. Official Journal of the European Union. 2008.

[16] AENOR. Envases y embalajes. Requisitos de los envases y embalajes valorizables mediante compostaje y biodegradación. Programa de ensayo y criterios de evaluación para la aceptación final del envase o embalaje. 2001.

[17] European Committee for Standardization (CEN). 2010:ftp://ftp.cen.eu/CEN/Sectors/List/bio_basedproducts/BTWG209finalreport.pdf.

[18] Song JH, Murphy RJ, Narayan R, Davies GBH. Biodegradable and compostable alternatives to conventional plastics. Philosophical Transactions of the Royal Society B-Biological Sciences. 2009;364(1526):2127-2139.

[19] Armentano I, Bitinis N, Fortunati E, Mattioli S, Rescignano N, Verdejo R, et al. Multifunctional nanostructured PLA materials for packaging and tissue engineering. Progress in Polymer Science. 2013;38(10–11):1720-1747.

[20] European Bioplastic. http://en.european-bioplastics.org/market/.

[21] Drumright RE, Gruber PR, Henton DE. Polylactic acid technology. Advanced Materials. 2000;12(23):1841-1846.

[22] Martino VP, Jimenez A, Ruseckaite RA, Averous L. Structure and properties of clay nano-biocomposites based on poly(lactic acid) plasticized with polyadipates. Polymers for Advanced Technologies. 2011;22(12):2206-2213.

[23] Hwang SW, Shim JK, selke SEM, Soto-Valdez H, Matuana L, Rubino M, et al. Poly(L-lactic acid) with added a-tocopherol and resveratrol: optical, physical, thermal and mechanical properties. Polymer International. 2012;61(3):418-425.

[24] Badia JD, Stromberg E, Ribes-Greus A, Karlsson S. Assessing the MALDI-TOF MS sample preparation procedure to analyze the influence of thermo-oxidative ageing and thermo-mechanical degradation on poly (Lactide). European Polymer Journal. 2011;47(7):1416-1428.

[25] Conn RE. Safety assessment of polylactide (PLA) for use as a food-contact polymer. Food and Chemical Toxicology. 1995;33(4):273-283.

[26] Auras R, Harte B, Selke S. Polylactides. A new era of biodegradable polymers for packaging application. Annual Technical Conference - ANTEC 2005a;Conference Proceedings, 8:320-324.

[27] Arrieta MP, Parres-García FJ, López-Martínez J, Navarro-Vidal R, Ferrandiz S. Pyrolysis of bioplastic waste: Obtained products from Poly(Lactic acid)(PLA). DYNA. 2012a;87(4):395-399.

[28] Liu H, Zhang J. Research progress in toughening modification of poly(lactic acid). 2011;49(15):1051- 1083.

[29] Sodergard A, Stolt M. Properties of lactic acid based polymers and their correlation with composition. Progress in Polymer Science. 2002;27(6):1123-1163.

[30] Tripathi AD, Srivastava SK. Kinetic Study of Biopolymer (PHB) Synthesis in Alcaligenes sp in Submerged Fermentation Process Using TEM. Journal of Polymers and the Environment. 2011;19(3):732-738.

[31] Vink ETH, Rábago KR, Glassner DA, Gruber PR. Applications of life cycle assessment to NatureWorks™ polylactide (PLA) production. Polymer Degradation and Stability. 2003;80(3):403-419.

[32] Sinclair RG. The case for polylactic acid as a commodity packaging plastic. Journal of Macromolecular Science - Pure and Applied Chemistry. 1996;33(5):585-597.

[33] Bordes P, Pollet E, Avérous L. Nano-biocomposites: Biodegradable polyester/nanoclay systems. Progress in Polymer Science (Oxford). 2009;34(2):125-155.

[34] Carrasco F, Pages P, Gamez-Perez J, Santana OO, Maspoch ML. Processing of poly(lactic acid): Characterization of chemical structure, thermal stability and mechanical properties. Polymer Degradation and Stability. 2010;95(2):116-125.

[35] Inkinen S, Hakkarainen M, Albertsson A-C, Sodergard A. From Lactic Acid to Poly(lactic acid) (PLA): Characterization and Analysis of PLA and Its Precursors. Biomacromolecules. 2011;12(3):523-532.

[36] Velazquez-Infante JC. Relación estructura-propiedades de films de nanocompuestos de PLA. Barcelona: Universitat Politècnica de Catalunya; 2012.

[37] Zhang J, Tashiro K, Tsuji H, Domb AJ. Disorder-to-order phase transition and multiple melting behavior of poly(L-lactide) investigated by simultaneous measurements of WAXD and DSC. Macromolecules. 2008;41(4):1352-1357.

[38] Sarasua JR, Arraiza AL, Balerdi P, Maiza I. Crystallization and thermal behaviour of optically pure polylactides and their blends. Journal of Materials Science. 2005;40(8):1855-1862.

[39] Kakuta M, Hirata M, Kimura Y. Stereoblock polylactides as high-performance bio-based polymers. Polymer Reviews. 2009;49(2):107-140.

[40] Burgos N, Martino VP, Jiménez A. Characterization and ageing study of poly(lactic acid) films plasticized with oligomeric lactic acid. Polymer Degradation and Stability. 2013;98(2):651-658.

[41] Carrasco F, Pérez-Maqueda LA, Sánchez-Jiménez PE, Perejón A, Santana OO, Maspoch ML. Enhanced general analytical equation for the kinetics of the thermal degradation of poly(lactic acid) driven by random scission. Polymer Testing. 2013;32(5):937-945.

[42] Tsuji H. Poly(lactide) stereocomplexes: Formation, structure, properties, degradation, and applications. Macromolecular Bioscience. 2005;5(7):569-597.

[43] Gamez-Perez J, Velazquez-Infante JC, Franco-Urquiza E, Pages P, Carrasco F, Santana OO, et al. Fracture behavior of quenched poly(lactic acid). Express Polymer Letters. 2011;5(1):82-91.

[44] Cailloux J, Santana OO, Franco-Urquiza E, Bou JJ, Carrasco F, Maspoch ML. Sheets of branched poly(lactic acid) obtained by one-step reactive extrusion-calendering process: physical aging and fracture behavior. Journal of Materials Science. 2014:1-15.

[45] Carlson D, Dubois P, Nie L, Narayan R. Free radical branching of polylactide by reactive extrusion. Polymer Engineering and Science. 1998;38(2):311-321.

[46] Yu H, Huang N, Wang C, Tang Z. Modeling of poly(L-lactide) thermal degradation: Theoretical prediction of molecular weight and polydispersity index. Journal of Applied Polymer Science. 2003;88(11):2557-2562.

[47] Aoyagi Y, Yamashita K, Doi Y. Thermal degradation of poly[(R)-3-hydroxybutyrate], poly[ε-caprolactone], and poly[(S)-lactide]. Polymer Degradation and Stability. 2002;76(1):53-59.

[48] Kopinke FD, Remmler M, Mackenzie K, Möder M, Wachsen O. Thermal decomposition of biodegradable polyesters - II. Poly(lactic acid). Polymer Degradation and Stability. 1996;53(3):329-342.

[49] Kopinke FD, Mackenzie K. Mechanistic aspects of the thermal degradation of poly(lactic acid) and poly(β-hydroxybutyric acid). Journal of Analytical and Applied Pyrolysis. 1997;40-41:43-53.

[50] Westphal C, Perrot C, Karlsson S. Py-GC/MS as a means to predict degree of degradation by giving microstructural changes modelled on LDPE and PLA. Polymer Degradation and Stability. 2001;73(2):281-287.

[51] Khabbaz F, Karlsson S, Albertsson AC. Py-GC/MS an effective technique to characterizing of degradation mechanism of poly (L-lactide) in the different environment. Journal of Applied Polymer Science. 2000;78(13):2369-2378.

[52] Nascimento L, Gamez-Perez J, Santana OO, Velasco JI, Maspoch ML, Franco-Urquiza E. Effect of the Recycling and Annealing on the Mechanical and Fracture Properties of Poly(Lactic Acid). Journal of Polymers and the Environment. 2010;18(4):654-660.

[53] Burgos N. Desarrollo de bionanocompuestos en base a poli(ácido láctico) y plastificantes de alta compatibilidad para el envasado de alimentos: University of Alicante; 2013.

[54] Martin O, Averous L. Poly(lactic acid): plasticization and properties of biodegradable multiphase systems. Polymer. 2001;42(14):6209-6219.

[55] Auras RA. Solubility of gases and vapors in polylactide polymers. 2007. p. 343-368.

[56] Auras RA, Singh SP, Singh JJ. Evaluation of oriented poly(lactide) polymers vs. existing PET and oriented PS for fresh food service containers. Packaging Technology and Science. 2005b;18(4):207-216.

[57] Courgneau C, Domenek S, Guinault A, Averous L, Ducruet V. Analysis of the Structure-Properties Relationships of Different Multiphase Systems Based on Plasticized Poly(Lactic Acid). Journal of Polymers and the Environment. 2011;19(2):362-371.

[58] Martino VP, Jimenez A, Ruseckaite RA. Processing and Characterization of Poly(lactic acid) Films Plasticized with Commercial Adipates. Journal of Applied Polymer Science. 2009a;112(4):2010-2018.

[59] Arrieta MP, Peltzer MA, López J, Garrigós MdC, Valente AJM, Jiménez A. Functional properties of sodium and calcium caseinate antimicrobial active films containing carvacrol. Journal of Food Engineering. 2014;121(0):94-101.

[60] Cocca M, Lorenzo MLD, Malinconico M, Frezza V. Influence of crystal polymorphism on mechanical and barrier properties of poly(l-lactic acid). European Polymer Journal. 2011;47(5):1073-1080.

[61] Guinault A, Sollogoub C, Ducruet V, Domenek S. Impact of crystallinity of poly(lactide) on helium and oxygen barrier properties. European Polymer Journal. 2012;48(4):779-788.

[62] Martucci JF, Ruseckaite RA. Tensile Properties, Barrier Properties, and Biodegradation in Soil of Compression-Molded Gelatin-Dialdehyde Starch Films. Journal of Applied Polymer Science. 2009;112(4):2166-2178.

[63] Food and Drog Administration (FDA). http://wwwaccessdatafdagov/scripts/cdrh/cfdocs/cfcfr/CFRSearchcfm?fr=1841061.

[64] Commission of the European Communities. relating to plastic materials and articles intended to come into contact with foodstuff. Official Journal of the European Communities; 2002.

[65] European Commision. on plastic materials and articles intended to come into contact with food. Official Journal of the European Communities; 2011.

[66] Dopico-García MS, Ares-Pernas A, González-Rodríguez MV, López-Vilariño JM, Abad-López MJ. Commercial biodegradable material for food contact: Methodology for assessment of service life. Polymer International. 2012;61(11):1648-1654.

[67] Stoffers NH, Störmer A, Bradley EL, Brandsch R, Cooper I, Linssen JPH, et al. Feasibility study for the development of certified reference materials for specific migration testing. Part 1: Initial migrant concentration and specific migration. Food Additives and Contaminants. 2004;21(12):1203-1216.

[68] Siracusa V, Rocculi P, Romani S, Rosa MD. Biodegradable polymers for food packaging: a review. Trends in Food Science and Technology. 2008;19(12):634-643.

[69] Martino VP, Ruseckaite RA, Jimenez A. Ageing of poly(lactic acid) films plasticized with commercial polyadipates. Polymer International. 2009b;58(4):437-444.

[70] Gómez-Estaca J, López-de-Dicastillo C, Hernández-Muñoz P, Catalá R, Gavara R. Advances in antioxidant active food packaging. Trends in Food Science and Technology. 2014;35(1):42-51.

[71] Jin T, Liu L, Zhang H, Hicks K. Antimicrobial activity of nisin incorporated in pectin and polylactic acid composite films against Listeria monocytogenes. International Journal of Food Science & Technology. 2009;44(2):322-329.

[72] Fortunati E, Armentano I, Iannoni A, Barbale M, Zaccheo S, Scavone M, et al. New multifunctional poly(lactide acid) composites: Mechanical, antibacterial, and degradation properties. Journal of Applied Polymer Science. 2012a;124(1):87-98.

[73] Manzanarez-López F, Soto-Valdez H, Auras R, Peralta E. Release of α-Tocopherol from Poly(lactic acid) films, and its effect on the oxidative stability of soybean oil. Journal of Food Engineering. 2011;104(4):508-517.

[74] Iñiguez-Franco F, Soto-Valdez H, Peralta E, Ayala-Zavala JF, Auras R, Gámez-Meza N. Antioxidant activity and diffusion of catechin and epicatechin from antioxidant active films made of poly(l-lactic acid). Journal of Agricultural and Food Chemistry. 2012;60(26):6515-6523.

[75] Ortiz-Vazquez H, Shin J, Soto-Valdez H, Auras R. Release of butylated hydroxytoluene (BHT) from Poly(lactic acid) films. Polymer Testing. 2011;30(5):463-471.

[76] Soto-Valdez H, Auras R, Peralta E. Fabrication of poly(lactic acid) films with resveratrol and the diffusion of resveratrol into ethanol. Journal of Applied Polymer Science. 2011;121(2):970-978.

[77] Introzzi L, Fuentes-Alventosa JM, Cozzolino CA, Trabattoni S, Tavazzi S, Bianchi CL, et al. "Wetting enhancer" pullulan coating for antifog packaging applications. ACS Applied Materials and Interfaces. 2012;4(7):3692-3700.

[78] Shah AA, Hasan F, Hameed A, Ahmed S. Biological degradation of plastics: A comprehensive review. Biotechnology Advances. 2008;26(3):246-265.

[79] Kale G, Auras R, Singh SP. Degradation of commercial biodegradable packages under real composting and ambient exposure conditions. Journal of Polymers and the Environment. 2006;14(3):317-334.

[80] Rhim JW, Park HM, Ha CS. Bio-nanocomposites for food packaging applications. Progress in Polymer Science. 2013;38(10-11):1629-1652.

[81] Jung JH, Ree M, Kim H. Acid- and base-catalyzed hydrolyses of aliphatic polycarbonates and polyesters. Catalysis Today. 2006;115(1–4):283-287.

[82] Lucas N, Bienaime C, Belloy C, Queneudec M, Silvestre F, Nava-Saucedo JE. Polymer biodegradation: Mechanisms and estimation techniques - A review. Chemosphere. 2008;73(4):429-442.

[83] Bucci DZ, Tavares LBB, Sell I. PHB packaging for the storage of food products. Polymer Testing. 2005;24(5):564-571.

[84] Kijchavengkul T, Auras R, Rubino M, Selke S, Ngouajio M, Fernandez RT. Biodegradation and hydrolysis rate of aliphatic aromatic polyester. Polymer Degradation and Stability. 2010;95(12):2641-2647.

[85] Chandra R, Rustgi R. Biodegradable polymers. Progress in Polymer Science (Oxford). 1998;23(7):1273-1335.

[86] Lemmouchi Y, Murariu M, Dos Santos AM, Amass AJ, Schacht E, Dubois P. Plasticization of poly(lactide) with blends of tributyl citrate and low molecular weight poly(D,L-lactide)-b-poly(ethylene glycol) copolymers. European Polymer Journal. 2009;45(10):2839-2848.

[87] Fortunati E, Rinaldi S, Peltzer M, Bloise N, Visai L, Armentano I, et al. Nano-biocomposite films with modified cellulose nanocrystals and synthesized silver nanoparticles. Carbohydrate Polymers. 2014;101(0):1122-1133.

[88] European Food Safety Authority. Scientific Opinion on the safety evaluation of the active substances, iron, polyethyleneglycol, disodium pyrophosphate, monosodium phosphate and sodium chloride for use in food contact materials. EFSA Journal. 2013;11(6):3245.

[89] European Food Safety Authority. Scientific Opinion on Flavouring Group: Aliphatic primary and secondary saturated and unsaturated alcohols, aldehydes, acetals, carboxylic acids and esters containing an additional oxygenated functional group

and lactones from chemical groups 9, 13 and 30.Evaluation 10, Revision 3 (FGE.10Rev3). EFSA Journal. 2012;10(3):2563.

[90] Auras R, Harte B, Selke S. Effect of water on the oxygen barrier properties of poly(ethylene terephthalate) and polylactide films. Journal of Applied Polymer Science. 2004b;92(3):1790-1803.

[91] Martucci JF, Ruseckaite RA. Three-layer sheets based on gelatin and poly(lactic acid), part 1: Preparation and properties. Journal of Applied Polymer Science. 2010;118(5):3102-3110.

[92] Rhim JW, Mohanty KA, Singh SP, Ng PKW. Preparation and properties of biodegradable multilayer films based on soy protein isolate and poly(lactide). Industrial and Engineering Chemistry Research. 2006;45(9):3059-3066.

[93] Cho SW, Gällstedt M, Hedenqvist MS. Properties of wheat gluten/poly(lactic acid) laminates. Journal of Agricultural and Food Chemistry. 2010;58(12):7344-7350.

[94] Bartczak Z, Galeski A, Kowalczuk M, Sobota M, Malinowski R. Tough blends of poly(lactide) and amorphous poly([R,S]-3-hydroxy butyrate) - Morphology and properties. European Polymer Journal. 2013;49(11):3630-3641.

[95] Zhang M, Thomas NL. Blending Polylactic Acid with Polyhydroxybutyrate: The Effect on Thermal, Mechanical, and Biodegradation Properties. Advances in Polymer Technology. 2011;30(2):67-79.

[96] Carrasco F, Gámez-Pérez J, Santana OO, Maspoch ML. Processing of poly(lactic acid)/organomontmorillonite nanocomposites: Microstructure, thermal stability and kinetics of the thermal decomposition. Chemical Engineering Journal. 2011;178:451-460.

[97] Fortunati E, Armentano I, Iannoni A, Kenny JM. Development and thermal behaviour of ternary PLA matrix composites. Polymer Degradation and Stability. 2010;95(11):2200-2206.

[98] Fortunati E, Armentano I, Zhou Q, Iannoni A, Saino E, Visai L, et al. Multifunctional bionanocomposite films of poly(lactic acid), cellulose nanocrystals and silver nanoparticles. Carbohydrate Polymers. 2012b;87(2):1596-1605.

[99] Mekonnen T, Mussone P, Khalil H, Bressler D. Progress in bio-based plastics and plasticizing modifications. Journal of Materials Chemistry A. 2013;1(43):13379-13398.

[100] Murariu M, Ferreira ADS, Alexandre M, Dubois P. Polylactide (PLA) designed with desired end-use properties: 1. PLA compositions with low molecular weight ester-like plasticizers and related performances. Polymers for Advanced Technologies. 2008;19(6):636-646.

[101] Bruins PF. Plasticizer Technology. London. : Reinhold Publishing Corporation; 1965. p. 248.

[102] Singh A, Kamal M. Synthesis and characterization of polylimonene: Polymer of an optically active terpene. Journal of Applied Polymer Science. 2012;125(2):1456-1459.

[103] Dias MV, de Medeiros HS, Soares NdFF, Melo NRd, Borges SV, Carneiro JdDS, et al. Development of low-density polyethylene films with lemon aroma. LWT - Food Science and Technology. 2013;50(1):167-171.

[104] Sánchez-González L, Cháfer M, González-Martínez C, Chiralt A, Desobry S. Study of the release of limonene present in chitosan films enriched with bergamot oil in food simulants. Journal of Food Engineering. 2011;105(1):138-143.

[105] Sánchez-González L, Cháfer M, Hernández M, Chiralt A, González-Martínez C. Antimicrobial activity of polysaccharide films containing essential oils. Food Control. 2011;22(8):1302-1310.

[106] Salazar R, Domenek S, Courgneau C, Ducruet V. Plasticization of poly(lactide) by sorption of volatile organic compounds at low concentration. Polymer Degradation and Stability. 2012;97(10):1871-1880.

[107] Labrecque LV, Kumar RA, Dave V, Gross RA, McCarthy SP. Citrate esters as plasticizers for poly(lactic acid). Journal of Applied Polymer Science. 1997;66(8):1507-1513.

[108] Coltelli M-B, Della Maggiore I, Bertold M, Signori F, Bronco S, Ciardelli F. Poly(lactic acid) properties as a consequence of poly(butylene adipate-co-terephthalate) blending and acetyl tributyl citrate plasticization. Journal of Applied Polymer Science. 2008;110(2):1250-1262.

[109] Baiardo M, Frisoni G, Scandola M, Rimelen M, Lips D, Ruffieux K, et al. Thermal and mechanical properties of plasticized poly(L-lactic acid). Journal of Applied Polymer Science. 2003;90(7):1731-1738.

[110] Kulinski Z, Piorkowska E. Crystallization, structure and properties of plasticized poly(L-lactide). Polymer. 2005;46(23):10290-10300.

[111] Gracida J, Alba J, Cardoso J, Perez-Guevara F. Studies of biodegradation of binary blends of poly(3-hydroxybutyrate-co-3-hydroxyvalerate) (PHBHV) with poly(2-hydroxyethylmetacrilate) (PHEMA). Polymer Degradation and Stability. 2004;83(2):247-253.

[112] Llorente Uceta MA, Horta Zubiaga A. Técnicas de Caracterización de Polímeros. Madrid: UNED; 1991.

[113] Balart R, López J, Sánchez L, Nadal A. Introducción a la ciencia e ingeniería de polímeros. Alcoy: Alfagràfic S.A; 2001.

[114] Corre Y-M, Bruzaud S, Audic J-L, Grohens Y. Morphology and functional properties of commercial polyhydroxyalkanoates: A comprehensive and comparative study. Polymer Testing. 2012;31(2):226-235.

[115] Bittmann B, Bouza R, Barral L, Diez J, Ramirez C. Poly(3-hydroxybutyrate-co-3-hydroxyvalerate)/clay nanocomposites for replacement of mineral oil based materials. Polymer Composites. 2013;34(7):1033-1040.

[116] Moire L, Rezzonico E, Poirier Y. Synthesis of novel biomaterials in plants. Journal of Plant Physiology. 2003;160(7):831-839.

[117] Lenz RW, Marchessault RH. Bacterial polyesters: Biosynthesis, biodegradable plastics and biotechnology. Biomacromolecules. 2005;6(1):1-8.

[118] Calvao PS, Chenal J-M, Gauthier C, Demarquette NR, Bogner A, Cavaille JY. Understanding the mechanical and biodegradation behaviour of poly(hydroxybutyrate)/rubber blends in relation to their morphology. Polymer International. 2012;61(3):434-441.

[119] Grassie N, Murray EJ, Holmes PA. The thermal degradation of poly(-(d)-β-hydroxybutyric acid): Part 3-The reaction mechanism. Polymer Degradation and Stability. 1984;6(3):127-134.

[120] Villegas M, Castro Vidaurre EF, Habert AC, Gottifredi JC. Sorption and pervaporation with poly(3-hydroxybutyrate) membranes: methanol/methyl tert-butyl ether mixtures. Journal of Membrane Science. 2011;367(1-2):103-109.

[121] Sanchez-Garcia MD, Gimenez E, Lagaron JM. Morphology and barrier properties of nanobiocomposites of poly(3-hydroxybutyrate) and layered silicates. Journal of Applied Polymer Science. 2008;108(5):2787-2801.

[122] Weng YX, Wang L, Zhang M, Wang XL, Wang YZ. Biodegradation behavior of P(3HB,4HB)/PLA blends in real soil environments. Polymer Testing. 2013;32(1):60-70.

[123] Vogel C, Siesler HW. Thermal degradation of poly(epsilon-caprolactone), poly(L-lactic acid) and their blends with poly(3-hydroxy-butyrate) studied by TGA/FT-IR spectroscopy. Macromolecular Symposia. 2008;265:183-194.

[124] Chang L, Woo EM. Crystallization of poly(3-hydroxybutyrate) with stereocomplexed polylactide as biodegradable nucleation agent. Polymer Engineering and Science. 2012;52(7):1413-1419.

[125] Ni C, Luo R, Xu K, Chen G-Q. Thermal and Crystallinity Property Studies of Poly (L-Lactic Acid) Blended with Oligomers of 3-Hydroxybutyrate or Dendrimers of

Hvdroxyalkanoic Acids. Journal of Applied Polymer Science. 2009;111(4):1720-1727.

[126] Furukawa T, Sato H, Murakami R, Zhang JM, Duan YX, Noda I, et al. Structure, dispersibility, and crystallinity of poly(hydroxybutyrate)/poly(L-lactic acid) blends studied by FT-IR microspectroscopy and differential scanning calorimetry. Macromolecules. 2005;38(15):6445-6454.

[127] Blümm E, Owen AJ. Miscibility, crystallization and melting of poly(3-hydroxybutyrate)/ poly(l-lactide) blends. Polymer. 1995;36(21):4077-4081.

[128] Hu Y, Sato H, Zhang J, Noda I, Ozaki Y. Crystallization behavior of poly(l-lactic acid) affected by the addition of a small amount of poly(3-hydroxybutyrate). Polymer. 2008;49(19):4204-4210.

[129] Focarete ML, Ceccorulli G, Scandola M, Kowalczuk M. Further evidence of crystallinity-induced biodegradation of synthetic atactic poly(3-hydroxybutyrate) by PHB-depolymerase A from Pseudomonas lemoignei. Blends of atactic poly(3-hydroxybutyrate) with crystalline polyesters. Macromolecules. 1998;31(24):8485-8492.

[130] Zhang L, Xiong C, Deng X. Miscibility, crystallization and morphology of poly(β-hydroxybutyrate)/poly(d,l-lactide) blends. Polymer. 1996;37(2):235-241.

[131] Arora A, Padua GW. Review: Nanocomposites in food packaging. Journal of Food Science. 2010;75(1):R43-R49.

[132] Chivrac F, Pollet E, Avérous L. Progress in nano-biocomposites based on polysaccharides and nanoclays. Materials Science and Engineering: R: Reports. 2009;67(1):1-17.

[133] Avérous L, Pollet E. Green Nano-Biocomposites. 2012. p. 1-11.

[134] Raquez JM, Habibi Y, Murariu M, Dubois P. Polylactide (PLA)-based nanocomposites. Progress in Polymer Science. 2013;38(10-11):1504-1542.

[135] Azizi Samir MAS, Alloin F, Dufresne A. Review of Recent Research into Cellulosic Whiskers, Their Properties and Their Application in Nanocomposite Field. Biomacromolecules. 2005;6(2):612-626.

[136] Sanchez-Garcia MD, Lagaron JM. On the use of plant cellulose nanowhiskers to enhance the barrier properties of polylactic acid. Cellulose. 2010;17(5):987-1004.

[137] Rayón E, Ferrandiz S, Rico MI, López J, Arrieta MP. Microstructure, mechanical and thermogravimetric characterization of cellulosic by-products obtained from the biomass seeds. International Journal of Food Properties. 2014;0(0):0.

[138] Brinchi L, Cotana F, Fortunati E, Kenny JM. Production of nanocrystalline cellulose from lignocellulosic biomass: Technology and applications. Carbohydrate Polymers. 2013;94(1):154-169.

[139] Siqueira G, Bras J, Dufresne A. Cellulosic bionanocomposites: A review of preparation, properties and applications. Polymers. 2010;2(4):728-765.

[140] Eichhorn SJ, Dufresne A, Aranguren M, Marcovich NE, Capadona JR, Rowan SJ, et al. Review: Current international research into cellulose nanofibres and nanocomposites. Journal of Materials Science. 2010;45(1):1-33.

[141] Lavoine N, Desloges I, Dufresne A, Bras J. Microfibrillated cellulose – Its barrier properties and applications in cellulosic materials: A review. Carbohydrate Polymers. 2012;90(2):735-764.

[142] Habibi Y, Lucia LA, Rojas OJ. Cellulose Nanocrystals: Chemistry, Self-Assembly, and Applications. Chemical Reviews. 2010;110(6):3479-3500.

[143] Cranston ED, Gray DG. Morphological and optical characterization of polyelectrolyte multilayers incorporating nanocrystalline cellulose. Biomacromolecules. 2006;7(9):2522-2530.

[144] Fernandes EM, Pires RA, Mano JF, Reis RL. Bionanocomposites from lignocellulosic resources: Properties, applications and future trends for their use in the biomedical field. Progress in Polymer Science. 2013;38(10-11):1415-1441.

[145] Rayón E, López J, Arrieta MP. Mechanical characterization of microlaminar structures extracted from cellulosic materials using nanoindentation technique. Cellulose Chemistry and Technology. 2013;47(5-6):345-351.

[146] Fortunati E, Peltzer M, Armentano I, Torre L, Jiménez A, Kenny JM. Effects of modified cellulose nanocrystals on the barrier and migration properties of PLA nano-biocomposites. Carbohydrate Polymers. 2012c;90(2):948-956.

[147] Bitinis N, Fortunati E, Verdejo R, Bras J, Kenny JM, Torre L, et al. Poly(lactic acid)/natural rubber/cellulose nanocrystal bionanocomposites. Part II: Properties evaluation. Carbohydrate Polymers. 2013;96(2):621-627.

[148] Patrício PSDO, Pereira FV, Dos Santos MC, De Souza PP, Roa JPB, Orefice RL. Increasing the elongation at break of polyhydroxybutyrate biopolymer: Effect of cellulose nanowhiskers on mechanical and thermal properties. Journal of Applied Polymer Science. 2013;127(5):3613-3621.

[149] Pei A, Zhou Q, Berglund LA. Functionalized cellulose nanocrystals as biobased nucleation agents in poly(l-lactide) (PLLA) - Crystallization and mechanical property effects. Composites Science and Technology. 2010;70(5):815-821.

[150] Fortunati E, Puglia D, Luzi F, Santulli C, Kenny JM, Torre L. Binary PVA bio-nanocomposites containing cellulose nanocrystals extracted from different natural sources: Part I. Carbohydrate Polymers. 2013;97(2):825-836.

[151] Martínez-Sanz M, Abdelwahab MA, Lopez-Rubio A, Lagaron JM, Chiellini E, Williams TG, et al. Incorporation of poly(glycidylmethacrylate) grafted bacterial cellulose nanowhiskers in poly(lactic acid) nanocomposites: Improved barrier and mechanical properties. European Polymer Journal. 2013;49(8):2062-2072.

[152] Bondeson D, Mathew A, Oksman K. Optimization of the isolation of nanocrystals from microcrystalline cellulose by acid hydrolysis. Cellulose. 2006;13(2):171-180.

[153] Aranguren MI, Marcovich NE, Salgueiro W, Somoza A. Effect of the nano-cellulose content on the properties of reinforced polyurethanes. A study using mechanical tests and positron anihilation spectroscopy. Polymer Testing. 2013;32(1):115-122.

[154] Roman M, Winter WT. Effect of sulfate groups from sulfuric acid hydrolysis on the thermal degradation behavior of bacterial cellulose. Biomacromolecules. 2004;5(5):1671-1677.

[155] Fortunati E, Armentano I, Zhou Q, Puglia D, Terenzi A, Berglund LA, et al. Microstructure and nonisothermal cold crystallization of PLA composites based on silver nanoparticles and nanocrystalline cellulose. Polymer Degradation and Stability. 2012d;97(10):2027-2036.

[156] Kose R, Kondo T. Size effects of cellulose nanofibers for enhancing the crystallization of poly(lactic acid). Journal of Applied Polymer Science. 2013;128(2):1200-1205.

[157] Satyanarayana KG, Arizaga GGC, Wypych F. Biodegradable composites based on lignocellulosic fibers-An overview. Progress in Polymer Science (Oxford). 2009;34(9):982-1021.

[158] Bitinis N, Verdejo R, Bras J, Fortunati E, Kenny JM, Torre L, et al. Poly(lactic acid)/natural rubber/cellulose nanocrystal bionanocomposites Part I. Processing and morphology. Carbohydrate Polymers. 2013;96(2):611-620.

[159] Pei A, Malho JM, Ruokolainen J, Zhou Q, Berglund LA. Strong nanocomposite reinforcement effects in polyurethane elastomer with low volume fraction of cellulose nanocrystals. Macromolecules. 2011;44(11):4422-4427.

[160] López De Dicastillo C, Castro-López MDM, Lasagabaster A, López-Vilariño JM, González-Rodríguez MV. Interaction and release of catechin from anhydride maleic-grafted polypropylene films. ACS Applied Materials and Interfaces. 2013;5(8):3281-3289.

[161] López de Dicastillo C, Castro-López MDM, López-Vilariño JM, González-Rodríguez MV. Immobilization of green tea extract on polypropylene films to control the

antioxidant activity in food packaging. Food Research International. 2013;53(1):522-528.

[162] Castro López MDM, De Dicastillo CL, Vilariño JML, Rodríguez MVG. Improving the capacity of polypropylene to be used in antioxidant active films: Incorporation of plasticizer and natural antioxidants. Journal of Agricultural and Food Chemistry. 2013;61(35):8462-8470.

[163] Castro-López MDM, López-Vilariño JM, González-Rodríguez MV. Analytical determination of flavonoids aimed to analysis of natural samples and active packaging applications. Food Chemistry. 2014;150:119-127.

[164] Arrieta MP, Peltzer M, Garrigós MC, A J. Structure and mechanical properties of sodium and calcium caseinate edible active films with carvacrol. Journal of Food Engineering. 2012c.

[165] Samper MD, Fages E, Fenollar O, Boronat T, Balart R. The potential of flavonoids as natural antioxidants and UV light stabilizers for polypropylene. Journal of Applied Polymer Science. 2013;129(4):1707-1716.

[166] Nijveldt RJ, Van Nood E, Van Hoorn DEC, Boelens PG, Van Norren K, Van Leeuwen PAM. Flavonoids: A review of probable mechanisms of action and potential applications. American Journal of Clinical Nutrition. 2001;74(4):418-425.

[167] Castro López MDM, Cela Pérez MC, Dopico García MS, López Vilariño JM, González Rodríguez MV, Barral Losada LF. Preparation, evaluation and characterization of quercetin-molecularly imprinted polymer for preconcentration and clean-up of catechins. Analytica Chimica Acta. 2012;721:68-78.

[168] Castro López MDM, Vilariño JML, Rodríguez MVG, Losada LFB. Development, validation and application of Micellar Electrokinetic Capillary Chromatography method for routine analysis of catechins, quercetin and thymol in natural samples. Microchemical Journal. 2011;99(2):461-469.

[169] Dopico-García MS, Castro-López MM, López-Vilariño JM, González-Rodríguez MV, Valentão P, Andrade PB, et al. Natural extracts as potential source of antioxidants to stabilize polyolefins. Journal of Applied Polymer Science. 2011;119(6):3553-3559.

[170] Castro López MDM, Dopico García S, Ares Pernas A, López Vilariño JM, González Rodríguez MV. Effect of PPG-PEG-PPG on the tocopherol-controlled release from films intended for food-packaging applications. Journal of Agricultural and Food Chemistry. 2012;60(33):8163-8170.

[171] UNE-EN ISO. Paper, board and pulps - Determination of dry matter content - Oven-drying method. 2008.

# III. RESULTS and DISCUSSION

The present work is focused on the development of bio-based and biodegradable PLA films for food packaging. PLA is currently considered a good alternative to some commodities in this application, but some properties, such as its low thermal stability, poor barrier properties and reduced stretchability are major issues limiting the use of PLA in the preparation of films for packaging. Therefore, some modifications in PLA formulations are required.

The modification strategy followed in this work consists of blending PLA with other biopolymer (PHB) and/or some additives in the melt state to get a practical approach to their suitability for processing at the industrial scale. In addition, some key aspects of the PLA degradation processes during PLA processing, use and further elimination are also studied. Section III of this document integrates and discuss all results, which are briefly described and in the paragraphs below.

Some aspects of the thermal degradation under pyrolysis conditions of PLA were initially studied by using a Py/GC-MS methodology with a complete analysis of the PLA thermal degradation products. The main results of this study are reported in Chapter III.1.

The use of a natural plasticizer, such as D-limonene, to obtain flexible PLA-based materials was studied in Chapter III.2. The objective of that chapter was also to give added value to D-limonene, from a low-grade by-product of citrus processing industries to a useful plasticizer. Subsequently, the addition of PHB, a highly crystalline bio-based polymer, to improve barrier properties in plasticized PLA was reported in Chapter III.3 where ternary PLA-PHB-Limonene systems were fully characterized with regards to the proposed applications in food packaging. In addition the disintegrability under composting conditions was suggested as the end of life option of the developed PLA-PHB-Limonene blends.

PLA-PHB blends were blended with two commercial plasticizers, PEG and ATBC, in Chapter III.4. The complete characterization of the obtained films was carried out in consideration of their thermal stability and intended use. Meanwhile, the changes in the plasticized PLA-PHB properties during composting were studied in Chapter III.5.

The introduction of a third nanocomponent to PLA-PHB blends was considered to improve some of their properties. Pristine cellulose nanocrystals (CNC) were synthesized from microcrystalline cellulose, and they were further modified in their surface by the addition of a surfactant agent (CNC-s). Processing conditions of these nano-biocomposites was optimized in Chapter III.6, where both CNC and CNC-s were blended with PLA-PHB systems improving the PLA-PHB processability and interaction between both polymers. These nano-biocomposites were processed into films and properties related with food

packaging were studied and reported in Chapter III.7 as well as their disintegration under composting conditions.

The use of PLA-PHB blends as support of antioxidants for active food packaging application was also considered. Chatechin was added to plasticized PLA-PHB blends and the release of this agent to food simulants was studied and reported in Chapter III.8 to get information about kinetics and the ability of these blends to reduce oxidation processes and to extend food shelf-life during storage. In the mean time, the potential material degradation during foodstuff storage was also evaluated.

## 1. Development of a novel pyrolysis-gas chromatography/mass spectrometry method for the analysis of poly(lactic acid) thermal degradation products

*Marina Patricia Arrieta[a,b], Francisco Parres[a], Juan López Martínez[a], Alfonso Jiménez[b]*

[a] Instituto de Tecnología de Materiales, Universitat Politècnica de València, Plaza Ferrándiz y Carbonell 1, 03801 Alcoy, Alicante Spain.

[b] Analytical Chemistry, Nutrition and Food Sciences Department, University of Alicante, P.O. Box 99, E-03080 Alicante, Spain.

**Journal of Analytical and Applied Pyrolysis**

**101: 150-155 (2013)**

**Abstract**

Thermal degradation of PLA is a complex process since it comprises many simultaneous reactions. The use of analytical techniques, such as differential scanning calorimetry (DSC) and thermogravimetry (TGA), yields useful information but a more sensitive analytical technique would be necessary to identify and quantify the PLA degradation products. In this work the thermal degradation of PLA at high temperatures was studied by using a pyrolyzer coupled to a gas chromatograph with mass spectrometry detection (Py-GC/MS). Pyrolysis conditions (temperature and time) were optimized in order to obtain an adequate chromatographic separation of the compounds formed during heating. The best resolution of chromatographic peaks was obtained by pyrolyzing the material from room temperature to 600 °C during 0.5 seconds. These conditions allowed identifying and quantifying the major compounds produced during the PLA thermal degradation in inert atmosphere. The strategy followed to select these operation parameters was by using sequential pyrolysis based on the adaptation of mathematical models. By application of this strategy it was demonstrated that PLA is degraded at high temperatures by following a non-linear behaviour. The application of logistic and Boltzmann models leads to good fittings to the experimental results, despite the Boltzmann model provided the best approach to calculate the time at which 50% of PLA was degraded. In conclusion, the Boltzmann method can be applied as a tool for simulating the PLA thermal degradation.

**Key words:** Poly(lactic acid), thermal degradation, Pyrolysis, Py-GC/MS, Logistic model, Boltzmann model.

## 1. INTRODUCTION

Biopolymers are becoming more and more interesting for many industrial sectors, such as packaging, automotive and many others since they are obtained from renewable resources and they are intrinsically biodegradable. Several biopolymers have been investigated as alternatives to non-degradable commodities to produce materials with similar properties to those of the common polymers [1].

Among all commercial biopolymers, poly(lactic acid) (PLA) is one of the most attractive and mainly used in many applications, being biocompatible and biodegradable [2]. Currently, PLA is used in food packaging industry for short shelf life products [3, 4]. Although the inherent biodegradable and compostable characteristics of PLA, the high growth on its production in the last years and application in the packaging market represents an upcoming new main source of polymer waste and new strategies for PLA waste management should be proposed [5]. Therefore, the fact that biodegradable polymers, and particularly PLA, should be considered as waste suggests that pyrolysis may offer an alternative option for waste treatment of biomass and biopolymers [6]. In this sense, PLA has a high potential energy content making it suitable for thermal processes with energy recovery. It has been reported that PLA waste is suitable to be used in pyrolysis facilities due to the high conversion efficiency of the polymer [7]. Therefore, pyrolysis of PLA may offer an alternative to this polymer waste management, while being economically and environmentally attractive [2]. The application of thermo-chemical operations to PLA must be carefully tackled, taking into account healthy and environmental issues and guaranteeing the right management of emitted gases [7]. Although some research work has been published on the PLA pyrolysis [8], only semi-quantitative results of the PLA degradation products were reported [8-10].

The study of polymers thermal degradation is especially important because it is relevant for their processing, characterization, potential applications and thermal recycling [9] as well as to guarantee their complete life cycle. The obtained products during thermal degradation depend on the selected conditions. Furthermore, degradation mechanisms of a particular polymer are dependent on its structure and they can follow different paths by the complexity of the polymeric chains and their breaking under heat [11]. In this sense, PLA thermal stability is often evaluated by thermogravimetric analysis (TGA) and differential scanning calorimetry (DSC). However these techniques lack on the identification of the thermal degradation products and pyrolysis coupled to gas chromatography/mass spectrometry (Py-GC/MS) is an alternative to identify these products in polymers and biodegradable polymers [12, 13]. To the best of our knowledge,

no methodologies for the quantification of PLA thermal degradation products by using Py-GC/MS have been already reported.

The main objective of this work was to develop a Py-GC/MS method for the simultaneous identification and quantification of PLA thermal degradation products by optimization Py-GC/MS experimental parameters: pyrolysis time and temperature. This methodology was successfully applied to PLA film samples by using sequential pyrolysis.

## 2. MATERIALS AND METHODS

### 2.1. Materials

Poly(lactic acid) (PLA 2002D, $M_n$ = 98000 Da, 4 wt% D-isomer) was supplied by NatureWorks (USA). Chloroform (99.8% purity) was obtained from Sigma Aldrich (Móstoles, Spain).

### 2.2. Films preparation

PLA was processed into films by compression molding following the methodology developed by Martino et al. (2009) [14]. Since PLA is highly hygroscopic [15], pellets were previously dried in a vacuum oven (60 °C for 6 h) and then moulded at 170 º C in a hot press (Mini C 3850, Caver, Inc. USA) at atmospheric pressure for 5 min until melting and then it was submitted to the following pressure cycles, 3 MPa for 1 min, 5 MPa for 1 min, and 10 MPa for 3 min, with the aim to eliminate the trapped air bubbles [16]. Film samples were then quenched at room temperature at atmospheric pressure.

### 2.3. Samples and standards preparation

1.0 g of PLA in pellets (for standards) or PLA films previously prepared as described (for sample solutions) were dissolved in 30 mL of chloroform. 10 µL of each solution were then put in the pyrolysis tube to get a complete solvent evaporation. Samples were prepared at the lowest quantity used for standard solutions (0.34 µg).

### 2.4. Py-GC/MS analyses

Samples were pyrolyzed with the use of a Pyroprobe 1000 instrument (CDS Analytical, Oxford, PA, USA), which was coupled to a gas chromatograph (6890N, Agilent

Technologies, Madrid, Spain) equipped with a 5973N mass selective detector (Agilent Technologies). The column used for the analysis was 30 m long HP-5 (0.25 mm thickness) using helium as carrier gas with a 50:1 split ratio. The GC oven was programmed at 40 °C for 2 min, followed by a stepped increase of 5 °C $min^{-1}$ to 200 °C, where it was held for 15 min, and then the temperature was increased by 20 °C $min^{-1}$ to 300 °C, where it was held for 5 min. The mass selective detector was programmed to detect masses between 30 and 650 amu. PLA samples were pyrolyzed at 600 °C for 0.5 s. Samples were repeatedly subjected to sequential pyrolysis under the same conditions up to 36 cycles were completed. The identification of PLA degraded products was confirmed by the characteristic fragmentation patterns observed in Py-GC/MS spectra or by comparison with literature mass spectra.

### 2.5. Validation

Linear relationships between the instrumental response and product concentrations were established by using least-squares regression (peak area vs. concentration, ranging from 0.34 to 1.36 μg). Intra-day repeatability of peak-areas expressed as relative standard deviations (RSD) were calculated. The method reproducibility was evaluated by the variation coefficients of five measurements of the same standard at different days (inter-day precision). The sensitivity and limit of detection (LOD) were estimated as three times the standard deviation provided by the relationship between the signal-to-noise ratio and the slope of the corresponding calibration curve, determined as the curve sensitivity [17].

### 2.6. Data statistical analysis and fitted models

The relationship between the cumulative mass of each degraded PLA and the pyrolysis time was fitted to two non-linear regression models based on the empirical use of the Logistic and Boltzmann equations in OriginPro 8.0 software. Firstly data were adjusted to a sigmoidal fit using a logistic type equation (Equation III.1. 1):

$$m = \frac{(mi - m_\infty)}{1 + (\frac{t}{t_0})^p} + m_\infty \qquad \textbf{Equation III.1. 1}$$

where $m_i$ and $m_\infty$ are the initial and final mass values at the initial and final asymptotes, *p is* the Hill slope coefficient [19], and $t_0$ is the time at which cumulative mass reaches the average value between $m_i$ and $m_\infty$, known as the half-maximal degradation.

Secondly, the Boltzmann equation (Equation III.1. 2) was fitted to the data.

$$m = \frac{(m_i - m_\infty)}{1 + e^{\frac{(t-t_0)}{d_t}}} + m_\infty \qquad \textbf{Equation III.1. 2}$$

where *dt* is a parameter that describes the shape of the curve between the upper and lower asymptotes [19].

## 3. RESULTS AND DISCUSSION

### 3.1. Optimization of pyrolysis conditions

The selection of experimental parameters is a critical issue for an accurate analysis of pyrolytic products. These parameters, in particular pyrolysis temperatures and times, are the key factors to achieve a good separation and further identification of compounds from degraded materials. Several pyrolysis conditions for PLA were proposed in previous works. Westphal et al. proposed pyrolysis of PLA for 2 s at 400 and 500 °C [20]. Kopinke and Mackenzie [21] proposed the study of PLA pyrolysis for 10 s at temperatures between 400 and 600 °C. Aoyagi et al. [9] also used 10 s but lower temperatures, i.e. 280 °C. In the present work different times and temperatures were evaluated. The starting pyrolysis time was 2 s and pyrolysis temperature was firstly selected at 400 °C, with further increases to 500 °C and 600 °C. Under these conditions, the high number of compounds involved in the PLA pyrolysis gave highly complex chromatograms. As expected, a higher number of reaction products was obtained when the pyrolysis temperature increased, resulting in poor separation of the degradation compounds. In order to improve the chromatographic resolution between the pyrolizates, the influence of pyrolysis time was also evaluated maintaining the pyrolysis temperature at 600 °C. It is known that the use of short pyrolysis times can improve the chromatographic separation of the pyrolyzates. Therefore, a reduction in pyrolysis time was considered 1.5, 1 and 0.5 s were used in tests. The best resolution was reached when the selected time was 0.5 s since good chromatographic separation between peaks was achieved (Figure III.1.1). Under these conditions, seven PLA pyrolizated products were detected and identified by getting the mass spectra of each main chromatographic peak (Table III.1. 4). It was observed that the

thermal degradation of PLA under these conditions showed a dominant series of signalswith *m/z = 56 + (n x 72)* in which *n* assumed values of 1, 2, 3 and 4. Figure III.1.1 shows the presence of two peaks (1 and 2) with very similar mass spectra (Figure III.1.2), where their main fragments were those with *m/z = 32, 43, 45* and *56*.

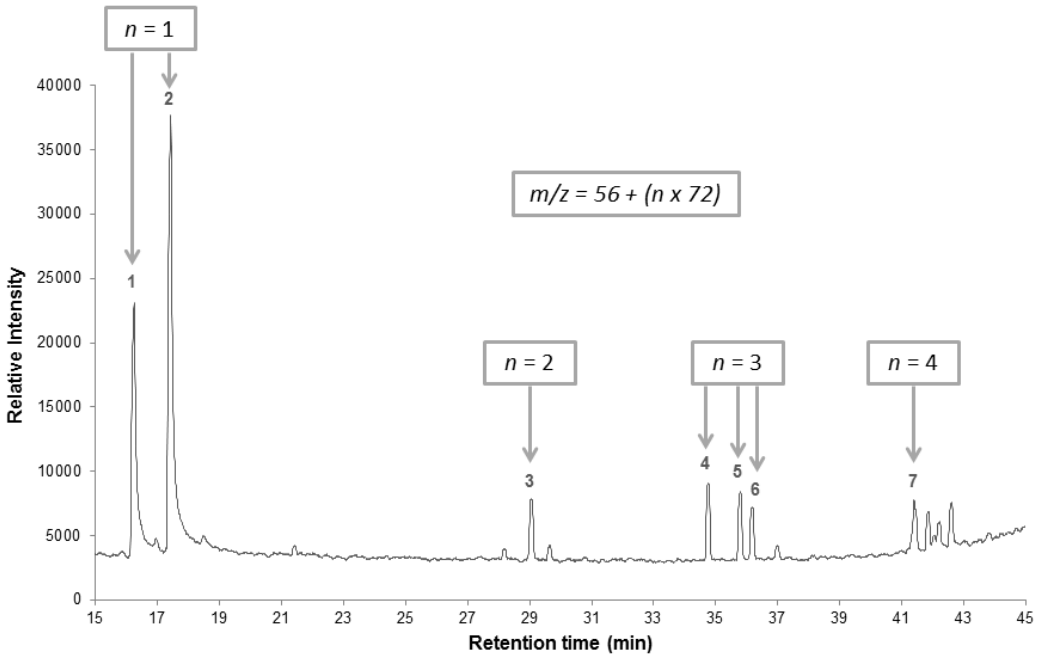


**Figure III.1.1.** Py-GC/MS chromatogram of PLA pyrolizates for 0.5 s at 600 °C.

**Table III.1. 4.** List of products formed during Py-GC-MS at 600°C for 0.5s

| Peak number | Retention Time (min) | Compound | Ion EI (*m/z*)[a] |
|---|---|---|---|
| 1 | 16.2 | Mesolactide | 32, 43, 45, **56** |
| 2 | 17.4 | Lactide | 32, 43, 45, **56** |
| 3 | 29.5 | Dimer: *56+(2 x 72)* | 32, 56, 100, **128**, 200 |
| 4 | 34.6 | Trimer: *56+(3 x 72)a* | 32, 56, 100, 128, **200**, 272 |
| 5 | 35.6 | Trimer: *56+(3 x 72)b* | 32, 56, 100, 128, **200**, 272 |
| 6 | 36.7 | Trimer: *56+(3 x 72)c* | 32, 56, 100, 128, **200**, 272 |
| 7 | 42.4 | Tetramer: *56+(4 x 72)* | 32, 56, 100, 128, **200**, 272, 344 |

[a] Main ion (base peak in bold) for electron ionization (EI).

These two peaks were assigned to mesolactide and lactide, respectively [8, 21, 22]. The groups of peaks appearing periodically at retention times higher than 20 minutes were assigned to higher cyclic lactide oligomers [8, 10, 22]. Three trimer peaks were

observed with very similar spectra. This is due to the fact that lactide oligomers are diastereomers derived from the asymmetric C atom [8, 21] in the lactic acid monomer, suggesting that the dominant reactions during pyrolysis of PLA followed an intramolecular *trans* esterification [10, 20].

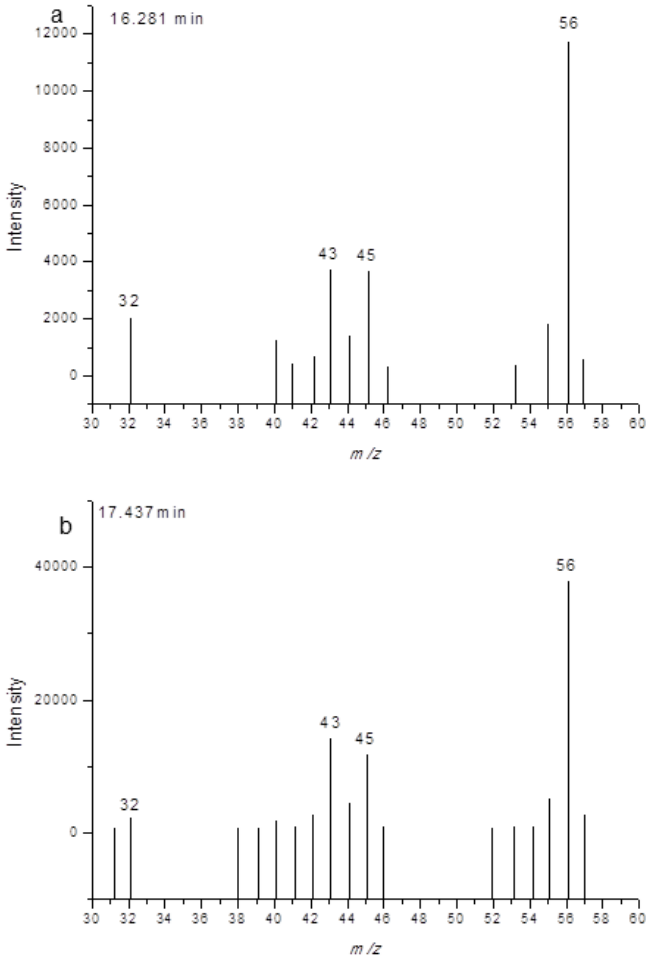


**Figure III.1.2.** Py-GC/MS spectra of peak 1 (a) and peak 2 (b)

### 3.2. Validation of the analytical method

The validation of this method was carried out by evaluating the main analytical parameters, in particular limit of detection (LOD), limit of quantification (LOQ), linearity, and repeatability for each compound (Table III.1. 5). Linear calibration curves for all these reaction products were evaluated at 6 calibration points in the range 0.34 µg - 1.36 µg, using triplicates at each standard. Linear relationships between instrumental responses for each compound, in terms of PLA amount, were verified by the analysis of the variance of the regression curve. The linear correlation between each compound (axis x) and

chromatographic peak areas (axis y) was given by the regression equation, $y = ax + b$ permitting the calculation of correlation coefficients ($r^2$). It could be observed in Table III.1. 5 that nearly all compounds showed a linear correlation coefficient above 0.900 over the whole concentration range. This is a reasonably good result since it is a complex separation and no better results have been reported in literature. Only two exceptions were observed, for *56+(3 x 72)a* and *56+(2 x 72)* oligomers that showed lower correlation coefficients (0.841 and 0.880 respectively).

**Table III.1. 5.** Validation parameters of the development analytical method

| **Compound** | **$r^2$** | **LOD** (μg) [a] | **Repeatability RSD** ($n$ = 5)[b] | **Reproducibility RSD** ($n$ = 5) |
|---|---|---|---|---|
| Mesolactide | 0.921 | 0.15 | 4.18 | 3.89 |
| Lactide | 0.968 | 0.20 | 4.09 | 2.65 |
| *56+(2 x 72)* | 0.880 | 0.22 | 3.49 | 3.42 |
| *56+(3 x 72)a* | 0.841 | 0.27 | 2.83 | 4.23 |
| *56+(3 x 72)b* | 0.925 | 0.26 | 3.05 | 4.56 |
| *56+(3 x 72)c* | 0.947 | 0.10 | 3.56 | 4.32 |
| *56+(4 x 72)* | 0.985 | 0.23 | 4.68 | 4.48 |

[a] μg: responses of each compound in terms of μg of PLA

[b] n: number of replicates

Table III.1. 5 shows that the LOD of the developed method increased when the molar mass of PLA pyrolysis products decreased, and consequently the lowest detection limit when applying this analytical method was calculated for the lactide peak. The relationship between areas corresponding to mesolactide and lactide peaks was reported as a semi-quantitative indication of the pyrolysis mechanism of PLA [8, 20]. In this work this mesolactide:lactide relationship was 1:7.7, remaining constant for all the calibration samples with a standard deviation 0.7, demonstrating the good reproducibility of the method. This parameter was also validated by the variation coefficients of five measurements of the same standard at different days (inter-day precision), while repeatability of the method was evaluated by the variation coefficient for the measurement of five identical samples during one working day (intra-day precision). This parameter was evaluated and results are shown in Table III.1. 5 reflected by the relative standard deviation (%RSD). It was observed that all %RSD values were lower than 5%, indicating that the Py-GC/MS method proposed in this study can be carried out with a satisfactory level of precision for the determination of PLA pyrolysis products.

### 3.3. Application of the sequential pyrolysis to PLA films

This method was successfully applied to the quantification of PLA thermal degraded products in PLA films by using sequential pyrolysis, defined as the consecutive pyrolysis reactions applied to the same sample under identical experimental conditions, until no more products are detected [23]. In this procedure, sample sizes should be small enough to discard any diffusion effect. Thus, a first pyrolysis run was performed and the total product peaks were recorded. A second pyrolysis was then performed to the residue remaining from the first pyrolysis, and this sequence was repeated until no more products evolved [24]. Data obtained from sequential pyrolysis were further used to create a plot of cumulative areas as a function of time in a variety of polymers, such as polysulfones [23], poly(butyl acrylate) [25], polyamide-6 [26], poly(epichlorohydrin-co-ethylene oxide)[24], poly(methyl methacrylate) [25, 27], and polystyrene [25, 27], where the system is expected to show a first order behavior with exponential growth. No studies on sequential pyrolysis of PLA have been previously reported.

The introduction of the $m_\infty$ term in the equations used in this study ensures that the asymptotic value for the pyrolysis limit might be different from 100% [28]. But, in this work, samples were repeatedly subjected to sequential pyrolysis under the same pyrolysis conditions until no more products were detected. Consequently, the $m_\infty$ term could be attributed to the total amount of PLA degraded during pyrolysis. It was observed that PLA thermal degradation under the selected conditions did not show the expected exponential growth, as it was reported for other materials [23, 26]. However, the thermal decomposition pattern of PLA showed a sigmoidal pyrolysis behaviour for all compounds. In this sense, Sánchez-Jiménez et al reported a non-first order behaviour for another biodegradable polymer [29]. Sigmoidal curves were obtained during the study of the kinetics of cellulose pyrolysis by TGA. They showed that this sigmoidal model fits better to the experimental degradation curves for cellulose. They proposed a new kinetic model based on the assumption that random scission of the polymer chains occurs. A random scission mechanism implies the cleavage of the polymeric chains followed by the release of fragments once they become small enough to volatilize [30]. This explanation could be extended to PLA pyrolysis, since it should be expected that a random scission could lead to the formation of the lactide monomer as well as dimers, trimers and tetramers, as indicated in Table III.1. 4. Moreover, in the case of PLA, it has been reported that processed PLA showed lower thermal stability than unprocessed PLA due to a certain depolymerization reactions caused by PLA melting with the result of volatilization of the the small molecules formed during melting [31].

A further analysis of these results makes necessary the use of empirical equations to permit the data treatment for each PLA thermal degradation product. Therefore, the cumulative mass of PLA degradation products was studied by using non-linear regression methods. The Logistic (Equation III.1. 1) and Boltzmann (Equation III.1. 2) methods were used to fit the cumulative experimental masses vs. the cumulative pyrolysis time for each product in order to correlate the observed sigmoidal behavior (Figure III.1.3). The estimated regression parameters of the two non-linear models, $m_\infty$ and $t_0$, were calculated from these curves and they are shown in Table III.1. 6. The correlation coefficients between theoretical and experimental data ($r^2$) were higher than 0.995 in all cases, indicating that only minor differences were observed between the two applied models in their fitting to experimental values. Therefore, the cumulative amount of these seven degradation products seems to be well described by both models. Logistic model provided slightly higher values of m∞ than Boltzmann for all PLA thermal degradation products. In the case of t0 calculations, which represent the time at which 50% of each PLA product was degraded, results were significantly different when applying the Logistic (Equation III.1. 1) and the Boltzmann (Equation III.1. 2) approaches (see Table III.1. 6).

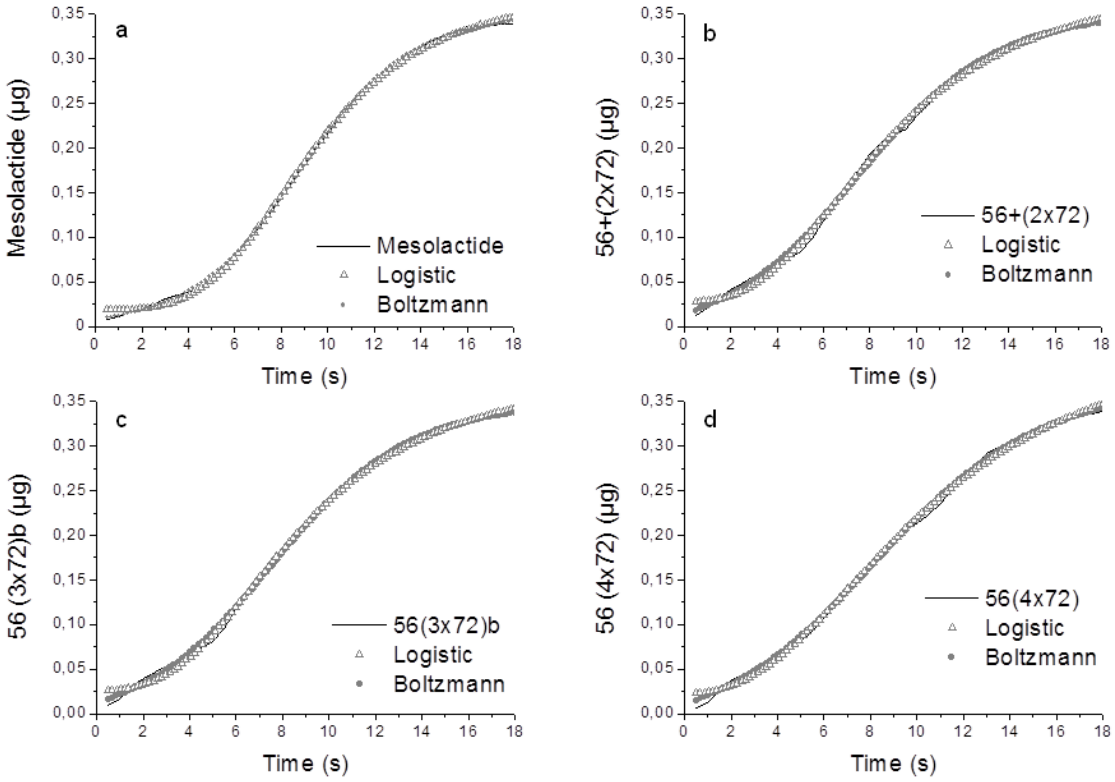


**Figure III.1.3.**Cumulative amount of PLA products (µg PLA) as a function of time, after consecutive pyrolysis for a) mesolactide, b) dimer, c) trimer and d) tetramer.

We can conclude that although both models lead to good fitting to experimental results, the Boltzmann model provided the best approach to calculate the value for $t_0$ since the $m_\infty$ value proposed by Boltzmann model was closer to the initial mass (0.34 μg).

**Table III.1. 6.** Parameters estimated for PLA sequential pyrolysis by using the Logistic and Boltzmann models

| **Compound** | **Parameter estimation** | | | | | |
|---|---|---|---|---|---|---|
| | **Logistic** (Equation 1) | | | **Boltzmann** (Equation 2) | | |
| | **$m_\infty$** (μg) [a] | **$t_0$** (min) | **$r^2$** | **$m_\infty$** (μg) [a] | **$t_0$** (min) | **$r^2$** |
| Mesolactide | 0.378 ± 0.004 | 9.4 ± 0.1 | 0.999 | 0.348 ± 0.001 | 8.8 ± 0.1 | 0.999 |
| Lactide | 0.370 ± 0.006 | 8.2 ± 0.1 | 0.996 | 0.346 ± 0.002 | 7.5 ± 0.1 | 0.999 |
| *56+(2 x 72)* | 0.391 ± 0.002 | 8.8 ± 0.2 | 0.997 | 0.346 ± 0.002 | 7.5 ± 0.1 | 0.998 |
| *56+(3 x 72)a* | 0.412 ± 0.003 | 9.2 ± 0.3 | 0.997 | 0.355 ± 0.005 | 7.2 ± 0.2 | 0.998 |
| *56+(3 x 72)b* | 0.386 ± 0.008 | 8.7 ± 0.2 | 0.998 | 0.346 ± 0.003 | 7.6 ± 0.1 | 0.998 |
| *56+(3 x 72)c* | 0.385 ± 0.006 | 8.6 ± 0.1 | 0.998 | 0.348 ± 0.002 | 7.6 ± 0.1 | 0.999 |
| *56+(4 x 72)* | 0.437 ± 0.002 | 10.4 ± 0.4 | 0.997 | 0.340 ± 0.005 | 8.2 ± 0.1 | 0.998 |

[a] μg: responses of each compound in terms of μg of PLA

## 4. CONCLUSIONS

A Py-GC/MS method for the identification and quantification of PLA thermal degradation products has been developed and successfully applied to PLA films. The optimum pyrolysis conditions were set at 600 °C for 0.5 s and the analytical methodology was successfully validated. Seven different compounds produced during the PLA thermal degradation were identified and quantified in terms of PLA amount. It was observed that the pyrolized PLA gave a dominant series of signals with *m/z = 56 + (n x 72).* This work demonstrated that the use of short pyrolysis times and diluted film samples were key factors to achieve good chromatographic resolutions and to avoid diffusion effects, respectively. The validated methodology was applied to PLA films by using sequential pyrolysis to the same sample until no more products were detected. It was found that the thermal degradation of PLA revealed a sigmoidal behavior and this could be an indication of the PLA complex degradation mechanism. The use of processed PLA in this study and the obtained results could lead to the conclusion that the hot-melt treatment to produce films could significantly change the polymer behaviour at high temperatures. However, further work should be carried out to assess such complex mechanism since it is known

that a variety of experimental factors could be also co-responsible of such differences in PLA thermal degradation. The Logistic and Boltzmann models could describe well this behaviour since the complete sample was pyrolizated before the end of the test. Therefore, sequential pyrolysis allowed assuming that the final mass ($m_\infty$) should be equal to the initial amount. Although both models lead to good fittings to experimental results, it could be concluded that the Boltzmann model provided the best approach to calculate the value for $t_0$ at which 50% of each PLA compound was degraded. In conclusion, it could be expected that the Boltzmann model could be applied to PLA other formulations with different additives by using low amount of materials and short pyrolysis times.

**Acknowledgements**

This research was supported by the Ministry of Science and Innovation of Spain (MAT2011-28468-C02-02). Marina P. Arrieta thanks Generalitat Valenciana (Spain) for a Santiago Grisolía Grant (GRISOLIA/2011/007).

**REFERENCES**

[1] Martino VP, Ruseckaite RA, Jimenez A. Thermal and mechanical characterization of plasticized poly (L-lactide-co-D,L-lactide) films for food packaging. J Therm Anal Calorim. 2006;86(3):707-712.

[2] Chien YC, Liang CJ, Yang SH. Exploratory study on the pyrolysis and PAH emissions of polylactic acid. Atmos Environ. 2011;45(1):123-127.

[3] Auras R, Harte B, Selke S. An overview of polylactides as packaging materials. Macromolecular Bioscience. 2004;4(9):835-864.

[4] Fortunati E, Peltzer M, Armentano I, Torre L, Jimenez A, Kenny JM. Effects of modified cellulose nanocrystals on the barrier and migration properties of PLA nano-biocomposites. Carbohydrate Polymers. 2012;90(2):948-956.

[5] Badia JD, Santonja-Blasco L, Martinez-Felipe A, Ribes-Greus A. Hygrothermal ageing of reprocessed polylactide. Polym Degrad Stabil. 2012;97(10):1881-1890.

[6] Cornelissen T, Jans M, Stals M, Kuppens T, Thewys T, Janssens GK, et al. Flash co-pyrolysis of biomass: The influence of biopolymers. J Anal Appl Pyrolysis. 2009;85(1-2):87-97.

[7] Badia JD, Santonja-Blasco L, Martinez-Felipe A, Ribes-Greus A. A methodology to assess the energetic valorization of bio-based polymers from the packaging industry: Pyrolysis of reprocessed polylactide. Bioresource technology. 2012;111:468-475.

[8] Khabbaz F, Karlsson S, Albertsson AC. Py-GC/MS an effective technique to characterizing of degradation mechanism of poly (L-lactide) in the different environment. J Appl Polym Sci. 2000;78(13):2369-2378.

[9] Aoyagi Y, Yamashita K, Doi Y. Thermal degradation of poly (R)-3-hydroxybutyrate , poly epsilon-caprolactone , and poly (S)-lactide. Polym Degrad Stabil. 2002;76(1):53-59.

[10] Kopinke FD, Remmler M, Mackenzie K, Moder M, Wachsen O. Thermal decomposition of biodegradable polyesters .2. Poly(lactic acid). Polym Degrad Stabil. 1996;53(3):329-342.

[11] Jimenez A, Lopez J, Torre L, Kenny JM. Kinetic analysis of the thermal degradation of PVC plastisols. J Appl Polym Sci. 1999;73(6):1069-1079.

[12] Parres F, Balart R, Crespo JE, Lopez J. Effects of the injection-molding temperatures and pyrolysis cycles on the butadiene phase of high-impact polystyrene. J Appl Polym Sci. 2007;106(3):1903-1908.

[13] Parres F, Sanchez L, Balart R, Lopez J. Determination of the photo-degradation level of high impact polystyrene (HIPS) using pyrolysis-gas chromatography-mass spectrometry. J Anal Appl Pyrolysis. 2007;78(2):250-256.

[14] Martino VP, Jimenez A, Ruseckaite RA. Processing and Characterization of Poly(lactic acid) Films Plasticized with Commercial Adipates. J Appl Polym Sci. 2009;112(4):2010-2018.

[15] Badia JD, Stromberg E, Ribes-Greus A, Karlsson S. Assessing the MALDI-TOF MS sample preparation procedure to analyze the influence of thermo-oxidative ageing and thermo-mechanical degradation on poly (Lactide). European Polymer Journal. 2011;47(7):1416-1428.

[16] Martino VP, Jimenez A, Ruseckaite RA, Averous L. Structure and properties of clay nano-biocomposites based on poly(lactic acid) plasticized with polyadipates. Polymers for Advanced Technologies. 2011;22(12):2206-2213.

[17] Arrieta M, Prats Moya MS. Free amino acids and biogenic amines in Alicante Monastrell wines. Food Chemstry 2012;135(3):1511-1519.

[18] Scharfman HE, Hintz TM, Gomez J, Stormes KA, Barouk S, Malthankar-Phatak GH, et al. Changes in hippocampal function of ovariectomized rats after sequential low doses of estradiol to simulate the preovulatory estrogen surge. European Journal of Neuroscience. 2007;26(9):2595-2612.

[19] Mosquera LH, Moraga G, de Cordoba PF, Martinez-Navarrete N. Water Content-Water Activity-Glass Transition Temperature Relationships of Spray-Dried Borojo as Related to Changes in Color and Mechanical Properties. Food Biophys. 2011;6(3):397-406.

[20] Westphal C, Perrot C, Karlsson S. Py-GC/MS as a means to predict degree of degradation by giving microstructural changes modelled on LDPE and PLA. Polymer Degradation and Stability. 2001;73(2):281-287.

[21] Kopinke FD, Mackenzie K. Mechanistic aspects of the thermal degradation of poly(lactic acid) and poly(beta-hydroxybutyric acid). Journal of Analytical and Applied Pyrolysis. 1997;40-1:43-53.

[22] Fan YJ, Nishida H, Shirai Y, Endo T. Racemization on thermal degradation of poly(L-lactide) with calcium salt end structure. Polym Degrad Stabil. 2003;80(3):503-511.

[23] Almen P, Ericsson I. Studies of the thermal degradation of polysulfones by filament-pulse pyrolysis gas chromatography. Polym Degrad Stabil. 1995;50(2):223-228.

[24] Soto-Oviedo MA, Lehrle RS, Parsons IW, De Paoli MA. Thermal degradation mechanism and rate constants of the thermal degradation of

poly(epichlorohydrin-co-ethylene oxide), deduced from pyrolysis-GC-MS studies. Polym Degrad Stabil. 2003;81(3):463-472.

[25] Bate DM, Lehrle RS, Pattenden CS, Place EJ. A critical comparison of procedures for evaluating rate constants in thermal degradation, illustrated by pyrolysis-gc results from four polymers. Polym Degrad Stabil. 1998;62(1):73-83.

[26] Parres F, Crespo JE, Nadal-Gisbert A. Thermal Degradation Analysis of Polyamide 6 Processed at Different Cycles Using Sequential Pyrolysis. J Appl Polym Sci. 2009;114(2):713-719.

[27] Bate DM, Lehrle RS. Kinetic measurements by pyrolysis-gas chromatography, and examples of their use in deducing mechanisms. Polym Degrad Stabil. 1996;53(1):39-44.

[28] Costa D, Valente AJM, Graca Miguel M, Lindman B. Light triggered release of solutes from covalent DNA gels. Colloids and Surfaces a-Physicochemical and Engineering Aspects. 2011;391(1-3):80-87.

[29] Sanchez-Jimenez PE, Perez-Maqueda LA, Perejon A, Pascual-Cosp J, Benitez-Guerrero M, Criado JM. An improved model for the kinetic description of the thermal degradation of cellulose. Cellulose. 2011;18(6):1487-1498.

[30] Sanchez-Jimenez PE, Perez-Maqueda LA, Perejon A, Criado JM. Nanoclay Nucleation Effect in the Thermal Stabilization of a Polymer Nanocomposite: A Kinetic Mechanism Change. Journal of Physical Chemistry C. 2012;116(21):11797-11807.

[31] Carrasco F, Pags P, Gámez-Pérez J, Santana OO, Maspoch ML. Kinetics of the thermal decomposition of processed poly(lactic acid). Polym Degrad Stabil. 2010;95(12):2508-2514.

## 2. Characterization of PLA-limonene blends for food packaging applications

*Marina P. Arrieta[a], Juan López[a], Santiago Ferrándiz[a], Mercedes A. Peltzer[b]*

[a] Instituto de Tecnología de Materiales, Universitat Politècnica de València, Plaza Ferrándiz y Carbonell 1, 03801 Alcoy, Alicante Spain.

[b] Analytical Chemistry, Nutrition and Food Sciences Department, University of Alicante, P.O. Box 99, E-03080 Alicante, Spain.

**Polymer Testing**

**32: 760-768 (2013)**

**Abstract**

Polymers derived from renewable resources are now considered as promising alternatives to traditional petro-polymers as they mitigate current environmental concerns (raw renewable materials/biodegradability). D-limonene can be found in a variety of citrus, indeed is the main component of citrus oils and one of most important contributors to citrus flavor. The incorporation of limonene in PLA matrix was evaluated and quantified by Pyrolysis Gas Chromatography Mass Spectrometry (Py-GC/MS). Transparent films were obtained after the addition of the natural compound. Mechanical properties were evaluated by tensile tests. The effect of limonene on mechanical properties of PLA films was characterized by an increase in the elongation at break and a decrease in the elastic modulus. The fracture surface structure of films was evaluated by scanning electron microscopy (SEM), and homogeneous surfaces were observed in all cases. Barrier properties were reduced due to the increase of the chain mobility produced by the D-limonene.

**Keywords:** PLA; limonene; plasticizer; packaging.

## 1. INTRODUCTION

Polymers derived from renewable resources are now considered as promising alternatives to traditional petro-polymers as they mitigate current environmental concerns (raw renewable materials/biodegradability). It is widely accepted that the use of long-lasting polymers for short-term and disposable applications, such as packaging, is not entirely satisfactory [1]. As a result, the biopolymer industry is growing rapidly since biodegradables polymers made from renewable resources have a less negative effect on the environment compared to the conventional petroleum based materials largely used in commodities [2].

Polylactide (PLA) is one of the most promising bio-based polyesters for food packaging [1] and [2] because of its good mechanical, superior transparency, ease of processing and availability in the market [3]. In this sense, poly(lactic acid) (PLA) is one of the most attractive biopolymers with many short-term or disposable applications, such as disposable cutlery (plates, cups, lids and drinking straws), bags and film packaging [4] and [5]. PLA is also widely used in rigid and flexible food packaging applications [6] since it has been approved by the US Food and Drug Administration (FDA) as a food contact substance [7] and [8]. However, the use of PLA for food packaging is somewhat limited because of its poor ductility, thermal and oxygen barrier properties [3].

Recent studies have been conducted on the use of limonene as a new novel monomer to obtain polyterpenes [9]. D-limonene can be found in a variety of citrus, indeed is the main component of citrus oils and one of most important contributors to citrus flavor [10] and [11]. Is the most abundant monocyclic monoterpene in nature and represents more than 90% of orange peel oil, being the most important residue in the citrus industry [12]. The limonene diffusion through packaging has been widely studied in different food contact materials such as polyethylene (PE) [13], low density polyethylene (LDPE) [14], high density polyethylene (HDPE), polystyrene (PS) [15] and PLA [15] and [16]. Furthermore, the sorption of aroma compounds through packaging materials have been reported recently by Salazar et al. (2012) [17], who found a plasticization effect of PLA films by aroma compounds after the sorption studies.

For many practical food packaging applications, it is desirable to modify the polymer matrix and many modifications have been proposed to improve PLA's performance. It is widely known that PLA plasticization is required in order to improve ductility [18] and [19]. Although the addition of plasticizer increases the PLA gas permeability, this could be detrimental for food packaging use [3] since polymer barrier properties are of fundamental importance for food packaging applications [20]. López-

Rubio & Lagaron (2009) reported that the addition of the β-carotene to PLA showed a significant plasticization of polymer matrix [21]. In addition, the control of light transmission through packaging is an important parameter to preserve and protect some food products until they reach the consumer. So, additives are required for transparent PLA films to block light transmission [22]. Furthermore, PLA modified with natural origin compounds has been proposed as active packaging [8], [23] and [24]. In this way, Hwang et al. (2011) proposed PLA with added α-tocopherol and resveratrol as promising active functional membranes [8]. Jamshidian et al. (2012) studied PLA with ascorbyl palmitate although they reported high loss of antioxidant during polymer preparation and negatives results on PLA transparency [24].

Polymer modifiers should be miscible with polymer matrix, so it becomes necessary to analyze the effects of the additives on the thermal stability of the modified PLA formulations. Thermal degradation is responsible for serious damage to many polymeric materials during processing and use under high temperature conditions [25]. Therefore, it becomes necessary to study the incorporation of modifiers into polymer matrix with the effect depending on the chemical nature of the molecules and their interaction.

The aim of this work is to evaluate the performance of PLA films when two concentrations (15 wt% and 20 wt%) of D-limonene were added to the PLA matrix to obtain sustainable films. The amount of limonene incorporated into PLA matrix was studied by thermogravimetric analysis (TGA) and also with pyrolysis coupled with gas chromatography and mass spectrometric detection (Py-GC/MS). In order to evaluate the applicability for flexible food packaging materials, optical, mechanical and oxygen barrier properties of PLA and PLA-limonene films were also assessed.

## 2. MATERIALS AND METHODS

### 2.1. Materials

Poly(lactic acid) pellets (PLA 4032D, $M_n$ = 217,000 Da, 2 wt% D-isomer) was supplied by NatureWorks LLC (USA). D-limonene ($M_w$ = 136.24 g/mol) was provided by Acros Organic (USA). The chemical structures of PLA and limonene are provided in Figure III.2.1.

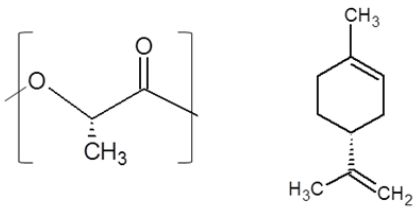


**Figure III.2. 1.** Chemical structures of PLA and limonene

## 2.2. Film preparation

The preparation of PLA with D-limonene was performed by adding limonene monomer to the PLA matrix. Since PLA is very hygroscopic, PLA pellets were previously dried in a vacuum oven at 60 °C for 6 h. Blends were obtained by mixing PLA pellets and D-limonene in appropriate amounts, 15 wt% or 20 wt%, in a Haake Polylab mixer (Thermo Fischer Scientific Walham, USA). Samples were designated as PLA, PLA-Lim15 and PLA-Lim20. The melt mixing was performed at 180 °C with 50 rpm rotor speed for 5 min for PLA pellets followed by 3 min after limonene addition. The blends were then molded into films at 170 °C in a press (Mini C 3850, Caver, Inc. USA). The material was kept between the plates at atmospheric pressure for 5 min until melted and then submitted to the following pressure cycle, 3 MPa for 1 min, 5 MPa for 1 min and 10 MPa for 3 min, with the aim of liberating trapped air bubbles [19]. Film samples were then quenched at room temperature at atmospheric pressure.

## 2.3. FTIR analysis

Fourier transformed infrared spectroscopy (FTIR) measurements were carried out at ambient temperature in transmission mode by using a Perkin-Elmer Spectrum BX infrared spectrometer (Perkin–Elmer, Spain, S.L., Madrid Spain). Spectra were obtained in the 4000–600 $cm^{-1}$ region, using 128 scans and 4 $cm^{-1}$ resolution. A blank spectrum was obtained before each test to compensate for the humidity effect and the presence of carbon dioxide in the air by spectra subtraction.

## 2.4. Scanning electron microscopy (SEM)

Scanning electron microscopy (SEM) was used to observe the fracture surface morphology of the films samples generated from the tensile test in a Phenom SEM (FEI

Company, Eindhoven, The Netherlands) using an acceleration voltage of 10 kV. Samples were covered with an Au layer in vacuum conditions prior to each measurement.

### 2.5. Thermogravimetric analysis

Thermogravimetric analysis (TGA) tests were carried out using a TGA/SDTA 851 Mettler Toledo thermal analyzer (Schwarzenbach, Switzerland). Samples weighing around 5–10 mg were heated under dynamic mode. Measurements were performed at 10 °C $min^{-1}$ from 30 to 600 °C under nitrogen atmosphere (flow rate 50 mL $min^{-1}$) in order to prevent any thermoxidative degradation.

### 2.6. Py-GC/MS analysis

The amount of D-limonene incorporated into PLA films was measured by Py-GC/MS. Film samples were pyrolyzed with the use of a Pyroprobe 1000 instrument (CDS Analytical, Oxford, Pennsylvania, USA), which was coupled to a gas chromatograph (6890N, Agilent Technologies, Spain S.L., Madrid, Spain). The column used for the analysis was 30 m long HP-5 (0.25 mm thickness) using helium as carrier gas with a 50:1 split ratio. The GC oven was programmed at 40 °C to 50 °C by a stepped increase of 5 °C $min^{-1}$ and then the temperature was increased by 10 °C $min^{-1}$ to 300 °C, where it was held for 5 min. For mass spectral detection, a Agilent 5973N mass selective detector was used. The transfer temperature from the GC to MS was set at 280 °C. The mass selective detector was programmed to detect masses between 30 and 650 amu. Film samples were pyrolyzed at 1000 °C for 0.5 s. The identification of PLA and PLA-limonene degradation products was confirmed by the characteristic fragmentation patterns observed in Py-GC/MS spectra or by comparison with literature mass spectra. The concentration of limonene incorporated into the film sample was determined from the peak area of the limonene component and by using the calibration curve from limonene standard solutions. The limit of detection (LOD), was calculated as three times the standard deviation which provided the signal-to-noise ratio in the lowest concentration standard, divided by slope of the calibration curve (LOD = 3 SD/$m$). The slope ($m$) represents the sensitivity of the method [26].

### 2.7. Differential scanning calorimetry (DSC)

Differential scanning calorimetry (DSC) experiments were carried out in a TA Instrument Q100 calorimeter (New Castle, DE, USA). The heating and cooling rate for the runs was 10 °C $min^{-1}$ in a nitrogen atmosphere, the typical sample weight was around 4 mg. Calibration was performed using an indium sample. The cycle program consisted of a first heating stage from −90 to 180 °C at a rate of 10 °C $min^{-1}$, followed by cooling to −90 °C and subsequent heating up to 200 °C at 10 °C $min^{-1}$. The glass transition temperature ($T_g$) was calculated from the first heating and was taken at the mid-point of heat capacity changes. The melting temperature ($T_m$) and cold crystallization temperature ($T_{cc}$) were obtained from the second heating, and degree of crystallinity ($\chi_c$) was determined by using Equation III.2. 1:

$$\chi_c = 100 \times \left[\frac{\Delta H_m - \Delta H_{cc}}{\Delta H_m^c}\right] \frac{1}{1 - m_f} \qquad \textbf{Equation III.2. 1}$$

where $\Delta H_m$ is the enthalpy of fusion, $\Delta H_{cc}$ is the enthalpy of cool crystallization, $\Delta H^c_m$ is the heat of melting of purely crystalline PLA, taken as 93 J/g [27], [28], [29], [30] and [31], and $(1 - m_f)$ is the weight fraction of PLA in the sample.

### 2.8. Mechanical properties

Tensile tests were conducted at room temperature on a universal testing machine IBERTEST ELIB 30 equipped with a 5 kN cell (S.A.E. Iberstest, Madrid, Spain) according to the standard procedure UNE-EN ISO 527-3 [32]. Tests were performed on rectangular test pieces (10 mm × 100 mm) with initial grip separation of 50 mm and crosshead speed of 5 mm $min^{-1}$. Average percentage deformation at break ($\varepsilon_B$%), elastic modulus ($E$) and tensile strength (TS) were calculated from the resulting stress-strain curves as the average of five measurements from three films of each composition.

### 2.9. Film color properties

Film color properties were evaluated measuring colour coordinates in the CIELAB colour space L* (lightness), a* (red-green) and b* (yellow-blue) were analyzed using a KONICA CM-3600d COLORFLEX-DIFF2, HunterLab, Hunter Associates Laboratory, Inc,

(Reston, Virginia, USA). The instrument was calibrated with a white standard tile. Measurements were carried out in quintuplicate at random positions over the film surface. Average values for these five tests were calculated. Total color differences ($\Delta E$), induced by limonene incorporation, with respect to the control PLA film was evaluated Equation III.2. 2:

$$\Delta E = \sqrt{\Delta a^2 + \Delta b^2 + \Delta L^2} \qquad \textbf{Equation III.2. 2}$$

The yellowness index (YI) was also measured.

### 2.10. Oxygen permeability measurement

The oxygen transition rate (OTR) measurements were accomplished using an oxygen permeation analyzer from Systech Instruments-Model 8500 (Metrotec S.A, Spain) at a pressure of 2.5 atm. Measurements were conducted at room temperature. Films were clamped in the diffusion chamber and pure oxygen (99.9% purity) was then introduced into the upper half of the sample chamber, while nitrogen was injected into the lower half of the chamber where there was an oxygen sensor. Measurements were done in triplicate and were expressed as oxygen transmission rate per film thickness (OTR.$e$). Thickness was measured at 25 °C using a Digimatic Micrometer Series 293 MDC-Lite (Mitutoyo, Japan) accurate to 0.001 mm from 10 readings taken at random positions over the 14 cm diameter circle films.

### 2.11. Wettability

Water contact angle measurements were performed at room temperature with an EasyDrop Standard goniometer FM140 (KRÜSS GmbH, Hamburg, Germany) equipped with a camera and analysis software (Drop Shape Analysis SW21; DSA1). The contact angle was measured by randomly putting 10 drops of distiller water (2 µl) onto the surface film with a syringe. Five measurements were carried out for each sample an average values were calculated.

## 3. RESULTS AND DISCUSSION

Figure III.2.2 shows the visual appearance of pure PLA films and PLA films with 15 wt% and 20 wt % of limonene. The films have good transparency even at high limonene concentrations; therefore limonene has no effect on the transparency of the PLA.

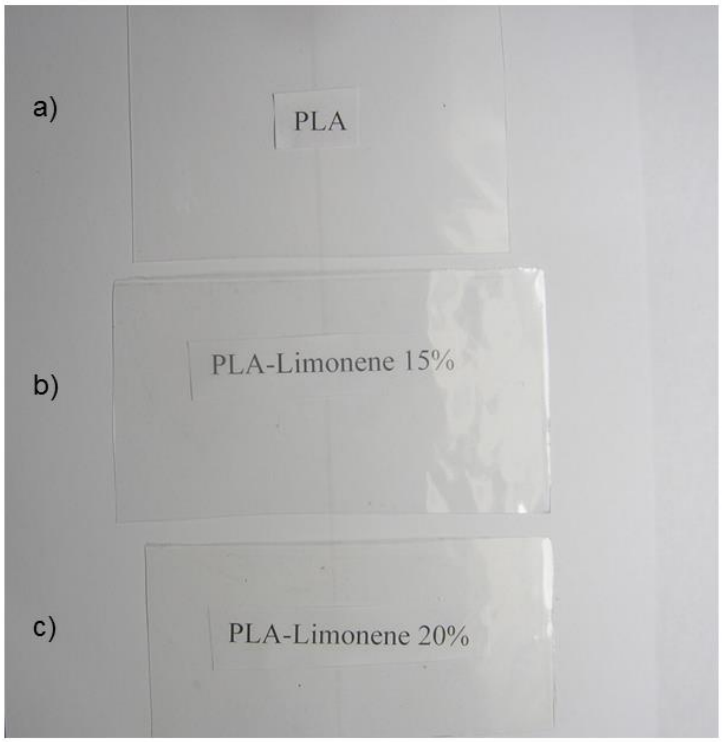


**Figure III.2.2.** Visual appearance of films: a) PLA, b) PLA-Lim15 and c) PLA-Lim20

### 3.1. FTIR

FTIR spectra were recorded for PLA and PLA-limonene films in order to investigate the chemical structure of the films and to study the characteristic peaks of the blend. The spectra are showed in Figure III.2.3, being arbitrarily offset for comparison. The spectrum region between 3000 $cm^{-1}$ and 2860 $cm^{-1}$ is characterized by –CH stretching bands [33]; this region shows a high absorption for PLA, with the intensities of these peaks decreasing with increase of limonene content. There is also a broad absorption due to the absorption of cyclohexene group at ≈3000 $cm^{-1}$ which overlap –CH peaks (Figure III.2.3) [34]. In Figure III.2.3-b, the most relevant spectrum bands are identified. The typical asymmetric stretching of carbonyl group (C═O) by lactide is present at 1760 $cm^{-1}$ [35]. The 1450 $cm^{-1}$ band is assigned to the $CH_3$ group [22]. The symmetric and asymmetric deformation bands of –CH appeared at 1380 $cm^{-1}$ and 1360 $cm^{-1}$, respectively. In the

region between of 1000 $cm^{-1}$ and 800 $cm^{-1}$, the deformation vibration of ═CH groups can be observed.

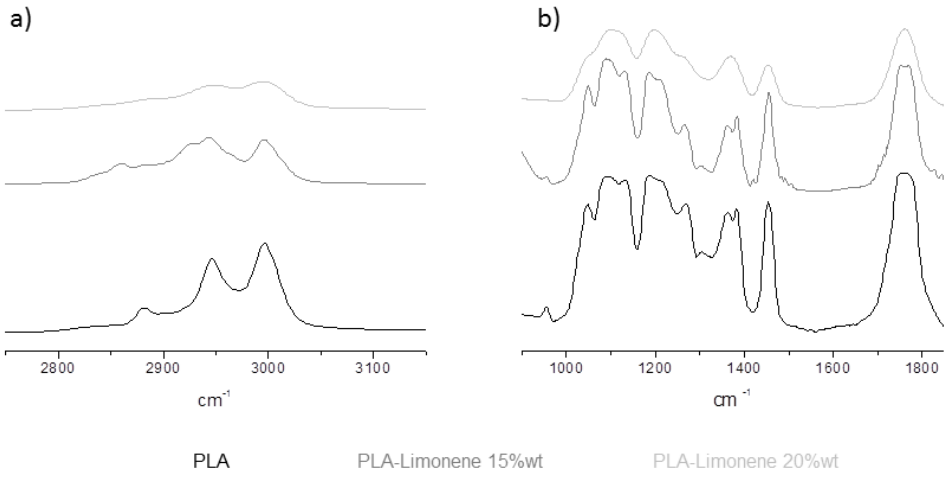


**Figure III.2.3.** FTIR spectra of PLA and PLA limonene films

### 3.2. Thermogravimetric analysis

The effect of limonene on the thermal stability of PLA was studied by TGA. PLA decomposes in a single step process with an initial degradation temperature ($T_0$) of 322 °C and maximum degradation rate temperature ($T_{max}$) centered at 370 °C (Figure III.2.4). The addition of Limonene in the polymer matrix resulted in a two step degradation process, where the first degradation step, between 80–160 °C, corresponds to the degradation of limonene, while the second step corresponds to the degradation of the PLA. From these results, it is possible to estimate the remaining amount of limonene in the PLA matrix after processing, which is approximately 6.5 wt% and 8.5 wt% for the sample PLA-Lim15 and PLA-Lim20%, respectively. The $T_0$ and $T_{max}$ of the studied samples are showed in Table III.2.1. Figure III.2.4 also shows the derivative curves (DTG) and it could be observed that there is another step process overlapping PLA decomposition and may be also related to limonene. Similar behavior was observed by Martino et al. (2006) when PLA was plasticized with commercial adipates [36].

**Table III.2.1.** DSC and TGA results of PLA and PLA-Limonene films.

| Parameter | PLA | PLA-Lim15 | PLA-Lim20 |
|---|---|---|---|
| $\mathbf{T}_{0(\alpha=0,01)}$ (°C) | 322 | 109 | 105 |
| $\mathbf{T}_{max}$ (°C) | 370 | 338 | 367 |
| $\mathbf{T}_{g}$ (°C) | 60.3 | 30.2 | 33.8 |
| $\mathbf{T}_{cc}$ (°C) | 99.8 | 75.1 | 72.7 |
| $\mathbf{T}_{m}$ (°C) | 167.4 | 164.2 | 166.3 |
| $\chi_c$ (%) | 4.54 | 3.54 | 1.80 |

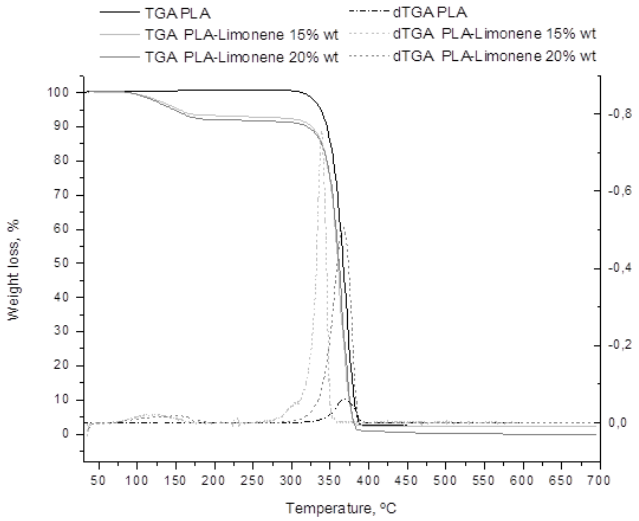


**Figure III.2.4.** TGA and dTGA curves for PLA and PLA-Limonene films

### 3.3. Py-GC/MS

The quantification of the remaining amount of limonene after film processing was carried out by Py-GC/MS. This technique presents high sensitivity and it could be useful to study smaller variations in material structure [5], [37] and [38]. The optimization of Py-GC/MS conditions was based in the use of 0.5 s and 1000 °C, since short pyrolysis time allowed achieving good chromatographic resolution [38] and high temperature was in order to elute the total amount of limonene in the sample in one pyrolysis. Therefore, these pyrolysis conditions allow limonene to be eluted in one and it could be quantified by using standard solutions. The peak at 7.5 min in the pyrogram corresponds to D-limonene while the peak at 9.7 min corresponds to L-lactide (Figure III.2.5). There is another smaller peak at around 9.1 min that has been identified as mesolactide [38]. The limonene limit of detection (LOD) was 0.05 wt%. The results indicated that after processing there were

remaining amounts of D-limonene of 8.9 wt% and 11.2 wt% in PLA-Lim15 and PLA-Lim20, respectively. Therefore, there is a loss of limonene during processing and the lost was more pronounced when the concentration of limonene was increased. These results are in good agreement with Soto-Valdez et al., 2011 who reported that the amount of resveratrol lost during extrusion of PLA-resveratrol films increased with higher resveratrol concentrations [39].

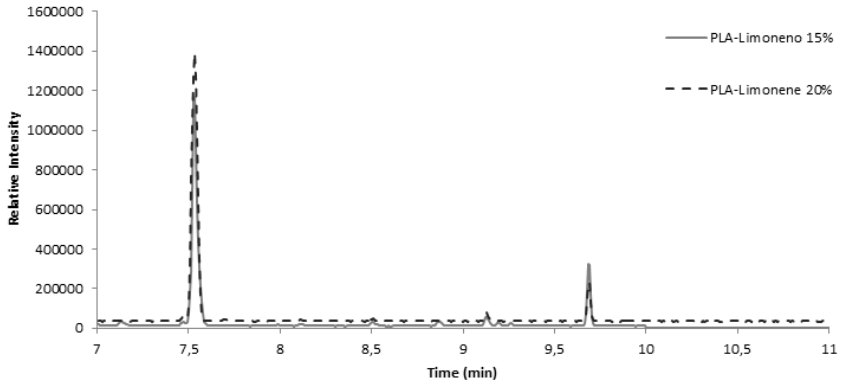


**Figure III.2.5.** Pyrogram obtained for PLA-Limonene films at 1000°C for 0.5s

### 3.4. Differential Scanning Calorimetry

DSC curves showed a single $T_g$ for the limonene added samples indicating the miscibility between limonene and PLA. In addition, a significant reduction in $T_g$ was observed (Table III.2.1) accompanied by a decrease in the value of $T_{cc}$ with the addition of D-limonene to the polymer matrix. These changes are due to the increase in the polymer chain mobility, indicating a plasticization effect. Moreover, degree of crystallinity ($\chi_c$) of the blends decreased with increasing limonene content, due to enhanced polymer chain mobility [40] and the plasticization effect [39]. The low $\chi c$ values obtained indicate that the all films are essentially amorphous. The lower amounts of crystals present when melt occurs in the sample containing limonene, produce a slight shifting of $T_m$ to lower temperatures with respect to the neat PLA film.

### 3.5. Mechanical properties

The plasticizer effect of limonene was also observed in the mechanical tests. The incorporation of limonene caused a reduction in elastic modulus and tensile stress values in accordance with $\chi_c$ decrease, and increased the elongation at break of the films (Figure

III.2.6). Consequently, PLA-limonene films presented less brittleness than neat PLA. The most significant difference between the films with limonene and neat PLA film was the elongation at break, which was significantly lower for control PLA film. It is known that films for packaging require high flexibility to avoid breaking during processing and use [36]. The elongation increased from 1.5% (PLA) to 150% for PLA-lim15 and reached a maximum of 165% for PLA-Lim20 film. These results display a significant improvement in the flexibility of PLA due of the plasticization effect achieved by limonene addition.

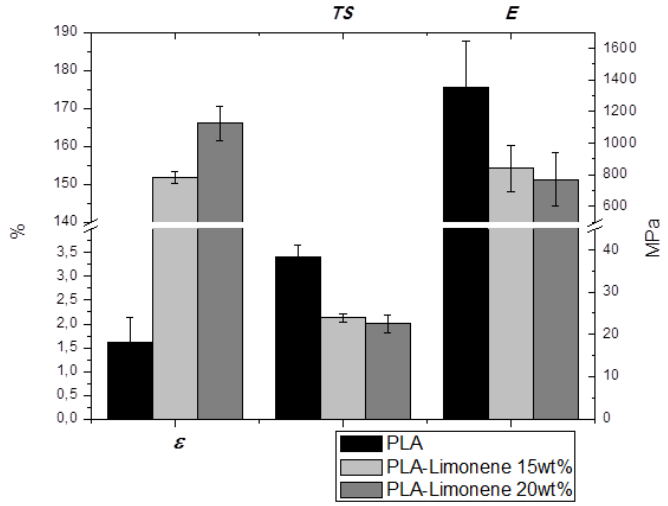


**Figure III.2.6.** Elongation at break (ε, %), tensile stress (TS, MPa) and modulus (E, MPa) of PLA and PLA-Limonene films

### 3.6. Scanning Electron Microscopy

Scanning electron microscopy (SEM) images were taken of the fractured surfaces after the tensile tests and are shown in Figure III.2.7. A smooth broken surface was observed for neat PLA film sample corresponding to brittle nature of PLA (Figure III.2.7-a). PLA-Lim15 (Figure III.2.7-b) and PLA-Lim20 (Figure III.2.7-c) fracture surfaces show great evidence of plastic deformation with a uniform dispersion of limonene in the PLA matrix. Limonene addition significantly influences the morphological structural showing blended-PLA ductile behavior in accordance with the increased deformation at break.

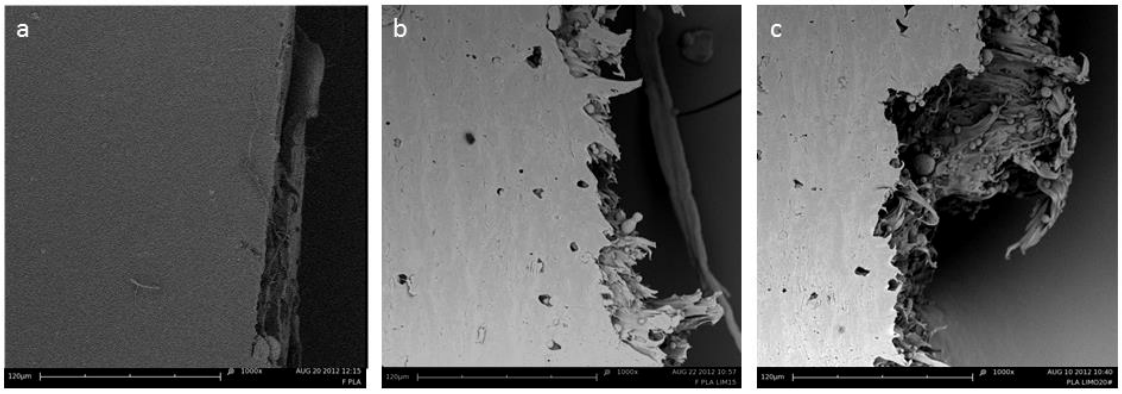


**Figure III.2.7.** Fracture surface of a) neat PLA film, b) PLA-Lim15 film and c) PLA-Lim20 film

### 3.7. Film color properties

Table III.2.2 shows the results obtained from the colorimeter analysis. When limonene is added to the film sample, a slight decrease in lightness values ($L^*$) was observed. However, PLA and also both PLA-limonene samples presented high $L^*$ values showing their high brightness. Furthermore, no major differences were found for total color difference values. This result suggested high transparency for films containing limonene and the possibility to see through the film is one of the most important requirements for consumers [41]. Negative values obtained for $a^*$ coordinate are indicative of a deviation towards green. However, these values are close to zero so the green tone was not noticeable. Positive values obtained of $b^*$ coordinate indicate a slight deviation towards yellow. Therefore, yellowness index was also determined. The YI is used to describes the change in color of a sample from clear toward yellow [22]. It was observed that the YI values increased with the limonene content increase. However, the highest YI value, achieved by PLA-Lim20, is a similar value that has been reported for other packaging plastic films such as PET [22].

**Table III.2.2.** Color parameters from CIELab space, wettability and oxygen barrier properties of PLA, PLA-Lim15 and PLA-Lim20.

| **Parameter** | | **PLA** | **PLA-Lim15** | **PLA-Lim20** |
|---|---|---|---|---|
| *Color* | $L^*$ | 94.08 ± 0.07 | 93.86 ± 0.10 | 93.32 ± 0.33 |
| | $a^*$ | -1.03 ± 0.01 | -0.99 ± 0.01 | -1.31 ± 0.08 |
| | $b^*$ | 1.33 ± 0.05 | 1.27 ± 0.06 | 2.55 ± 0.47 |
| | $\Delta E$ | - | 0.24 ± 0.04 | 1.46 ± 0.50 |
| | Y313 (65/10) | 3.47 ± 0.07 | 3.49 ± 0.10 | 5.65 ± 0.85 |
| *Oxygen Barrier* | OTR.*e* ($cm^3.mm.m^{-2}.d^{-1}$) | 44.4 ± 0.9 | 84.0 ± 4.9 | 99.3 ± 2.6 |
| *Wettability* | $\theta^o$ | 58.4 ± 3.7 | 75.3 ± 1.3 | 78.3 ± 2.1 |

### 3.8. Oxygen permeability measurement

The incorporation of limonene leads to an increase in the oxygen permeation (Table III.2.2). This result is in accordance with $T_g$ values. The increase in polymer chain mobility caused by limonene plasticization effect reduced the resistance of the PLA film to oxygen transmission, allowing the mobility of the oxygen molecules in the polymer matrix. Increases in OTR.*e* values with increasing amount of plasticizer in the PLA matrix have been well reported in the literature [19], [42] and [43]. Although, OTR.*e* values increased with limonene present they were still better than the levels obtained for commercial LDPE films in comparable conditions (OTR.*e* = 160 $cm^3$ mm $m^{-2}$ $d^{-1}$) [19].

### 3.9. Wettability

The hydrophilicity of films samples was investigated by water contact angle measurement. When limonene was added to the PLA matrix, the contact angle with water was increased from 58° to ≈75, showing a higher hydrophobic character of PLA-limonene blends. This behavior could be attributed to the limonene hydrophobic character. It has been reported that modifying the physicochemical properties of the material surface can control the water adsorption [41]. Therefore, PLA films containing limonene are also expected to have higher resistance to water adsorption than neat PLA film. PLA-limonene blends could be used in packaging formulations with reduced water adsorption requirements.

## 4. CONCLUSIONS

A complete characterization of PLA blended with d-limonene was carried out. PLA-limonene films maintained their transparency after the addition of the natural compound, but minor positive values of *b** coordinate indicated a slight deviation towards yellow. Py-GC/MS analysis demonstrated that there was a remaining amount of limonene in the PLA matrix after processing. The results revealed that the addition of limonene into the PLA matrix decreases the glass transition temperature of the films. The $T_{cc}$ and $\chi_c$ were also decreased while Tm was slightly reduced. Mechanical properties of the films were altered by the presence of limonene and good plasticization was observed. Barrier properties to oxygen were reduced due to the plasticization of the PLA matrix, but presented acceptable values for food packaging applications. Furthermore, d-limonene reduced the water adsorption of PLA matrix.

These results show the feasibility of using d-limonene as a natural PLA plasticizer to obtain flexible films for food contact materials, and even to be tested as active compound in active packaging systems.

**Acknowledgements**

This research was supported by the Ministry of Science and Innovation of Spain (MAT2011-28468-C02-02). Marina P. Arrieta thanks Generalitat Valenciana (Spain) for a Santiago Grisolía Fellowship. Authors thank Professor Alfonso Jiménez from the University of Alicante, for his useful discussions.

**REFERENCES**

[1] Averous L. Biodegradable multiphase systems based on plasticized starch: A review. Journal of Macromolecular Science-Polymer Reviews. 2004;C44(3):231-274.

[2] Fortunati E, Armentano I, Iannoni A, Kenny JM. Development and thermal behaviour of ternary PLA matrix composites. Polymer Degradation and Stability. 2010;95(11):2200-2206.

[3] Martino VP, Jimenez A, Ruseckaite RA, Averous L. Structure and properties of clay nano-biocomposites based on poly(lactic acid) plasticized with polyadipates. Polymers for Advanced Technologies. 2011;22(12):2206-2213.

[4] Chien Y-C, Liang C, Yang S-h. Exploratory study on the pyrolysis and PAH emissions of polylactic acid. Atmospheric Environment. 2011;45(1):123-127.

[5] Arrieta MP, Parres García FJ, López Martínez J, Navarro Vidal R, Ferrándiz S. Pyrolysis of Bioplastic waste: Obtained poducts from Poly(lactic Acid). DYNA. 2012;87(4):395-399.

[6] Boonyawan D, Sarapirom S, Tunma S, Chaiwong C, Rachtanapun P, Auras R. Characterization and antimicrobial properties of fluorine-rich carbon films deposited on poly(lactic acid). Surface & Coatings Technology. 2011;205:S552-S557.

[7] FDA AU. Inventory of Effective Food Contact Substance (FCS) 2005.

[8] Hwang SW, Shim JK, selke SEM, Soto-Valdez H, Matuana L, Rubino M, et al. Poly(L-lactic acid) with added a-tocopherol and resveratrol: optical, physical, thermal and mechanical properties. Polymer International. 2012;61(3):418-425.

[9] Singh A, Kamal M. Synthesis and characterization of polylimonene: Polymer of an optically active terpene. Journal of Applied Polymer Science. 2012;125(2):1456-1459.

[10] Perez AG, Luaces P, Oliva J, Rios JJ, Sanz C. Changes in vitamin C and flavour components of mandarin juice due to curing of fruits. Food Chemistry. 2005;91(1):19-24.

[11] Sanchez-Vicente Y, Perez E, Cabanas A, Urieta JS, Renuncio JAR, Pando C. Excess molar enthalpies for mixtures of supercritical carbon dioxide and limonene. Fluid Phase Equilibria. 2006;246(1-2):153-157.

[12] Bicas JL, Pastore GM. Isolation and screening of D-limonene-resistant microorganisms. Brazilian Journal of Microbiology. 2007;38(3):563-567.

[13] Cava D, Catala R, Gavara R, Lagaron JM. Testing limonene diffusion through food contact polyethylene by FT-IR spectroscopy: Film thickness, permeant concentration and outer medium effects. Polymer Testing. 2005;24(4):483-489.

[14] Pieper G, Borgudd L, Ackermann P, Fellers P. Absorption of aroma volatiles of orange juice into laminated carton packages did not affect sensory quality. Journal of Food Science. 1992;57(6):1408-1411.

[15] Haugaard VK, Weber CJ, Danielsen B, Bertelsen G. Quality changes in orange juice packed in materials based on polylactate. European Food Research and Technology. 2002;214(5):423-428.

[16] Auras R, Harte B, Selke S. Sorption of ethyl acetate and d-limonene in poly(lactide) polymers. Journal of the Science of Food and Agriculture. 2006;86(4):648-656.

[17] Salazar R, Domenekb S, Courgneaub C, Ducruet V. Plasticization of poly(lactide) by sorption of volatile organic compounds at low concentration. Polymer Degradation and Stability. 2012.

[18] Courgneau C, Domenek S, Guinault A, Averous L, Ducruet V. Analysis of the Structure-Properties Relationships of Different Multiphase Systems Based on Plasticized Poly(Lactic Acid). Journal of Polymers and the Environment. 2011;19(2):362-371.

[19] Martino VP, Jimenez A, Ruseckaite RA. Processing and Characterization of Poly(lactic acid) Films Plasticized with Commercial Adipates. Journal of Applied Polymer Science. 2009;112(4):2010-2018.

[20] Rial-Otero R, Galesio M, Capelo JL, Simal-Gándara J. A review of synthetic polymer characterization by pyrolysis-GC-MS. Chromatographia. 2009;70(3-4):339-348.

[21] Lopez-Rubio A, Lagaron JM. Improvement of UV stability and mechanical properties of biopolyesters through the addition of beta-carotene. Polymer Degradation and Stability. 2010;95(11):2162-2168.

[22] Auras R, Harte B, Selke S. An overview of polylactides as packaging materials. Macromolecular Bioscience. 2004;4(9):835-864.

[23] Jamshidian M, Tehrany EA, Cleymand F, Leconte S, Falher T, Desobry S. Effects of synthetic phenolic antioxidants on physical, structural, mechanical and barrier properties of poly lactic acid film. Carbohydrate Polymers. 2012;87(2):1763-1773.

[24] Jamshidian M, Tehrany EA, Imran M, Akhtar MJ, Cleymand F, Desobry S. Structural, mechanical and barrier properties of active PLA-antioxidant films. Journal of Food Engineering. 2012;110(3):380-389.

[25] Peltzer M, Wagner JR, Jimenez A. Thermal characterization of UHMWPE stabilized with natural antioxidants. Journal of Thermal Analysis and Calorimetry. 2007;87(2):493-497.

[26] Arrieta MP, Prats-Moya MS. Free amino acids and biogenic amines in Alicante Monastrell wines. Food Chemistry. 2012;135(3):1511-1519.

[27] Fortunati E, Armentano I, Zhou Q, Iannoni A, Saino E, Visai L, et al. Multifunctional bionanocomposite films of poly(lactic acid), cellulose nanocrystals and silver nanoparticles. Carbohydrate Polymers. 2012b;87(2):1596-1605.

[28] Auras RA, Singh SP, Singh JJ. Evaluation of oriented poly(lactide) polymers vs. existing PET and oriented PS for fresh food service containers. Packaging Technology and Science. 2005b;18(4):207-216.

[29] Gamez-Perez J, Velazquez-Infante JC, Franco-Urquiza E, Pages P, Carrasco F, Santana OO, et al. Fracture behavior of quenched poly(lactic acid). Express Polymer Letters. 2011;5(1):82-91.

[30] Nam JY, Ray SS, Okamoto M. Crystallization behavior and morphology of biodegradable polylactide/layered silicate nanocomposite. Macromolecules. 2003;36(19):7126-7131.

[31] Hwang SW, Lee SB, Lee CK, Lee JY, Shim JK, Selke SEM, et al. Grafting of maleic anhydride on poly(L-lactic acid). Effects on physical and mechanical properties. Polymer Testing. 2012;31(2):333-344.

[32] ISO. UNE-EN ISO 527-3. Plastics: determination of tensile properties. Part 3: test conditions for films and sheets. 1995.

[33] Siracusa V, Blanco I, Romani S, Tylewicz U, Rocculi P, Dalla Rosa M. Poly(lactic acid)-modified films for food packaging application: Physical, mechanical, and barrier behavior. Journal of Applied Polymer Science. 2012;125:E390-E401.

[34] Pretsch E BP, Affolter C, Herrera A, Martínez R. Determinación estructural de compuestos orgánicos. Barcelona, Spain: Masson, SA; 2002.

[35] Fortunati E, Armentano I, Iannoni A, Barbale M, Zaccheo S, Scavone M, et al. New multifunctional poly(lactide acid) composites: Mechanical, antibacterial, and degradation properties. Journal of Applied Polymer Science. 2012;124(1):87-98.

[36] Martino VP, Ruseckaite RA, Jimenez A. Thermal and mechanical characterization of plasticized poly (L-lactide-co-D,L-lactide) films for food packaging. Journal of Thermal Analysis and Calorimetry. 2006;86(3):707-712.

[37] Parres F, Balart R, Crespo JE, Lopez J. Effects of the injection-molding temperatures and pyrolysis cycles on the butadiene phase of high-impact polystyrene. Journal of Applied Polymer Science. 2007;106(3):1903-1908.

[38] Arrieta MP, Parres F, López J, Jiménez A. Development of a novel pyrolysis-gas chromatography/mass spectrometry method for the analysis of poly(lactic acid) thermal degradation products. Journal of Analytical and Applied Pyrolysis. 2013.

[39] Soto-Valdez H, Auras R, Peralta E. Fabrication of Poly(lactic acid) Films with Resveratrol and the Diffusion of Resveratrol into Ethanol. Journal of Applied Polymer Science. 2011;121(2):970-978.

[40] Martin O, Averous L. Poly(lactic acid): plasticization and properties of biodegradable multiphase systems. Polymer. 2001;42(14):6209-6219.

[41] Introzzi L, Fuentes-Alventosa JM, Cozzolino CA, Trabattoni S, Tavazzi S, Bianchi CL, et al. "Wetting enhancer" pullulan coating for antifog packaging applications. ACS Applied Materials and Interfaces. 2012;4(7):3692-3700.

[42] Auras R, Harte B, Selke S. Effect of water on the oxygen barrier properties of poly(ethylene terephthalate) and polylactide films. Journal of Applied Polymer Science. 2004b;92(3):1790-1803.

[43] Cho S-W, Gallstedt M, Hedenqvist MS. Properties of Wheat Gluten/Poly(lactic acid) Laminates. Journal of Agricultural and Food Chemistry. 2010;58(12):7344-7350.

## 3. Ternary PLA-PHB-Limonene blends intended for biodegradable food packaging applications

*Marina P. Arrieta[a,d], Juan López[a], Alberto Hernández[b], Emilio Rayón[c]*

[a] Instituto de Tecnología de Materiales, Universitat Politècnica de València, Plaza Ferrándiz y Carbonell 1, 03801 Alcoy, Alicante Spain.

[b] Servicio de Microscopía Óptica y Confocal, Centro de Investigación Príncipe Felipe, Eduardo Primo Yúfera, 3 E46012. Valencia, Spain.

[c] Instituto de Tecnología de Materiales, Universitat Politècnica de València, Camí de Vera s/n. E46022. Valencia, Spain

[d] Analytical Chemistry, Nutrition and Food Sciences Department, University of Alicante, P.O. Box 99, E-03080 Alicante, Spain.

**European Polymer Journal**

**50: 255-270 (2014)**

**Abstract**

In this work poly(lactic acid) PLA, and poly(hydroxybutyrate) PHB, were blended and plasticized with a natural terpene D-limonene (LIM) with the dual objective to increase PLA crystallinity and to obtain flexible films intended for food packaging applications. Materials were melt-blended and processed in transparent films. Structural and surfaces properties were evaluated. Moreover, functional properties were studied by means colorimetric parameters, oxygen permeation and water resistant measurements. In addition, thermal stability, crystallization behavior, mechanical as well as nanomechanical properties were investigated. FTIR spectra showed the characteristic bands corresponding to PLA and PHB and their rather molecular interaction. Py-GC/MS showed the characteristics peak of D-limonene as well as the thermal degradation products of PLA and PHB. D-limonene amount after processing was higher in PHB incorporated samples. PHB produced a reinforcing effect in PLA matrix and therefore an improvement in the oxygen barrier properties and the surface water resistance. Moreover, Scanning Confocal Microscopy surface images showed the dispersion of PHB crystal in PLA matrix. The influences of plasticization process on the mechanical properties showed that D-limonene provoked an increase in elongation at break. Disintegrability under composting conditions was also investigated and it was observed that PHB delays the PLA disintegrability under composting while D-limonene speed it up. In brief, the best results regarding structural, thermal, barrier and mechanical properties were found for the ternary PLA–PHB–LIM film.

**Keywords:** Poly(lactic acid) PLA; Poly(hydroxybutyrate) PHB; Limonene; food packaging; biodegradable.

## 1. INTORDUCTION

Increasing ecological concern towards a reduction on the environmental impact produced by plastics is contributing to the growth of the biodegradable polymer industry. During the last two decades, the great interest in the reduction of environmental impact caused by food packaging and their indiscriminate use, have increasingly received the scientist attention specially focused in the development of new biodegradable materials as a way to reduce the petroleum-based plastic residue. In this sense, poly(lactic acid) (PLA) is becoming increasingly popular as a biodegradable plastic owing to its high mechanical strength, superior transparency and easy processability compared to other biodegradables polymers [1]. Nowadays, PLA is an economically feasible material [2] derived from renewable resources [3], in particular from sugar and starch [4], chemically synthesized, commercially available with good performance characteristics as a packaging material [5] that is currently being used for many short-term applications, such as disposable cutlery (plates, cups, lids and drinking straws), bags and film packages [6]. Moreover, its waste is suitable to be used in pyrolysis facilities to produce green energy [7] and also it is a compostable material [8]. Therefore, the PLA is suitable for food packaging applications [3]. Nevertheless, the use of PLA for food packaging is limited because of PLA has lower water vapor permeability, poor mechanical and thermal properties, low ductility, and its thermal and oxygen barrier properties are quite poor compared with equivalent petroleum based polymers [9].

Moreover, although the addition of plasticizer increases PLA gas permeability, owing to its poor ductility PLA plasticization is required for film applications [10]. Polymer barrier properties are of fundamental importance for food packaging applications. For instance, there are many food products sensitive to oxidation and to overcome this trouble packages with reduced oxygen permeability are desirable. On the other hand, the water resistant is also important, particularly for materials intended for direct contact with high moisture foods as well as materials to be submitted under high humidity conditions during storage and/or transport [5]. PLA barrier properties are decided by the crystalline and molecular characteristics [11]. Thus, research on modifications of PLA has mainly focused on the increase of PLA crystallinity.

There are many studies focusing on PLA modification such as the addition of modifiers, copolymerization or blending. Blending PLA with another bio-based and/or biodegradable material allow to adjust some properties in wide range while legislation also favors completely compostable materials with minimal carbon-footprint [12], such as are those provided by the physical blend processing technology. In this sense, poly-

hydroxybutyrate (PHB), another biodegradable thermoplastic, is the most common representative of Poly-hydroxyalkanoates (PHA) that has been proposed for short term food applications [13]. It is also a brittle polymer, as its enzymatic polymerization leads to the formation of macromolecules with highly ordered stereochemical structure, as a result large crystallinity [12]. One of the great advantages of PHB over many other biodegradable polymers is it biodegradability under both, aerobic and anaerobic conditions [14]. For this reason, PLA and PHB and their blends are biodegradable materials commonly investigated for food packaging applications [15], [16], [17] and [18]. One of the potential application fields of these materials is as a film. It has been reported that 25 wt% of PHB produced a reinforcement effect on PLA matrix [18] due to PHB could be used as a nucleating agent [17]. In this sense, Zhang and colleagues studied blends of PLA and poly(hydroxybutirate) (PHB) in different proportions and concluded that blending PLA with 25 wt% of PHB some interactions between both polymers matrices were observed. Furthermore, their results also showed improved mechanical properties [18]. However, PLA and PHB films are rigid and need to be modified. One common practice for film manufacturing is the plasticizers addition to increase the molecular mobility and consequently enhance the material flexibility. The composition of materials in contact with foodstuffs is tightly regulated, so food grade plasticizers are required. Furthermore, when consumers decide to purchase food products the aspect of packaging could influence the decision, and therefore high transparency in food packaging is required.

The use of additives in the developed of biodegradable materials to be in contact with food is limited not only by safety, but for environmental concern. Essential oil rich in monoterpens are of great interest as stabilizers for polymers. Terpenes, such as limonene, are abundant and inexpensive [19]. It was found that D-limonene is easily absorbed for plastic polymers [20] and also it has no effect on aroma quality on foodstuff [21]. Moreover, limonene, extracted from citrus peel, is one of the most important byproduct in the citrus industry [22]. Thus, it is highly available in the market at low-price and it would be positive to increase its added value from a low-grade by-product to a useful plasticizer. In this sense, in our previous work we showed that different amounts of D-limonene provoke a positive plasticization effect in PLA matrix [10]. D-limonene was also selected because it is derived from renewable resources and it is colorless reducing some drawbacks in the transparency that occurs with other natural additives such as several essential oils.

For materials intended to be used in short term applications, such as food packaging, not only the renewable nature of its components but also their inert degradation is highly desirable [16]. PLA may not biodegrade at room temperature, but it

is biodegradable under severe degradation conditions as those provided by composting systems [9]. Composting is the controlled and natural decomposition of organic matter by strong active microorganisms [8]. Biodegradable polymers exposed to compost conditions first become susceptible to hydrolysis, the attack of water molecules lead to polymer random decomposition into oligomers [23] and chemical degradation initiates the polymer erosion as a result of hydrolysable functional groups in the polymer backbone [8]. The degradation behavior of PLA strongly depends on the stereochemical composition, molecular weight and the initial crystallinity as well as the percentage of L-lactide content [6, 8]. The final degradation product formed during the degradation process of PLA is lactid acid which is easily assimilated by the microorganisms [23, 24]. Likewise, PHB hydrolytic degradation products (R) and (S)-hydroxybutyrates are as well nontoxic compounds [16].

This work is focused on the developing of fully biodegradable films intended for film food packaging applications based on PLA–PHB blends plasticized with D-limonene. The obtained films were full characterized by the determination of structural, thermal, mechanical, nanomechanical and morphological properties. Same functional properties such as optical, wettability and oxygen barrier properties were also assayed to demonstrate the potential of PLA–PHB blends incorporated with D-limonene for food packaging sector. Moreover, the disintegration under composting conditions was also tested by studding the thermal degradation, surface changes and the meso-lactide to lactide relationship of PLA based formulations after the exposition to compost, with the main objective to supply information about the environmentally friendly end-life option proposed for these developed biomaterials.

## 2. MATERIALS AND METHODS

### 2.1. Materials

Poly(lactic acid) pellets (PLA 4032D, $M_n$ = 217,000 Da, 2 wt% D-isomer, $M_w/M_n$ = 2) was supplied by NatureWorks LLC (USA), PHB pellets (PHB P226, $M_w$ = 426,000) was provided by Biomer (Krailling, Germany) and D-limonene ($M_w$ = 136.24 g/mol) was provided by Acros Organic (USA).

## 2.2. Film samples preparation

The preparation of PLA-PHB blends was performed by mixing PLA and PHB pellets in 75 wt% and 25 wt% proportion respectively in a Haake Polylab mixer (Thermo Fischer Scientific Walham, USA) at 180 °C and a rotation speed of 50 rpm for 4 min. PLA pellets were previously dried in a vacuum oven at 80 °C overnight, meanwhile PHB pellets were dried at 40 °C during 4 h. PLA and PLA–PHB were added with 15 wt% of d-limonene. Furthermore, PLA and PHB neat films were also prepared using the same conditions as a reference material. The d-limonene was added into the mixer after 3 min when PLA and PLA–PHB blend achieved the melt state. Blends were then molded into films at 180 °C in a hot press (Mini C 3850, Caver, Inc. USA). The material was kept between the plates at atmospheric pressure for 2 min until melting and then it was submitted to the following pressure cycles, 3 MPa for 1 min, 5 MPa for 1 min, and 10 MPa for 2 min. Finally, film samples were quenched at room temperature at atmospheric pressure. Five formulations were obtained and were named as PLA, PLA-LIM, PHB, PLA-PHB and PLA-PHB-LIM.

## 2.3. Samples characterization

### *2.3.1. Structural characterization*

#### 2.3.1.1. *Fourier transformed infrared spectroscopy analysis (FTIR)*

Fourier transformed infrared spectroscopy (FTIR) tests were performed in transmission mode at ambient temperature using a Perkin–Elmer BX infrared spectrometer (Perkin Elmer Spain, S.L., Madrid Spain). Spectra were obtained in the 4000–600 $cm^{-1}$ region, using 128 scans and 4 $cm^{-1}$ resolution. A background spectrum was obtained before each test to compensate the humidity effect and the presence of carbon dioxide in the air by spectra subtraction.

#### 2.3.1.2. *Pyrolysis gas chromatography/ mass spectrometry (Py-GC/MS)*

Film samples were pyrolyzed at 1000 °C for 0.5 s with the use of a Pyroprobe 1000 instrument (CDS Analytical, Oxford, Pennsylvania, USA), which was coupled to a gas chromatograph (6890N, Agilent Technologies, Spain S.L., Madrid, Spain) equipped with a 30 m long HP-5 (0.25 mm thickness) column and using helium as carrier gas with a 50:1

split ratio. The GC oven was programmed at 40–50 °C by a stepped increase of 5 °C min$^{-1}$ and then the temperature was increased by 10 °C min$^{-1}$ to 300 °C, where it was held for 5 min. For mass spectral detection, an Agilent 5973N mass selective detector was used. The transfer temperature from the GC to MS was set at 280 °C. The mass selective detector was programmed to detect masses between 30 and 650 amu. The identification of PLA and PHB degraded products were confirmed by the characteristic fragmentation pattern observed in Py-GC/MS spectra. While the amount of D-limonene incorporated into polymer matrices was measured by pyrolysis coupled with gas chromatography and mass spectrometric detection (Py-GC/MS) following a previous developed method [10] and it was determined from the peak area of the limonene component and by using the calibration curve from D-limonene standard solutions.

### *2.3.2. Thermal characterization*

#### 2.3.2.1. *Differential Scanning Calorimetry (DSC)*

DSC experiments were carried out in a TA Instrument Q100 calorimeter (New Castle, DE, USA). The heating and cooling rate for the runs was 10 °C/min in a nitrogen atmosphere, the typical sample weight was around 4 mg. Calibration was performed using an indium sample. The materials were exposed to a heat-cool cycle. The cycle program consisted in a first heating stage from −90 to 180 °C at a heating rate of 10 °C min$^{-1}$, followed by a cooling process up to −90 °C and subsequent heating up to 200 °C at 10 °C min$^{-1}$. The glass transition temperature ($T_g$) was taken at the mid-point of heat capacity changes. The melting temperature ($T_m$) and cold crystallization temperature ($T_{cc}$) were obtained from the first heating and degree of crystallinity ($\chi_c$) was determined by using Equation III.3. 1:

$$\chi_c = 100 \times \left[\frac{\Delta H_m - \Delta H_{cc}}{\Delta H_m^c}\right] \frac{1}{1 - m_f} \qquad \textbf{Equation III.3. 1}$$

where $\Delta H_m$ is the enthalpy of fusion, $\Delta H_{cc}$ is the enthalpy of cool crystallization, $\Delta H_m{}^c$ is the heat of melting of purely crystalline PLA by considering this value as 93 J/g [6] and [25] and $W_{PLA}$ is the weight fraction of PLA in the sample [1]. For neat PHB Equation III.3. 2 was used to calculate the degree of crystallinity ($\chi_c$). Where $\Delta H_m{}^c$ is the heat of melting of purely crystalline PHB considering this value as 146 J/g [26].

$$\chi_c = 100 \times \left[\frac{\Delta H_m}{\Delta H_m^c}\right]$$ **Equation III.3. 2**

#### 2.3.2.2. *Thermogravimetric analysis (TGA)*

Dynamic and isothermal thermal degradation analysis were carried out using thermogravimetric analyzer TGA/SDTA 851 Mettler Toledo (Schwarzenbach, Switzerland). Dynamic measurements were run at 10 °C/min constant heating rates. Temperature was raised from 30 to 600 °C under nitrogen atmosphere (flow rate 50 mL/min) to avoid any thermo-oxidative degradation. The initial degradation temperature ($T0$) was calculated at 5% mass loss, while temperatures at the maximum degradation rate ($T$max) for each stage were determined from the first derivatives of the TGA curves (DTG). Isothermal measurements were carried out at 40 °C under air conditions.

### *2.3.3. Mechanical properties*

#### 2.3.3.1. *Tensile test*

The film Young's modulus ($E$), tensile strength ($TS$) and percentage deformation at break ($\varepsilon_B$%), were conducted at room temperature on a universal testing machine IBERTEST ELIB 30 (S.A.E. Iberstest, Madrid, Spain) equipped with a 5 kN cell, according to the standard procedure ASTM D882-01 [27]. Tests were performed in rectangular probes (10 mm × 100 mm), with an initial grip separation 50 mm, and crosshead speed 5 mm $min^{-1}$. Results were calculated from the resulting stress-strain curves as the average of five measurements from two films of each composition.

#### 2.3.3.2. *Nanoindentation procedure*

Nanomechanical properties were acquired by a nanoindenter machine G-200 (Agilent Technologies, USA) with a previously calibrated Berkovich diamond tip. Experiments were carried out by Continuous Stiffness Measurement (CSM) under a 70 Hz harmonic oscillation frequency and 2 nm of harmonic amplitude maintaining a constant 0.05 $s^{-1}$ indentation rate. An array of 5 × 5 indentations distanced between them 50 μm, were programmed at a constant 200 nm depth, calculating the average values between the

100 nm and 200 nm depth. The reduced elastic modulus ($E_r$) was calculated instead of the Young's Modulus because the Poisson's coefficient is unknown for these blends and plasticized polymers.

### *2.3.4. Surface characterization*

#### 2.3.4.1. *Scanning Electron Microscopy (SEM)*

Fracture surfaces morphology generated from the tensile test were coated with a gold layer to be observed in a Phenom Scanning Electron Microscopy SEM (FEI Company, Eindhoven, Netherlands) with an operating voltage of 10 kV.

#### 2.3.4.2. *Optical Microscopy*

Surfaces of films before and after disintegrability under composting conditions were observed by a LV-100 Nikon Eclipse optical microscope equipped with a Nikon sight camera at 20× magnifications using the extended depth of field (EDF) imaging technique.

#### 2.3.4.3. *Scanning Confocal Microscopy (SCM)*

Surfaces of the sample slices before and after composting were examined and imaged using a Leica TCS SP2 AOBS (Leica Microsystems Heidelberg GmbH, Mannheim, Germany) inverted laser scanning confocal microscope. Samples were mounted in a universal stage, on slides and then illuminated with the 488 nm line from an argon laser. Reflection light from sample surfaces was collected (detecting spectral range = 480–500 nm) with a 63× Plan-Apochromat-Lambda Blue oil objective (numerical aperture = 1.4) in a single 8-bit channel and Airy 0.75 pinhole diameter; begin and end limits of the vertical series were set visually in the Z-wide scan control. Gain and black levels for the photomultiplier were adjusted through digital control in the glow/over/under look-up-table and two-dimensional pseudo color images (255 color levels) were gathered with a size of 119 × 119 μm (Zoom = 2) and 1024 × 1024 pixels. Image stacks with the optimal number of sections for maximal z-resolution (for the lens) were transformed into topographical images for measurements in the Leica LCS Materials software package and converted to 3-D images.

### 2.3.5. *Light transmission and color properties*

The light transmission test performed in the visible light region (400-700 nm) and film color properties were evaluated by using the CIELAB color space by means a KONICA CM-3600d COLORFLEX-DIFF2, HunterLab, Hunter Associates Laboratory, Inc, (Reston, Virginia, USA). Color coordinates, $L$ (lightness), $a^*$(red–green) and $b^*$ (yellow–blue), and yellowness index ($YI$) were measured. The instrument was calibrated with a white standard tile. Measurements were carried out in quintuplicate at random positions over the film surface. Average values for these five tests were calculated. Total color difference ($\Delta E$) was calculated with respect to the control neat PLA film or PLA-PHB film as follow:

$$\Delta E = \sqrt{\Delta a^{*2} + \Delta b^{*2} + \Delta L^2} \qquad \textbf{Equation III.3. 3}$$

### 2.3.6. Oxygen permeability

The oxygen transition rate (OTR) was measured with an oxygen permeation analyzer from Systech Instruments-Model 8500 (Metrotec S.A, Spain) at a pressure of 2.5 atm at room temperature. Films (14 cm diameter circle) were compressed between the upper and lower diffusion chamber. Pure oxygen (99.9% purity) was introduced into the upper half of the sample chamber while nitrogen was injected into the lower half where there was an oxygen sensor. The oxygen volumetric flow rate per unit area of the film and per time (OTR, $cm^3\ m^2\ day^1$) was continuously monitored until a steady state was reached. Measurements were done in triplicate and were expressed as oxygen transmission rate per film thickness (OTR·$e$).

### 2.3.7. Wettability

The surface hydrophobicity of films was studied by measuring the water contact angle by means an Easy-Drop Standard goniometer FM140 (KRÜSS GmbH, Hamburg, Germany) equipped with a camera and analysis software (Drop Shape Analysis SW21; DSA1). The contact angle was measured by randomly adding six drops of distilled water (2 µL) with a syringe to the film's surfaces at room temperature [10]. Ten contact angle measurements were carried out for each drop and the average values were reported.

### 2.3.8. Disintegration under composting conditions

The disintegrability under composting conditions was studied according to ISO 22000 [28]. All formulations cut in 3 × 3 $cm^2$ were buried inside an iron mesh (to allow the removal of the disintegrated samples but also allowing the access of microorganisms and moisture) [29] at 4–6 cm depth [9] in plastic reactors containing solid biodegradable synthetic wet waste and subjected to disintegration under aerobic conditions at 58 °C in an air circulation DO/200 draping oven (Carbolite, UK) during a period of 35 days. For the preparation of solid synthetic waste, 10% of compost (containing of total organic matter, 40% vegetal matter, 30% of humidity and pH 6.5) supplied by Mantillo, Spain, it was mixed with 30% rabbit food, 10% starch, 5% sugar, 1% urea, 10% corn oil and 40% sawdust. Finally, the solid synthetic waste was mixed with water in 45:55 proportions and water was added periodically to maintain the humidity. Each film formulation was recovered at 7, 14, 21 and 28 days cleaned with distilled water, dry at 40 ± 2 °C for 24 h and weighed. The disintegration degree was calculated by normalizing the sample weight, at different days of incubation, to the initial weight [9].

### 2.3.9. Statistical analysis

Significance in the mechanical data differences were statistically analyzed by one-way analysis of variance (ANOVA) using OriginPro 8 software. To identify which groups were significantly different from other groups means comparison were done employing a Tukey's test with a 95% confidence level.

## 3. RESULTS AND DISCUSSION

### 3.1. Light transmission and colorimetric properties

Figure III.1-B shows the visual appearance of developed films. As it was expected, neat PLA results colorless and transparent while neat PHB presents amber color with slightly transparency. After PHB addition, light yellow films were obtained. No apparent differences in transparency and color can be reported for samples added with D-limonene (LIM). Since high transparency in food packaging is required because of the aspect of packaging could influence the decision of consumers [10] the light transmission analysis

in the visible light region and colorimetric analysis were performed and results are shown in Figure III.3.1 and Table III.3.1

, respectively. The light transmission showed that no significance differences were observed between PLA and PLA-LIM (Figure III.3.1-A). This result is in agreement with a previous work where we reported that D-limonene did not influence the characteristic high brightness of PLA [10]. Meanwhile, neat PHB showed the minimum transparency in the visible light region (Figure III.3.1-A) with the highest *L* value (Table III.3.1). Small but positive values in $a^*$ coordinate showed a slight trend to red in neat PHB. Neat PLA and neat PHB showed a big total color difference. PHB presents a clear visual amber tonality which was less pronounced in PLA–PHB blends (Figure III.3.1-B).

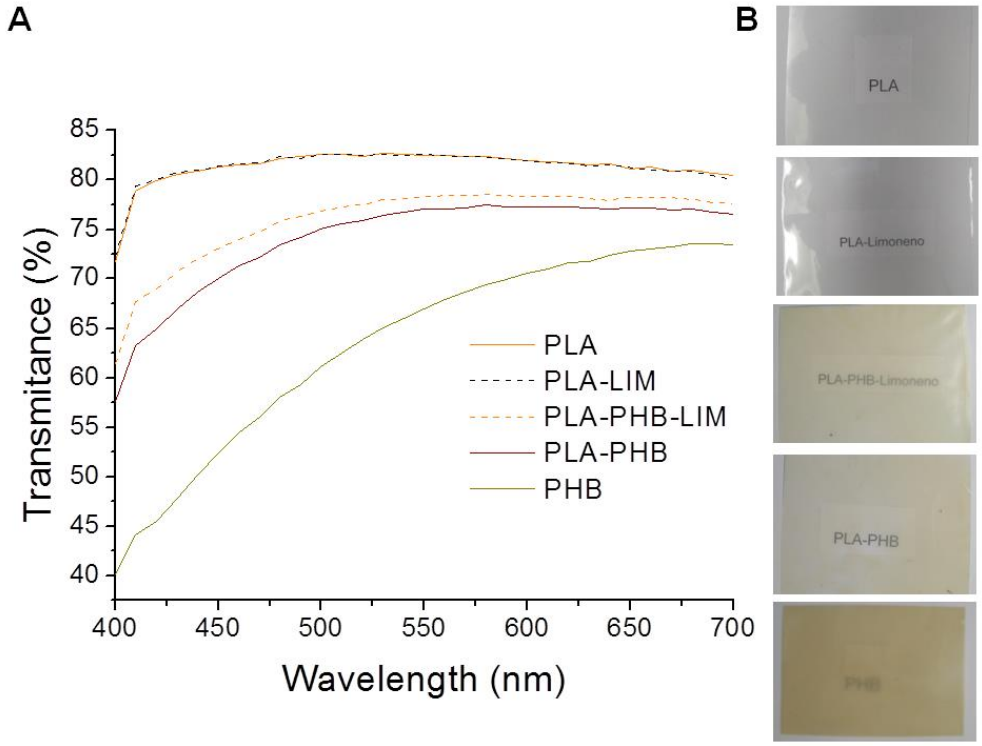


**Figure III.3.1. (A)** Light transmission of films at the range of 400-700 nm. **(B)** Visual aspect of films.

Positive values of coordinate $b^*$ indicate the trend to yellow. All samples containing PHB presented positive values of $b^*$. *YI* was also used to judge the yellowness and neat PHB was the sample with the highest *YI* value. In PLA–PHB blends, *L* value significant decreased with respect to the neat PLA ($p < 0.05$) but it was still showing a high brightness. However, PHB presence produced a stronger tendency towards yellow showing an increment in $b^*$ coordinate and in *YI* value. Meanwhile, $a^*$ coordinate showed a trivial tendency to green. Comparing the total color difference between PLA-PHB and PLA-

PHB-LIM films they resulted not significant different from each other ($p > 0.05$), but they showed a significant difference with respect to neat PLA. Moreover, PLA-PHB-LIM formulation showed a decrease in *YI* and $b^*$ coordinate indicating a somewhat limonene improvement in color properties compared with PLA–PHB blend ($p < 0.05$).

**Table III.3.1.** Colour parameters from CIELab space and YI.

| Formulation | *L* | a* | b* | ΔE | *YI* |
|---|---|---|---|---|---|
| PLA | 94.08 ± 0.07[a] | -1.03 ± 0.01[a] | 1.33 ± 0.05[a] | - | 3.47 ± 0.07[a] |
| PLA-LIM | 93.86 ± 0.10[a] | -0.81 ± 0.17[a] | 1.58 ± 0.04[a] | 0.24 ± 0.04[*] | 3.49 ± 0.10[a] |
| PHB | 83.30 ± 2.16[b] | 1.49 ± 0.87[b] | 22.48 ± 3.34[b] | 23.87 ± 3.99[*] | 45.12 ± 3.15[b] |
| PLA-PHB | 89.09 ± 1.0[c] | -1.29 ± 0.12[a] | 10.95 ± 2.13[c] | 10.84 ± 2.29[*]<br>13.20 ± 3.85[Δ] | 21.74 ± 3.10[c] |
| PLA-PHB-LIM | 90.98 ± 0.25[c] | -1.73 ± 0.02[c] | 8.73 ± 0.11[c] | 8.05 ± 0.19[*]<br>2.95 ± 2.17[Δ] | 17.04 ± 0.02[d] |

[*] Calculated by using PLA colour coordinates as reference.

[Δ] Calculated by using PHB colour coordinates as reference.

[a-d] Different superscripts within the same column indicate significant differences between formulations ($p < 0.05$).

### 3.2. Fourier transformed infrared spectroscopy analysis (FTIR)

The chemical structure of the obtained films was investigated by means FTIR analysis and the obtained spectra are showed in Figure III.3.2-a, being arbitrarily offset for comparison. The spectrum region between 3000 $cm^{-1}$ and 2860 $cm^{-1}$ was characterized by –CH stretching bands showed the characteristic broad absorption of PLA (not shown)[30]. At 1760 $cm^{-1}$ the typical asymmetric stretching of carbonyl group (C═O) in PLA and PLA-LIM films is attributed to lactide [10], while a broad absorption band was observed in neat PHB film attributed to the crystalline carbonyl stretching of PHB [17] and [18]. However, in PLA–PHB binary and ternary films this peak result was narrow and showed the interaction between both polymers. This behavior has been related with the miscibility between PLA and PHB at the selected proportion (75:25) where a transesterification reaction occurred during processing [18]. The –C–O– bond stretching of –CH–O– group of PLA appeared at 1182 $cm^{-1}$[9] and its intensity almost vanished in PLA-PHB blends spectrum. Similar situation was observed in the 1450 $cm^{-1}$ peak, assigned to the lactides – $CH_3$ group [2]. These two peaks intensity decreased with the presence of LIM or PHB, as

expected due to the lesser proportion of PLA in the final formulation showing the lowest intensity in the PLA-PHB-LIM film.

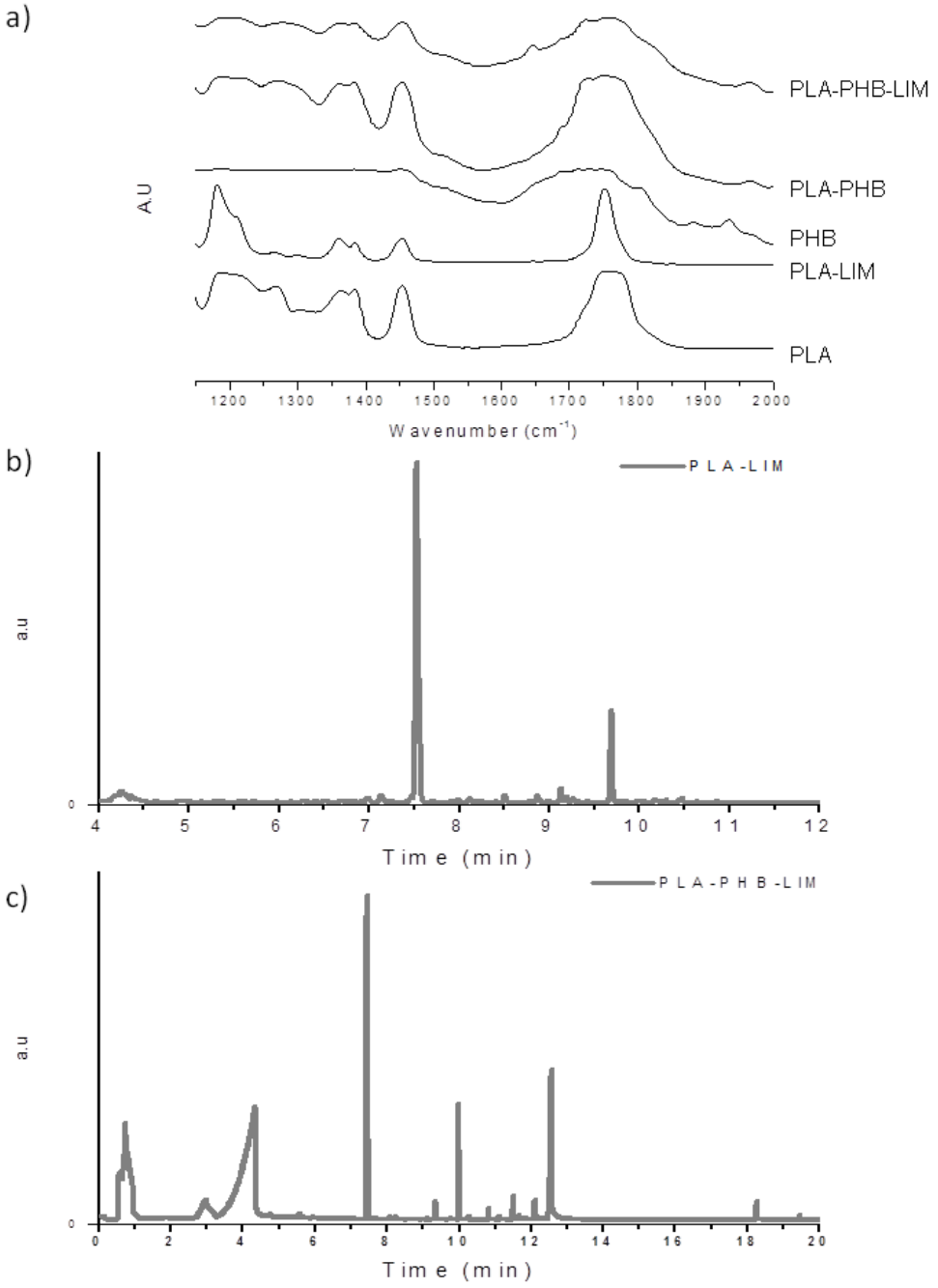


**Figure III.3.2. (a)** FTIR spectra of films.

Pyrogram obtained for: **(b)** PLA-LIM film and **(c)** PLA-PHB-LIM film.

### 3.3. Py-GC/MS characterization and D-limonene amount after processing

Py-GC/MS analysis showed the thermal degradation products of PLA and PHB and also D-limonene presence. Each product was detected and identified by getting the mass

spectra of each main chromatographic peak. Figure III.3.2-b and c show some distinctive peaks of PLA where the peak at 7.5 min in the pyrogram corresponds to D-limonene [10]. Meanwhile the peaks at 9.7 min and the smaller peak at around 9.1 min have been assigned to mesolactide and (L) or (D)-lactide respectively with highly similar mass spectra (with $m/z$ = 32, 43, 45 and 56) [7] and [31]. Furthermore, some more small peaks were present at higher retention time showing the characteristic series of signals attributed to the PLA degradation products with $m/z = 56 + (n \times 72)$ [7], in which $n$ = 1 for mesolactide and (L) or (D)-lactide. The obtained pyrogram of PLA-PHB-LIM (Figure III.3.2 -c) shows the characteristic PHB pyrolysis degradation pattern with a broad peak corresponding to crotonic acid at 4.3 min revealing the characteristic signals $m/z$ = 39, 41, 68, 69, and 86. The peak at 12.6 min as well as the group of smaller peaks appearing between 10.5 min and 12 min could be assigned to the dimmers and trimers of crotonic acid [32] with very similar spectra where their main fragments were those with $m/z$ = 39, 41, 68, 69, 86, 103, 113 and 154, in accordance with previous published works [32] and [33]. The amount of D-limonene after processing was also calculated by Py-GC/MS using our previous developed method to quantify the remaining amount of D-limonene after processing which resulted in 8.90 ± 0.05 wt% for PLA–LIM film [10] and it was higher in the case of PLA-PHB-LIM, 10.45 ± 0.05 wt%. This result confirms that D-limonene was more efficiently retained in PHB incorporated samples (PLA-PHB-LIM) than in PLA–LIM counterpart.

### 3.4. Differential Scanning Calorimetry (DSC)

DSC thermal properties are summarized in Table III.3.2. PHB slightly increased $T_m$ temperature respect to the neat PLA. Materials seem to be compatible since only one $T_g$ was observed in all formulations. In previous work we showed that D-limonene presence induced the depression in $T_g$ of PLA [10]. The plasticization effect of D-limonene was also observed in PLA-PHB-LIM blend where the $T_g$ value decreases about 20 °C.

A reduction in the cold crystallization temperature ($T_{cc}$) was observed for PLA–PHB. This result underlined the compatibility between polymer matrices, where as a result of the decrease in $T_g$ a consequently lowering in the transport barrier for crystallization occurred, which results in a lower crystallization temperature [16]. This behavior was more evident in the case of D-limonene presence with a shift to even lower temperatures. This is in good agreement with Abdelwahab et al. (2012) who studied PLA-PHB blends

plasticized with Lapol 108 and find a reduction in $T_{cc}$ of PLA with an increase in plasticizer content [15].

**Table III.3.2.** Thermal parameters of film samples obtained from TGA and from DSC at the first heating scan

| Formulation | | PLA | PLA-LIM | PHB | PLA-PHB | PLA-PHB-LIM |
|---|---|---|---|---|---|---|
| $\mathbf{T_0}$ (°C) | | 332 | 145 | 268 | 282 | 154 |
| | Stage I | - | 140 | - | | 140 |
| $\mathbf{T_{max}}$ (°C) | Stage II | 366 | 355 | - | 286 | 278 |
| | Stage III | - | - | 285 | 349 | 345 |
| $\mathbf{T_g}$ (°C) | | 59.51 | 30.23 | - | 57.97 | 38.81 |
| $\mathbf{T_{cc}}$ (°C) | | 123,2 | 75.1 | - | 96.9 | 77.4 |
| $\mathbf{T_m}$ (°C) | | 164.2 | 164.2 | 167.7 | 166.7 | 164.9 |
| $\mathbf{\Delta H_{cc}}$ (J/g) | | 23.3 | 19.7 | - | 31.4 | 10.7 |
| $\mathbf{\Delta H_m}$ (J/g) | | 40.0 | 34.2 | 65.9 | 39.9 | 37.6 |
| $\mathbf{\chi_c}$ (%) | | 15.7 | 18.3 | 45.1* | 20.7 | 45.3 |

* $\chi_c$ (%), calculated using $\Delta H_m^c$ of PHB

While $T_m$ values did not change significantly respect to the neat PLA or PLA-PHB blend, the melting behavior showed somewhat differences. Melting consists of two overlapped peaks (Figure III.3.3-a). The temperature of the lower melting peak related to the melting and recrystallization of original crystals into more stable form and the second melting peak a higher temperature is related to melting of more stable crystals [16]. For D-limonene incorporated samples the melting peak became broader. The reason of such behave could be provable due to D-limonene favors the compatibility between PLA and PHB crystallizing simultaneously both type of crystals. During the cooling scan (Figure III.3.3-b) all samples containing PLA presented a jump in the heat flow at around 59 °C which was attributed to the PLA glass transition. PHB and PLA-PHB blends showed an exothermic event corresponding to the cold crystallization with a maximum at 104 °C. Meanwhile, no signals of crystallization process were observed for PLA and PLA-LIM. Moreover, neat PHB film showed its high crystallinity with a high $\chi_c$ (Table III.3.2). The degree of crystallinity augmented from 15.7% to 20.7% when PHB is incorporated into PLA matrix. This behavior is due to PHB can enhance the recrystallization of PLA [18] owing to its ability to act as a nucleating agent [17]. It is known that the presence of plasticizers alters the crystalline structure of PLA [34]. In this study, PLA-PHB-LIM

system reached the highest crystallinity (45.3%). It has been reported that the increase in crystallinity in plasticized PLA-PHB systems could be attributable to the interface interaction between PLA and PHB with the plasticizer, which influences the nucleation and generates a better packaging of segments [15].

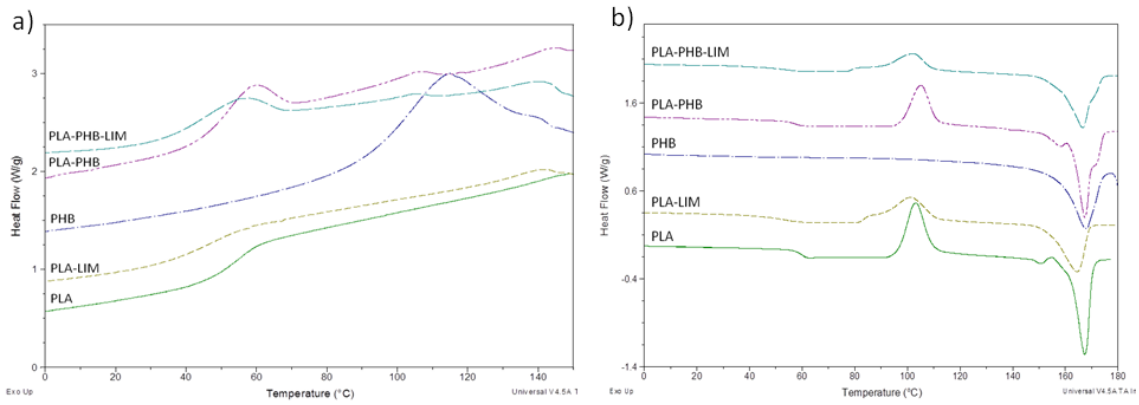


**Figure III.3.3.** DSC thermograms during the (a) cooling scan and (b) second heating scan at 10 °C min−1 for all formulations.

### 3.5. Thermogravimetric analysis (TGA)

The thermal decomposition was studied by TGA and DTG, as shown in Figure III.3.4. One step process was observed for neat PLA and neat PHB. PLA showed the typical decomposition with a maximum degradation rate centered at 366 °C (Figure III.3.4-a). Meanwhile, PHB was less thermal stable with a smaller $T_0$ and $T_{max}$ (Figure III.3.4). PHB decomposes firstly, so when PHB was incorporated into PLA matrix; it decreases the thermal stability of the final film. However, films incorporated with D-limonene showed a first degradation step at about 140 °C and then the thermal degradation of the polymer matrix. There is a loss of D-limonene during the blend procedure which could be estimated from TGA and it is approximately 9% and 8.5% for PLA-LIM and PLA-PHB-LIM, respectively. This result confirms that in ternary systems D-limonene is slightly more efficiently retained. Isothermal experiments were also carried out at 40 °C (not shown) in order to corroborate films stability at eventual working conditions (storage, handling and transport). Moreover, $T_0$ is shifted from 145 °C in PLA-LIM and to 154 °C in ternary systems (PLA-PHB-LIM). D-limonene presences also shift the $T_{max}$ to lower temperatures Figure III.3.4-b) decreasing the thermal stability of the final film. This behavior confirms the interface interactions between both polymer matrices with D-limonene. Moreover, it could be related with some loss of remaining amount of D-limonene. All formulations

showed low pyrolyzate residual wastes at 800 °C, showing a complete degradation and their inherent low environmental impact.

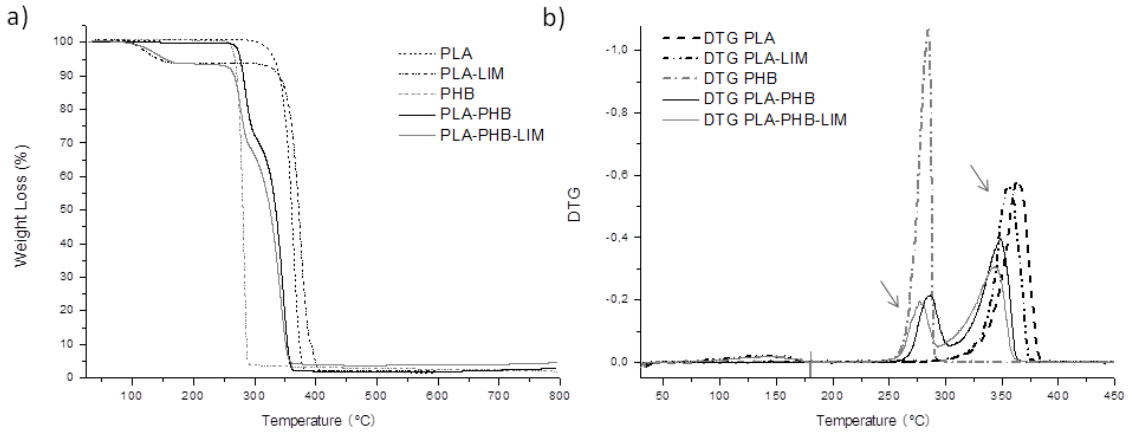


**Figure III.3.4. a)** TGA and **b)** DTG curves of film samples at 10°C $min^{-1}$

### 3.6. Mechanical and nanomechanical characterization

The films intended for food packaging applications are subjected to elongation during the packaging procedure, being important their elastic modulus and elongation characteristics. Furthermore, the stressed films require a minimum of hardness to avoid perforations during their transport and exposition lifecycle. In order to study the final mechanical features after the addition of PHB and plasticizers into PLA matrix, mechanical tests were performed and tensile test results are summarized in Table III.3.3.

**Table III.3.3.** Tensile properties of films (n=5) and oxygen permeation rate of films (n=3).

| **Formulation** | $\varepsilon_{B\%}$ (%) | ***TS*** (MPa) | ***E*** (MPa) | **OTR.*e*** ($cm^3mm$ / $m^2day$) |
|---|---|---|---|---|
| PLA | 1.5 ± 0.3[a] | 38.5 ± 2.3[a] | 1150 ± 100[a] | 44.4 ± 0.9[a] |
| PLA-LIM | 151.7 ± 0.6[b] | 24.6 ± 2.0[b] | 840 ± 30[b] | 84.0 ± 4.9[b] |
| PHB | 2.0 ± 0.4[a] | 48.8 ± 5.3[a] | 1670 ± 50[c] | 11.5 ± 4.7[c] |
| PLA-PHB | 2.1 ± 0.4[a] | 21.3 ± 6.9[b] | 1390 ± 100[d] | 24.9 ± 3.8[d] |
| PLA-PHB-LIM | 8.0 ± 0.2[c] | 20.7 ± 1.4[b] | 630 ± 20[e] | 53.9 ± 2.3[a] |

[a-e] Different superscripts within the same column indicate significant differences between formulations ($p < 0.05$).

PLA–PHB films showed Young modulus significant higher than neat PHB and neat PLA ($p > 0.05$). This result highlights the effect of PHB as nucleating agent for PLA. On the

other hand, the introduction of D-limonene into the system provoked a significant reduction in Young modulus and tensile strength. Systems without D-limonene presented low elongation; meanwhile films containing limonene significant increased their $\varepsilon_{B\%}$ values showing its efficiency as plasticizer. This result is in a good accordance with DSC results. Elongation was greatly increased for PLA-LIM sample resulting in superior flexibility than PLA-PHB-LIM ($p > 0.05$), in accordance with $T_g$ tendency.

The indentation elastic modulus ($E_r$) was also obtained by nanoindentation technique. This technique obtains the elastic and hardness features of small volumes of material of thin films performing indentations at very low loads [35]. The $E_r$ values obtained for each film are shown in Figure III.3.5-a.

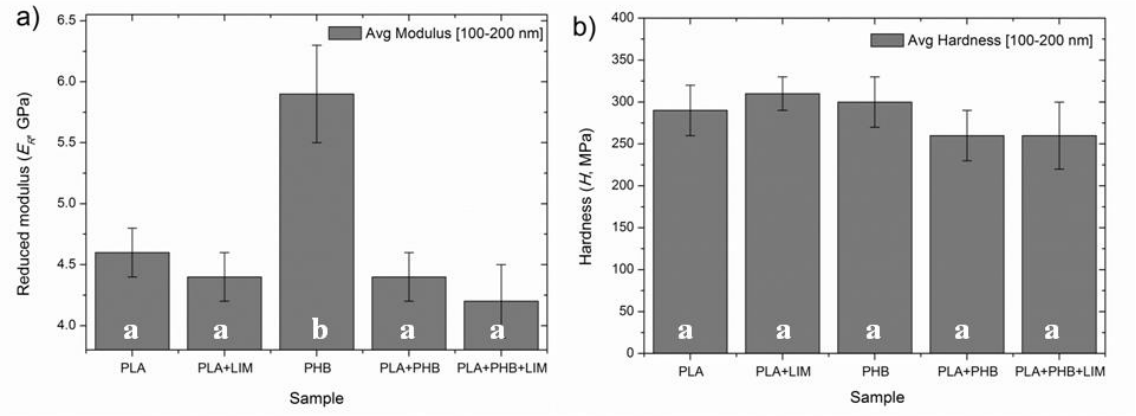


**Figure III.3.5.** Nanoindentation modulus **(a)** and hardness **(b)** results averaged between the 100nm and 200nm in depth.

[a-b] Different letters on the bars within the same image indicate significant differences between formulations ($p < 0.05$).

The significant higher values obtained by nanoindentation compared with those obtained by tensile test is probably due to the creep character of polymers [36] and because while the entire film is deformed under a tensile stress test, only a very small volume of material is assayed by nanoindentation. These results corroborate that the addition of D-limonene reduces the elastic modulus, showing its plasticizer role. The highest modulus was found for the PHB film ($p > 0.05$) due to its greater crystallinity, indicating that the reinforcement effect of the PHB in PLA matrix plays an important role in the tensile deformation. Nanoindentation results for PLA-PHB blend show the influence of PLA concentration. The nanoindentation hardness results (Figure III.3.5-b) revealed similar average results with slightly or unappreciable differences ($p < 0.05$) between samples which values are in the range of 275–350 MPa.

### 3.7. Morphological characterization

Films surfaces were observed by Optical Microscopy and micrograph observations are shown in Figure III.3.6-A. All films formulations showed mostly homogeneous surfaces with no apparent phase separation as evidenced from optical (Figure III.3.6-A) and SEM (Figure III.3.6-B) observations.

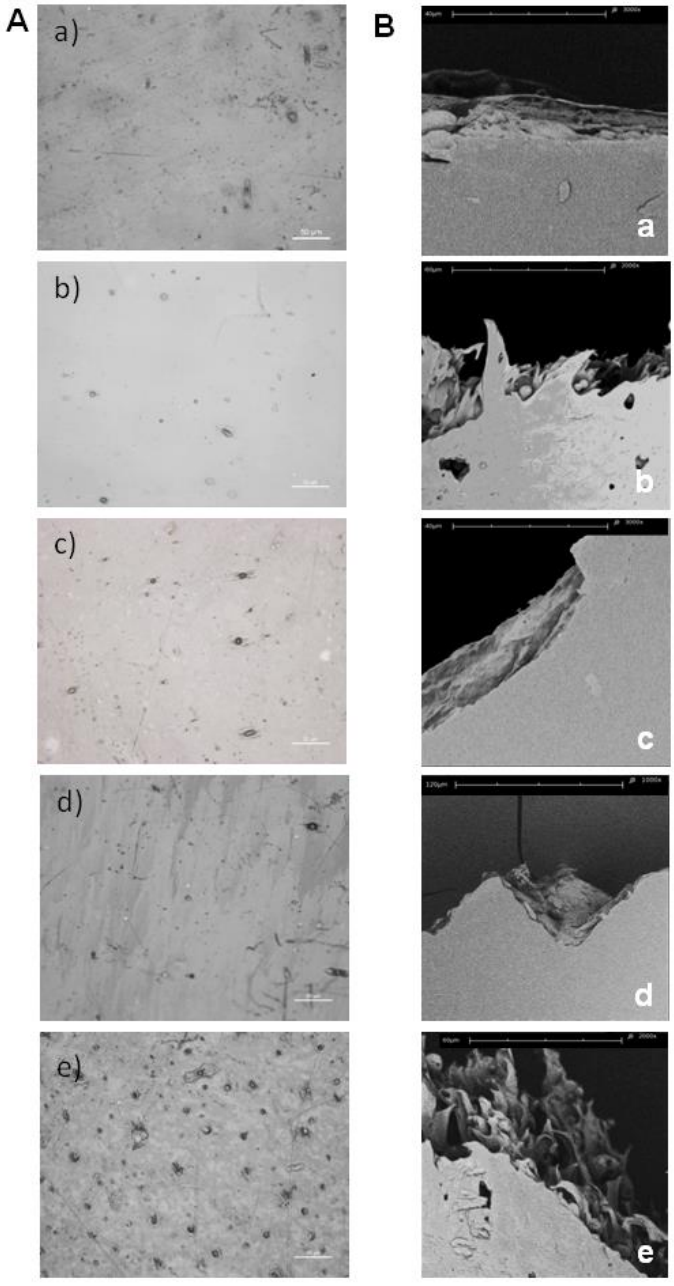


**Figure III.3.6. (A)** Optical microscope 3D surface images of films (20 x): **a)** PLA, **b)** PLA-LIM, **c)** PHB, **d)** PLA-PHB, **e)** PLA-PHB-LIM.
**(B)** SEM images of the tensile fracture surfaces of a) PLA, b) PLA-LIM, c) PHB, d) PLA-PHB and e) PLA-PHB-LIM films.

SEM images were taken on the fracture surfaces of films after the tensile tests (Figure III.3.6-B). Neat PLA, neat PHB and PLA-PHB films (Figure III.3.6-B.a, c and d) showed a smooth fracture where no plastic region could be observed. Meanwhile, the expected plastic fracture was observed in PLA-LIM film (Figure III.3.6-B.b) since D-limonene significantly influences PLA morphological structure [10]. A similar plastic behavior was observed in PLA-PHB-LIM sample (Figure III.3.6-B.e) showing the effectiveness of D-limonene to plasticize the PLA-PHB blend.

Films surfaces were also studied by means confocal microscopy (Figure III.3.9-A) While smooth surfaces were showed by PLA and PLA-LIM films, neat PHB (Figure III.3.9-A.c) was characterized by the presence of small particles that could be associated with the crystals owing to the highly crystalline matrix of PHB. In PLA-PHB blend (Figure III.3.9-A.d) it could be notice that small crystal phases of PHB were well dispersed in the continuous amorphous PLA phase. Figure III.3.9-A.e shows the ternary PLA-PHB-LIM system and reveals homogeneous distribution of D-limonene within both PLA and PHB matrices among reduced PHB crystals.

### 3.8. Oxygen permeability

The oxygen transmission rate was studied and the obtained results are shown in Table 3. It is well known that plasticizers addition increases the free volume in PLA matrix [37] and as a result a reduction in the oxygen barrier properties is produced. In a previous work we reported an enhance in PLA chains mobility caused by D-limonene presence and consequently an augment in OTR.*e* values with increasing amount of D-limonene [10]. In the present work, while D-limonene increased the oxygen permeation, it was considerably reduced with the addition of PHB (Table III.3.3). This improvement in the resistance to oxygen transmission is due to the small dispersed phases of PHB in PLA matrix reduces the solubility of gases in film, resulting in a more tortuous path for oxygen molecules to transport through the film [11] and [38]. The OTR·*e* value of PLA–PHB was in the same order of magnitude as the values found in the literature for nanoreinforced PLA films [39] and [40]. The combination of the improvement in oxygen barrier properties generated by PHB presence owing the development of crystalline order with the contrary effect produced by limonene leads to a good result for the final ternary system (PLA-PHB-LIM) showing comparable values as the neat PLA and besides acceptable values for film food packaging applications.

### 3.9. Wettability

It was already discussed that water resistant is an important issue in materials intended for food contact. Thus, water contact angle measurements were conducted to study the water absorption of film surfaces. Smaller water contact angle values than 65° obtained for neat PLA film ($\theta_{PLA}$ = 58 ± 3) implies a hydrophilic surface [41], while the addition of D-Limonene with hydrophobic nature caused an increase in the water contact angle ($\theta_{PLA-LIM}$ = 75 ± 1)[10] showing an hydrophobic surface character of film. As well, D-limonene caused an increase in the surface hydrophobicity of ternary systems being the PLA-PHB-LIM films slightly ($p < 0.05$) more hydrophobic ($\theta_{PLA-PHB-LIM}$ = 74 ± 1) with respect to that of PLA-PHB blend ($\theta_{PLA-PHB}$ = 70 ± 1).

### 3.10. Disintegration under composting conditions

Disintegration under composting conditions of all film samples was also studied. Visual appearance of the recovered films at different disintegration days of exposure to composting conditions are shown in Figure III.3.7-a. It was observed that PLA films samples changed their color and became more opaque after 7 days in accordance with Fortunati and colleagues [9]. Figure III.3.7-b shows the degree of disintegration as a function of time in which the line at 90% of disintegrations represents the goal of disintegrability test [9]. Neat PHB reached only to 1.5% after 35 days under composting. It has been reported that neat PHB needs approximately six weeks to be disintegrated in compost [42]. The rate of disintegration under composting conditions was longer for PLA-PHB with respect to PLA counterparts. In this sense, while formulations without PHB addition were disintegrated in 28 days, PLA–PHB needed 35 days to overcome the 90% of disintegrability. This is because of the crystalline phase of PHB presents a slower degradation rate compared with PLA amorphous phase. The kinetic of disintegration is mainly ruled by the amorphous phase [43], thus the more amorphous PLA-PHB blend was easily disintegrated in 35 days while no significant weight loss was observed in PHB film.
Regarding D-limonene added samples, it was observed that disintegration got higher in D-limonene incorporated films, particularly noticeable for PLA-PHB-LIM ternary system. While PLA-PHB reached 12% of disintegration in 21 days PLA-PHB-LIM showed two times higher rate of disintegration and it reached the goal of disintegration in 28 days whereas PLA-PHB still was in 50% of disintegration.

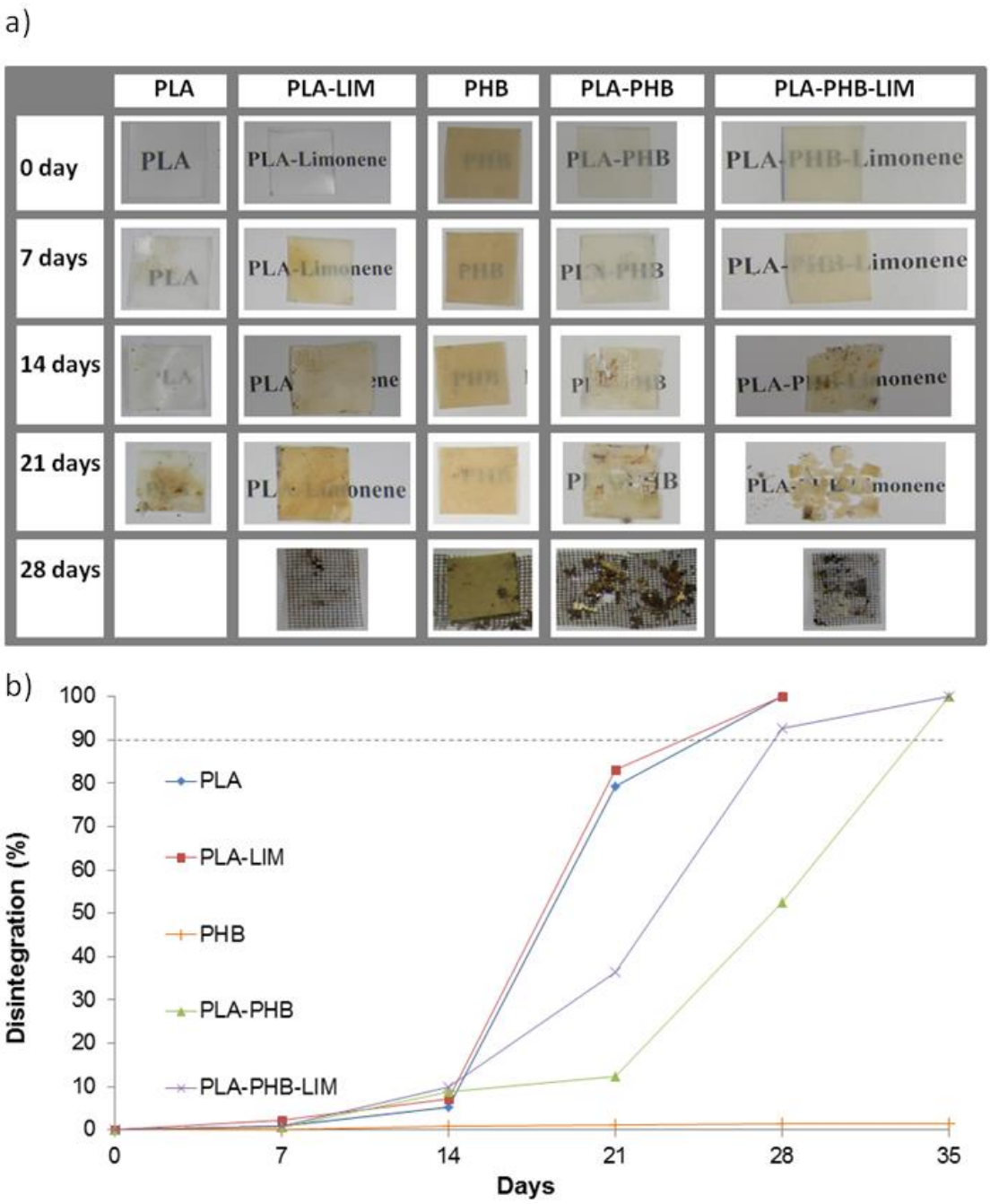


**Figure III.3.7. a)** Visual appearance of film samples before and after different recovered days of disintegration under composting conditions.

**b)** Degree of disintegration of films under composting conditions as a function of time.

This was confirmed by TG and DTG results before and after different exposed times to composting conditions as shown Table III.3.4. The D-limonene amount was reduced from 6%, 3.5%, 2.5% to 2% in PLA–LIM binary systems (PLA-LIM) at 0, 7, 14 and 21 days under composting, correspondingly. Meanwhile, D-limonene amount is reduced

from 6.5%, 2%, 1.5% to 1% in ternary systems (PLA-PHB-LIM) at 0, 7, 14 and 21 days under composting, respectively.

**Table III.3.4.** TGA and DTG results for films at different time of disintegration

| *Formulation* | **Time** (Day) | **$T_0$** (°C) | **$T_{max}$ LIM** (°C) | **$T_{max}$ PHB** (°C) | **$T_{max}$ PLA** (°C) |
|---|---|---|---|---|---|
| **PLA** | 0 | 332 | - | - | 366 |
| | 7 | 331 | - | - | 363 |
| | 14 | 261 | - | - | 346 |
| | 21 | 240 | - | - | 341 |
| **PLA-LIM** | 0 | 145 | 140 | - | 355 |
| | 7 | 240 | 138 | - | 360 |
| | 14 | 247 | 138 | - | 353 |
| | 21 | 237 | 136 | - | 341 |
| **PHB** | 0 | 268 | - | 285 | - |
| | 7 | 273 | - | 288 | - |
| | 14 | 273 | - | 287 | - |
| | 21 | 272 | - | 286 | - |
| **PLA-PHB** | 0 | 282 | - | 286 | 349 |
| | 7 | 268 | - | 283 | 353 |
| | 14 | 229 | - | 265 | 304 |
| | 21 | 230 | - | 256 | 298 |
| **PLA-PHB-LIM** | 0 | 154 | 140 | 278 | 345 |
| | 7 | 250 | 139 | 276 | 345 |
| | 14 | 238 | 138 | 275 | 325 |
| | 21 | 241 | 138 | 260 | 323 |

At 7 days of incubation, the $T_0$ of D-limonene incorporated samples greatly increased with respect to their initial values as a consequence of a high loss of D-limonene. In addition, $T_0$ and $T_{max}$ decreased to lower temperatures with the degradation time increased for all formulations, with the exception of neat PHB. During the initial phases of disintegration, as a result of water absorption [8] the high molecular polyester chains hydrolyzed to smaller molecules [8], [9] and [44] which are more susceptible for microorganisms to enzymatic reactions [8] and [45] and also presented less thermal stability. This result is in agreement with degree of disintegration test results (Figure

III.3.7-b) in which it is noticeable that samples with D-limonene (PLA-LIM and PLA-PHB-LIM) were disintegrated previously than their counterparts without D-limonene (PLA and PLA-PHB). This behavior was more evident in the ternary system, where the D-limonene's losses produced some weakness in the packaging of segments among PLA and PHB matrices.

The recovered samples were also pyrolyzed at 1000 °C for 0.5 s and the pyrolyzates were identified by means GC/MS. The Py-GC/MS chromatogram of PLA, PLA-LIM, PLA-PHB and PLA-PHB-LIM samples (not shown) revealed the presence of the two characteristic peaks of pyrolysis of PLA assigned to mesolactide and (L) or (D)-lactide already commented [7]. The relationship between meso-lactide and lactide peaks was reported as a semi-quantitative sign of the degradation mechanism of PLA in biotic media [24], [31], and [46]. In the present work, before the composting all PLA based composites showed that lactide was the dominant oligomer. Whereas, the ratio of meso-lactide to lactide decrease during composting time (Table III.3.5) suggesting that meso-lactide form increased in the polymer matrix during the compost incubation. This result is because of microorganisms prefer de L-lactide than D-lactide form, thus the decrease in L-lactide in the polymer matrix influences the formation of meso-lactide during high pyrolysis temperatures [24].

It seems that during the disintegration under composting conditions the biodegradable polymers degradation is caused by surface hydrolysis [47]. Therefore, in order to clarify the possible disintegration in the aspect of films surfaces, they were observed by optical and scanning electron microscopy. Micrographs observations after 21 days in composting are shown in Figure III.3.8. No evident signs of disintegration after 21 days of incubation were observed for net PHB (Figure III.3.8-A.c) in well accordance with the measured disintegration (Figure III.3.7-b). The rest of films showed a homogeneous surface aspect before exposed to composting (Figure III.3.6-A). Nevertheless, it was observed that after 21 days in composting the surfaces became breakable. This behavior was strong noticeable for neat PLA and PLA–PHB blends which displayed evident surface signs of disintegration by means of deeper fractures, Figure III.3.8.A.a and Figure III.3.8-A.d, respectively. SEM observations (Figure III.3.8-B) showed that after 21 days in composting PLA–LIM Figure III.3.8-B.b shows deep fractures on the surface more evident than in the other films, followed by neat PLA Figure III.3.8-B.a and then by ternary PLA–PHB–LIM (Figure III.3.8-B.d) in agreement with degree of disintegration test results (Figure III.3.7-b).

**Table III.3. 6.** Roughness parameters registered by the confocal microscope on films' surfaces and meso-lactide : lactide ratio obtained by Py-GC/MS before and after 21 days in composting conditions.

| | **$P_a$** (um) | | **$P_q$ RMS** (um) | | ***meso*-lactide : lactide** | | **Reduction in *meso*-lactide : lactide** (%) |
|---|---|---|---|---|---|---|---|
| **Exposed time** (days) | **0** | **21** | **0** | **21** | **0** | **21** | **21** |
| **PLA** | 0.31 | 1.51 | 0.38 | 1.93 | 1 : 3.1 | 1 : 1.7 | 46.2 |
| **PLA-LIM** | 0.85 | 2.72 | 1.22 | 3.32 | 1 : 11.3 | 1 : 6.8 | 40 |
| **PHB** | 2.62 | 2.77 | 3.41 | 3.69 | - | - | - |
| **PLA-PHB** | 2.03 | 1.89 | 2.89 | 2.58 | 1 : 7.9 | 1 : 2.6 | 66.7 |
| **PLA-PHB-LIM** | 1.38 | 4.19 | 2.15 | 5.26 | 1 : 5.0 | 1 : 2.8 | 44.3 |

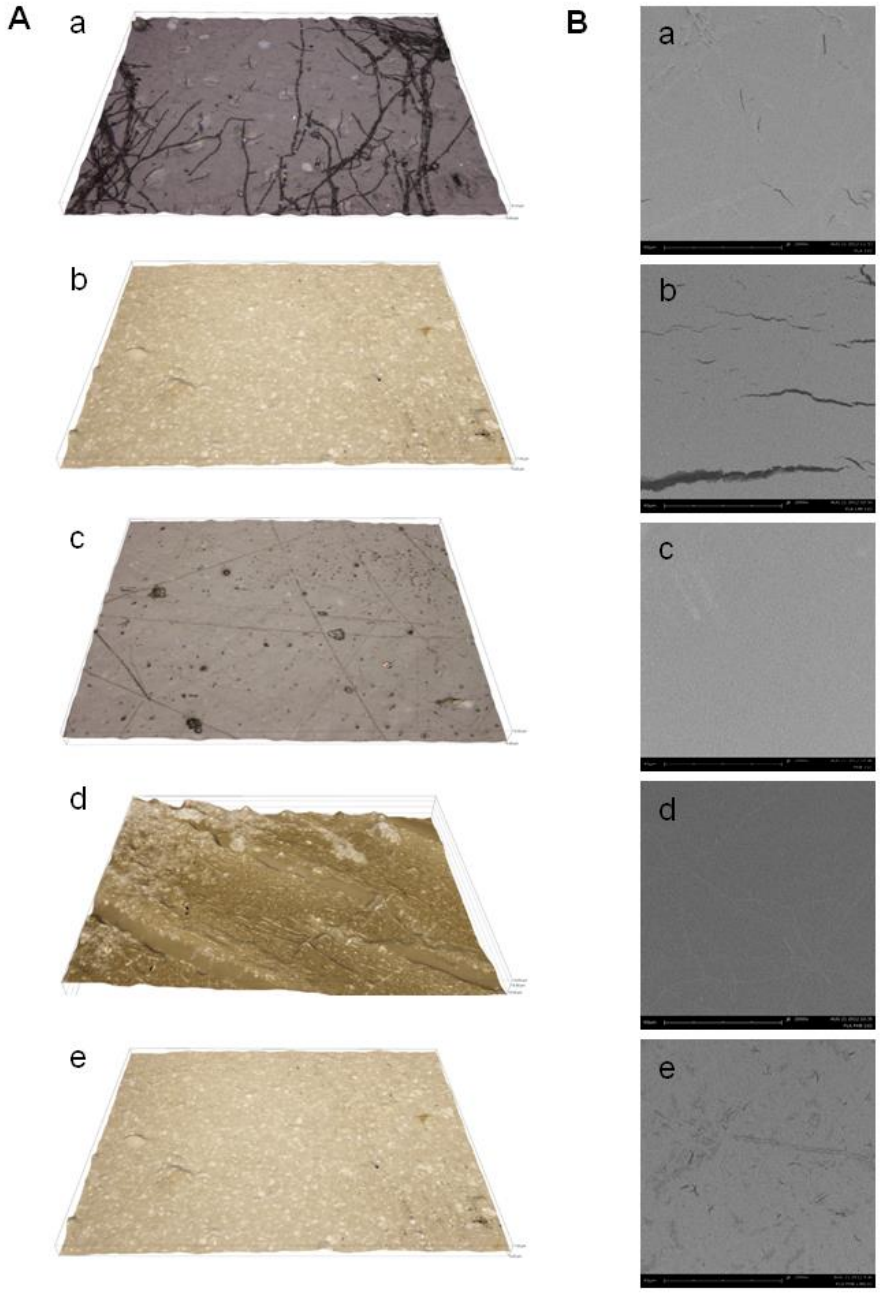


**Figure III.3.8.** Surface of films after 21 days under composting exposure

**(A)** Optical microscope images of the (20 x). **a)** PLA $t_{21}$, **b)** PLA-LIM $t_{21}$, **c)** PHB $t_{21}$, **d)** PLA-PHB $t_{21}$ and **e)** PLA-PHB-LIM $t_{21}$.The 3D surface Images were acquired by extended depth field method.

**(B)** SEM observations (2000 x) of **a)** PLA $t_{21}$, **b)** PLA-LIM $t_{21}$, **c)** PHB $t_{21}$, **d)** PLA-PHB $t_{21}$ and **e)** PLA-PHB-LIM $t_{21}$

In order to resolve with more details the different states of the films surfaces it were studied by means confocal microscopy (Figure III-3.9).

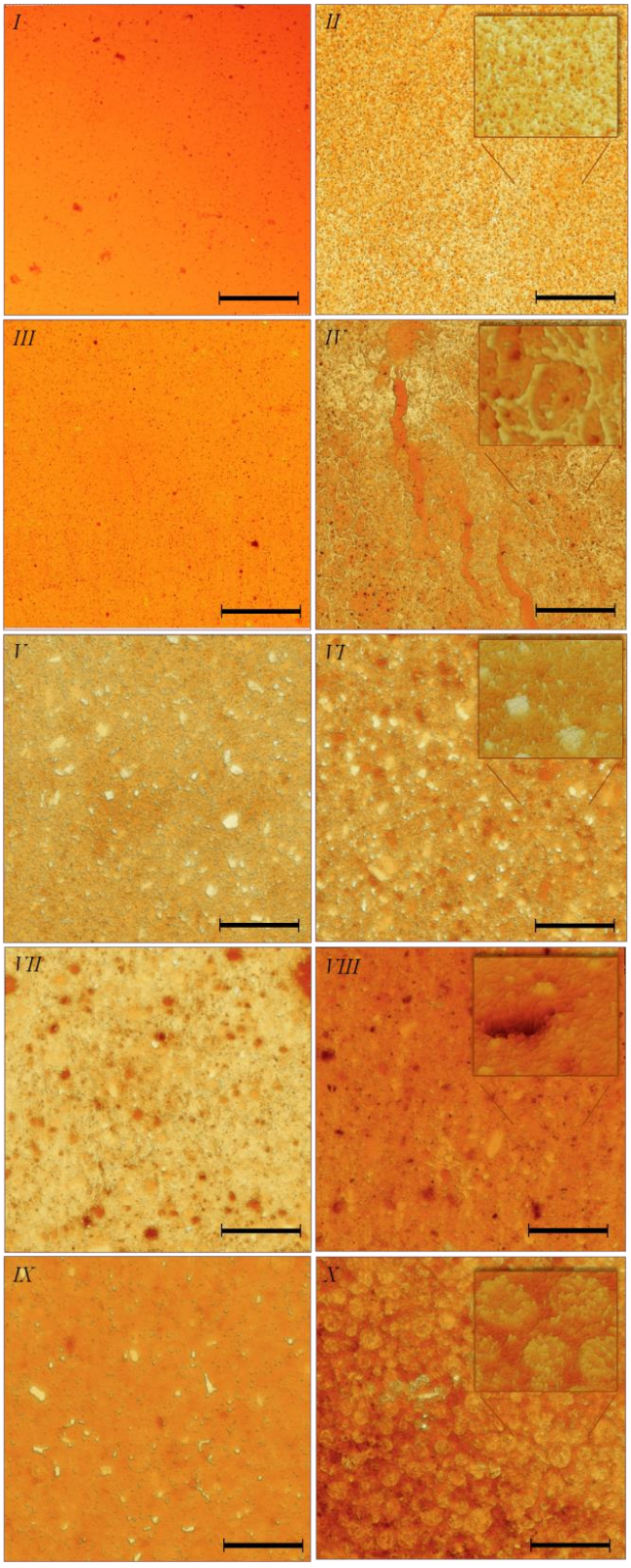


**Figure III-3.9.** Confocal images of films before ($t_0$) and after 21 days ($t_{21}$) under composting exposure. The bar scale corresponds to 50 μm.
**I)** PLA $t_0$, **II)** PLA $t_{21}$, **III)** PLA-LIM $t_0$, **IV)** PLA-LIM $t_{21}$, **V)** PHB $t_0$, **VI)** PHB $t_{21}$, **VII)** PLA-PHB $t_0$, **VIII)** PLA-PHB $t_{21}$, **IX)** PLA-PHB-LIM $t_0$ and **X)** PLA-PHB-LIM $t_{21}$.
Inset figures are details of surfaces at a higher magnification.

This technique confirmed that films with D-limonene, PLA-LIM (Figure III-3.9-IV) and PLA–PHB–LIM (Figure III-3.9-X), after 21 days in composting presented large fissures. This could be explained due to the loss of D-limonene which accelerated the hydrolysis process of the ester linkage. It was also established that PHB delayed the PLA disintegration because of while larger differences were observed between PLA before (Figure III-3.9-I) and after 21 days in compost (Figure III-3.9-II), no big differences were observer in neat PHB film were the structure is characterized by the presence of small spherulites related with the highly crystalline matrix of PHB (Figure III-3.9-V and VI). Additionally, PLA–PHB film presented somewhat differences before (Figure III-3.9-VII) and after (Figure III-3.9-VIII) exposition to compost stating that the amorphous phase of PLA ruled the disintegration of the blend.

The visual aspect quality of films is also governed by their smoothness. The surface profiles from confocal examination were studied and recorded (Figure III-3.10).

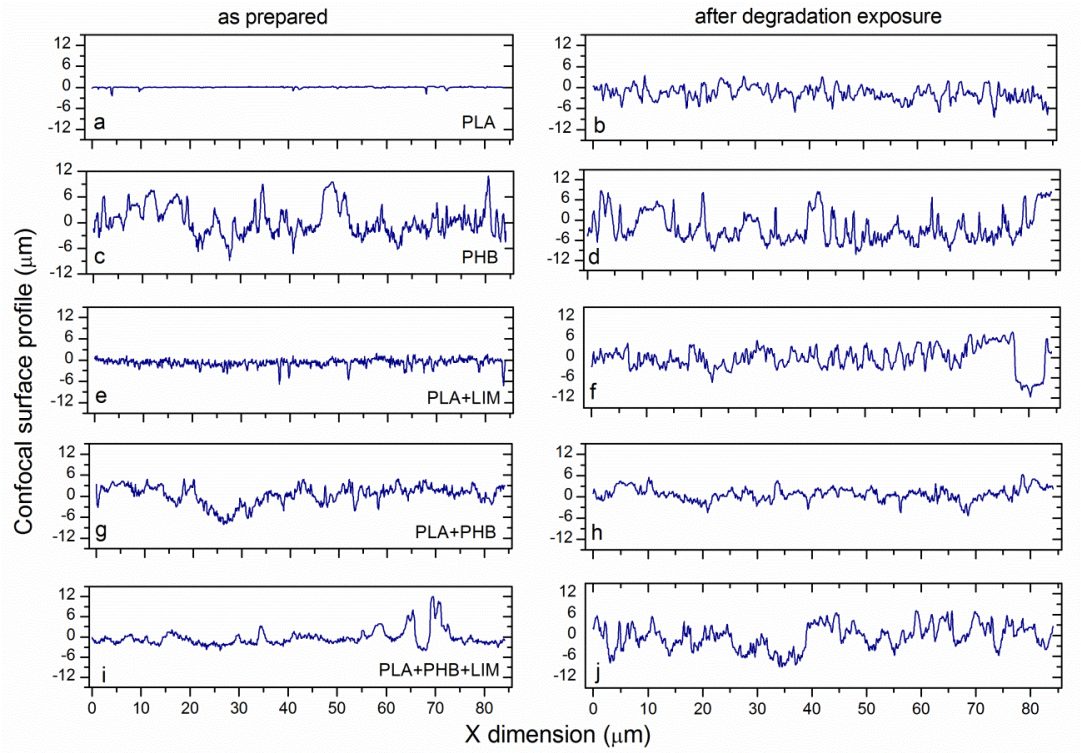


**Figure III.3.10.** Confocal profiles of films before and after 21 days under composting.

Firstly, it is noticeable the difference in roughness profile measured on undisintegrated films. While the neat PLA film shows the smoothest surface and neat PHB the roughest, the addition of D-limonene to PLA seems to have a low effect on this parameter. For an easier comparison, Table III.3.5 resumes the roughness parameters recorded by the confocal microscope for each analyzed surface, being $P_a$ the arithmetic

average of the profile (average height) and $P_q$ the quadratic average of the profile, following ISO 4287 definitions [48]. These curves reveal that films after 21 days under composting exposure have much higher roughness with great ridges and valleys, indicating preferential localized zones disintegration.

## 4. CONCLUSIONS

PLA and PHB were successfully melt blended and incorporated with D-limonene to obtain transparent films. While structural characterization indicate that there is a molecular interaction between PLA and PHB blends, DSC analysis revealed that blends were miscible showing only one $T_g$ which decreased with D-limonene addition and also the reinforcing effect of PHB. The ability of PHB to act as a nucleating agent made evident an improvement in PLA oxygen barrier properties where the addition of D-limonene resulted in an increase of oxygen permeation. Moreover, the surface wettability was also increased in PLA-PHB-LIM due to the combination of the increase in the crystallinity and the hydrophobic character provided by PHB and D-limonene, respectively. Morphological studies showed a well dispersion of PHB crystals in the amorphous PLA matrix and also that D-limonene generates a better packaging. D-limonene is more efficient retained after processing in ternary PLA-PHB-LIM than in binary PLA-LIM. Tensile tests underlined that the addition of D-limonene produced plasticization because of D-limonene incorporated films presented some characteristic of flexible materials, whereas nanoindentation showed that hardness did not present big differentiation between film formulations. The disintegrability under composting conditions revealed that while D-limonene facilitated the hydrolysis process, PHB delays the disintegration of PLA matrix. The rate of disintegration was longer for PLA-PHB blends with respect to PLA counterparts due to the increased crystal phase and the surface water resistant. However, all formulations resulted fully disintegrated under composting in times compatible with the regular composting time. According to all these results, it can be said that the combination of PLA-PHB blend (75:25) with the addition of D-limonene may offer good perspective for transparent flexible films, with enhanced oxygen barrier and water resistant properties, biodegradable in compost, and therefore suitable for biodegradable food packaging applications.

**Acknowledgements**

This work has been supported by the Spanish Ministry of Science and Innovation (MAT2011-28468-C02-01 and MAT2011-28468-C02-02). M.P. Arrieta is granted by Santiago Grisolía program (GRISOLIA/2011/007). Authors gratefully acknowledge Prof. Alfonso Jiménez (University of Alicante) for his assistance with OTR measurements and Prof. Mª Dolores Salvador (Polytechnic University of Valencia) for her assistance with nanomechanical and optical microscope analysis.

**REFERENCES**

[1] Fortunati E, Armentano I, Zhou Q, Iannoni A, Saino E, Visai L, et al. Multifunctional bionanocomposite films of poly(lactic acid), cellulose nanocrystals and silver nanoparticles. Carbohydrate Polymers. 2012;87(2):1596-1605.

[2] Auras R, Harte B, Selke S. An overview of polylactides as packaging materials. Macromolecular Bioscience. 2004;4(9):835-864.

[3] Boonyawan D, Sarapirom S, Tunma S, Chaiwong C, Rachtanapun P, Auras R. Characterization and antimicrobial properties of fluorine-rich carbon films deposited on poly(lactic acid). Surface & Coatings Technology. 2011;205:S552-S557.

[4] Molinaro S, Cruz Romero M, Boaro M, Sensidoni A, Lagazio C, Morris M, et al. Effect of nanoclay-type and PLA optical purity on the characteristics of PLA-based nanocomposite films. Journal of Food Engineering. 2013;117(1):113-123.

[5] Rhim JW, Lee JH, Hong SI. Increase in water resistance of paperboard by coating with poly(lactide). Packaging Technology and Science. 2007;20(6):393-402.

[6] Auras RA, Singh SP, Singh JJ. Evaluation of oriented poly(lactide) polymers vs. existing PET and oriented PS for fresh food service containers. Packaging Technology and Science. 2005;18(4):207-216.

[7] Arrieta MP, Parres F, López J, Jiménez A. Development of a novel pyrolysis-gas chromatography/mass spectrometry method for the analysis of poly(lactic acid) thermal degradation products. Journal of Analytical and Applied Pyrolysis. 2013;101:150-155.

[8] Kale G, Auras R, Singh SP. Comparison of the degradability of poly(lactide) packages in composting and ambient exposure conditions. Packaging Technology and Science. 2007;20(1):49-70.

[9] Fortunati E, Armentano I, Iannoni A, Barbale M, Zaccheo S, Scavone M, et al. New multifunctional poly(lactide acid) composites: Mechanical, antibacterial, and degradation properties. Journal of Applied Polymer Science. 2012;124(1):87-98.

[10] Arrieta MP, López J, Ferrándiz S, Peltzer MA. Characterization of PLA-limonene blends for food packaging applications. Polymer Testing. 2013;32(4):760-768.

[11] Lahtinen K, Kotkamo S, Koskinen T, Auvinen S, Kuusipalo J. Characterization for water vapour barrier and heat sealability properties of heat-treated paperboard/polylactide structure. Packaging Technology and Science. 2009;22(8):451-460.

[12] Imre B, Pukanszky B. Compatibilization in bio-based and biodegradable polymer blends. European Polymer Journal. 2013;49(6):1215-1233.

[13] Bucci DZ, Tavares LBB, Sell I. Biodegradation and physical evaluation of PHB packaging. Polymer Testing. 2007;26(7):908-915.

[14] Bittmann B, Bouza R, Barral L, Diez J, Ramirez C. Poly(3-hydroxybutyrate-co-3-hydroxyvalerate)/clay nanocomposites for replacement of mineral oil based materials. Polymer Composites. 2013;34(7):1033-1040.

[15] Abdelwahab MA, Flynn A, Chiou B-S, Imam S, Orts W, Chiellini E. Thermal, mechanical and morphological characterization of plasticized PLA-PHB blends. Polymer Degradation and Stability. 2012;97(9):1822-1828.

[16] Bartczak Z, Galeski A, Kowalczuk M, Sobota M, Malinowski R. Tough blends of poly(lactide) and amorphous poly([R,S]-3-hydroxy butyrate) - morphology and properties. European Polymer Journal. 2013.

[17] Furukawa T, Sato H, Murakami R, Zhang J, Duan YX, Noda I, et al. Structure, dispersibility and crystallinity of poly (hydroxybutyrate)/ poly(l-lactic acid) blends studied by FT-IR microspectroscopy and differential scanning calorimetry. Macromolecules. 2005;54:3593.

[18] Zhang M, Thomas NL. Blending polylactic acid with polyhydroxybutyrate: The effect on thermal, mechanical, and biodegradation properties. Advances in Polymer Technology. 2011;30(2):67-79.

[19] Wilbon PA, Chu F, Tang C. Progress in renewable polymers from natural terpenes, terpenoids, and rosin. Macromolecular Rapid Communications. 2013;34(1):8-37.

[20] Marin AB, Acree TE, Hotchkiss JH, Nagy S. Gas-Chromatography olfactometry of orange juice to assess the effects of plastic polymers on aroma character. Journal of Agricultural and Food Chemistry. 1992;40(4):650-654.

[21] Fisher K, Phillips C. Potential antimicrobial uses of essential oils in food: is citrus the answer? Trends in Food Science & Technology. 2008;19(3):156-164.

[22] Firdaus M, Montero De Espinosa L, Meier MAR. Terpene-based renewable monomers and polymers via thiol-ene additions. Macromolecules. 2011;44(18):7253-7262.

[23] Fortunati E, Puglia D, Santulli C, Sarasini F, Kenny JM. Biodegradation of Phormium tenax/poly(lactic acid) composites. Journal of Applied Polymer Science. 2012;125(SUPPL. 2):E562-E572.

[24] Khabbaz F, Karlsson S, Albertsson AC. Py-GC/MS an effective technique to characterizing of degradation mechanism of poly (L-lactide) in the different environment. Journal of Applied Polymer Science. 2000;78(13):2369-2378.

[25] Gamez-Perez J, Velazquez-Infante JC, Franco-Urquiza E, Pages P, Carrasco F, Santana OO, et al. Fracture behavior of quenched poly(lactic acid). Express Polymer Letters. 2011;5(1):82-91.

[26] Corre YM, Bruzaud S, Audic JL, Grohens Y. Morphology and functional properties of commercial polyhydroxyalkanoates: A comprehensive and comparative study. Polymer Testing. 2012;31(2):226-235.

[27] ASTM. Standard test method for tensile properties of thin plastic sheeting, standards designation: D882-01 Philadelphia, USA.2001.

[28] AENOR. Determination of the degree of disintegration of plastic materials under simulated composting conditions in a laboratory-scale test. UNE EN ISO 220002006.

[29] Martucci JF, Ruseckaite RA. Biodegradation of three-layer laminate films based on gelatin under indoor soil conditions. Polymer Degradation and Stability. 2009;94(8):1307-1313.

[30] Siracusa V, Blanco I, Romani S, Tylewicz U, Rocculi P, Dalla Rosa M. Poly(lactic acid)-modified films for food packaging application: Physical, mechanical, and barrier behavior. Journal of Applied Polymer Science. 2012;125:E390-E401.

[31] Arrieta MP, Parres García FJ, López Martínez J, Navarro Vidal R, Ferrándiz S. Pyrolysis of Bioplastic waste: Obtained poducts from Poly(lactic Acid). DYNA. 2012;87(4):395-399.

[32] Aoyagi Y, Yamashita K, Doi Y. Thermal degradation of poly[(R)-3-hydroxybutyrate], poly[ε-caprolactone], and poly[(S)-lactide]. Polymer Degradation and Stability. 2002;76(1):53-59.

[33] Ariffin H, Nishida H, Shirai Y, Hassan MA. Anhydride production as an additional mechanism of poly(3-hydroxybutyrate) pyrolysis. Journal of Applied Polymer Science. 2009;111(1):323-328.

[34] Liu L, Jin TZ, Coffin DR, Hicks KB. Preparation of Antimicrobial Membranes: Coextrusion of Poly(lactic acid) and Nisaplin in the Presence of Plasticizers. Journal of Agricultural and Food Chemistry. 2009;57(18):8392-8398.

[35] Roa JJ, Rayon E, Morales M, Segarra M. Contact mechanics at nanometric scale using nanoindentation technique for brittle and ductile materials. Recent Patents on Nanotechnology. 2012;6(2):142-152.

[36] Arenz RJ. Stress states and nonlinear mechanical behavior associated with nanoindentation testing of polymers. Mechanics of Time-Dependent Materials. 2009;13(4):317-332.

[37] Auras R, Harte B, Selke S. Effect of water on the oxygen barrier properties of poly(ethylene terephthalate) and polylactide films. Journal of Applied Polymer Science. 2004;92(3):1790-1803.

[38] Siró I, Plackett D, Sommer-Larsen P. A comparative study of oxygen transmission rates through polymer films based on fluorescence quenching. Packaging Technology and Science. 2010;23(6):301-315.

[39] Martino VP, Jimenez A, Ruseckaite RA, Averous L. Structure and properties of clay nano-biocomposites based on poly(lactic acid) plasticized with polyadipates. Polymers for Advanced Technologies. 2011;22(12):2206-2213.

[40] Fortunati E, Peltzer M, Armentano I, Torre L, Jiménez A, Kenny JM. Effects of modified cellulose nanocrystals on the barrier and migration properties of PLA nano-biocomposites. Carbohydrate Polymers. 2012;90(2):948-956.

[41] Arrieta MP, Peltzer MA, López J, Garrigós MdC, Valente AJM, Jiménez A. Functional properties of sodium and calcium caseinate antimicrobial active films containing carvacrol. Journal of Food Engineering. 2014;121(0):94-101.

[42] Rutkowska M, Krasowska K, Heimowska A, Adamus G, Sobota M, Musiol M, et al. Environmental Degradation of Blends of Atactic Poly (R,S)-3-hydroxybutyrate with Natural PHBV in Baltic Sea Water and Compost with Activated Sludge. Journal of Polymers and the Environment. 2008;16(3):183-191.

[43] Calvao PS, Chenal J-M, Gauthier C, Demarquette NR, Bogner A, Cavaille JY. Understanding the mechanical and biodegradation behaviour of poly(hydroxybutyrate)/rubber blends in relation to their morphology. Polymer International. 2012;61(3):434-441.

[44] Drumright RE, Gruber PR, Henton DE. Polylactic acid technology. Advanced Materials. 2000;12(23):1841-1846.

[45] Kijchavengkul T, Auras R. Compostability of polymers. Polymer International. 2008;57(6):793-804.

[46] Westphal C, Perrot C, Karlsson S. Py-GC/MS as a means to predict degree of degradation by giving microstructural changes modelled on LDPE and PLA. Polymer Degradation and Stability. 2001;73(2):281-287.

[47] Corrêa MCS, Rezende ML, Rosa DS, Agnelli JAM, Nascente PAP. Surface composition and morphology of poly(3-hydroxybutyrate) exposed to biodegradation. Polymer Testing. 2008;27(4):447-452.

[48] AENOR. Geometrical product specifications (GPS). Surface texture: Profile method. Terms, definitions and surface texture parameters (ISO 4287:1997 + Technical Corrigendum 1). UNE EN ISO 42871999

## 4. Combined effect of poly(hydroxybutyrate) and plasticizers on polylactic properties for film intended for food packaging

*Marina P. Arrieta[a,b], María Dolores Madrigal[a], Juan López[a], Alfonso Jiménez[c]*

[a] Instituto de Tecnología de Materiales, Universitat Politècnica de València, Plaza Ferrándiz y Carbonell 1, 03801 Alcoy, Alicante Spain.

[b] Catholic University of Cordoba, Camino a Alta Gracia Km 7½, 5017 Córdoba, Argentina.

[c] Analytical Chemistry, Nutrition and Food Sciences Department, University of Alicante, P.O. Box 99, E-03080 Alicante, Spain.

**Journal of Polymers and the Environment**

**(2014)**

**Abstract**

Poly (lactic acid), PLA, and poly(hydroxybutyrate), PHB, blends were processed as films and characterized for their use in food packaging. PLA was blended with PHB to enhance the crystallinity. Therefore, PHB addition strongly increased oxygen barrier while decreased the wettability. Two different environmentally-friendly plasticizers, poly(ethylene glycol) (PEG) and acetyl(tributyl citrate) (ATBC), were added to these blends to increase their processing performance, while improving their ductile properties. ATBC showed higher plasticizer efficiency than PEG directly related to the similarity solubility parameters between ATBC and both biopolymers. Moreover, ATBC was more efficiently retained to the polymer matrix during processing than PEG. PLA-PHB-ATBC blends were homogeneous and transparent blends that showed promising performance for the preparation of films by a ready industrial process technology for food packaging applications, showing slightly amber colour, improved elongation at break, enhanced oxygen barrier and decreased wettability.

**Keywords**: Poly(lactic acid); poly(hydroxybutyrate); blend; barrier properties; ductility.

## 1. INTRODUCTION

The concerns on the environmental impact of food packaging materials after use are currently increasing by their high consumption and short shelf-life [1]. Some fractions of the plastic waste generated from food packaging materials may be recycled, but most of these residues are disposed in landfills by technical and/or economical reasons [2]. Therefore, the use of non-renewable and non-biodegradable plastics for short shelf-life applications should be considered as potentially hazardous to the environment [3, 4]. Consequently, the development of new bio-based and biodegradable packaging materials is currently growing. In this sense, poly(lactic acid) (PLA) and poly(hydroxybutyrate) (PHB) are thermoplastic bio-based polyesters with highly promising perspectives for short-life applications [5-8]. PLA is currently the most used biobased materials by the food packaging industry in disposable cutlery, plates, lids [9], cups [5], postharvest packaging of fresh vegetables [10] and fast-food containers [11]. It is obtained by fermentation of renewable agricultural sources, such as corn [12, 13], cellulose [14] and other polysaccharides [12, 15]. However, the use of PLA in flexible films is restricted by its poor ductility, thermal and barrier properties [13].

Considerable academic and industrial efforts have been focused on PLA modification for extending PLA applications in food packaging industry, such as the addition of modifiers, nanotechnology, copolymerization or blending. It is known that the increase of crystallinity level could improve the use of PLA as food packaging material, due to its direct impact on gas permeation [8]. Melt blending PLA with other polymers can lead to significant improvement of the final properties through a cost-effective, easy and readily available processing technology. PHB is a highly crystalline bio-polyester produced by controlled bacterial fermentation [7] with relatively high melting point (173-180 °C) [3, 7] similar to that of PLA allowing physically blending both polymers in the melt state. After processing it yields stiff and brittle materials with poor mechanical properties [1, 16] and thermal degradation close to its melting point, limiting its processability [17]. These limitations have hampered the use of both bio-polymers in the preparation of flexible films for food packaging.

It has been reported that the addition of PHB to PLA matrices could enhance its crystallinity [18], while PHB mechanical properties could be improved [19]. PLA-PHB blends have been widely studied during the last years [7, 8, 18-20]. For instance, Ni and colleagues (2009) blended oligomers of 3-hydroxybutyrate (OHB) and PLA to enhance the PLA crystallization when OHB was introduced in amounts lower than 40 wt%, with phase separation at higher loadings [18]. Besides, Zhang and Thomas studied PLA-PHB blends at

different mass ratios (100:0, 75:25, 50:50, 25:75, 0:100) and reported that PLA-PHB (75:25) blends showed higher mechanical properties than neat PLA [7].

The inherent brittleness of PLA and PHB makes necessary the addition of plasticizers to improve their ductile properties and to get the flexibility required for films manufacturing. It is known that compatibility between plasticizers and polymers is a major issue for effective plasticization [21]. In a previous work it was observed that the addition of D-limonene improved the interaction between PLA and PHB due to a plasticization effect [8]. In this sense, some works were reported where PHB was blended with poly(ethylene glycol) (PEG) [22] and citrate esters, such as acetyl tributyl citrate (ATBC) [1, 3] and both are considered as efficient plasticizers for PLA [3, 23, 24]. Moreover, the European Food Safety Authority (EFSA) reported that the use of PEG [25] and ATBC [26] do not raise a safety concern for food contact materials. It was reported that ATBC was more effective in enhancing the PLA flexibility at concentrations higher than 10 wt% [27, 28]. However, Coltelli and colleagues (2008) reported enhanced crystallinity in PLA plasticized with ATBC at concentrations lower than 20 wt% [29]. Courgneau and colleagues (2011) studied PLA plasticized with PEG and ATBC. They reported that the addition of ATBC at concentrations higher than 13 wt% resulted in a significant decrease in Tg and the corresponding increase in elongation at break with no phase separation up to 17 wt%, while PEG-300 showed phase separation at contents higher than 9 wt% [23]. Kulinski and Piorkowska (2005) observed phase separation in PLA-PEG blends at 20 wt% of PEG-200 and 30 wt% of PEG-400 [30]. Martin and Avérous (2001) reported that PEGs with low molar masses showed good miscibility with PLA matrices [31].

The aim of this work was to prepare PLA-PHB blends (75:25) for food packaging applications. These developments were focused on the reinforcement of PLA by blending with PHB to increase crystallinity and to improve barrier properties, while the addition of plasticizer aimed to increase the blend's ductility. Two different plasticizers, PEG and ATBC, were tested to produce flexible films. Structural, thermal, mechanical and oxygen barrier properties of these films were evaluated to assess the most adequate formulation for the intended application.

## 2. MATERIALS AND METHODS

### 2.1. Materials

PLA pellets (Ingeo™ 4032D, Mn = 217000 Da, 2 wt% D-isomer, Mw/ Mn = 2) was supplied by NatureWorks LLC (Minnetonka, MIN, USA), PHB (PHB P226, Mw = 426,000 Da) was provided by Biomer (Krailling, Germany). ATBC (M = 402 g $mol^{-1}$, 98% purity) and PEG (Mn= 300 g $mol^{-1}$) were purchased from Sigma-Aldrich (Móstoles, Madrid, Spain).

### 2.2. Films preparation and processing

PLA pellets and plasticizers were dried overnight at 80 °C in a vacuum oven to prevent PLA hydrolysis during processing [32]. Meanwhile, PHB pellets were dried at 40 °C for 4 hours. Blends were prepared by mixing PLA and PHB pellets (75:25 wt% ratio) in a Haake PolyLab QC mixer (Thermo Fischer Scientific Inc., Waltham, MA, USA), equipped with a pair of high-shear rolls, at 180 °C and rotation speed 50 rpm for 4 min. ATBC and PEG were added at 15 wt% after 3 minutes when PLA or PLA-PHB blends had achieved the melt state. Each blend was then processed into films by compression molding at 180 °C in a hot press (Mini C 3850, Caver, Inc., Wabash, IN, USA) by using a film mold (15 x 15 cm2). 8g of each blend were kept between the plates at atmospheric pressure for 2 min until melting and they were further submitted to the following pressure cycle, 3 MPa for 1 min, 5 MPa for 1 min and finally 10 MPa for 2 min with the aim to eliminate the trapped air bubbles [33]. Films were then quenched to room temperature at atmospheric pressure. Their average thickness was measured with a Digimatic Micrometer Series 293 MDC-Lite (Mitutoyo, Japan) ± 0.001 mm at ten random positions over the film surface for barrier properties testing and at five positions along the strips surface for the mechanical properties determination. The films average thickness was 200 ± 50 μm.

### 2.3. Characterization

#### 2.3.1. Thermal characterization

Thermogravimetric analysis (TGA) tests were carried out by using a TGA/SDTA 851e Mettler Toledo thermal analyzer (Schwarzenbach, Switzerland). Raw materials were heated (isothermal mode) at 180 °C for 25 minutes under air (flow rate 50 mL $min^{-1}$) to evaluate the thermal stability of raw materials at the processing conditions. Films were

heated at 10 °C $min^{-1}$ from 30 to 600 °C under nitrogen atmosphere (flow rate 50 mL $min^{-1}$). In both cases samples masses were between 5-7 g.

Differential scanning calorimetry (DSC) tests were carried out in a DSC Q-2000 (TA Instruments, New Castle, DE, USA) under nitrogen (flow rate 50 mL $min^{-1}$). Samples (around 4 mg) were introduced in aluminum pans, which were sealed with a Tzero press (TA Instruments). All tests consisted of a first heating stage from -90 °C to 180 °C at 10 °C $min^{-1}$, followed by a cooling process up to -90 °C at the maximum rate given by the instrument and subsequent heating up to 200 °C at 10 °C $min^{-1}$. Glass transition ($T_g$), cold-crystallization ($T_{cc}$) and melting temperatures ($T_m$) were determined during the second heating scan. The degree of crystallinity ($\chi_c$) was calculated by using Equation III.4. 1, where $\Delta H_m$ is the melting enthalpy, $\Delta H_{cc}$ is the cold crystallization enthalpy, $\Delta H_{mc}$ is the melting heat associated to pure crystalline PLA, reported to be 93 J $g^{-1}$ [34] and WPLA the proportion of PLA in the blend.

$$\chi_c = 100\% \times \left[\frac{\Delta H_m - \Delta H_c}{\Delta H_m^c}\right] \times \frac{1}{W_{PLA}} \qquad \textbf{Equation III.4. 1}$$

For the neat PHB film the $\chi_c$ was calculated by following the Equation III.4. 2, were $\Delta H_m^c$ is the melting heat associated to pure crystalline PHB, reported to be 146 J $g^{-1}$ [35].

$$\chi_c = 100\% \times \left[\frac{\Delta H_m}{\Delta H_m^c}\right] \qquad \textbf{Equation III.4. 2}$$

### 2.3.2. Scanning Electron Microscopy (SEM)

SEM micrographs of both, surface and cross-section areas after tensile tests, were obtained with a Phenom SEM (FEI Company, Eindhoven, The Netherlands), operated at 10 kV. Samples were coated with a gold layer (10-25 nm thickness) in vacuum conditions prior to their analysis to increase their electrical conductivity. Micrographs were registered at 1000× magnification.

### 2.3.3. Mechanical characterization

Tensile tests were carried out at room temperature with a IBERTEST ELIB 30 (S.A.E. Ibertest, Madrid, Spain) machine by following the ASTM D882-01 Standard [36].Tests were performed in rectangular strips (dimensions: 100 × 10 $mm^2$), initial grip separation 50 mm, crosshead speed 25 mm $min^{-1}$ and load cell 5 kN. The average percentage

deformation at break ($\varepsilon_{B\%}$), elastic modulus ($E$) and tensile strength (TS) were calculated from the resulting stress-strain curves as the average of five measurements from three films of each composition.

### 2.3.4. Oxygen Transmission Rate (OTR)

OTR measurements were carried out with an 8500 oxygen permeation analyzer (Systech Instruments, Metrotec, SA. Spain). Circular films (140 mm diameter) were conditioned at 50 ± 2 % relative humidity and 25.0 ± 0.1 °C prior to testing. Pure oxygen (99.9%) was introduced into the upper half of the chamber while pure nitrogen was injected into the lower half where one oxygen sensor is placed. Values were expressed as OTR·$e$ where $e$ is the film thickness (mm).

### 2.3.5. Total soluble matter (TSM)

TSM was determined as the percentage in dry basis of every sample solubilized in distilled water after 24 h [37] and it was calculated by using Equation III.4.3:

$$TSM = 100 \times \frac{m_0 - m_f}{m_0} \qquad \textbf{Equation III.4. 3}$$

where $m_0$ is the initial dry weight of a square sample (20 x 20 $mm^2$) calculated after drying in an air-circulating oven at 105 °C for 24 h. Samples were then immersed in 30 mL of a 0.02 % (w/w) aqueous sodium azide solution at room temperature for 24 h. Samples were further rinsed with distilled water, dried at 105 °C and re-weighed until constant weight (± 0.0001 g) to determine the final weight ($m_f$). Three films of each composition were tested and the average value was determined as the TSM. Sample weights were determined with an AG-245 Mettler Toledo analytical balance.

### 2.3.6. Water contact angle

A standard goniometer (EasyDrop-FM140, KRÜSS GmbH, Hamburg, Germany) equipped with a camera and Drop Shape Analysis SW21; DSA1 software was used to test the water contact angle ($\theta^{o}$) at room temperature. The contact angle was determined by randomly putting 6 drops of distiller water (≈ 2 μL) onto the films surface with a syringe and the average values of ten measurements for each drop were calculated [4].

### 2.3.7. Film transparency and color

These properties were evaluated by using a COLORFLEX-DIFF2 45º/0º HunterLab colorimeter, (Hunter Associates Laboratory Inc., Reston, VI, USA). The instrument was calibrated with a white standard tile and the average value of five measurements at random positions over the samples surface (20 x 20 $mm^2$) was calculated. Transparency was calculated by following Equation III.4. 4:

$$Transparency = \frac{A_{600}}{e} \qquad \textbf{Equation III.4. 4}$$

where $A_{600}$ is the absorbance at 600 nm and *e* the film thickness (mm) [38].

The color coordinates, L (lightness), a* (red-green) and b* (yellow-blue) were used to determine the total color differences (ΔE) induced by the presence of plasticizer in films when compared to the control PLA or PLA-PHB formulations by following Equation III.4.5:

$$\Delta E^*_{CIE} = \sqrt{(\Delta L)^2 + (\Delta a^*)^2 + (\Delta b^*)^2} \qquad \textbf{Equation III.4. 5}$$

Yellowness index (YI) was used to evaluate the color change from clear to yellow.

### 2.3.8. Statistical analysis

Significance in the data differences were statistically analyzed by one-way variance analysis (ANOVA) by using Origin-Pro 8 software. Tukey's test with a 95% confidence level was used to identify which data groups were significantly different from others.

## 3. RESULTS AND DISCUSSION

### 3.1. Blends preparation and homogeneity

It is known that the effective blending of two polymers requires high affinity between them. Two substances with similar solubility parameters (δ) should be mutually soluble [39]. This effect can be predicted by calculating their respective δ values [5], calculated by following Equation III.4. 6.

$$\delta = \frac{D\sum G}{M} \qquad \textbf{Equation III.4. 6}$$

where δ ((cal $cm^{-3}$)$^{1/2}$) is the solubility parameter for each component, *D* (g $cm^{-3}$) is the density, G ((cal $cm^{-3}$)$^{1/2}$$mol^{-1}$) is the group molar cohesive energy and *M* (g $mol^{-1}$) is the molar mass per repetitive unit. The PLA solubility parameter has been reported to range between 19.5 and 20.5 $MPa^{1/2}$ [5], while the solubility parameter for PHB ranges between 18.5 and 20.1 $MPa^{1/2}$ [16]. Differences are relatively low and consequently good miscibility between both polymers should be expected.

In the case of plasticizers, they should be compatible with the polymer matrix [40, 41], and the relative affinity of the polymer and plasticizer can be assessed by calculating their δ values [39]. The solubility parameters for PEG and ATBC were calculated as 16.7 $MPa^{1/2}$ and 20.2 $MPa^{1/2}$, respectively. Therefore, since ATBC shows solubility parameter close to PLA and PHB values, good miscibility should be expected. The addition of PEG to the PLA-PHB matrix was also checked, since their δ values are in the same order of magnitude. Seven different plasticized and unplasticized PLA and PLA-PHB films were prepared as summarized in Table III.4.1 and their aspect is shown in Figure III.4.1. All films were mostly transparent and colorless except those with high amounts of PHB in their formulations. These differences in color will be further discussed.


**Figure III.4.1.** Visual appearance of: a) PLA, b) PLA-PEG, c) PLA-ATBC, d) PHB, e) PLA-PHB, f) PLA-PHB-PEG and g) PLA-PHB-ATBC.

**Table III.4.1.** Film formulations prepared in this study

| *Film designation* | PLA (wt%) | PHB (wt%) | PEG (wt%) | ATBC (wt%) |
|---|---|---|---|---|
| PLA | 100 | - | - | - |
| PLA-PEG | 85 | - | 15 | - |
| PLA-ATBC | 85 | - | | 15 |
| PHB | 100 | - | - | - |
| PLA-PHB | 75 | 25 | - | - |
| PLA-PHB-PEG | 63.75 | 21.25 | 15 | - |
| PLA-PHB-ATBC | 63.75 | 21.25 | - | 15 |

## 3.2. Thermal characterization

### 3.2.1. Thermogravimetric analysis (TGA)

The thermal stability of raw materials at the blends processing temperature (180 °C) is shown in Figure III.4.2-a. As expected, while both polymers did not show significant weight losses at this temperature, some plasticizer evaporation was observed, suggesting possibilities of plasticizer losses during processing. ATBC showed higher thermal stability at the processing temperature than PEG. However, the actual weight loss was low in both cases, since their losses were lower than 0.5% after one minute at 180 °C. Figure III.4.2-b shows the TGA curves of all blends at 180 °C. It was observed that both plasticizers improved the thermal stability of the PLA-PHB blend for times lower than 9 minutes. All samples showed a weight loss lower than 1% after 6 minutes, which is the actual time that blends were processed into films. Plasticized PLA and plasticized PLA-PHB formulations with ATBC were slightly more thermally stable than those with PEG.

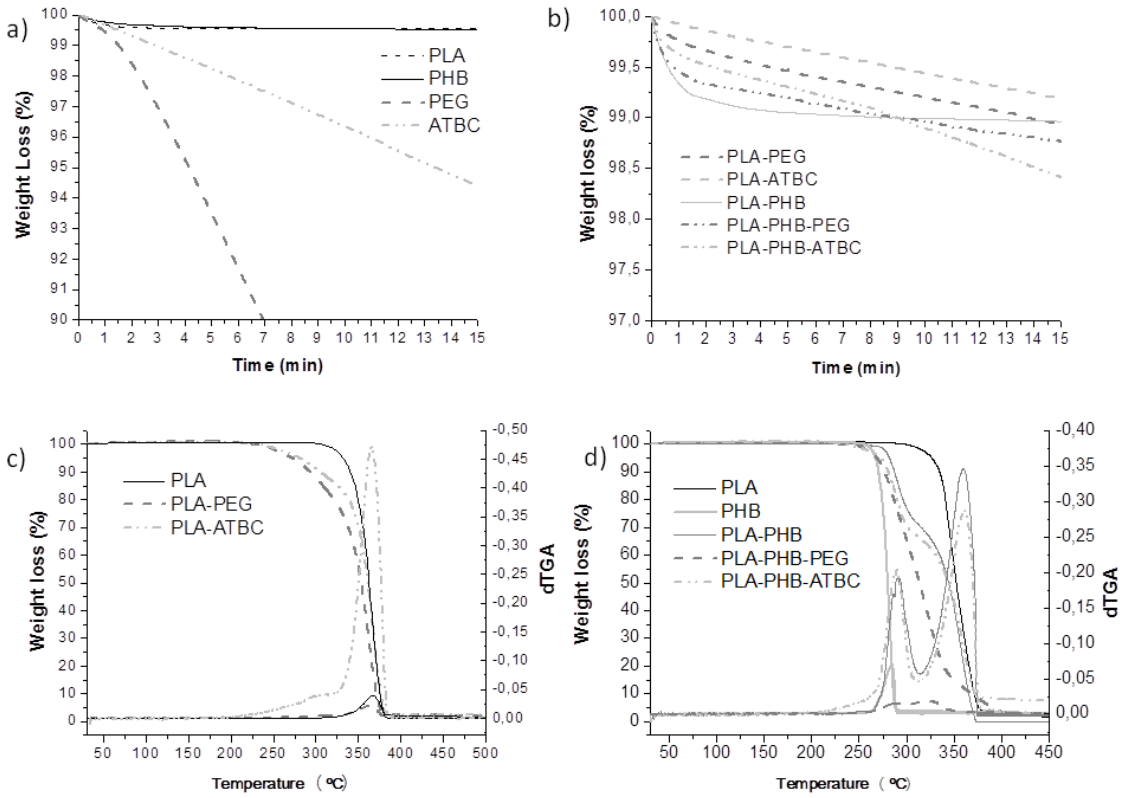


**Figure III.4.2. a)** TGA isothermal curves of raw materials at 180 °C, **b)** TGA isothermal curves of blends at 180 °C, **c)** TGA and DTG dynamic curves of plasticized PLA and **d)** TGA and DTG dynamic curves of plasticized PLA-PHB.

TGA curves representing the thermal behavior of plasticized PLA and PLA-PHB blends are plotted in Figure III.4.2-c and d, respectively. The main thermal parameters obtained from these curves are summarized in Table III.4.2. As expected, plasticized PLA films degraded in a single step, while plasticized PLA-PHB blends degradation was a two-step process. In both cases a peak corresponding to the plasticizer vaporization was observed prior to the main degradation peak(s), as indicated for other plasticized polymers [42]. The first degradation process of the PLA-PHB blend was assigned to the PHB decomposition with onset temperature ($T_0$) 272 °C and maximum degradation rate ($T_{max}$) 291 °C (Table III.4.2). PLA decomposition took place in the second stage at higher temperatures (onset 315 °C, maximum 360 °C). In this work, the values of $T_0$ for the second degradation stage in PLA-PHB blends were estimated since this process was overlapped with the end of the first stage, characteristic of the PHB degradation. The addition of PHB resulted in the decrease of the PLA $T_0$ value (Table III.4.2). It was also observed that plasticized PLA-PHB showed higher $T_0$ value than plasticized PLA films suggesting some stabilization of the PLA continuous phase caused by blending with PHB. It should be noted that the lowest value obtained for $T_0$ was 239 °C for the PLA-PEG blend,

temperature which is higher than those used in food processing or distribution, ensuring their thermal stability with no apparent degradation after processing.

PLA-PHB blends showed some increase in the $T_{max}$ value corresponding to the PHB degradation, while $T_{max}$ for the second stage was slightly lower than the value obtained for the neat PLA. It could be concluded that blending of PLA with PHB resulted in small modifications in their individual thermal stability, but not significant changes at processing and use temperatures were observed, ensuring the good thermal stability of these bio-films. In the case of the plasticized PLA-PHB blends, the addition of ATBC had no significant influence ($p < 0.05$) on the thermal stability of the final formulation while the PLA-PHB-PEG film showed some decrease in the $T_{max}$ value in the second degradation stage.

**Table III.4.2 .** TGA and DSC results

| Formulation | TGA and DTG parameters | | | DSC parameters | | | |
|---|---|---|---|---|---|---|---|
| | Stage | $T_0$ (°C) | $T_{max}$ (°C) | $T_g$ (°C) | $T_{cc}$ (°C) | $T_m$ (°C) | $\chi_c$ (%) |
| PLA | - | 315 | 366 | 60.4 | 103.0 | 167.3 | 5.1 |
| PLA-PEG | - | 239 | 366 | 26.8 | 70.0 | 160.0 | 18.4 |
| PLA-ATBC | - | 245 | 365 | 34.6 | 74.1 | 161.3 | 8.1 |
| PHB | - | 261 | 285 | - | - | 174.2 | 40.7* |
| PLA-PHB | I | 272 | 291 | 58.1 | 105.2 | 167.4 | 16.4 |
| | II | 315 | 360 | | | | |
| PLA-PHB-PEG | I | 250 | 285 | 25.1 | 64.2 | 160.2 | 36.5 |
| | II | 300 | 324 | | | | |
| PLA-PHB-ATBC | I | 247 | 290 | 31.8 | 76.4 | 160.4 | 27.0 |
| | II | 313 | 361 | | | | |

$T_0$, calculated at 1% mass loss (10 °C $min^{-1}$).

* $\chi_c$ (%), calculated using $\Delta H_m^c$ of PHB

### 3.2.2. Differential Scanning Calorimetry (DSC)

Figure III.4.3 and Figure III.4.4 show the DSC thermograms for all samples, while Table III.4.2 reports the numerical values of the main thermal events. Only one $T_g$ value was observed for all formulations, suggesting the good miscibility between the different components in the amorphous region. A relevant shift to lower values in the $T_g$ was observed for the PLA-PHB blend, giving another indication of the good interaction between both polymers after processing. A clear effect of the addition of ATBC or PEG to

the polymer matrices was observed, since they induced the $T_g$ depression in all plasticized films. This effect was due to their ability to increase the free volume between the polymer chains [23] and consequently their mobility. This reduction in $T_g$ was higher in films plasticized with PEG, as expected, since plasticizers with low molecular weight are usually more efficient in lowering $T_g$ values [28].

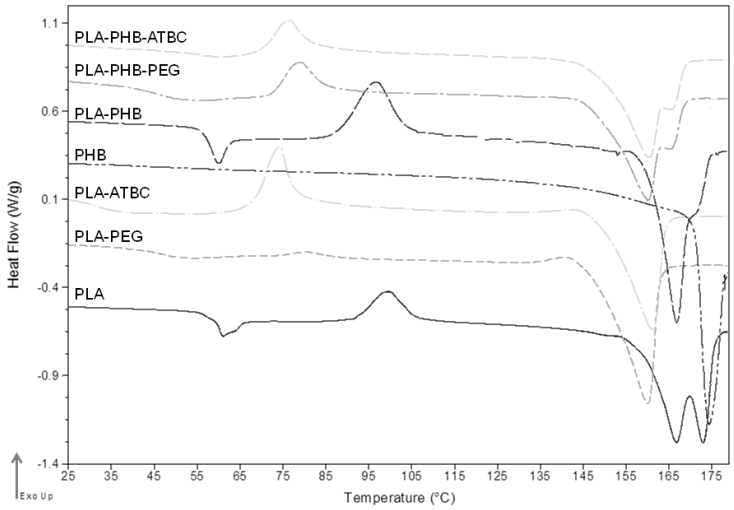


**Figure III.4.3.** DSC thermograms during the first heating scan at 10 °C $min^{-1}$ for all formulations

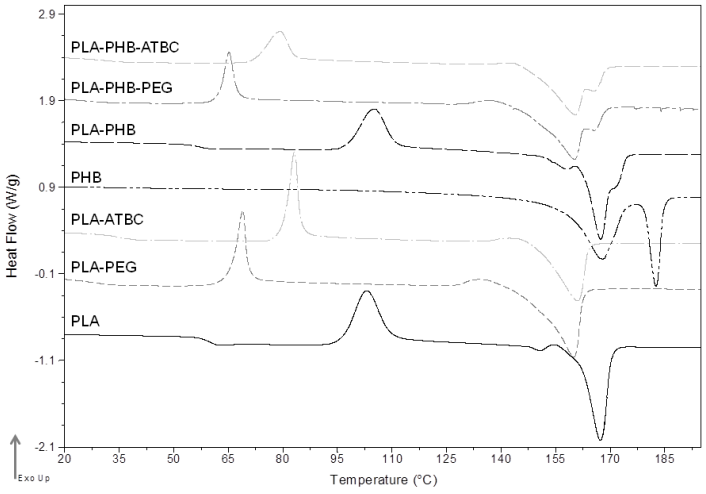


**Figure III.4.4**. DSC thermograms during the second heating scan at 10 °C $min^{-1}$ for all formulations

The endothermic peak corresponding to the enthalpic relaxation right after $T_g$ was observed during the PLA and PLA-PHB first heating (Figure III.4.3.). This peak can be related to the physical aging of polymers, probably PLA, before testing [43]. In these

formulations the cold crystallization exotherm and two melting endothermic peaks were also observed. Double melting peaks in PLA films were related to the formation of crystalline structures with different perfection and thermodynamic stability [44, 45]. This behavior was previously observed in plasticized PLA formulations, since disordered α'-crystals were formed when $T_{cc}$ was around 100 °C [32, 46].

Recently Bartczak and colleagues (2013) reported a decrease in a cold crystallization of PLA in with different proportions of PHB and ascribed this behavior to a partial miscibility between both polymers [47]. In this work, it was observed that $T_{cc}$ shifted from 103 °C to 105 °C during the second heating scan, suggesting that PHB could promote the cold crystallization of the PLA matrix. As expected in plasticized materials, the incorporation of ATBC or PEG induced a higher decrease in $T_{cc}$ due to the important increase in the polymers chain mobility. One of the goals of blending PLA with PHB is to increase the blends crystallinity to further control their properties. The crystallinity degree for all materials was calculated from DSC tests and results are reported in Table III.4.2. As expected, the PHB film showed the highest $\chi_c$, while PLA-PHB blends increased their crystallinity in comparison to neat PLA, since PHB acted as nucleating agent of the PLA matrix [7]. In plasticized samples, PLA-ATBC films showed lower $\chi_c$ evidencing the formation of amorphous materials in agreement with the visual aspect of highly transparent films (Figure III.4.1). Meanwhile, PLA-PEG films showed high $\chi_c$ values and this could be related to the fact that PEG can interact with PLA resulting in higher chain mobility. Moreover, the macroscopic observation of PLA-PEG films showed that they were brittle, due to some phase separation in these blends [23] induced by the increase in the crystalline phase [42]. This observation is in agreement with the higher differences observed between PEG and PLA solubility parameters.

### 3.3. Mechanical Properties

The influence of the addition of PHB and plasticizers in the tensile properties of PLA was evaluated. Results of the tensile properties for all formulations are shown in Figure III.4.5.

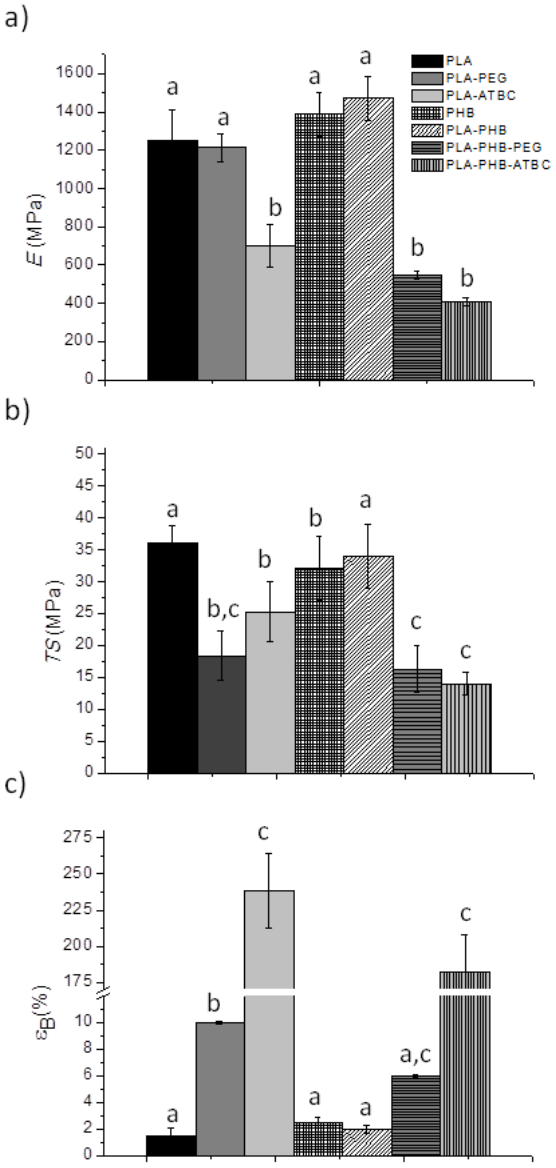


**Figure III.4.5.** Modulus (*E*), tensile strength (*TS*) and elongation at break ($\varepsilon_B$) of films (n=5).

[a-c] Different letters on the bars indicate significant differences between formulations ($p < 0.05$)

Neat PLA and PHB showed similar elastic modulus (*E*) values ($p < 0.05$) while it slightly increased for the PLA-PHB blend due to the reinforcement effect of PHB, enhancing toughness (Figure III.4.5-a). Moreover, the PLA-PHB blend showed comparable tensile strength (*TS*) values to the PLA film ($p = 0.05$) (Figure III.4.5-b). As expected, all blends with ATBC or PEG showed *E* and *TS* values lower than those for their unplasticized counterparts, since plasticizers induced ductile fracture, particularly in plasticized PLA-PHB films. These results are in good agreement with DSC tests where PLA-PHB-PEG and

PLA-PHB-ATBC films showed lower $T_g$ values than the plasticized PLA counterparts. These reductions of these mechanical properties for the PLA-PHB-ATBC formulation were significant ($p > 0.05$), since these films showed a reduction in 70% in $E$ and 65% in $TS$ when compared with pure PLA.

A noticeable improvement in elongation at break ($\varepsilon_B$) was observed for plasticized PLA films (Figure III.4.5-c), in full agreement with the decrease in their $T_g$ values. This improvement was less pronounced for PLA-PHB films because of the reinforcement effect caused by the addition of PHB, while PLA, PHB and PLA-PHB films did not show stretchable behavior. It was also observed that ATBC produced much higher increase in $\varepsilon_B$ than PEG in all blends ($p > 0.05$). In fact the addition of PEG did not show any clear improvement in ductile properties of PLA and/or PLA-PHB blends. A similar behavior was reported by Courgneau et al. (2011) who observed that the addition of PEG resulted in the decrease in the PLA $\varepsilon_B$ due to the drop in PLA molar mass induced by PEG [23]. These results are in agreement with the clear increase in blends crystallinity already discussed by the addition of PEG to PLA-based formulations.

The higher plasticization effectiveness of ATBC for PLA and PLA-PHB matrices was in agreement with their high similarity in solubility parameters. These interactions resulted in a two-order of magnitude increase in $\varepsilon_B$ for the plasticized blends (from 1.5% for PLA to 238% for the PLA-ATBC film and from 2.0% for the PLA-PHB blend to 182% for the PLA-PHB-ATBC formulation). It should be noted that these values for $\varepsilon_B$ are similar to those of commercial plasticized PVC stretching films. Therefore, it could be concluded that PLA-ATBC and PLA-PHB-ATBC blends could be considered a sustainable alternative to current non-natural and non-biodegradable materials for food packaging films in terms of flexibility and possibilities for processing at the industrial level.

### 3.4. Scanning electron microscopy (SEM)

SEM images of films surfaces (not shown) showed smooth surfaces for PLA and PHB films with no relevant heterogeneities. The PLA-PHB blend also showed homogeneous surface, with no apparent phase separation, suggesting the good interaction between both polymers in agreement with DSC results. As well, no apparent differences in surface homogeneity were observed in plasticized films surfaces, suggesting the good dispersion of plasticizers in both, PLA and PLA-PHB matrices.

SEM micrographs of fractured surfaces after tensile tests are shown in Figure III.4.6. Neat rigid fracture surfaces were clearly noticed for PLA, PHB and PLA-PHB films (Figure III.4.6 a-c), while plasticized samples showed ductile fracture patterns where plastic

deformations were present, particularly in films plasticized with ATBC (Figure III.4.6 d-g). It is known that the introduction of relatively low-size molecules, such as those in ATBC, reduces molecular interactions between atoms in polymer chains [48], making easier the solubilization of the plasticizer into the polymer matrix resulting in a ductile behavior [40].

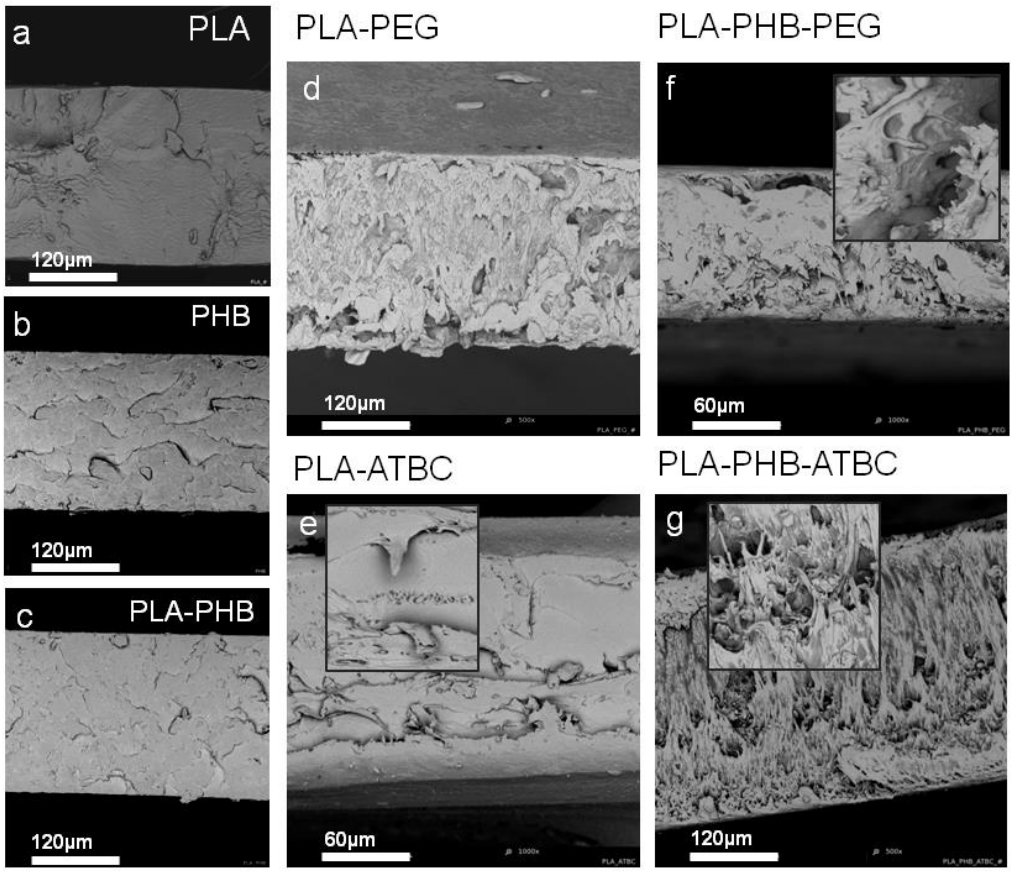


**Figure III.4.6.** Fractured SEM micrographs of: **a)** PLA, **b)** PHB, **c)** PLA-PHB, **d)** PLA-PEG, **e)** PLA-ATBC, **f)** PLA-PHB-PEG and **g)** PLA-PHB-ATBC.

### 3.5. Oxygen Transmission rate (OTR)

Oxygen barrier is one of the most important issues to be considered in materials intended to be used in food packaging, since the presence of oxygen in some cases and mainly for respiring foods (e.g. fruits and vegetables), it may lead to detrimental changes in quality and inducing a depression of food shelf-life [49]. OTR at the steady-state can be related to the oxygen permeation through the polymer structure and it is dependent on the film thickness. Thus, OTR·*e* values were obtained and results are shown in Table III.4.3.

**Table III.4.3.** Yellow Index (YI), CIELAB color parameters, transparency, OTR·*e,* TSM and water contact angle measurements ($\theta$º) for all film formulations

| **Formulation** | ***L*** | **a*** | **b*** | **YI** | **Δ*E**** | $A_{600}$/mm | OTR·*e* ($cm^3mm\ m^{-2}day^{-1}$) | *TSM* | $\theta$º |
|---|---|---|---|---|---|---|---|---|---|
| PLA | 94.1 ± 0.1[a] | -1.1 ± 0.1[a,d] | 1.3 ± 0.1[a] | 3.5 ± 0.1[a] | - | 279.9 ± 2.8[a] | 44.1 ± 0.5[a] | 0.08 ± 0.01[a] | 58.4 ± 3.7[a,c] |
| PLA-PEG | 91.1 ± 0.1[b] | -0.8 ± 0.2 [a] | 1.6 ± 0.1[a] | 4.2 ± 0.2[a] | 3.1 ± 0,2[A] | 264.5 ± 0.6[b] | 61.2 ± 1.4[b] | 8.57 ± 0.14[b] | 53.2 ± 3.4[a] |
| PLA-ATBC | 93.5 ± 0.1 [a] | -0.8 ± 0.1 [a] | 1.4 ± 0.1[a] | 3.8 ± 0.1[a] | 0.7 ± 0,1[A] | 263.7 ± 0.1[b] | 51.8 ± 1.2[c] | 0.92 ± 0.02[c] | 70.7 ± 1.3[b] |
| PHB | 83.3 ± 2.2[c] | 1.0 ± 1.0 [b] | 22.5 ± 3.3[b] | 45.1 ± 3.1[b] | - | 237.7 ± 0.8[c] | 24.9 ± 1.3[d] | 0.09 ± 0.04[a] | 61.3 ± 2.5[c] |
| PLA-PHB | 89.1 ± 1.0[d] | -1.3 ± 0.1 [a,c] | 10.9 ± 2.1[c] | 21.7 ± 3.1[c] | 10.8 ± 2.0[A] | 259.3 ± 0.1[d] | 11.0 ± 0.7[e] | 0.08 ± 0.06[a] | 70.0 ± 0.6[d] |
| PLA-PHB-PEG | 89.5 ± 0.5 [b,d] | -1.6 ± 0.2 [c,d] | 9.4 ± 0.7[c] | 18.5 ± 1.2[c] | 1.7 ± 0,5[B] | 240.4 ± 0.1[c] | 62.9 ± 1.3[b] | 7.41 ± 0.08[d] | 57.2 ± 2.0[a,c] |
| PLA-PHB-ATBC | 89.8 ± 0.5[b,d] | -1.2 ± 0.3[a,d] | 9.5 ± 0.8[c] | 19.1 ± 1.4[c] | 1.6 ± 0,5[B] | 236.8 ± 0.7[c] | 22.8 ± 2.8[d] | 0.50 ± 0.05[e] | 66.9 ± 3.1[b] |

[a-e] Different superscripts within the same column indicate significant differences between formulations ($p < 0.05$).

[A] Calculated by using PLA film color coordinates as control reference.

[B] Calculated by using PLA-PHB film color coordinates as control reference.

In general, PHB showed significant ($p > 0.05$) higher barrier to oxygen than neat PLA, as expected from its higher intrinsic crystallinity and more efficient molecules distribution in the polymer structure. Therefore, the PLA-PHB blend resulted in improved barrier properties compared to neat PLA films. This effect could be caused by the increase in the PLA crystallinity by the addition of PHB.

It is well known that the addition of plasticizers to polymer matrices increases their oxygen transmission rate [4, 23, 32, 50]. In this case, films plasticized with PEG showed the highest OTR.*e* values. Courgenau et al. already reported this effect and they concluded that PLA crystallization caused by physical aging might induce plasticizer segregation towards the amorphous phase and free volume around macromolecular chains in the polymer structure would increase [51].

The addition of PHB to the plasticized PLA matrix induced a general reduction in oxygen permeability, in particular for PLA-PHB-ATBC films, showing the good interaction between components in this ternary blend. However, no significant improvement in oxygen barrier was observed for the PLA-PHB-PEG film when compared to the PLA-PEG formulation ($p < 0.05$). It should be noted that the OTR.*e* results for these blends, particularly for those with PHB, suggested that these films could be used as sustainable materials for food packaging with values clearly lower than those calculated for low density polyethylene (LDPE), 160 $cm^3 \cdot mm\ m^2\ day^{-1}$ [50]. Even plasticized formulations showed OTR.*e* results lower than those obtained for LDPE and plasticized PVC films (around 80 $cm^3 \cdot mm\ m^2\ day^{-1}$).

### 3.6. Total soluble matter

The weight difference between the initial dry matter and the material remaining after treatment in aqueous environments was determined by calculating the total soluble matter (TSM). Results are summarized in Table III.4.3. PLA, PHB and PLA-PHB blends remained almost unaltered after treatment. Plasticized films showed a significant increase in water solubility that could be related to the plasticizer loss, which was clearly higher for PEG than for ATBC. It was also observed that the PLA-PHB blend was more effective preventing the plasticizer loss in aqueous environments than PLA due to the stabilization of the PLA continuous phase by blending with PHB, as it was previously discussed.

### 3.7. Water contact angle

Water contact angle measurements were used to evaluate the hydrophilic/hydrophobic behavior of these materials. Results are shown in Table III.4.3. It is known that the water contact angle increases with the surface hydrophobic character [40]. Thus, a water contact angle higher than 65º is typical in hydrophobic surfaces, while $\theta$º values lower than 65º are obtained in hydrophilic materials [52]. Neat PLA and PHB showed hydrophilic surfaces, while PLA-PHB blends showed a significant improvement in their hydrophobic character with reduced water adsorption ($p > 0.05$). In plasticized samples, the incorporation of PEG resulted in a slight decrease in the PLA contact angle suggesting some increase in the hydrophilic character, as it has been previously reported [53]. On the other hand, the contact angle for the PLA-ATBC film was around 12º higher, suggesting that the addition of ATBC produced some significant increase in the hydrophobic character of the PLA matrix ($p > 0.05$). Similar results were observed in PLA and PLA-PHB incorporated with D-limonene, and this behavior was attributed to the hydrophobic character of this additive [4, 8]. The significant difference in the effect of plasticizers in PLA and PLA-PHB contact angles could be caused by their differences in water solubility. PEG is soluble in water while this is not the case for ATBC. Films plasticized with ATBC could be used in packaging formulations with reduced water absorption requirements since they showed higher hydrophobic character.

Transparency and colorimetric properties

It was noticed that the addition of PHB to the transparent and colorless PLA films resulted in changes in color getting some yellowish tone (Figure III.4.1). The determination of transparency and color parameters in the CIELab space would permit to quantify these changes. Results are shown in Table III.4.3. Neat PLA showed the highest transparency and *L* value, characteristic of the high brightness of PLA films. The addition of plasticizers significantly affected transparency ($p < 0.05$) of polymer films, but no significant differences between PEG and ATBC were observed, either in PLA or PLA-PHB blends. Furthermore, the plasticizer addition resulted in a* values close to zero, while YI and b* sligthly increased and some decrease in *L* was also observed ($p < 0.05$).

PHB films showed the lowest transparency and *L* values and the highest b* and YI values. In consequence, PLA-PHB blends showed some color differences with neat PLA, but some improvement in transparency and lightness when compared to neat PHB. No significant differences in *L* between the PLA-PHB blends and their plasticized counterparts were observed. In addition, PLA-PHB films showed some increase in the yellow color, with intermediate b* values between neat PLA and neat PHB. In general, the addition of

plasticizers contributed to improve the colored aspect of blends, decreasing their yellowness index and slighty increasing their transparency, which is a important consumer's requirement in food packaging applications.

## 4. CONCLUSIONS

PLA was melt blended with PHB to increase crystallinity and further plasticized with PEG and ATBC to evaluate the possibility to obtain bio-based and biodegradable flexible films with improved properties for food packaging. Transparent and homogeneous films were obtained by melt-blending followed by compression molding processes. The addition of PHB increased the PLA crystallinity and the obtained PLA-PHB blends showed improved oxygen barrier properties and lowered water incorporation. Moreover, PHB improved the interface interaction between PLA and plasticizers. Those blends plasticized with ATBC showed higher flexibility and thermal stability than those with PEG. The best properties for the intended use in films manufacturing were found for the PLA-PHB-ATBC formulation, with moderate elongation at break, slightly amber color but still mostly transparent, reduced surface water absorption and a considerable improvement in oxygen barrier. In order to assess the use of these formulations in films manufacturing for biodegradable food packaging, migration studies in different environments as well as disintegrability under composting conditions are currently on-going.

## Acknowledgments

This work has been supported by the Spanish Ministry of Economy and Competitiveness (MAT2011-28648-C02-01 and MAT2011-28468-C02-02) M.P. Arrieta is granted by Santiago Grisolía program (GRISOLIA/2011/007). Authors gratefully acknowledge Prof. Arturo Horta Zubiaga from National University of Distance Education (UNED) Spain for his valuable discussion.

**REFERENCES**


[1] Erceg M, Kovacic T, Klaric I. Thermal degradation of poly(3-hydroxybutyrate) plasticized with acetyl tributyl citrate. Polym Degrad Stabil. 2005;90(2):313-318.

[2] Briassoulis D, Dejean C. Critical Review of Norms and Standards for Biodegradable Agricultural Plastics Part I (TM). Biodegradation in Soil. J Polym Environ. 2010;18(3):384-400.

[3] Averous L. Biodegradable multiphase systems based on plasticized starch: A review. J Macromol Sci C. 2004;44(3):231-274.

[4] Arrieta MP, López J, Ferrandiz S, Peltzer M. Characterization of PLA-limonene blends for food packaging applications. Polym Test. 2013;32(4):760-768.

[5] Auras R, Harte B, Selke S. An Overview of Polylactides as Packaging Materials. Macromol Biosci. 2004; 4(9):864.

[6] Fortunati E, Armentano I, Zhou Q, Iannoni A, Saino E, Visai L, et al. Multifunctional bionanocomposite films of poly(lactic acid), cellulose nanocrystals and silver nanoparticles. Carbohyd Polym. 2012;87(2):1596-1605.

[7] Zhang M, Thomas NL. Blending Polylactic Acid with Polyhydroxybutyrate: The Effect on Thermal, Mechanical, and Biodegradation Properties. Adv Polym Tech. 2011;30(2):67-79.

[8] Arrieta MP, López J, Hernández A, Rayón E. Ternary PLA–PHB–Limonene blends intended for biodegradable food packaging applications. (2014) Eur Polym J. 2014;33(2):289-296.

[9] Arrieta MP, Parres-García FJ, López-Martínez J, Navarro-Vidal R, Ferrándiz S. Pyrolysis of bioplastics waste: Obtained products from poly(lactic acid) (PLA). DYNA. 2012;87(4):395-399.

[10] Almenar E, Samsudin H, Auras R, Harte J. Consumer acceptance of fresh blueberries in bio-based packages. J Sci Food Agr. 2010;90(7):1121-1128.

[11] Conn RE, Kolstad JJ, Borzelleca JF, Dixler DS, Filer LJ, Ladu BN, et al. Safety assessment of polylactide (PLA) for use as a food-contact polymer. Food Chem Toxicol. 1995;33(4):273-283.

[12] Fortunati E, Armentano I, Iannoni A, Kenny JM. Development and thermal behaviour of ternary PLA matrix composites. Polym Degrad Stabil. 2010;95(11):2200-2206.

[13] Martino VP, Jimenez A, Ruseckaite RA, Averous L. Structure and properties of clay nano-biocomposites based on poly(lactic acid) plasticized with polyadipates. Polym Advan Technol. 2011;22(12):2206-2213.

[14] Jamshidian M, Tehrany EA, Imran M, Jacquot M, Desobry S. Poly-Lactic Acid: Production, Applications, Nanocomposites, and Release Studies. Compr Rev Food Sci F. 2010;9(5):552-571.

[15] Hwang SW, Shim JK, selke SEM, Soto-Valdez H, Matuana L, Rubino M, et al. Poly(L-lactic acid) with added a-tocopherol and resveratrol: optical, physical, thermal and mechanical properties. Polym Int. 2012;61(3):418-425.

[16] Calvao PS, Chenal J-M, Gauthier C, Demarquette NR, Bogner A, Cavaille JY. Understanding the mechanical and biodegradation behaviour of poly(hydroxybutyrate)/rubber blends in relation to their morphology. Polym Int. 2012;61(3):434-441.

[17] Malinova L, Brozek J. Mixtures poly((R)-3-hydroxybutyrate) and poly(l-lactic acid) subjected to DSC. J Therm Anal Calorim. 2011;103(2):653-660.

[18] Ni C, Luo R, Xu K, Chen G-Q. Thermal and Crystallinity Property Studies of Poly (L-Lactic Acid) Blended with Oligomers of 3-Hydroxybutyrate or Dendrimers of Hvdroxyalkanoic Acids. J Appl Polym Sci. 2009;111(4):1720-1727.

[19] Vogel C, Siesler HW. Thermal degradation of poly(epsilon-caprolactone), poly(L-lactic acid) and their blends with poly(3-hydroxy-butyrate) studied by TGA/FT-IR spectroscopy. Macromol Symp. 2008;265:183-194.

[20] Chang L, Woo EM. Crystallization of poly(3-hydroxybutyrate) with stereocomplexed polylactide as biodegradable nucleation agent. Polym Eng Sci. 2012;52(7):1413-1419.

[21] Tavera-Quiroz MJ, Urriza M, Pinotti A, Bertola N. Plasticized methylcellulose coating for reducing oil uptake in potato chips. J Sci Food Agr. 2012;92(7):1346-1353.

[22] Parra D, Rodrigues J, Ponce P, Lugao A. Biodegradable Polymeric Films of PHB from Burkholderia saccharia in Presence of Polyethylenglycol. Pakistan J Biol Sci. 2005;8(7):1041-1044.

[23] Courgneau C, Domenek S, Guinault A, Averous L, Ducruet V. Analysis of the Structure-Properties Relationships of Different Multiphase Systems Based on Plasticized Poly(Lactic Acid). J Polym Environ. 2011;19(2):362-371.

[24] Baiardo M, Frisoni G, Scandola M, Rimelen M, Lips D, Ruffieux K, et al. Thermal and mechanical properties of plasticized poly(L-lactic acid). J Appl Polym Sci. 2003;90(7):1731-1738.

[25] European Food Safety Authority. Scientific Opinion on the safety evaluation of the active substances, iron, polyethyleneglycol, disodium pyrophosphate, monosodium phosphate and sodium chloride for use in food contact materials. EFSA Journal. 2013;11(6):3245.

[26] European Food Safety Authority. Scientific Opinion on Flavouring Group Evaluation 10, Revision 3 (FGE.10Rev3): Aliphatic primary and secondary saturated and unsaturated alcohols, aldehydes, acetals, carboxylic acids and esters containing an additional oxygenated functional group and lactones from chemical groups 9, 13 and 30. EFSA Journal. 2012;10(3):2563.

[27] Labrecque LV, Kumar RA, Dave V, Gross RA, McCarthy SP. Citrate esters as plasticizers for poly(lactic acid). J Appl Polym Sci. 1997;66(8):1507-1513.

[28] Liu H, Zhang J. Research progress in toughening modification of poly(lactic acid). J Polym Sci Pol Phys. 2011;49(15):1051- 1083.

[29] Coltelli M-B, Della Maggiore I, Bertold M, Signori F, Bronco S, Ciardelli F. Poly(lactic acid) properties as a consequence of poly(butylene adipate-co-terephthalate) blending and acetyl tributyl citrate plasticization. J Appl Polym Sci. 2008;110(2):1250-1262.

[30] Kulinski Z, Piorkowska E. Crystallization, structure and properties of plasticized poly(L-lactide). Polymer. 2005;46(23):10290-10300.

[31] Martin O, Averous L. Poly(lactic acid): plasticization and properties of biodegradable multiphase systems. Polymer. 2001;42(14):6209-6219.

[32] Burgos N, Martino VP, Jiménez A. Characterization and ageing study of poly(lactic acid) films plasticized with oligomeric lactic acid. Polym Degrad Stabil. 2013;98(2):651-658.

[33] Martino VP, Ruseckaite RA, Jimenez A. Ageing of poly(lactic acid) films plasticized with commercial polyadipates. Polym Int. 2009;58(4):437-444.

[34] Auras RA, Singh SP, Singh JJ. Evaluation of oriented poly(lactide) polymers vs. existing PET and oriented PS for fresh food service containers. Packag Technol Sci. 2005;18(4):207-216.

[35] Corre Y-M, Bruzaud S, Audic J-L, Grohens Y. Morphology and functional properties of commercial polyhydroxyalkanoates: A comprehensive and comparative study. Polym Test. 2012;31(2):226-235.

[36] ASTM. Standard Test Method for Tensile Properties of Thin Plastic Sheeting. Philadelphia, PA.: ASTM Book Stand. 08.01:316.; 1993

[37] Martucci JF, Ruseckaite RA. Biodegradable three-layer film derived from bovine gelatin. J Food Eng. 2010;99(3):377-383.

[38] Molinaro S, Romero MC, Boaro M, Sensidoni A, Lagazio C, Morris M, et al. Effect of nanoclay-type and PLA optical purity on the characteristics of PLA-based nanocomposite films. J Food Eng. 2013;117(1):113-123.

[39] Auras R, Harte B, Selke S. Sorption of ethyl acetate and d-limonene in poly(lactide) polymers. J Sci Food Agr. 2006;86(4):648-656.

[40] Wu L-Y, Wen Q-B, Yang X-Q, Xu M-S, Yin S-W. Wettability, surface microstructure and mechanical properties of films based on phosphorus oxychloride-treated zein. J Sci Food Agr. 2011;91(7):1222-1229.

[41] Murariu M, Ferreira ADS, Alexandre M, Dubois P. Polylactide (PLA) designed with desired end-use properties: 1. PLA compositions with low molecular weight ester-like plasticizers and related performances. Polym Advan Technol. 2008;19(6):636-646.

[42] Martino VP, Ruseckaite RA, Jiménez A. Thermal and mechanical characterization of plasticized poly (L-lactide-co-D,L-lactide) films for food packaging. J Therm Anal Calorim. 2006;86(3):707-712.

[43] Gamez-Perez J, Velazquez-Infante JC, Franco-Urquiza E, Pages P, Carrasco F, Santana OO, et al. Fracture behavior of quenched poly(lactic acid). Express Polym Lett. 2011;5(1):82-91.

[44] Fortunati E, Armentano I, Iannoni A, Barbale M, Zaccheo S, Scavone M, et al. New multifunctional poly(lactide acid) composites: Mechanical, antibacterial, and degradation properties. J Appl Polym Sci. 2012;124(1):87-98.

[45] Scaffaro R, Botta L, Passaglia E, Oberhauser W, Frediani M, Di Landro L. Comparison of different processing methods to prepare poly(lactid acid)-hydrotalcite composites. Polym Eng Sci. 2013.

[46] Zhang J, Tashiro K, Tsuji H, Domb AJ. Disorder-to-order phase transition and multiple melting behavior of poly(L-lactide) investigated by simultaneous measurements of WAXD and DSC. Macromolecules. 2008;41(4):1352-1357.

[47] Bartczak Z, Galeski A, Kowalczuk M, Sobota M, Malinowski R. Tough blends of poly(lactide) and amorphous poly([R,S]-3-hydroxy butyrate) - Morphology and properties. European Polymer Journal. 2013;49(11):3630-3641.

[48] López J, Parres F, Rico I, Molina J, Bonastre J, Cases F. Monitoring the polymerization process of polypyrrole films by thermogravimetric and X-ray analysis. J Therm Anal Calorim. 2010;102(2):695-701.

[49] Cagnon T, Méry A, Chalier P, Guillaume C, Gontard N. Fresh food packaging design: A requirement driven approach applied to strawberries and agro-based materials. (2014) Innov Food Sci Emerg. (0).

[50] Martino VP, Jimenez A, Ruseckaite RA. Processing and Characterization of Poly(lactic acid) Films Plasticized with Commercial Adipates. J Appl Polym Sci. 2009;112(4):2010-2018.

[51] Courgneau C, Domenek S, Lebosse R, Guinault A, Averous L, Ducruet V. Effect of crystallization on barrier properties of formulated polylactide. Polym Int. 2012;61(2):180-189.

[52] Arrieta MP, Peltzer MA, López J, Garrigós MdC, Valente AJM, Jiménez A. Functional properties of sodium and calcium caseinate antimicrobial active films containing carvacrol. J Food Eng. 2014;121(0):94-101.

[53] Tu Q, Wang J-C, Liu R, Zhang Y, Xu J, Liu J, et al. Synthesis of polyethylene glycol- and sulfobetaine-conjugated zwitterionic poly(L-lactide) and assay of its antifouling properties. Colloid Surface B. 2013;102:331-340.

## 5. Disintegrability under composting conditions of plasticized PLA-PHB blends

*Marina P. Arrieta[a,b], Juan López[a], Emilio Rayón[c], Alfonso Jiménez[d]*

[a] Instituto de Tecnología de Materiales, Universitat Politècnica de València, Plaza Ferrándiz y Carbonell 1, 03801 Alcoy, Alicante Spain.

[b] Catholic University of Cordoba, Camino a Alta Gracia Km 7½, 5017 Córdoba, Argentina.

[c] Instituto de Tecnología de Materiales, Universitat Politècnica de València, Camí de Vera s/n. E46022. Valencia, Spain

[d] Analytical Chemistry, Nutrition and Food Sciences Department, University of Alicante, P.O. Box 99, E-03080 Alicante, Spain.

**Polymer Degradation and Stability**

**(2014)**

**Abstract**

The disintegration under composting conditions of films based on poly(lactic acid)-poly(hydroxybutyrate) (PLA-PHB) blends and intended for food packaging was studied. Two different plasticizers, poly(ethylene glycol) (PEG) and acetyl-tri-n-butyl citrate (ATBC), were used to limit the inherent brittleness of both biopolymers. Neat PLA, plasticized PLA and PLA-PHB films were processed by melt-blending and compression moulding and they were further treated under composting conditions in a laboratory-scale test at 58 ± 2 °C. Disintegration levels were evaluated by monitoring their weight loss at different times: 0, 7, 14, 21 and 28 days. Morphological changes in all formulations were followed by optical and scanning electron microscopy (SEM). The influence of plasticizers on the disintegration of PLA and PLA-PHB blends was studied by evaluating their thermal and nanomechanical properties by thermogravimetric analysis (TGA) and the nanoindentation technique, respectively. Meanwhile, structural changes were followed by Fourier transformed infrared spectroscopy (FTIR). The ability of PHB to act as nucleating agent in PLA-PHB blends slowed down the PLA disintegration, while plasticizers speeded it up. The relationship between the mesolactide to lactide forms of PLA was calculated with a Pyrolysis-Gas Chromatography-Mass Spectrometry device (Py-GC/MS), revealing that the mesolactide form increased during composting.

**Keywords:** Poly(lactic acid); Poly(hydroxybutyrate); blend; biodegradable; plasticizers.

## 1- Introduction

Poly(lactic acid), PLA, and poly-hydroxybutyrate (PHB) are two of the bio-based and biodegradable polymers which have focused some attention by their possibilities as environmentally-friendly food packaging materials. In this sense, PLA is currently the most used biopolymer in the food packaging sector for short shelf-life products [1], [2], [3] and [4], owing to its high mechanical strength, easy processability, superior transparency, availability and low cost. Poly(hydroxybutyrate) (PHB) is the most common representative of poly(hydroxyalkanoates) (PHA) [5], and it has been also proposed for short-term food packaging applications [6]. Conversely, there are not many commercial products of PHB by its narrow processing window, high brittleness, [5] and price [7].

A considerable number of research work has been reported on the misicibility between PLA and PHB and possible applications in food packaging [8], [9], [10] and [11]. It is known that PLA shows limited or partial miscibility with low molar mass PHB [10] and [12]. The temperature used during the blend preparation has also significant influence in the miscibility between both polymers. In this sense Zhang et al. (1996) reported that PLA-PHB blends prepared at high temperature exhibited greater miscibility than those prepared by solvent casting at room temperature [13] since PLA-PHB systems are fully miscible in the melt state [11] and [14]. This effect could be due to the transesterification reaction between PLA and PHB chains [13]. In addition, the miscibility between PLA and PHB is strongly dependent on their ratio in the blend. For instance, Furukawa et al. (2005) studied PLA/PHB films prepared by solvent casting in chloroform with blending ratios (w/w) 20/80, 40/60, 60/40, and 80/20 (PLA/PHB). They reported that PHB crystallized as very small spherulites that may act as nucleation sites of PLA in the 20/80 blend [8]. Similarly, Zhang and Thomas (2011) studied PLA/PHB blends in different proportions (100/0, 75/25, 50/50, 25/75 and 0/100, w/w) prepared by melt blending followed by compression moulding [9]. They found that PLA/PHB 75/25 films showed interesting properties for specific applications, with increased crystallinity and optimal miscibility between both polymers, resulting in improved tensile properties compared with neat PLA. More recently, Bartczak et al. (2013) proposed the modification of PLA by the addition of PHB up to 20 wt% for food packaging applications and they concluded that PHB can be considered as an effective impact modifier for PLA, increasing its impact resistance [10]. PLA-PHB blends (75:25, w/w) prepared by melt-blending and compression moulding have been proposed for films intended for food packaging [3] and [5] and it was observed that the addition of 25 wt% of PHB improved PLA mechanical and barrier properties due to the ability of PHB to act as a nucleating agent at this PLA/PHB ratio [5].

Films processed from PLA/PHB blends are still rigid and brittle, while their processing for films manufacturing remains an issue to avoid fractures [5]. This drawback can be overcome by plasticization to improve processability and ductility of these films [3] and [5]. But not all plasticizers could be adequate for such application. It should be taken into account that plasticizers should satisfy the strict requirements applied to materials intended to be in contact with food. They should be also miscible with the polymer matrix [1], [15] and [16] and stable at the high temperatures used during processing [16], providing suitable mechanical and barrier properties [15]. In this sense, poly(ethylene glycol) (PEG) and citrate esters have been proposed as efficient plasticizers for PLA [16] and [17], while PHB has been successfully plasticized with PEG [18] and acetyl-tri-n-butyl citrate (ATBC) [19]. PEG is water-soluble [20] and ATBC is obtained from naturally occurring citric acid. Both are non-toxic plasticizers [21].

These blends are promising candidates for sustainable post-use waste treatments, such as composting [22]. Disintegration in compost is governed by aerobic fermentation that mostly results in humus-rich soil, while landfill disposal is mediated by anaerobic fermentation producing hazardous methane. Even if methane produced in landfills could be used as an energy source [22], it is known that the huge amount of plastic waste disposal in landfills must be reduced [23] and [24]. Thus, composting would be adequate for short-term food packaging plastics as end-life option.

Biodegradation in composting conditions of PLA [25], [26] and [27] and PHB [5] and [6] has been already reported. It is known that PLA degradation in compost takes place in two main and consecutive stages, i.e. the hydrolytic and enzymatic degradation [23]. PLA disintegration starts by surface hydrolysis [28] leading to polymer random decomposition [4], while PHB disintegration is firstly caused by microorganisms that erode the polymer surface and gradually spreading to the bulk [29]. Lemmouchi et al. (2009) reported that the disintegration of PLA in composting conditions was enhanced by the presence of plasticizers [5].

The influence of PHB and plasticizers on the PLA disintegrability in composting conditions was evaluated in this work. Plasticized PLA/PHB films were prepared by melt-blending followed by compression moulding. The disintegration patterns during composting of plasticized PLA/PHB films were investigated and compared with their plasticized PLA counterparts. Disintegrability was followed by morphological, structural, nanomechanical and thermal analysis, with the main objective to obtain information on the compostability of plasticized PLA-PHB blends as end-life option for food packaging applications.

## 2. MATERIALS AND METHODS

### 2.1. Materials

Poly(lactic acid) (PLA Ingeo™ 4032D, $M_n$= 217 kDa, 2 wt% D-isomer, $M_w$/ $M_n$ = 2) was supplied in pellets by NatureWorks LLC (Minnetonka, MIN, USA), Poly(hydroxybutyrate) pellets (PHB, P226, $M_w$ = 426 kDa) was purchased from Biomer (Krailling, Germany). Poly(ethylene glycol) (PEG, $M_n$= 300 g $mol^{-1}$) and acetyl-tri-n-butyl citrate (ATBC, M = 402 g $mol^{-1}$, 98% purity) were purchased from Sigma-Aldrich (Madrid, Spain).

### 2.2. Films preparation

PLA-PHB blends were processed by mixing PLA (previously dried overnight at 80 °C in a vacuum oven) and PHB pellets (treated for 4 hours at 40 °C), in 75:25 wt% ratio in a Haake PolyLab QC mixer (Thermo Fischer Scientific Inc., Waltham, MA, USA) at 180 °C and a rotation speed of 50 rpm for 4 min. ATBC and PEG were further added (15 wt%) after 3 min once PLA or PLA-PHB blends had achieved the melt state. Each blend was then processed into films by compression moulding at 180 °C in a hot press (Mini C 3850, Carver, Inc., Wabash, IN, USA). Blends were kept between the plates at atmospheric pressure for 2 min until melting and they were further submitted to a pressure cycle of 3 MPa for 1 min, 5 MPa for 1 min and finally 10 MPa for 2 min, with the aim to eliminate the trapped air bubbles [30]. These films were then quenched to room temperature. Five formulations were obtained: control neat PLA film, PLA plasticized with PEG or ATBC (PLA-PEG and PLA-ATBC), and plasticized PLA-PHB blends (PLA/PHB-PEG and PLA/PHB-ATBC). The films average thickness, measured with a Digimatic Micrometer Series 293 MDC-Lite (Mitutoyo, Japan) ± 0.001 mm, was 200 ± 50 μm. Control films were stored at 25 °C and 30% relative humidity (RH) in an acrylic desiccator cabinet before testing.

### 2.3. Disintegration under composting conditions

Disintegration under composting conditions was performed by following the ISO-20200 standard [31]. Solid synthetic waste was prepared by mixing 10% of compost at pH 6.5 (supplied by Mantillo, Spain), 30% rabbit food, 10% starch, 5% sugar, 1% urea, 4% corn oil and 40% sawdust and it was mixed with water in 45:55 ratio. Water was added periodically to the reaction container to maintain the relative humidity in the compost

medium. Films were prepared (30 x 30 x 0.2 $mm^3$) and they were buried 6 cm depth in plastic reactors containing the solid synthetic wet waste. Each sample was contained in an iron mesh to allow their easy removal after treatment, but allowing the access of microorganisms and moisture [32]. Reactors were introduced in an air circulation oven (DO/200 Carbolite, Hope Valley, UK) at 58 °C for 35 days. The aerobic conditions were guaranteed by periodical gentle mixing of the solid synthetic wet waste [18] and [25]. Films were recovered from the disintegration container at different times (7, 14, 21 and 28 days), washed with distilled water, dried in an oven at 37 °C for 24 h, and weighed. Disintegrability was calculated by normalizing the sample weight at each time to the initial value [33], while photographs were taken to all samples once extracted from the composting medium.

### 2.4. Characterization techniques

#### 2.4.1. Color properties

Color properties of plasticized PLA and plasticized PLA/PHB films before and after 7 days of incubation were studied by measuring CIELab colour coordinates *L* (lightness), *a** (red-green) and *b** (yellow-blue), with a KONICA CM-3600d COLORFLEX-DIFF2, HunterLab (Hunter Associates Laboratory, Inc, Reston, VA, USA) colorimeter. The yellowness index (*YI*) was also determined. The instrument was calibrated with a white standard tile. Measurements were carried out in quintuplicate at random positions over the films surface and average values were calculated. Total color differences ($\Delta E$) induced by disintegration in samples after 7 days in composting conditions with the control films were calculated by using Equation III.5. 1:

$$\Delta E^*_{CIE} = \sqrt{\Delta a^{*2} + \Delta b^{*2} + \Delta L^2} \qquad \textbf{Equation III.5. 1}$$

#### 2.4.2. Surface microstructure

Differences in surface microstructures of plasticized PLA and plasticized PLA/PHB films before and after 21 days of treatment were evaluated by using a LV-100 Nikon Eclips optical microscope equipped with a Nikon sight camera at 20X magnification (Tokyo, Japan). The extended depth of field (EDF-z) imaging technique was used to improve resolution. Furthermore, surface microstructure of films before and after 14 and 21 days

of disintegration was studied by Scanning Electron Microscopy (SEM) with a Phenom (FEI Company, Eindhoven, The Netherlands) operated at 10 kV.

### 2.4.3. Fourier transformed infrared spectroscopy (FTIR)

FTIR analysis of films was carried out in the 600-4000 $cm^{-1}$ range in attenuated total reflection (ATR) mode with a Perkin-Elmer BX IR spectrometer (Perkin Elmer Spain, S.L., Madrid Spain). Tests were performed at room temperature using 128 scans and 4 $cm^{-1}$ resolution. A background spectrum was obtained before each test to compensate by spectra subtraction the humidity effect and the presence of carbon dioxide.

### 2.4.4. Thermogravimetric analysis (TGA)

Thermogravimetric analysis was performed with a thermogravimetric analyzer TGA/SDTA-851e Mettler Toledo (Schwarzenbach, Switzerland). Tests were run under dynamic mode from 30 to 600 °C at 10 °C $min^{-1}$in nitrogen flow (50 mL $min^{-1}$) to avoid thermo-oxidative degradation. The initial degradation temperatures ($T_0$) were determined at 5% mass loss while temperatures at the maximum degradation rate ($T_{max}$) were calculated from the first derivative of the TG curves (DTG).

### 2.4.5. Pyrolysis/ Gas Chromatography- Mass Spectrometry (Py/ GC-MS)

The relationship between mesolactide and (D, L)-lactide forms in the PLA structure before and after 21 days under composting conditions was evaluated with a Pyrolysis-Gas Chromatography-Mass Spectrometry device (Py-GC/MS). Film samples were pyrolyzed at 1000 °C for 0.5 s with a Pyroprobe 1000 (CDS Analytical, Oxford, PA, USA), coupled to a gas chromatograph (6890N, Agilent Technologies, Spain S.L., Madrid, Spain) equipped with a 30 m long HP-5 (0.25 mm thickness) column and using helium as carrier gas with a 50:1 split ratio. The GC oven was programmed as previously reported [34], the column program started at 40 °C for 2 min, followed by a stepped increase of 5 °C $min^{-1}$ to 200 °C (15 min hold), and further increase at 20 °C $min^{-1}$ to 300 °C (5 min hold). Detection was carried out with an Agilent 5973N mass selective instrument. The transfer temperature from the GC to the MS was set at 180 °C. The mass selective detector was programmed to detect masses between 30 and 650 amu. The identification of PLA and PHB degradation products was carried out by the characteristic fragmentation patterns observed in Py-GC/MS spectra.

### 2.4.6. Nanomechanical properties

Nanomechanical properties were measured with a nanoindenter machine G-200 (Agilent Technologies, Santa Clara, CA, USA) with a previously calibrated Berkovich diamond tip. Experiments were carried out by Continuous Stiffness Measurement (CSM) [35] and [36] under a 70 Hz harmonic oscillation frequency and 2 nm of harmonic amplitude [36] maintaining a constant 0.05 $s^{-1}$ indentation rate. An array of 5 x 5 indentations distanced 50 μm were programmed at a constant 2000 nm depth, calculating the average values between the 400 nm and 600 nm depth to avoid the roughness effect at the initial penetration depth. The reduced elastic modulus ($E_r$) was calculated instead of the Young's Modulus since the Poisson's coefficient is unknown for these blends and plasticized polymers.

## 3. RESULTS AND DISCUSSION

Figure III.5.1 shows the visual appearance of samples recovered at different testing times. In general terms, all materials increased their opacity during composting even at the first tested time (7 days). It is noticeable that PHB slowed down the PLA disintegration rate, since formulations with PHB were still visible after 28 days, while those with no PHB were completely disintegrated at that time. It was observed that disintegrability under composting started in the polymers amorphous phase and this was mostly attacked by microorganisms at the initial stage of this process. This effect was apparent by the loss of transparency in films after treatment.

The increase in crystallinity in all these materials decreased their degradation rate since the ordered structure in the crystalline fractions could retain the action of microorganisms. Thus, the addition of mostly crystalline PHB slowed down the disintegration of the PLA matrix. In fact, in a previous work we studied the disintegrability of neat PHB films in composting conditions and it was observed that it only reached 1.5% after 35 days [5]. On the other hand, the addition of plasticizers resulted in a clear increase in the disintegration phenomenon.

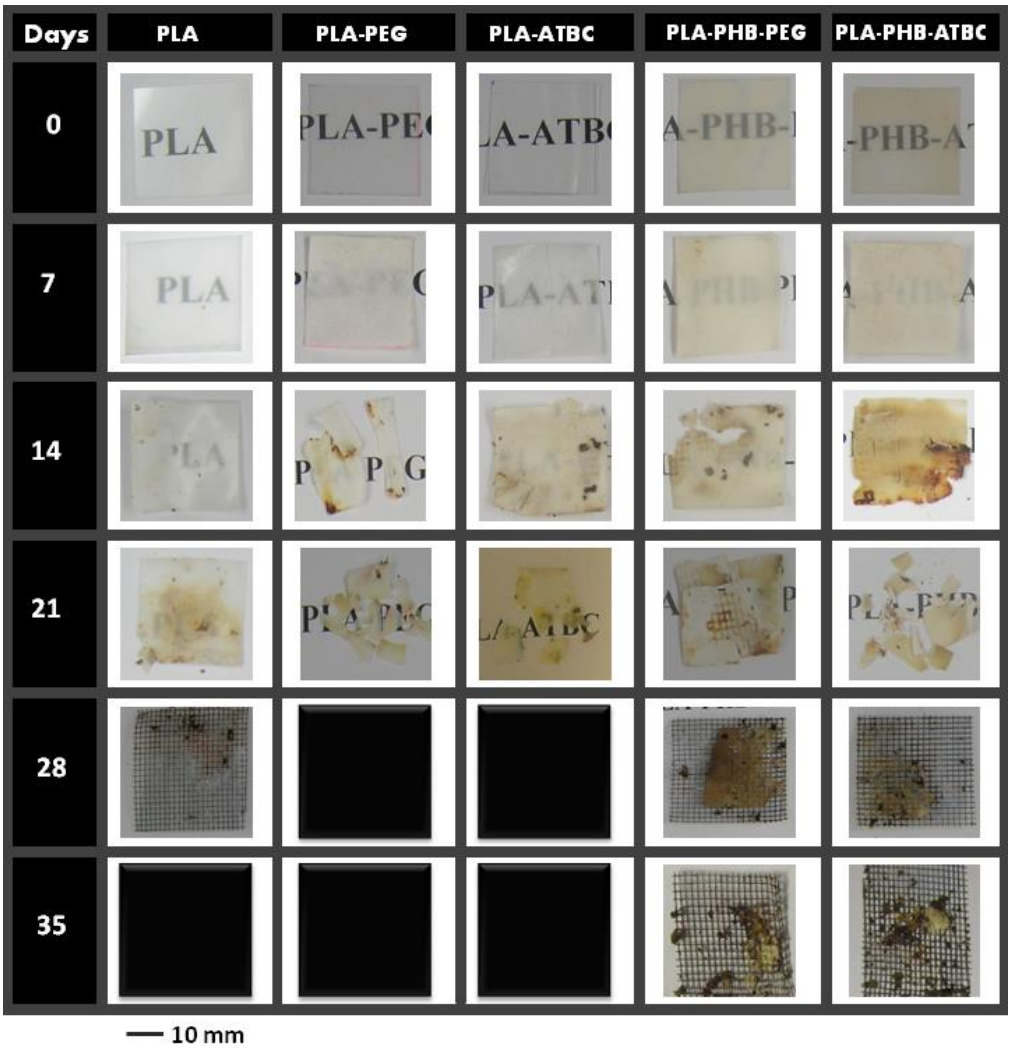


**Figure III.5.1.** Visual aspect of plasticized PLA and PLA-PHB films at different disintegration times.

Figure III.5.2 shows the colorimetric results obtained after 7 days of exposition to composting conditions. The characteristic high brightness of neat PLA decreased after 7 days in composting as evidenced by the decrease in the lightness value ($L$) (Figure III.5.2-a). A similar trend was observed for PLA and PLA-PHB blends plasticized with ATBC. However, a different behaviour was observed for films plasticized with PEG. These samples showed some increase in lightness with testing time. This effect could be due to some plasticizer losses and the consequent compression of macromolecular chains. The addition of PHB to the PLA matrix produced the increase in clear amber tone in PLA-PHB blends.

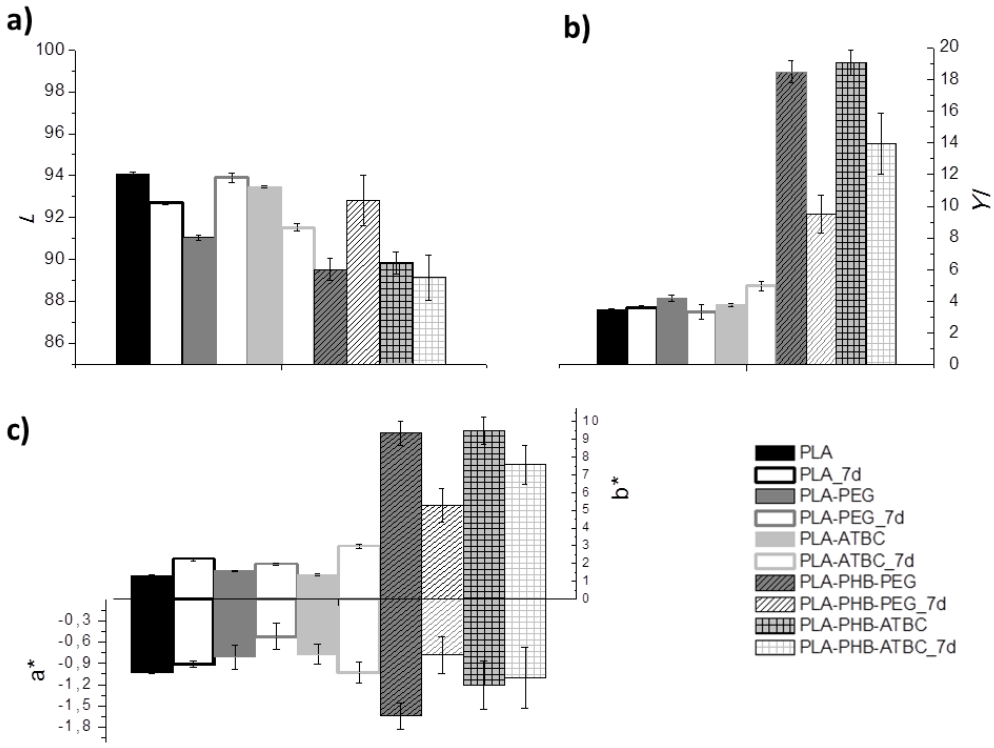


**Figure III.5.2**. Colorimetric parameters of plasticized PLA and PLA-PHB films before and after 7 days (7d) under composting conditions from the CIELab space: **a)** Lightness (*L*) values, **b)** yellowness index (*YI*) and **c)** a* and b* coordinates.

The yellowness index (*YI*) was measured and results are shown in Figure III.5.2-b. No significant differences in *YI* were observed between neat and plasticized PLA films before and after 7 testing days. Plasticized PLA/PHB blends showed a clear decrease in *YI* values, being this effect more evident in the PLA/PHB-PEG film. In addition, positive values of b*, indicative of a deviation towards yellow, as well as negative values of a*, indicative of a deviation towards green, corroborated this tendency to color change in PLA/PHB-PEG films (Figure III.5.2-c).

As can be seen in Figure III.5.1 some differences in visual appearance after 7 days of composting with respect to the corresponding formulation before the test start were observed. Total color difference ($\Delta E$) values indicated that neat PLA was the only sample with no apparent visual changes ($\Delta E$ = 1.7), since $\Delta E$ values higher than 2.0 represent the threshold of the perceptible color difference for the human eye [37]. The $\Delta E$ values for PLA-PEG and PLA-ATBC films were 2.9 and 2.5, respectively, while they were 5.3 and 2.1 for PLA/PHB-PEG and PLA/PHB-ATBC, correspondingly. In summary, all plasticized materials showed perceptible color changes after only 7 days of composting treatment. Changes in films color at the first stages of the composting test were related to the beginning of the hydrolytic degradation process, inducing some changes in the films

refraction index as a consequence of water absorption and/or the presence of hydrolysis products [33]. At higher testing times, films color could not be determined in the same way due to the samples rupture into small pieces and their irregular surfaces. Nevertheless, some qualitative observations could be drawn, since it was clearly noticeable that apparent color changes were related to the degradation stage. PLA/PHB blends tended to yellow at high testing times (Figure III.5.1), due to the PLA disintegration and the consequent increase in the PHB proportion in these formulations. Finally, at 28 days, samples showed a clear yellowness pattern due to the total disintegration of the PLA matrix (Figure III.5.1).

Visual observations were confirmed by calculating the disintegration degree (weight loss) as a function of time (Figure III.5.3) where 90% of disintegration was considered as the goal of samples disintegrability [33], as indicated in the current legislation for biodegradable materials [31]. No significant differences in weight loss were observed between samples after 7 days, but after 14 days the disintegration rate clearly increased for all formulations.

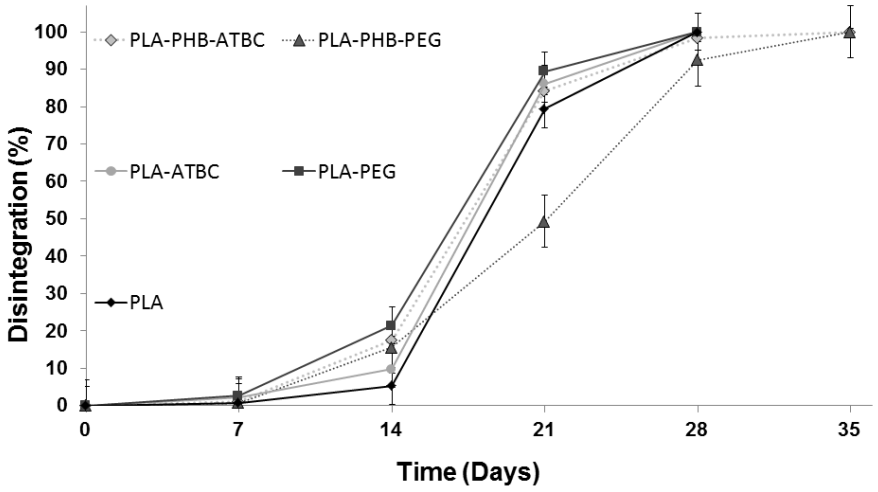


**Figure III.5.3.** Degree of disintegration of: control PLA film, plasticized PLA and plasticized PLA-PHB films under composting conditions as a function of time.

SEM micrographs (Figure III.5.4) showed deep fractures on the films surfaces after 7 testing days, and they were particularly notorious in plasticized materials. No significant differences were observed in plasticized PLA/PHB blends, but PLA-PEG showed higher disintegration rate than PLA-ATBC. This significant difference in plasticized PLA films could be explained by the hydrophilic nature of PEG, in contrast with the hydrophobic character of ATBC. Water absorption and diffusion through the polymer bulk in the initial phase of disintegration in PLA-PEG films was faster than in PLA-ATBC, resulting in higher

hydrolysis in the polymer chain leading to small molecules (monomers and short-chain oligomers) that are available for the microorganisms' attack [26].

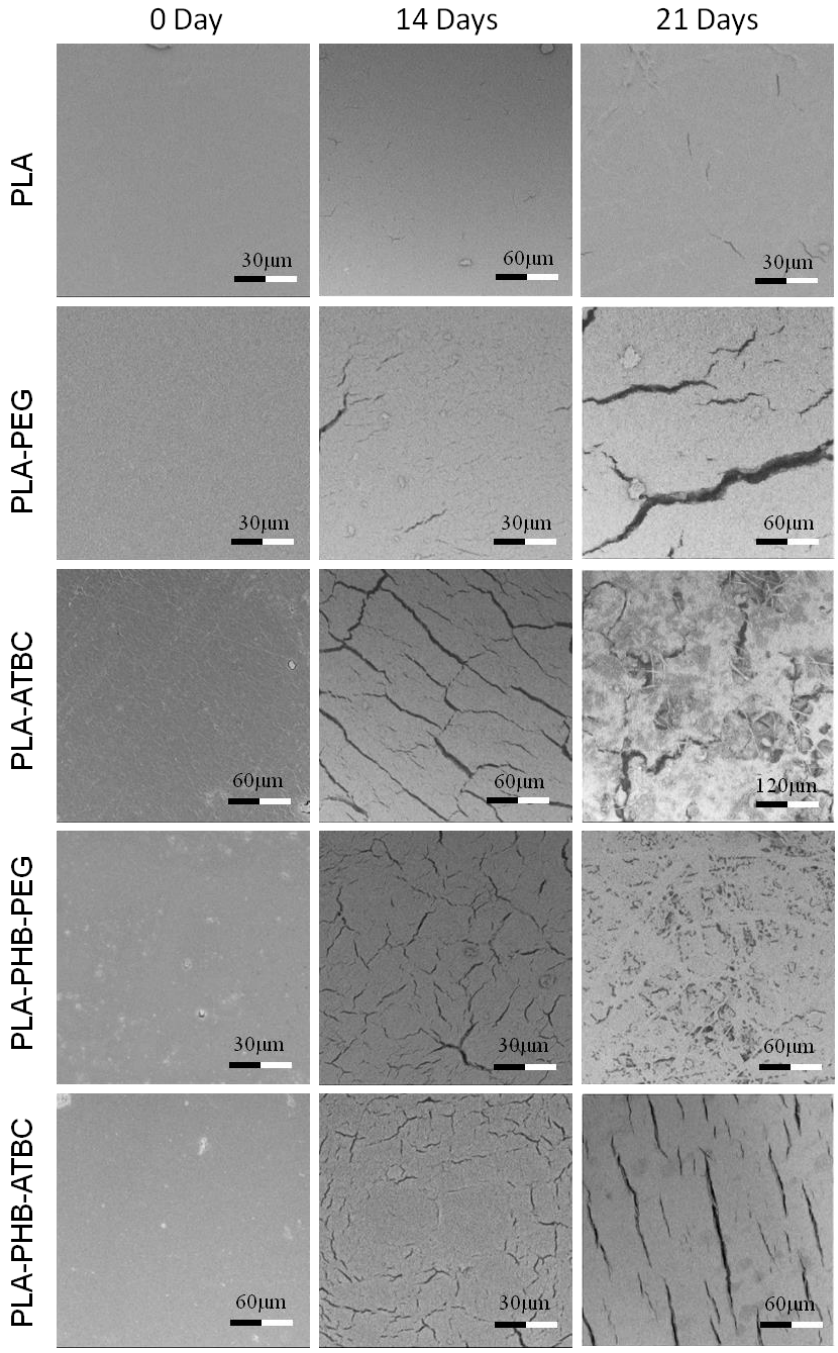


**Figure III.5.4**. SEM observations of neat PLA, plasticized PLA and plasticized PLA-PHB films at different degradation time under composting conditions.

However, PLA/PHB-ATBC blends showed higher disintegration rate (up to 65%) after 21 days of composting than PLA/PHB-PEG (below 50%). This different behaviour could be explained by the formation of acid groups during the plasticizer release in PLA/PHB-ATBC films, which are able to promote the hydrolysis of polymer chains

[33] and consequently accelerating the disintegration process. This result was confirmed by FTIR analysis where the formation of hydroxyl groups (3200-3600 $cm^{-1}$) in plasticized PLA-PHB blends showed higher intensity for the PLA/PHB-ATBC blend, as discussed below. Moreover, SEM micrographs of the PLA/PHB-ATBC blend after 21 days in composting conditions also showed evident signs of surface erosion with deep fractures, while the PLA/PHB-PEG blend showed a more regular surface. As observed in Figure III.5.3, plasticized PLA films achieved more than 85% of disintegration after 21 days and all materials showed weight losses higher than 90% after 28 days, indicating the compostable nature of all these blends.

The film surfaces were also investigated by optical microscopy and their roughness profiles were determined with the EDF-z technique (Figure III.5.5). In a previous work we observed that neat PLA films showed smooth surfaces which were rough in neat PHB films [5]. When applying this technique to PLA and plasticized PLA films, smooth surfaces were obtained (Figure III.5.5) in both cases, although plasticized PLA/PHB films showed some roughness. The more irregular surface profiles showed by films with PHB could be attributed to its higher crystallinity. After 21 days under composting conditions, all samples showed some increase in roughness when compared to the same formulation before the beginning of the test.

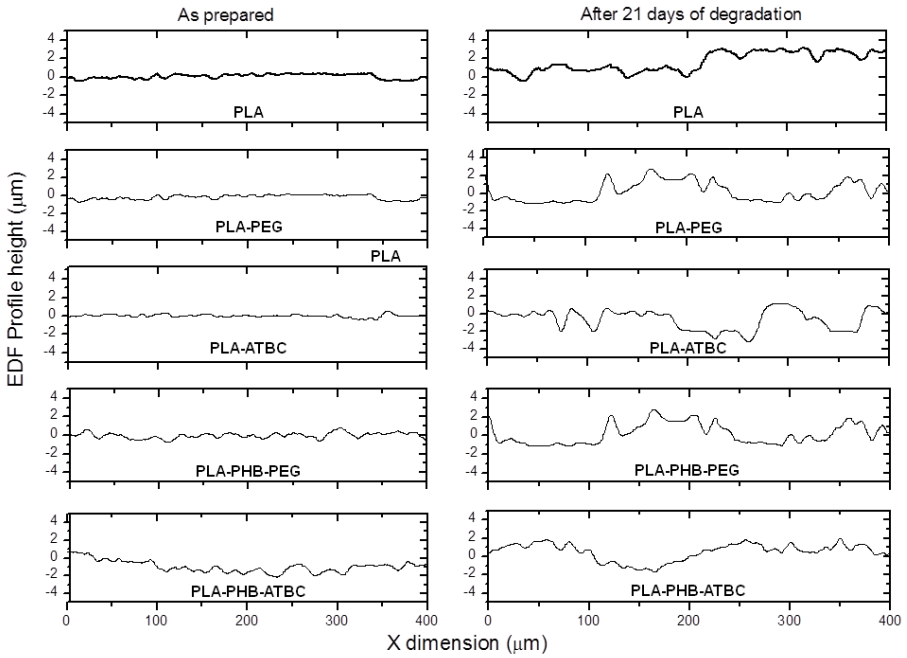


**Figure III.5.5**. EDF-z profiles of films before and after 21 days under composting.

Figure III.5.6 shows the FTIR spectra of each film at different testing times. All PLA based samples revealed the typical band at 1750$cm^{-1}$ assigned to the asymmetric

stretching of the carbonyl group (-C=O) by lactide [1] and [25]. At 1180 $cm^{-1}$ the -C-O- bond stretching in the -CH-O- group of PLA was also observed [25]. The 1450 $cm^{-1}$ band was assigned to the $-CH_3$ group [1] and [38]. It was reported that the intensity of the -C=O band increased with the composting time due to the hydrolytic degradation, resulting in some increase in the number of carboxylic end groups in the polymer chains [25]. In these materials, the -C=O band intensity increased with the composting time in both, PLA and plasticized PLA samples, while it showed broader absorption in films containing PHB. This result was related to the crystalline carbonyl group stretching in PHB at 1735 $cm^{-1}$ [29]. The good miscibility between PLA and PHB was related to the observation of a unique narrow band corresponding to the carbonyl group [9]. Two bands were clearly observed in the PLA/PHB-ATBC film at this wavenumber range at early disintegration stages (Figure III.5.6-e). This observation could be related to some loss of interaction between both polymers with the increase in disintegration time. Another important band was observed around 1600 $cm^{-1}$, corresponding to the formation of carboxylate ions by the action of microorganisms, able to consume lactic acid and PLA oligomers on the film surface leaving carboxylate ions at the chain ends [33]. This behaviour was particularly noticeable in PLA-ATBC films after 21 days under composting (Figure III.5.6-c). It should be also highlighted that this band appeared after 7 days in PLA and plasticized PLA samples and after 14 days in plasticized PLA/PHB films, confirming that PHB helps to slow down the PLA disintegration rate under composting conditions.

Two more bands corresponding to the amorphous and crystalline phases of PLA were observed at 866 $cm^{-1}$ and 756 $cm^{-1}$, respectively [38]. These bands seemed to be unmodified in all samples during the whole composting test with the exception of the PLA-ATBC film, in which the band at 866 $cm^{-1}$ clearly increased in intensity after 21 days (Figure III.5.6-c).

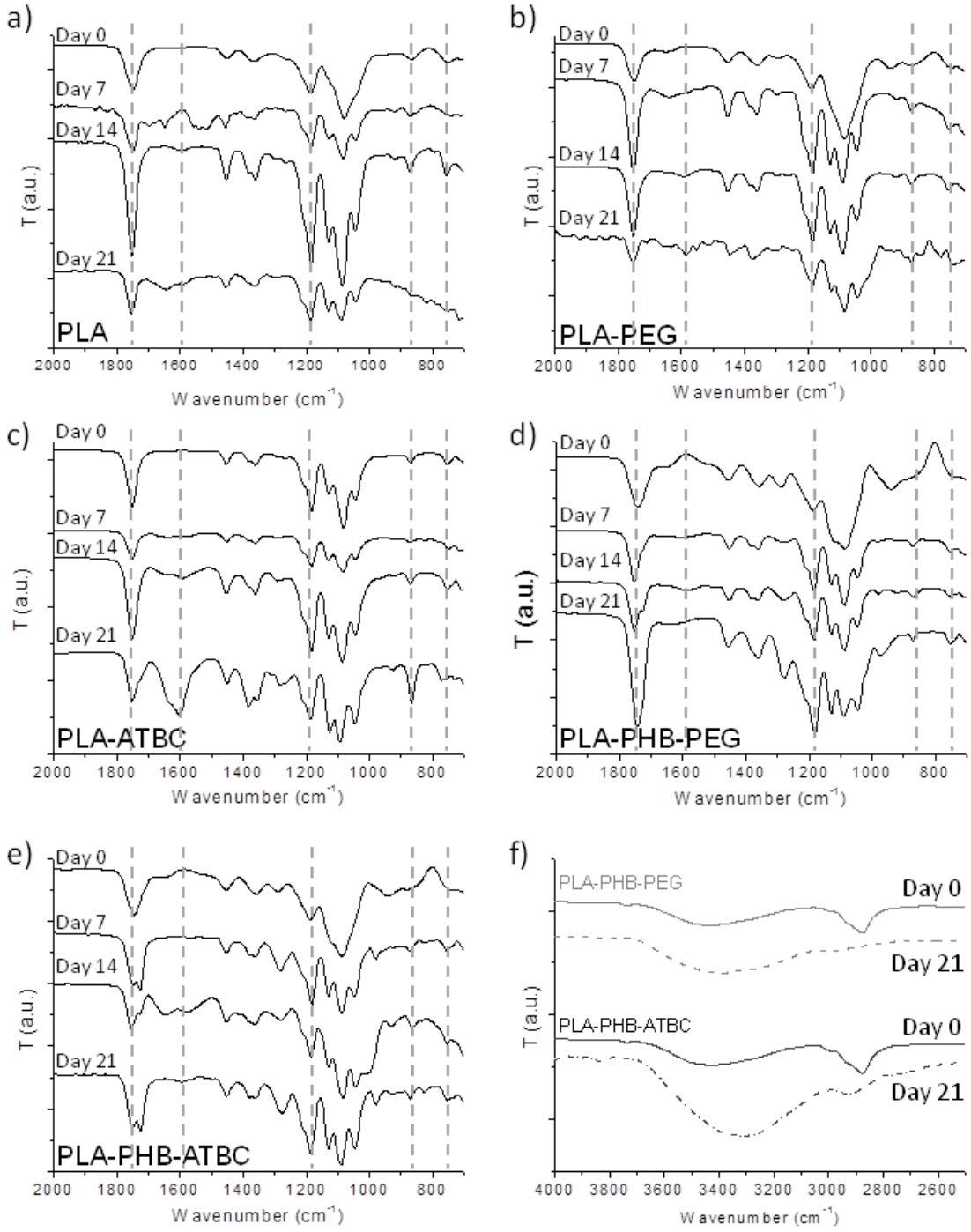


**Figure III.5.6**. Infrared spectra (2000-700 $cm^{-1}$) of: **a)** PLA, **b)** PLA-PEG, **c)** PLA-ATBC, **d)** PLA-PHB-PEG and **e)** PLA-PHB-ATBC at different disintegration times under composting conditions. **f)** Infrared spectra (4000-2500 $cm^{-1}$) of plasticized PLA-PHB blends at day 0 and 21.

TG and DTG curves (not shown) revealed the complete weight loss of PLA and plasticized PLA films in a single degradation step, while plasticized PLA/PHB blends were degraded in two steps, where the first one was assigned to the PHB decomposition and the

second one, at higher temperatures, was related to the PLA thermal degradation. The initial degradation temperature ($T_0$) was calculated for decomposition degree (α) 0.05 and the maximum degradation temperatures ($T_{max}$) were calculated from TG and DTG curves. The main results are summarized in Table III.5.1.

**Table III.5.1.** TG and DTG parameters for films at different disintegration times

| Formulation | Disintegration time (days) | $T_0$ (°C) | $T_{max}$ PHB (°C) | $T_{max}$ PLA (°C) |
|---|---|---|---|---|
| PLA | 0 | 332 | - | 366 |
| | 7 | 331 | - | 363 |
| | 14 | 261 | - | 346 |
| | 21 | 240 | - | 341 |
| PLA-PEG | 0 | 271 | - | 366 |
| | 7 | 240 | - | 350 |
| | 14 | 233 | - | 325 |
| | 21 | 218 | - | 298 |
| PLA-ATBC | 0 | 280 | - | 364 |
| | 7 | 253 | - | 278 |
| | 14 | 228 | - | 291 |
| | 21 | 224 | - | 278 |
| PLA-PHB-PEG | 0 | 269 | 285 | 324 |
| | 7 | 255 | 280 | 314 |
| | 14 | 224 | 282 | 337 |
| | 21 | 221 | 262 | - |
| PLA-PHB-ATBC | 0 | 272 | 290 | 361 |
| | 7 | 269 | 290 | 346 |
| | 14 | 220 | 271 | 332 |
| | 21 | 220 | 268 | 285 |

It was observed that both degradation temperatures decreased significantly with the disintegration time. While a slight decrease (around 0.3%) was observed for $T_0$ of neat PLA after 7 days, plasticized PLA films showed higher reductions (around 11% in PLA-PEG and 10% in PLA-ATBC). Lower reductions were observed for PLA/PHB-PEG and PLA/PHB-ATBC blends (5% and 1% in $T_0$, respectively). The decrease in $T_0$ after 7 testing days could be related with the high plasticizer loss caused by hydrolysis during the initial disintegration stages. It was also observed that plasticizers were more efficiently retained by PLA/PHB blends than by neat PLA. After 7 days the reduction of $T_{max}$ in PLA did not

show large differences between PLA, PLA-PEG and plasticized PLA/PHB blends (around 3-5%) but PLA-ATBC showed a considerable reduction in this value, close to 20%. The $T_{max}$ of PLA reached the maximum reduction (18-23%) after 21 days in plasticized PLA films. The corresponding peak of DTG associated with the PLA thermal degradation almost disappeared in the PLA/PHB-PEG film after 21 days, suggesting the gradual disappearance of PLA in the blend by being preferentially attacked by microorganisms during composting. Conversely, the reductions of $T_{max}$ corresponding to the PHB thermal degradation only reached 8% after 21 days of disintegration.

Figure III.5.7-a shows the chromatogram obtained after pyrolysis of the PLA/PHB-PEG film before composting. Py-GC/MS analysis of all films showed the typical thermal degradation products of PLA with the characteristic series of signals at m/z = 56 + (n x 72) attributed to the PLA degradation products [34]. Peaks at retention times 17.5 min and 18.5 min showed highly similar mass spectra for m/z = 56 + 72 (n=1) where the main fragments were those with m/z = 32, 43, 45 and 56 being assigned to mesolactide and (L,D)-lactide [34]. For PLA/PHB blends, the broad peak of crotonic acid showing the main fragmentation at m/z = 39, 41, 68, 69, and 86, was observed [5]. The peak at 23 min retention time was only observed in films plasticized with PEG with m/z = 32, 41, 68, 87, 103, 154, corresponding to the thermal degradation products of PEG. On the other hand, blends plasticized with ATBC showed two main peaks corresponding to tributyl propene-1,2,3-tricarboxylate (m/z = 41, 57, 112, 139, 156, 157, 168, 213 and 269) at 40.5 min and the characteristic peak of tributyl acetylcitrate (m/z = 29, 41, 57, 129, 139, 157, 185 and 259) at 42.5 min (Figure III.5.7-b and 7-c). It was observed that PLA/PHB-ATBC samples before and after 21 days under composting conditions showed the same ratio for these two peaks, while the PLA-ATBC film showed some decrease in the intensity of the tributyl propene-1,2,3-tricarboxylate peak after 21 days, suggesting that ATBC was easily released from the PLA matrix. This result is in agreement with the higher degradation rate in PLA-ATBC samples (Figure III.5.3). This behaviour could be explained by the preferential microorganisms attack to low molar mass fragments, which are more easily consumed when ATBC is available while these molecules are more difficult to reach in the non-plasticized PLA/PHB blend. Furthermore, smaller peaks at higher retention times also showed the characteristic series of signals of PLA (m/z = 56 + n x 72) with n = 2 and 3.

Table III.5.2 also shows the mesolactide to (D,L)-lactide ratio obtained from the Py-GC/MS chromatograms. These results showed the increase in the *meso*-lactide fraction of all materials during composting and they could be related to the preferential selection of microorganisms to attack the L-lactide fraction of the polymer structure [39].

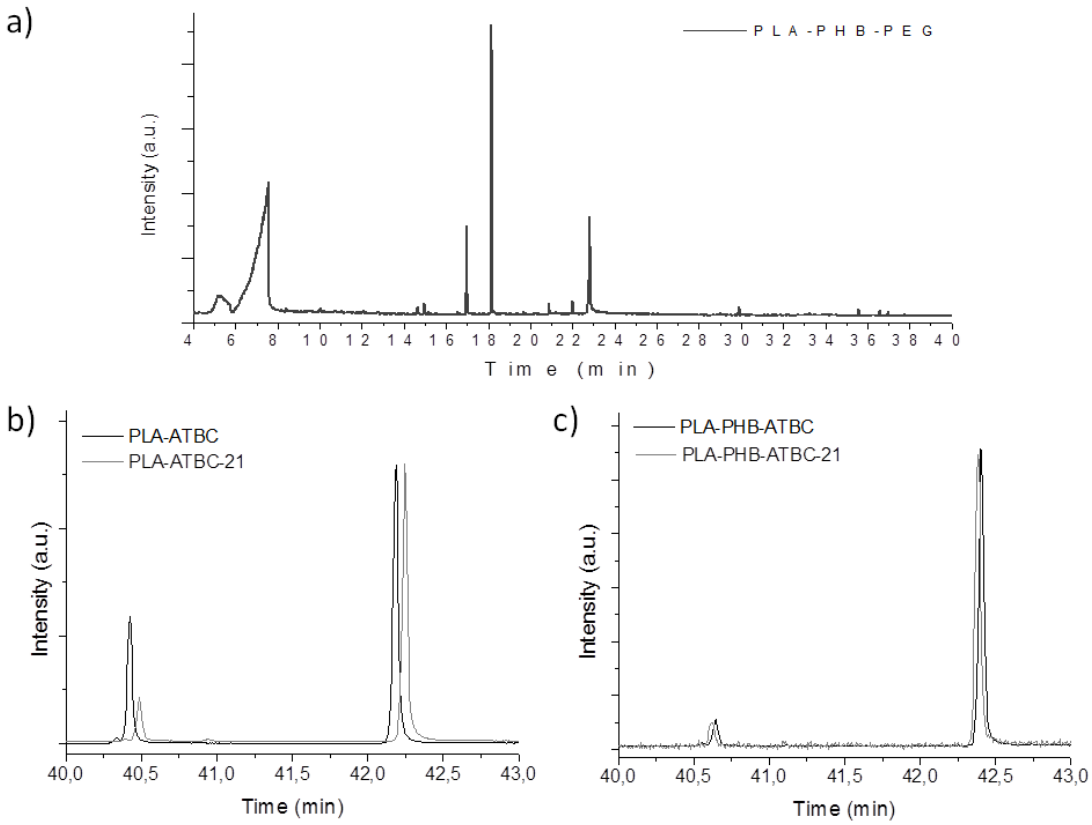


**Figure III.5.7. a)** Chromatogram obtained after pyrolysis of PLA-PHB-PEG. ATBC degradation products obtained after pyrolysis of: **b)** PLA-ATBC and **c)** PLA-PHB-ATBC before and after 21 days composting test.

**Table III.5.2**. Ratio between mesolactide and D,L-Lactide Py-GC/MS areas

| Formulation | Disintegrability day | *meso*-lactide : D,L-Lactide |
|---|---|---|
| PLA | 0 | 1 : 3.08 |
| | 21 | 1 : 1.66 |
| PLA-PEG | 0 | 1 : 7.15 |
| | 21 | 1 : 5.61 |
| PLA-ATBC | 0 | 1 : 6.33 |
| | 21 | 1 : 2.47 |
| PLA-PHB | 0 | 1 : 7.86 |
| | 21 | 1 : 2.62 |
| PLA-PHB-PEG | 0 | 1 : 7.36 |
| | 21 | 1 : 5.43 |
| PLA-PHB-ATBC | 0 | 1 : 4.43 |
| | 21 | 1 : 3.39 |

Nanomechanical properties were investigated with the nanoindentation technique. Only fresh samples (stored at 25°C and 30% RH) and those after 7 disintegration days could be tested, since those after 14 and 21 days were too fragile. The calculated hardness ($H$) and reduced modulus ($E_r$) in depth profiles are shown in Figure III.5.8.

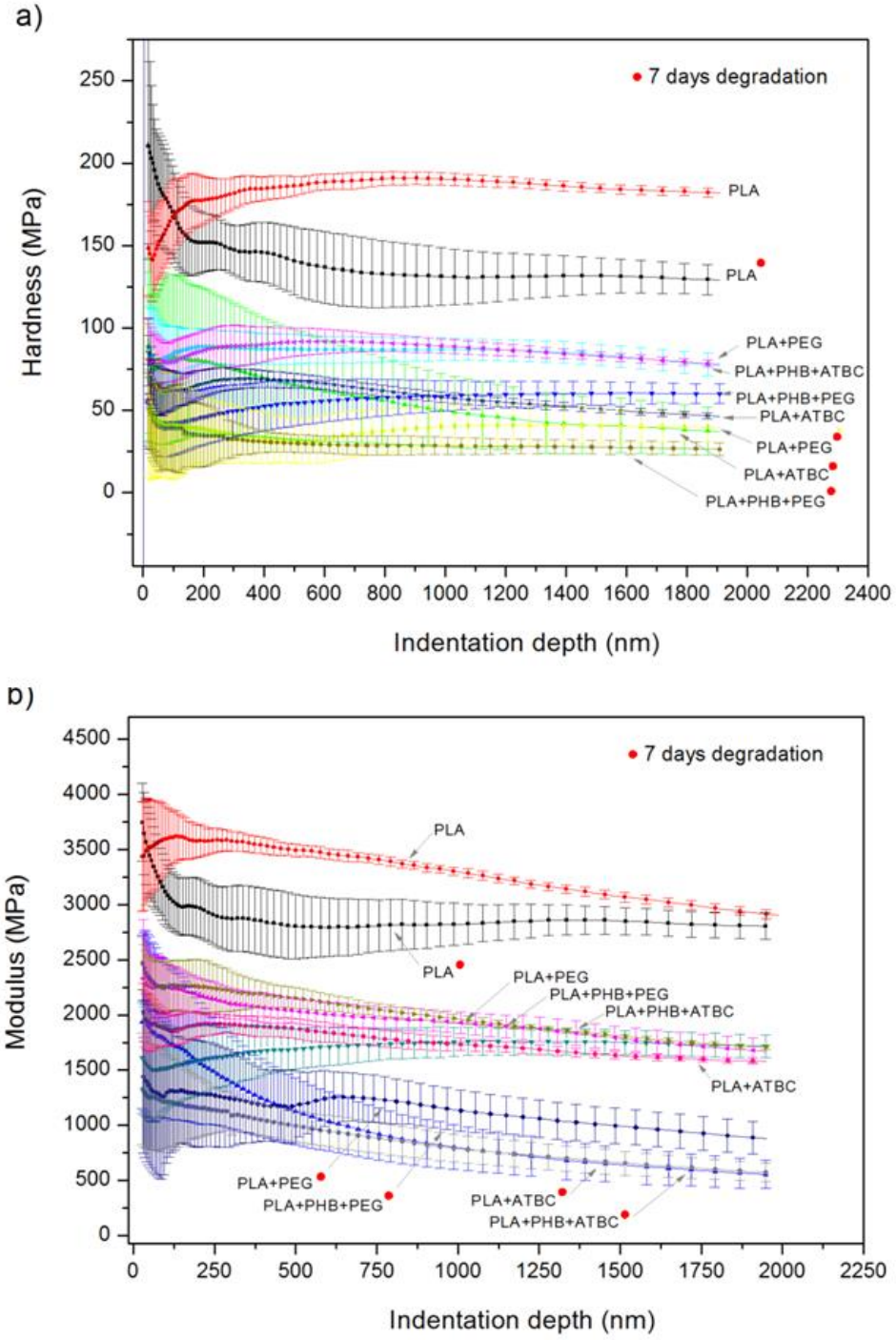


**Figure III.5.8. a)** Hardness and **b)** modulus curves obtained by nanoindentation of fresh films and those after 7 days in composting conditions.

Neat PLA showed the highest $H$ and $E_r$ values (around 200 MPa and 3500 MPa, respectively). The presence of either plasticizers or PHB in PLA formulations clearly reduced these parameters, even before the disintegration test, due to the plasticizer effect which reduced the inherent brittleness of both biopolymers [5]. All films after 7 testing days showed lower values than the fresh materials. These results demonstrated that nanoindentation is a powerful tool to evaluate the loss in mechanical properties of biopolymers submitted to composting [40] and [41]. The lowest values corresponded to plasticized films after 7 days, corroborating the observation of the higher degradation rate in plasticized materials. Although the reduction on mechanical properties is one of the main consequences of the degradation process occurring during composting, this process also favoured the microorganism's action. This effect could be explained since the loss in mechanical properties after 7 composting days produced a brittle material consisting in broken pieces with a high defects density, such as cracks and porous structure, permitting the easy access of microorganisms to the polymer bulk. The optical inspection of nanoindented samples (Figure III.5.9) revealed these defects.

Figure III.5.10 shows the $H$ and $E_r$ values averaged between 400 and 600 nm depth for plasticized and unplasticized materials. The reduction in both parameters after 7 composting days was more evident in films plasticized with PEG. While neat PLA lost around 20% in $H$ and $E_r$, all other materials lost approximately 50%, with the exception of the PLA/PHB-ATBC film that showed a similar behaviour than neat PLA. This result confirmed that ATBC increased the interaction between PLA and PHB and this blend showed higher mechanical resistance.

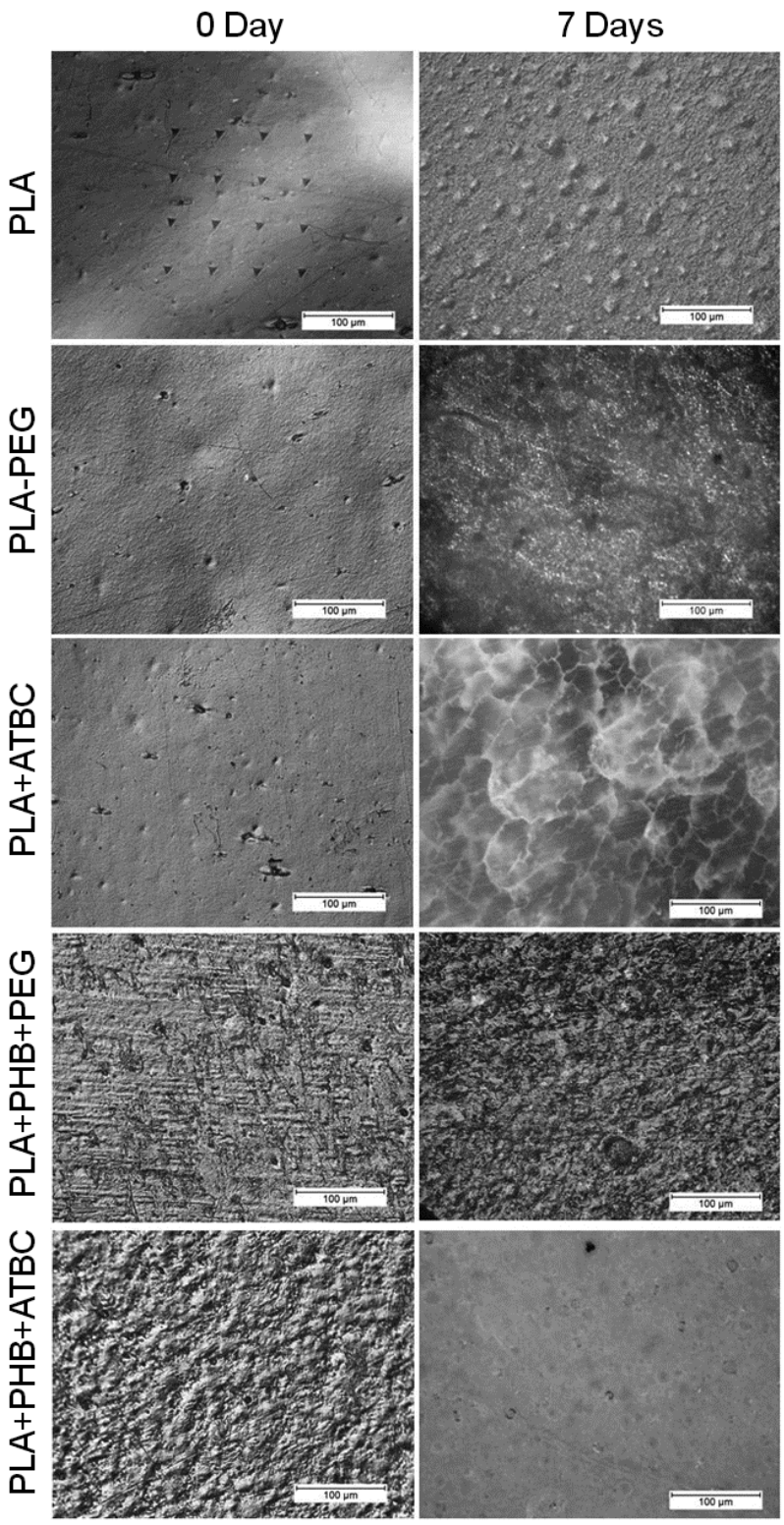


**Figure III.5.9.** Optical micrographs of the films surface of fresh films and after 7 composting days. Fresh PLA film shows the imprints of the Berckovich indenter.

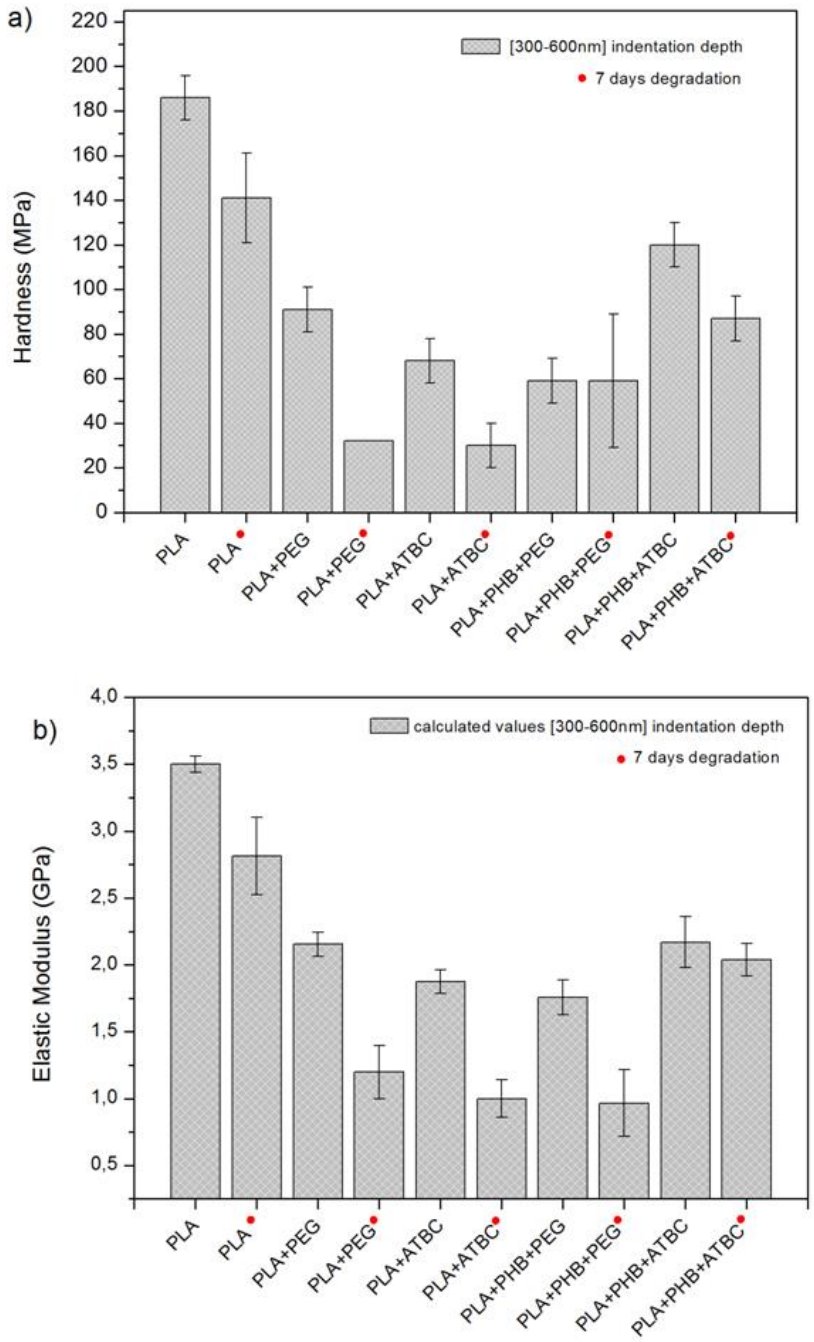


**Figure III.5.10.** Summary of $H$ and $E_r$ results for each film calculated (400-600 nm) in depth

## 5. CONCLUSIONS

Formulations based on plasticized PLA/PHB blends were successfully disintegrated under composting conditions in less than one month, stating their biodegradable character. The ability of PHB to act as nucleating agent in PLA/PHB blends slowed down the PLA disintegration, while plasticizers speeded it up. TGA analysis

revealed that plasticizers were mainly lost during the initial disintegration stages, while substantial losses in mechanical properties for all blends were also observed. The presence of plasticizers favoured the surface hydrolysis leading to the loss in mechanical properties, which also made disintegration easier. Py-GC/MS studies demonstrated the increase in the *meso*-lactide form for all blends due to the high microorganism's activity during composting. In summary, plasticized PLA/PHB blends may offer good perspective for biodegradable food packaging industry by improving the polymer performance in films manufacturing and use.

**Acknowledgements**

Authors thank Spanish Ministry of Economy and Competitiveness by financial support (MAT2011-28468-C02-01 and MAT2011-28468-C02-02). M.P. Arrieta thanks Generalitat Valenciana for Santiago Grisolía Fellowship (2011/007). Authors gratefully acknowledge Prof. Mª Dolores Salvador (Polytechnic University of Valencia) for her assistance with nanomechanical and optical microscope analysis.

**REFERENCES**

[1] Arrieta MP, López J, Ferrándiz S, Peltzer MA. Characterization of PLA-limonene blends for food packaging applications. Polymer Testing. 2013;32(4):760-768.

[2] Auras R, Harte B, Selke S. An Overview of Polylactides as Packaging Materials. Macromolecular Bioscience. 2004; 4(9):864.

[3] Abdelwahab MA, Flynn A, Chiou B-S, Imam S, Orts W, Chiellini E. Thermal, mechanical and morphological characterization of plasticized PLA-PHB blends. Polymer Degradation and Stability. 2012;97(9):1822-1828.

[4] Fortunati E, Armentano I, Iannoni A, Kenny JM. Development and thermal behaviour of ternary PLA matrix composites. Polymer Degradation and Stability. 2010;95(11):2200-2206.

[5] Arrieta MP, López J, Hernández A, Rayón E. Ternary PLA-PHB-Limonene blends intended for biodegradable food packaging applications. European Polymer Journal. 2014;50:255-270.

[6] Bucci DZ, Tavares LBB, Sell I. Biodegradation and physical evaluation of PHB packaging. Polymer Testing. 2007;26(7):908-915.

[7] Dong W, Ma P, Wang S, Chen M, Cai X, Zhang Y. Effect of partial crosslinking on morphology and properties of the poly(β-hydroxybutyrate)/poly(d,l-lactic acid) blends. Polymer Degradation and Stability. 2013;98(9):1549-1555.

[8] Furukawa T, Sato H, Murakami R, Zhang JM, Duan YX, Noda I, et al. Structure, dispersibility, and crystallinity of poly(hydroxybutyrate)/poly(L-lactic acid) blends studied by FT-IR microspectroscopy and differential scanning calorimetry. Macromolecules. 2005;38(15):6445-6454.

[9] Zhang M, Thomas NL. Blending Polylactic Acid with Polyhydroxybutyrate: The Effect on Thermal, Mechanical, and Biodegradation Properties. Advances in Polymer Technology. 2011;30(2):67-79.

[10] Bartczak Z, Galeski A, Kowalczuk M, Sobota M, Malinowski R. Tough blends of poly(lactide) and amorphous poly([R,S]-3-hydroxy butyrate) - Morphology and properties. European Polymer Journal. 2013;49(11):3630-3641.

[11] Blümm E, Owen AJ. Miscibility, crystallization and melting of poly(3-hydroxybutyrate)/ poly(l-lactide) blends. Polymer. 1995;36(21):4077-4081.

[12] Hu Y, Sato H, Zhang J, Noda I, Ozaki Y. Crystallization behavior of poly(l-lactic acid) affected by the addition of a small amount of poly(3-hydroxybutyrate). Polymer. 2008;49(19):4204-4210.

[13] Zhang L, Xiong C, Deng X. Miscibility, crystallization and morphology of poly(β-hydroxybutyrate)/poly(d,l-lactide) blends. Polymer. 1996;37(2):235-241.

[14] Focarete ML, Ceccorulli G, Scandola M, Kowalczuk M. Further evidence of crystallinity-induced biodegradation of synthetic atactic poly(3-hydroxybutyrate) by PHB-depolymerase A from Pseudomonas lemoignei. Blends of atactic poly(3-hydroxybutyrate) with crystalline polyesters. Macromolecules. 1998;31(24):8485-8492.

[15] Burgos N, Martino VP, Jiménez A. Characterization and ageing study of poly(lactic acid) films plasticized with oligomeric lactic acid. Polymer Degradation and Stability. 2013;98(2):651-658.

[16] Lemmouchi Y, Murariu M, Dos Santos AM, Amass AJ, Schacht E, Dubois P. Plasticization of poly(lactide) with blends of tributyl citrate and low molecular weight poly(D,L-lactide)-b-poly(ethylene glycol) copolymers. European Polymer Journal. 2009;45(10):2839-2848.

[17] Courgneau C, Domenek S, Guinault A, Averous L, Ducruet V. Analysis of the Structure-Properties Relationships of Different Multiphase Systems Based on Plasticized Poly(Lactic Acid). Journal of Polymers and the Environment. 2011;19(2):362-371.

[18] Bitinis N, Fortunati E, Verdejo R, Bras J, Kenny JM, Torre L, et al. Poly(lactic acid)/natural rubber/cellulose nanocrystal bionanocomposites. Part II: Properties evaluation. Carbohydrate Polymers. 2013;96(2):621-627.

[19] Erceg M, Kovacic T, Klaric I. Thermal degradation of poly(3-hydroxybutyrate) plasticized with acetyl tributyl citrate. Polymer Degradation and Stability. 2005;90(2):313-318.

[20] Parra DF, Fusaro J, Gaboardi F, Rosa DS. Influence of poly (ethylene glycol) on the thermal, mechanical, morphological, physical-chemical and biodegradation properties of poly (3-hydroxybutyrate). Polymer Degradation and Stability. 2006;91(9):1954-1959.

[21] Quintana R, Persenaire O, Lemmouchi Y, Sampson J, Martin S, Bonnaud L, et al. Enhancement of cellulose acetate degradation under accelerated weathering by plasticization with eco-friendly plasticizers. Polymer Degradation and Stability. 2013;98(9):1556-1562.

[22] Yagi H, Ninomiya F, Funabashi M, Kunioka M. Thermophilic anaerobic biodegradation test and analysis of eubacteria involved in anaerobic biodegradation of four specified biodegradable polyesters. Polymer Degradation and Stability. 2013;98(6):1182-1187.

[23] Armentano I, Bitinis N, Fortunati E, Mattioli S, Rescignano N, Verdejo R, et al. Multifunctional nanostructured PLA materials for packaging and tissue engineering. Progress in Polymer Science. 2013;38(10–11):1720-1747.

[24] Song JH, Murphy RJ, Narayan R, Davies GBH. Biodegradable and compostable alternatives to conventional plastics. Philosophical Transactions of the Royal Society B: Biological Sciences. 2009;364(1526):2127-2139.

[25] Fortunati E, Puglia D, Santulli C, Sarasini F, Kenny JM. Biodegradation of Phormium tenax/poly(lactic acid) composites. Journal of Applied Polymer Science. 2012;125(SUPPL. 2):E562-E572.

[26] Kale G, Auras R, Singh SP. Degradation of commercial biodegradable packages under real composting and ambient exposure conditions. Journal of Polymers and the Environment. 2006;14(3):317-334.

[27] Sarasa J, Gracia JM, Javierre C. Study of the biodisintegration of a bioplastic material waste. Bioresource Technology. 2009;100(15):3764-3768.

[28] Corrêa MCS, Rezende ML, Rosa DS, Agnelli JAM, Nascente PAP. Surface composition and morphology of poly(3-hydroxybutyrate) exposed to biodegradation. Polymer Testing. 2008;27(4):447-452.

[29] Weng YX, Wang L, Zhang M, Wang XL, Wang YZ. Biodegradation behavior of P(3HB,4HB)/PLA blends in real soil environments. Polymer Testing. 2013;32(1):60-70.

[30] Martino VP, Ruseckaite RA, Jimenez A. Ageing of poly(lactic acid) films plasticized with commercial polyadipates. Polymer International. 2009;58(4):437-444.

[31] UNE EN-ISO 20200. Determination of the degree of disintegration of plastic materials under simulated composting conditions in a laboratory-scale test. 2006.

[32] Martucci JF, Ruseckaite RA. Tensile Properties, Barrier Properties, and Biodegradation in Soil of Compression-Molded Gelatin-Dialdehyde Starch Films. Journal of Applied Polymer Science. 2009;112(4):2166-2178.

[33] Fortunati E, Armentano I, Iannoni A, Barbale M, Zaccheo S, Scavone M, et al. New multifunctional poly(lactide acid) composites: Mechanical, antibacterial, and degradation properties. Journal of Applied Polymer Science. 2012;124(1):87-98.

[34] Arrieta MP, Parres F, López J, Jiménez A. Development of a novel pyrolysis-gas chromatography/mass spectrometry method for the analysis of poly(lactic acid) thermal degradation products. J Anal Appl Pyrolysis. 2013;101:150-155.

[35] Pei A, Malho JM, Ruokolainen J, Zhou Q, Berglund LA. Strong nanocomposite reinforcement effects in polyurethane elastomer with low volume fraction of cellulose nanocrystals. Macromolecules. 2011;44(11):4422-4427.

[36] Rayón E, López J, Arrieta MP. Mechanical characterization of microlaminar structures extracted from cellulosic materials using nanoindentation technique. Cellulose Chemistry and Technology. 2013;47(5-6):345-351.

[37] Arrieta MP, Peltzer MA, López J, Garrigós MDC, Valente AJM, Jiménez A. Functional properties of sodium and calcium caseinate antimicrobial active films containing carvacrol. Journal of Food Engineering. 2014;121(1):94-101.

[38] Siracusa V, Blanco I, Romani S, Tylewicz U, Rocculi P, Rosa MD. Poly(lactic acid)-modified films for food packaging application: Physical, mechanical, and barrier behavior. Journal of Applied Polymer Science. 2012;125(SUPPL. 2):E390-E401.

[39] Khabbaz F, Karlsson S, Albertsson AC. Py-GC/MS an effective technique to characterizing of degradation mechanism of poly (L-lactide) in the different environment. Journal of Applied Polymer Science. 2000;78(13):2369-2378.

[40] Giró-Paloma J, Roa JJ, Díez-Pascual AM, Rayón E, Flores A, Martínez M, et al. Depth-sensing indentation applied to polymers: A comparison between standard methods of analysis in relation to the nature of the materials. European Polymer Journal. 2013.

[41] Roa JJ, Rayon E, Morales M, Segarra M. Contact mechanics at nanometric scale using nanoindentation technique for brittle and ductile materials. Recent Patents on Nanotechnology. 2012;6(2):142-152.

## 6. Multifunctional PLA-PHB/cellulose nanocrystal films. Processing, structural and thermal properties

*Arrieta, M.P.[a,e], Fortunati, E.[b], Dominici, F[b]., Rayón, E.[c], López, J.[1], Kenny, J.M.[b,d]*

[a]Instituto de Tecnología de Materiales. Universitat Politècnica de Valencia, 03801 Alcoy-Alicante, Spain.

[b]Materials Engineering Centre, UdR INSTM, NIPLAB, University of Perugia, 05100, Terni, Italy.

[c]Instituto de Tecnología de Materiales. Universitat Politècnica de Valencia, E-46022, Valencia, Spain.

[d]Institute of Polymer Science and Technology, CSIC, Juan de la Cierva 3, Madrid 28006, Spain.

[e]Analytical Chemistry, Nutrition and Food Sciences Department, University of Alicante, P.O. Box 99, E-03080 Alicante, Spain.

**Carbohydrate Polymers**

**107: 16-24 (2014)**

**Abstract**

Cellulose nanocrystals (CNC) synthesized from microcrystalline cellulose by acid hydrolysis were added into poly(lactic acid)-poly(hydroxybutyrate) (PLA-PHB) blends to improve the final properties of the multifunctional systems. CNC were also modified with a surfactant (CNCs) to increase the interfacial adhesion in the systems maintaining the thermal stability. Firstly, masterbatch pellets were obtained for each formulation to improve the dispersion of the cellulose structures in the PLA-PHB and then nanocomposite films were processed. The thermal stability as well as the morphological and structural properties of nanocomposites were investigated. While PHB increased the PLA crystallinity due to its nucleation effect, well dispersed CNC and CNCs not only increased the crystallinity but also improved the processability, the thermal stability and the interaction between both polymers especially in the case of the modified CNCs based PLA-PHB formulation. Likewise, CNCs were better dispersed in PLA-CNCs and PLA-PHB-CNCs, than CNC.

**Keywords:** Poly(lactic acid); Poly(hydroxybutyrate); Cellulose nanocrystals, Blends, Nanocomposites, Film processing; Thermal properties.

## 1. INTRODUCTION

Several biodegradable polymers have been investigated during the last few decades as alternatives to non-degradable polymers currently used in film production with particular attention to the food packaging sector [1, 2]. In this sense, poly(lactic acid) (PLA) is one of the most attractive biodegradable polymers used in short-term food commodities [3]. PLA can be processed by usual thermoplastic technologies such as extrusion, injection molding, sheet extrusion, blow molding, thermoforming and film forming) [4]. PLA is a semicrystalline polymer with low softening temperature and therefore it shows glasslike appearance at room temperature. Is being used in the food industry since seeing through the packaging is one of the most important requirements for consumers [5] and PLA shows high transparency. Unfortunately, so far the use of PLA as film for food packaging is limited because PLA shows high brittleness [4], low heat resistance [6] and poor barrier properties [7]. Interest in reducing PLA inherent brittleness and improving gas barrier properties, has led researchers and industries to develop new PLA matrices with increased crystallinity.

Poly(hydroxybutyrate) (PHB) is the best known poly(hydroxyalcanoate) (PHA) synthesized by controlled bacterial fermentation [8]. It presents high crystallinity [9]; nevertheless, the main drawback of PHB is that it has the melting temperature at about 170-180 °C [10, 11], close to the degradation temperature (typically around 270 °C) [12], showing a small processing window for melt extrusion [11, 12]. Thus, PHB processing temperature should be at least 180-190 °C but its thermal degradation proceeds very quickly at these temperatures [13]. Nevertheless, the melting temperature of PHB can be lowered far below the thermal decomposition temperature to make this material much easier to process [14] through chemical or physical modifications: introducing other structural units into the PHB backbone or blending with another polymer, respectively [11].

Many modifications have been proposed for extending biopolymers applications such as the addition of modifiers, copolymerization or blending. In this sense, blend process is a common and relatively simple approach to tuning the physical and mechanical properties of biopolymers [15]. The modification of biopolymers by blending with other bio-based and/or biodegradable polymer has many advantages, because it offers the opportunity to improve properties in a wide range, while legislation also favors completely compostable materials with minimal carbon-footprint [16].

PLA and PHB present similar melting temperatures, thus they can be blended in the melt state leading to a new biodegradable material that combine the advantages of

both polymers. It is expected that PHB crystals increase the crystallinity of PLA [8, 17], as well as PLA can significantly improve the stiffness of PHB [18]. It has been reported that the best synergic effect is achieved blending PLA and PHB in 75wt% and 25wt% ratio, respectively [8, 10, 19].

Alternatively, the use of natural reinforcements to improve the mechanical properties of biopolymers for food packaging applications represents a promising method without influencing the transparency [1, 20]. For millennia, natural lignocellulosic basic materials, referring to its main constituent cellulose, hemicelluloses and lignin have been used in the form of wood and plant fibers by number of industries in forest products, paper, textiles, etc [21]. It is known that the high mechanical and nanomechanical performance of natural materials extracted from the agriculture is conferred by cellulosic hieralchical structures [22]. The second generation of cellulosic based materials, focused in the nanometer scale, are represented by cellulose nanocrystals (CNC), which offer new properties including high biodegradability, better uniformity and durability [21]. Cellulose nanocrystals (CNC) have been successfully incorporated into the PLA matrix by Fortunati and colleagues [20, 23-25] and also into the PHB matrix [26] showing an improvement in the mechanical properties better than other reinforcing materials. The incorporation of CNC into the PLA matrix has shown to improve oxygen barrier properties of PLA [27]. Therefore they are suitable for food packaging applications. Moreover, the incorporation of CNC allows reducing the amount of biopolymer in the final formulation offering additional advantages such as they are fully renewable and biodegradable, and possess high stiffness and low density. CNC is commonly synthesized from the acid hydrolysis of microcrystalline cellulose (MCC) [28, 29]. However, the homogeneous dispersion of CNC in PLA matrix is not easy to achieve [6] due to its hydrophilic character [30]. One strategy to favor the CNC dispersion and therefore the final properties of the final formulation is using a surfactant for the CNC surface modification [29].

In this work the innovative combination of PLA-PHB blends reinforced with cellulose nanocrystals were prepared by melt compounding extrusion followed by film forming with the main purpose to produce new biodegradable ternary systems with increased interaction, crystallinity and thermal properties. The main objective is to evaluate the effect of synthesized cellulose nanocrystals (CNC) and surfactant modified cellulose nanocrystals (CNCs) in PLA-PHB blends with the aim of improving PLA-PHB processability and obtaining a fully biodegradable film based on PLA matrix with increased crystallinity intended for food packaging. With this propose, PLA-PHB masterbatchs were prepared by melt blending and then CNC and CNCs were added prior to film processing to improve the dispersion of the cellulose nanocrystals in the PLA and

PLA-PHB matrices. So, cellulose nanocrystals dispersion during processing and in the obtained nanocomposite films was specifically addressed and discussed. Another issue concerning the development of such systems is the thermal stability due to the cellulose nanocrystals introduction and their modification and/ or degradation during processing. Thus isothermal and dynamic thermal studies were also conducted. Moreover, fully morphological and structural characterizations of the obtained nanocomposite films were carried out.

## 2. MATERIALS AND METHODS

### 2.1. Materials

Poly(lactic acid) (PLA 2002D, $M_n$ = 98,000 g·mol$^{-1}$, 4 wt% D-isomer) was supplied by NatureWorks (USA), Poly(hydroxybutyrate) (PHB, under the trade name PHI002) was acquired by NaturePlast (France) and microcrystalline cellulose (MCC, dimensions of 10-15 μm) was purchased from Sigma-Aldrich.

### 2.2. Nanocrystal synthesis and modification

Cellulose nanocrystal suspension was prepared from 20g of MCC by acid hydrolysis following the recipe used by Fortunati et al., 2012 [29]. Sulphuric acid hydrolysis was carried out with 64% (w/w) at 45 °C for 30min with continuous stirring. The solution obtained was diluted in ultrapure water (1:200) and the acid was eliminated by centrifugation; the sediment deposits were then dialyzed until neutral pH. An ion exchange resin was added to the cellulose suspension for 24h and then was removed by filtration in order to ensure that all ionic materials were removed except the $H^+$ counter ions associated with the sulfate groups on the CNC surfaces. Ultrasonic treatment was also carried out in a Vibracell 75043, 750 W, Bioblock Scien-tific during 2 minutes in an ice bath. Cellulose nanocrystals were also modified by adding STEFAC TM 8170 (Stepan Company Norhfield) surfactant, an acid phosphate ester of ethoxylated nonylphenol, in 1/1 (w/w), and designed as CNCs. The dry content yield was calculated by the determination of dry matter content ($W_{dm}$) (Equation III.6. 1) following the oven drying method [171].

$$W_{dm} = \frac{m_1}{m_0} \times 100 \qquad \textbf{Equation III.6. 1}$$

where $m_0$ is the mass content before drying and $m_1$ is the mass content after drying. Nanocrystal solutions were neutralized by the addition of 1.0% (w/w) of 0.25 mol $l^{-1}$ NaOH and freeze-drying to obtain a power.

### 2.3. PLA-PHB blending and nanocomposite preparation

PLA-PHB were blended in 75:25 proportion, according to the literature [8, 10, 19]. Meanwhile, a cellulose nanocrystal content of 5% was selected according with previous results [29]. PLA matrix nanocomposites with CNC and CNCs were also produced for comparison. Sample blend formulations and their concentrations are summarized in Table III.6.1.

**Table III.6.1.** PLA and PLA-PHB nanocomposite film formulations

| **Materials** | **PLA** (wt%) | **PHB** (wt%) | **CNC** (wt%) | **CNCs** (wt%) |
|---|---|---|---|---|
| PLA | 100 | | | |
| PLA-CNC | 95 | | 5 | |
| PLA-CNCs | 95 | | | 5 |
| PLA-PHB | 75 | 25 | | |
| PLA-PHB-CNC | 71.25 | 23.75 | 5 | |
| PLA-PHB-CNCs | 71.25 | 23.75 | | 5 |

Nanocomposites were manufactured by using a twin-screw microextruder (DSM explorer 5&15 CC Micro Compounder). It is known that to prevent thermomechanical degradation during the extrusion process, screw speed, mixing time and temperature profile must be carefully selected [1]. Therefore, a screw speed of 150 rpm and mixing time of 3 minutes were used to optimize the material final properties [20, 29].

In the case of binary PLA and cellulose nanocrystal based systems, PLA pellets, previously dried, were put in the microextruder manually to reach a head force of 1200N while a temperature profile of mixing process with a maximum temperature of 200°C with three steps: 180-190-200°C, was selected. After 2 minutes, CNC or CNCs were added into the microextruder for 1 additional minute.

In the case of PLA-PHB blends a masterbatch was previously prepared (mixing time of 2 minutes). PLA-PHB masterbatch was granulated into pellets and then melted in the microextruder (1 minute) while CNC or CNCs were subsequently added and mixed during 1 supplementary minute.

Directly after the mixing process, a film forming process with a head force of 3000N was carried out to obtain PLA and PLA-PHB based nanocomposite films.

## 2.4. Characterization techniques

### 2.4.1. Transmission electron microscopy (TEM)

TEM images of cellulose nanocrystals and their nanocomposite films were obtained by Transmission Electron Microscopy (TEM, JEOL JEM-1010) operating at 100kV. One droplet of CNC or CNCs suspension were deposited on carbon-coated copper grids and dried at room temperature during 20 minutes before observations.

For the film characterization, they were embedded in epoxy resin and cured during 3 days at room temperature. To observe the cross section, the films were cut with an ultra-microtome (Leica CM1950, SCSIE Universitat de València) and were stained with a uranyl-acetate solution (2wt%) for about 5min.

### 2.4.2. Field emission scanning electron microscope (FESEM)

For the microstructural analysis of the nanocomposite films, the samples were previously frozen in liquid $N_2$, cryofractured and sputtered with a gold layer. The obtained cross-sections were investigated by FESEM, Supra 25-Zeiss.

### 2.4.3. Atomic Force Microscopy (AFM)

AFM analysis was performed to analyze the surface filler dispersion into the polymer matrices. The investigations were carried out by means a Multimode/NanoScope III (Veeco Metrology, Santa Barbara, CA) operating in the tapping mode under air conditions with drive amplitude of 200mV and an amplitude set point of 1.4 V. Surface roughness was calculated from the AFM topographical images by a Nanoscope Analysis 1.4 software using the root mean square (RMS) parameter.

### 2.4.4. Thermogravimetric analysis (TGA)

Thermogravimetric measurements were performed in a Seiko Exstar 6300 thermal analyzer. Masterbatch blends were heated under isothermic mode while processed film samples were heated under dynamic mode, both weighing around 5-10 mg. Isothermal

tests were carried out at a 200°C during 40min under air conditions while dynamic measurements were run from 30 to 900°C at 10°C $min^{-1}$ under nitrogen atmosphere.

### 2.4.5. Differential Scanning Calorimetry (DSC)

DSC experiments were carried out in a TA Instrument Q200 calorimeter (New Castle, DE, USA). The heating and cooling rate for the scans was 2°C/min under nitrogen atmosphere with sample weight about 4 mg in hermetic aluminum pans. Calibration was performed using an indium sample. The cycle program consisted in a first heating stage from -25 to 210°C at a heating rate of 2°C $min^{-1}$, followed by a cooling process up to -25°C and subsequent heating up to 210°C.

The glass transition temperature ($T_g$) was taken at the mid-point of heat capacity changes. The melting temperature ($T_m$) and cold crystallization temperature ($T_{cc}$) were obtained from the first heating and the degree of crystallinity ($\chi_c$) was calculated through Equation III.6.2:

$$\chi_c = 100\% \times \left[\frac{\Delta H_m - \Delta H_c}{\Delta H_m^c}\right] \times \frac{1}{W_{PLA}} \qquad \textbf{Equation III.6. 2}$$

where $\Delta H_m$ is the melting enthalpy, $\Delta H_{cc}$ is the cold crystallization enthalpy, $\Delta H_m^c$ is the melting heat associated to pure crystalline PLA (93J $g^{-1}$) [32] and $W_{PLA}$ the weightfraction of PLA in the blend.

### 2.4.6. X-ray diffraction

The crystalline phases of the nanocomposite films were examined by X-ray diffraction (XRD) equipment (BRUKER AXS D5005, SCSIE Universitat de València). Scanning was performed on square nanocomposite film surfaces (15mm x 15mm) mounted in an appropriate sample holder. The patterns for profile fitting were obtained from a diffractometer using Cu $K_\alpha$ radiation with a scanning step of 0.02º between 2.5º and 40º in 2θ with a collection time of 10s per step, while the voltage was held at 40kV.

### 2.4.7. Fourier transformed infrared spectroscopy (FTIR)

FTIR measurements of the nanocomposite films were carried out at room temperature in transmission mode by a Jasco FTIR spectrometer. Spectra were obtained in the 4000–600 $cm^{-1}$ region.

## 3. RESULTS AND DISCUSSION

### 3.1. Cellulose nanocrystal dispersion

CNC and CNCs yield reactions resulted in ca. 20.6 ± 5.3 %, in good accordance with previous reported works [20, 23, 33]. While pristine CNC suspension reached a constant pH between 8.5 and 9, the pH of CNCs solution after the modification procedure was around 3. Therefore, CNCs solutions were neutralized with NaOH and raised to pH 9 in order to improve the thermal stability of the final nanocrystals.

TEM images of the cellulose nanocrystals obtained (Figure III.6.1.A) show that synthesized CNC (Figure III.6.1.A-a) and CNCs (Figure III.6.1.A-b) exhibit dimensions ranging from 100 to 300 nm in length and between 5 and 10 nm in width confirming previous results [23, 29].

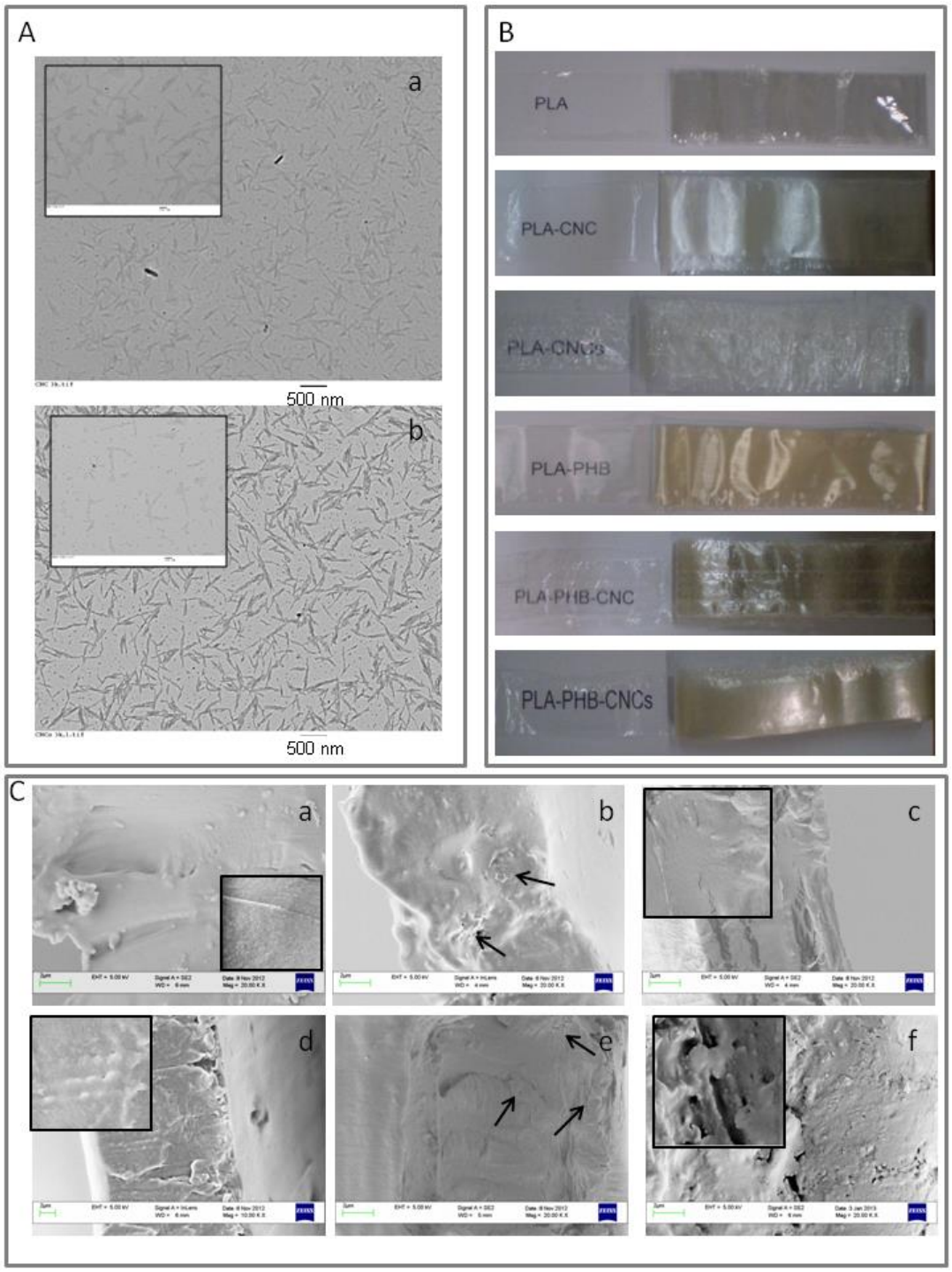


**Figure III.6.1. A)** TEM analysis of **(a)** CNC and **(b)** CNCs suspensions.

**B)** Visual appearance of PLA and PLA-PHB nanocomposite films.

**C)** Microstructure of fracture surface of **(a)** PLA, **(b)** PLA-CNC, **(c)** PLA-CNCs, **(d)** PLA-PHB, **(e)** PLA-PHB-CNC and **(f)** PLA-PHB-CNCs.

### 3.2. PLA-PHB-nanocomposite masterbatchs and film processing

The use of preformed masterbatches represents a useful technique for industrial end-applications. Therefore, masterbach processing parameters were studied. During masterbatch processing some changes in the force applied in the system were observed. Neat PLA process started with a 1000N, but after 1min the force decreased to around 600N showing that the material was completely in the melt state. In the case of PLA-PHB masterbatch melting, 30s after the process, the force notably increased from 1000N to 1200N owing to an increase in the viscosity of the system. This behaviour was more noticeable in the case of CNC and CNCs based formulations. After the addition of nanoreinforcements the force increased from 1000N to around 1200N after CNC incorporation while it increased drastically from 1000N to around 1400N with the addition of modified CNCs. This increment in the force was due to the viscosity change that increases with cellulose introduction, showing the effect of nanocrystals on the processing conditions and, consequently, on the final properties of both polymer matrixes.

A similar situation was observed during filming in which the force started at 1200N, then it reached a constant value of 400N and increased to around 600N in binary PLA-CNC and PLA-CNCs nanocomposite films. While for ternary PLA-PHB formulations the force decreased from 1200N to around 200N followed by an increase to around 400N with CNC and CNCs incorporation during film forming.

### 3.3. Morphological characterization of the nanocomposite films

PLA and PLA-PHB nanocomposite films with a thickness ranging between 10-30μm are shown in Figure III.6.1-B. It can be noticed when rolling the films that PHB presence produced a tendency to yellow, while CNC or CNCs slightly reduce this trend in PLA-PHB blends. However, all the formulations showed an evident transparency also in the case of PHB based systems, underlining that the presence of 25wt% of PHB does not affect the PLA original transparency.

Morphological aspects of the cross cryo-fractured sections of pure PLA, PLA-PHB blend, binary and ternary nanocomposite films were investigated by FESEM and the images are shown in Figure III.6.1-C. The pure PLA film (Figure III.6.1-C.a) shows a typical smooth and uniform surface of an amorphous polymer, while PLA-PHB blend (Figure III.6.1-C.d) shows a more toughness surface due of the increased crystallinity. At higher magnification (Figure III.6.1-C.d, insert) PHB particles appear dispersed as crystalline aggregates showing that no phase separation had taken place during the extrusion

process. In the case of nanocomposites, CNC based films (Figure III.6.1-C b and e) show some compact structures (arrows), suggesting that CNC are present in flakes with poor interfacial adhesion [33]. However, this structure is less pronounced in the PLA-PHB-CNC ternary film (Figure III.6.1-C.e), suggesting that nanocrystals are able to enhance the interfacial adhesion and influence the compatibility between PLA and PHB matrices. Moreover, surfactant modified nanocrystals seem to be better dispersed in both binary PLA-CNCs (Figure III.6.1-C.c) and ternary PLA-PHB-CNCs, (Figure III.6.1-C.f) nanocomposite films, highlighting the positive effect of cellulose modification.

The cellulose structures in the polymer matrices were also studied by transmission electron microscopy (TEM). Individual CNC and CNCs with dimensions ranging from 100 to 300 nm were actually identified in the cross section of the nanocomposite films, confirming the effective incorporation of the synthesized nanocrystals into the polymer matrices (Figure III.6.2-A). It was found that the size of the CNC and CNCs are in agreement with the TEM observations of the cellulose nanocrystal solutions conducted after the hydrolysis procedure (Figure III.6.2-A). Regardless the nanocrystals identification no information on their distribution could be observed by TEM analysis as a result of the low contrast between PLA, PHB and cellulose structures.

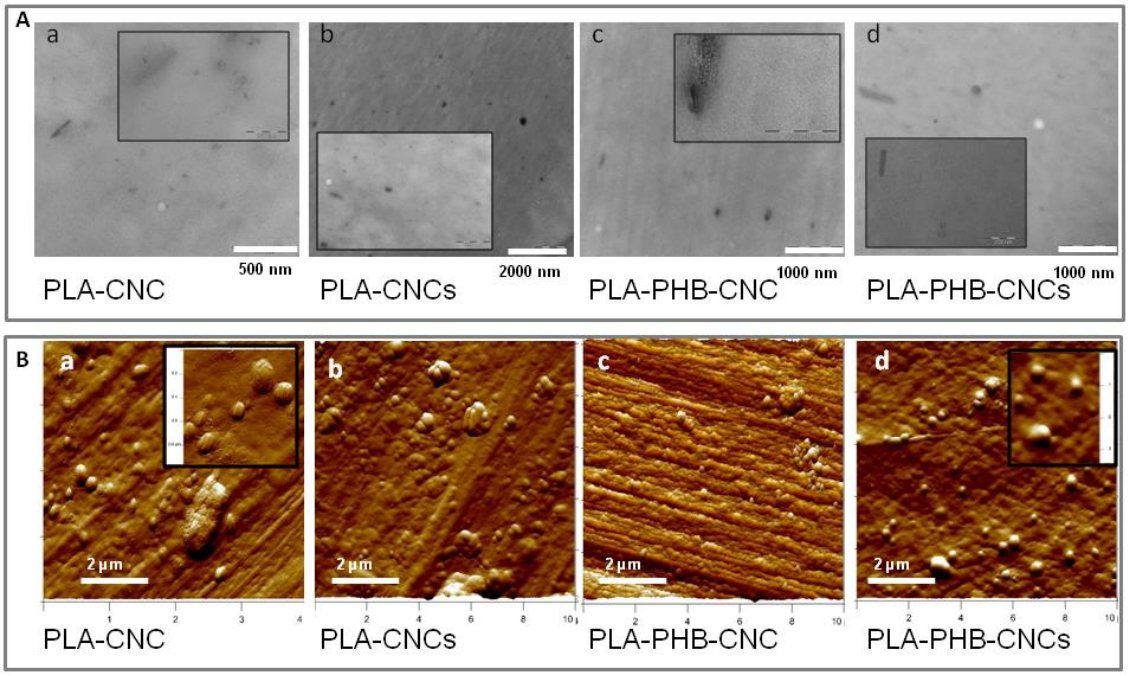


**Figure III.6.2. A)** TEM analysis of nanocomposite films with cellulose nanocrystals: **a)** PLA-CNC, **b)** PLA-CNCs, **c)** PLA-PHB-CNC and **d)** PLA-PHB-CNCs.
**B)** AFM images of nanocomposite films with cellulose nanocrystals incorporated films: **a)** PLA-CNC, **b)** PLA-CNCs, **c)** PLA-PHB-CNC and **d)** PLA-PHB-CNCs.

Therefore, nanocrystals dispersion was studied by means of AFM analysis on film surfaces in view of the fact that it represents a more sensitive technique without any limitations concerning contrast and resolution. The phase channel images of the cellulose nanocrystal based films are displayed in Figure III.6.2-B. The unmodified CNC based films showed that the nanocrystals appear somewhat agglomerated (Figure III.6.2-B a and c), while more individualized structures were detected for CNCs based systems (Figure III.6.2-B b and d) underlining that the surfactant presence allows the polymer chain penetration between the cellulose structures and confirming SEM and TEM results. Moreover, a topographical analysis was also carried out and it revealed that the RMS value increased from 10.2 nm for PLA-CNC to 49.7 nm for PLA-CNCs. Meanwhile, no significant differences were observed between ternary nanocomposite blend films, which showed RMS values of 14.0 nm for PLA-PHB-CNC and 14.8 nm for PLA-PHB-CNCs. Nevertheless, these differences in roughness surfaces are framed in the nanometer scale.

### 3.4. Thermal properties of nanocomposite films

The thermal stability of the masterbatches was studied by means of thermogravimetric analysis conducted under isothermal mode at the highest extrusion temperature of 200°C (Figure III.6.3-a). It was observed that CNC and CNCs slightly improved the thermal stability of pure PLA, PLA-CNC and PLA-CNCs losing less than 1% of the initial weight at the processing temperature. Whereas, nanocrystals based PLA-PHB blends showed lesser thermal stability than the neat PLA-PHB blend. It must be noticed that each masterbatch is melt blended using 180-190-200°C steps as temperature profile during 2 min and subsequently it is inmediately processed into film at 200°C during no more than 5 minutes. Thus, after the actual processing time of 7 minutes at 200°C, the PLA-PHB-CNC nanocomposite was the lesser thermally stable sample, losing aproximately 5% of the initial mass (Figure III.6.3-a). Meanwhile, sligthly better thermal stability was shown for PLA-PHB-CNCs and PLA-PHB, which presented a mass loss lower than 3%.

The effect of CNC and CNCs on the thermal properties of the PLA-PHB blends was also investigated by dynamic measurements. A one-step degradation process was observed for PLA and PLA-CNC, while PLA-CNCs degraded in two steps (Figure III.6.3-b). In PLA-CNCs the first degradation process, occurring at lower temperatures than the main degradation process, may be related with the loss of the surfactant. PLA-PHB blends and PLA-PHB nanocomposites (PLA-PHB, PLA-PHB-CNC and PLA-PHB-CNCs) degraded in two-steps (Figure III.6.3-c) with the first peak related to the PHB decomposition, and the second peak due to the PLA degradation.

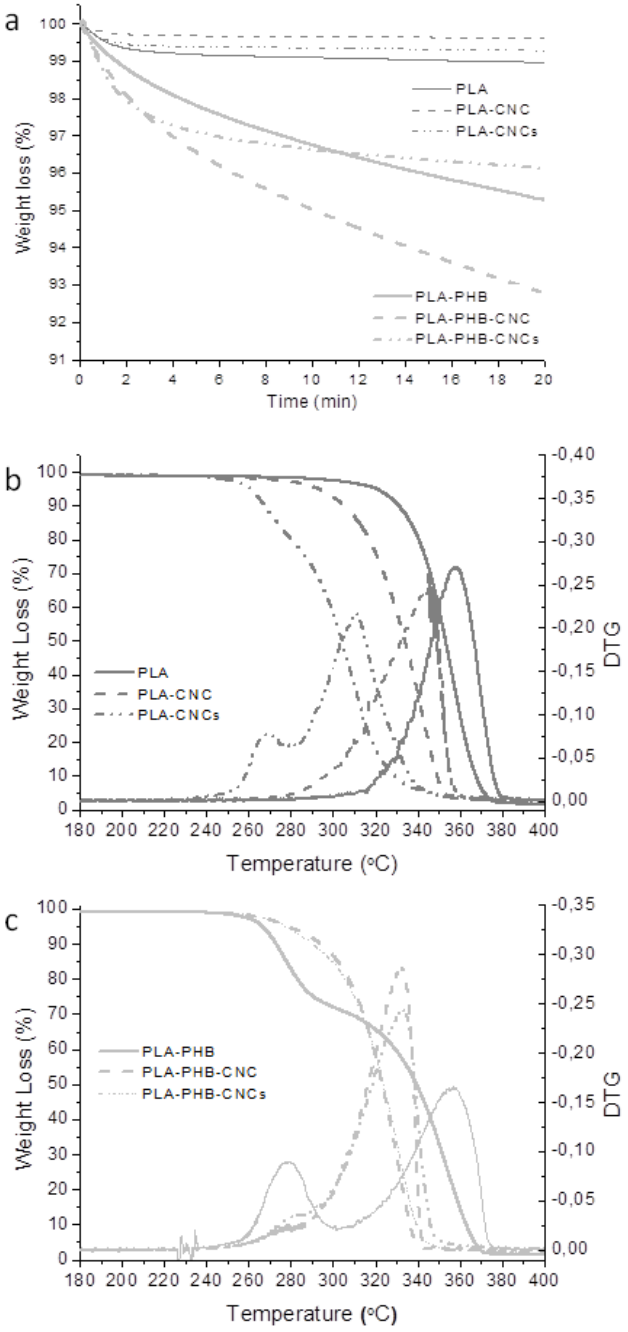


**Figure III.6. 3**. **(a)** Isothermal thermogravimetric analysis at 200°C of binary and ternary masterbatchs.

**(b)** Dynamic TGA and DTGA curves of binary PLA nanocomposite films.

**(c)** Dynamic TGA and DTGA curves of ternary PLA-PHB nanocomposite films.

In the binary systems the addition of cellulose fillers shifted the onset of the PLA degradation process towards lower temperatures (Figure III.6.3-b and Table III.6.2). The PLA maximum degradation rate ($T_{max}$) was also shifted to lower temperatures and with

the most evident decrease observed in PLA-CNCs (Table III.6.2). But it must be underlined that there was no degradation at temperatures below 200°C. As a consequence, PLA integrated with CNC or CNCs were thermally stable at the selected process conditions without risking thermal degradation.

**Table III.6.2.** TGA and DSC thermal properties of PLA and PLA-PHB nanocomposite films

| Formulations | TGA parameters | | | DSC parameters | | | | | |
|---|---|---|---|---|---|---|---|---|---|
| | | $T_0$ | $T_{max}$ | $T_g$ | $T_{cc}$ | $\Delta H_{cc}$ | $T_m$ | $\Delta H_m$ | $\chi_c$* |
| | Stage | (°C) | (°C) | (°C) | (°C) | (J g$^{-1}$) | (°C) | (J g$^{-1}$) | (%) |
| PLA | - | 320 | 357 | 58.8 | 82.5 | 12.6 | 149.0 | 17.7 | 5.6 |
| PLA-CNC | I | 293 | 343 | 56.3 | 74.1 | 9.7 | 150.2 | 20.1 | 11.7 |
| PLA-CNCs | I | 261 | 267 | 55.3 | 78.4 | 18.9 | 148.6 | 28.6 | 11.0 |
| | II | | 310 | | | | | | |
| PLA-PHB | I | 266 | 278 | 53.5 | 66.4 | 19.4 | 149.6/172.7 | 28.8 | 11.9 |
| | II | | 356 | | | | | | |
| PLA-PHB-CNC | I | 278 | 280 | 60.1 | 70.9 | 12.8 | 150.2 | 25.0 | 18.5 |
| | II | | 332 | | | | | | |
| PLA-PHB-CNCs | I | 278 | 280 | 62.5 | 72.1 | 13.1 | 148.8 | 27.2 | 21.3 |
| | II | | 333 | | | | | | |

$T_0$, calculated at 5% mass loss (10°C min$^{-1}$).

DSC parameters calculated at the first heating scan (2°C min$^{-1}$).

* $\chi_c$ (%), calculated using $\Delta H_m^c$ of PLA

On the other hand, the addition of CNC and CNCs shifted the onset of the PLA-PHB blend degradation process from 266°C to around 278°C and led to an improvement in the thermal stability of the ternary nanocomposites. No important changes in the temperature corresponding to the maximum degradation rate of the first stage process ($T_{max-I}$) were observed (Table III.6.2). However, while the temperature at the maximum degradation rate corresponding to the PLA degradation process was unaffected in the PLA-PHB blend, $T_{max-II}$ was shifted to lower temperatures (Table III.6.2) in ternary nanocomposites. The changes in the thermal stability due to cellulose nanocrystals introduction lead to enhance the interface interaction between PLA and PHB.

DSC thermal properties obtained for the first heating scan are summarized in Table III.6.2 while DSC thermograms for first and second heating scans are reported in Figure III.6.4. No significant changes were observed in the glass transition temperature ($T_g$) between neat PLA and PLA-CNC or PLA-CNCs in good accordance with a previous published work [29]. However, a slightly shift to lower $T_g$ values was observed in the PLA-

PHB blend while ternary systems showed higher $T_g$ values without significant differences respect to neat PLA. A reduction of PLA cold crystallization temperature was observed in all formulations. The shift of the cold crystallization to lower temperatures in binary PLA-CNC and PLA-CNCs indicates that the addition of cellulose nanocrystals favours PLA recrystallization [29]. This behaviour was more marked in the case of PHB addition, with a reduction of about 16°C, showing that PHB crystals act as nucleating agents of the PLA matrix [8]. However, a slight shift to higher temperature was observed in the case of ternary PLA-PHB-CNC and PLA-PHB-CNCs with respect to PLA-PHB blend. This increase of almost 5°C in the cold crystallization could be related to the difference in the flexibility of the chains and their ability to form different crystalline structures [11].

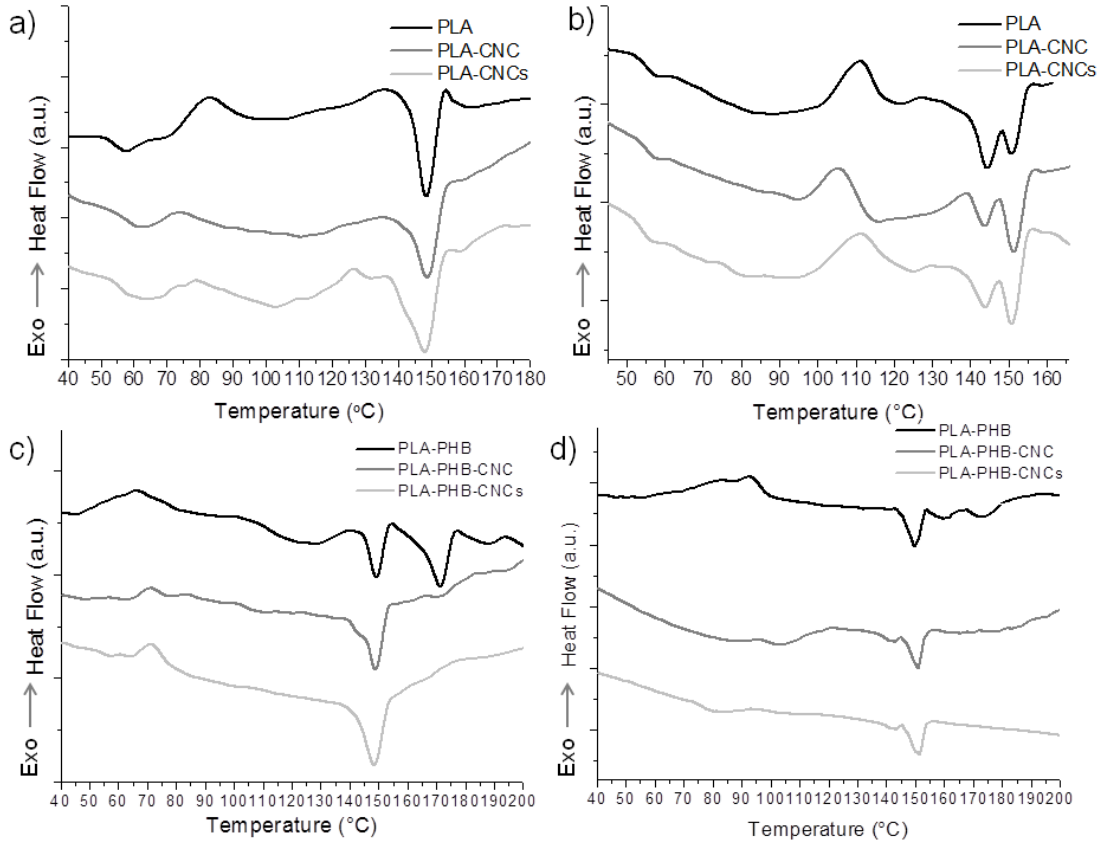


**Figure III.6.4**. DSC curves of nanocomposite films during first (**a** and **c**) and second (**d** and **e**) heating scans.

Moreover, the degree of crystallinity increased almost 5% in PLA-CNC, PLA-CNCs and PLA-PHB with respect to pure PLA, while in reinforced PLA-PHB it raised up 18.5% for PLA-PHB-CNC and 21.3% for PLA-PHB-CNCs. The higher crystallinity reached by PLA-PHB-CNCs than PLA-PHB-CNC is due to the presence of the surfactant on the nanocrystal surfaces leading to a better dispersion and thus a higher nucleation effect [29]. The

melting temperatures of the binary and ternary systems do not change significantly respect to the neat PLA, while the PLA-PHB film shows two peaks in the melting process (Figure III.6.4-c); the first one is due to the PLA component and the second corresponds to the melting of PHB component, suggesting no complete miscibility between the polymers. Conversely, for ternary PLA-PHB-CNC and PLA-PHB-CNCs only one melting peak was observed. This result evidences that well dispersed nanocrystals lead to a clear improvement in the interaction between PLA and PHB.

During the cooling (not shown), no crystallization phenomena were observed for the different formulations and only one deflection due to the glass transition temperature, was observed.

During the second heating scan a double melting behaviour, with one peak at around 145°C and the second one at 151°C, was observed for PLA, PLA-CNC and PLA-CNCs as it is shown in Figure III.6.4-b ascribed to the formation of small and imperfect crystals that change into more stable crystals through melting and recrystallization at low heating rates or to lamellar populations with two different crystalline phases [34]. In PLA-PHB blend after the PLA melting peak at around 150°C two more small melting peaks were present at around 160°C and 170°C corresponding to the as-formed PHB crystals during blending process and re-crystallized PHB crystals formed from the re-crystallization during DSC heating, respectively [8]. Whereas, PLA-PHB-CNC and PLA-PHB-CNCs films (Figure III.6.4-d) showed a similar behaviour to that of the first heating (Figure III.6.4-c). This result is related with the fact that cellulose nanocrystals are small and well dispersed phases able to enhance the interfacial adhesion and consequently improve the compatibility between PLA and PHB matrices. Thus, the melting and re-crystallization of PHB becomes faster than that of PLA-PHB blend in the subsequent heating processes due to CNC and CNCs presence.

### 3.5. Structural characterization of nanocomposite films

X-ray diffraction analysis was used to determine the crystalline structure of the nanocomposite films and the results are shown in Figure III.6.5-a. All films exhibited the characteristic peak of PLA at 2θ=16.5º. An increase in the intensity at around $2\theta$=22.5º is expected for PLA based systems with the CNC [27, 35] or CNCs [27] introduction. However, in this case, this peak was replaced by a broad shoulder in PLA-CNC and PLA-CNCs due to the low cellulose content. PLA-PHB blend exhibited the characteristic peak of PHB at $2\theta$=13.5 and the peak at 2θ=17º [8, 19] was overlapped by the peak at $2\theta$=16.5º attributed to PLA. PLA-PHB-CNC and PLA-PHB-CNCs ternary systems showed a clearly

different XRD pattern respect to the PLA-PHB blend behaviour, where the peaks in the $2\theta$=10-23º range have merged into a single broad peak. The broad X-ray diffraction peaks are indicative of small crystallites size and semi-crystalline character [32]. In this case, while the broad peak could be influenced by the small cellulose crystal size, the increased intensity at 2θ=16.5º shows that in ternary systems, PLA is re-crystallising confirming, as previous discussed, that the presence of CNC or CNCs is able to positively affect the interaction between PLA and PHB.

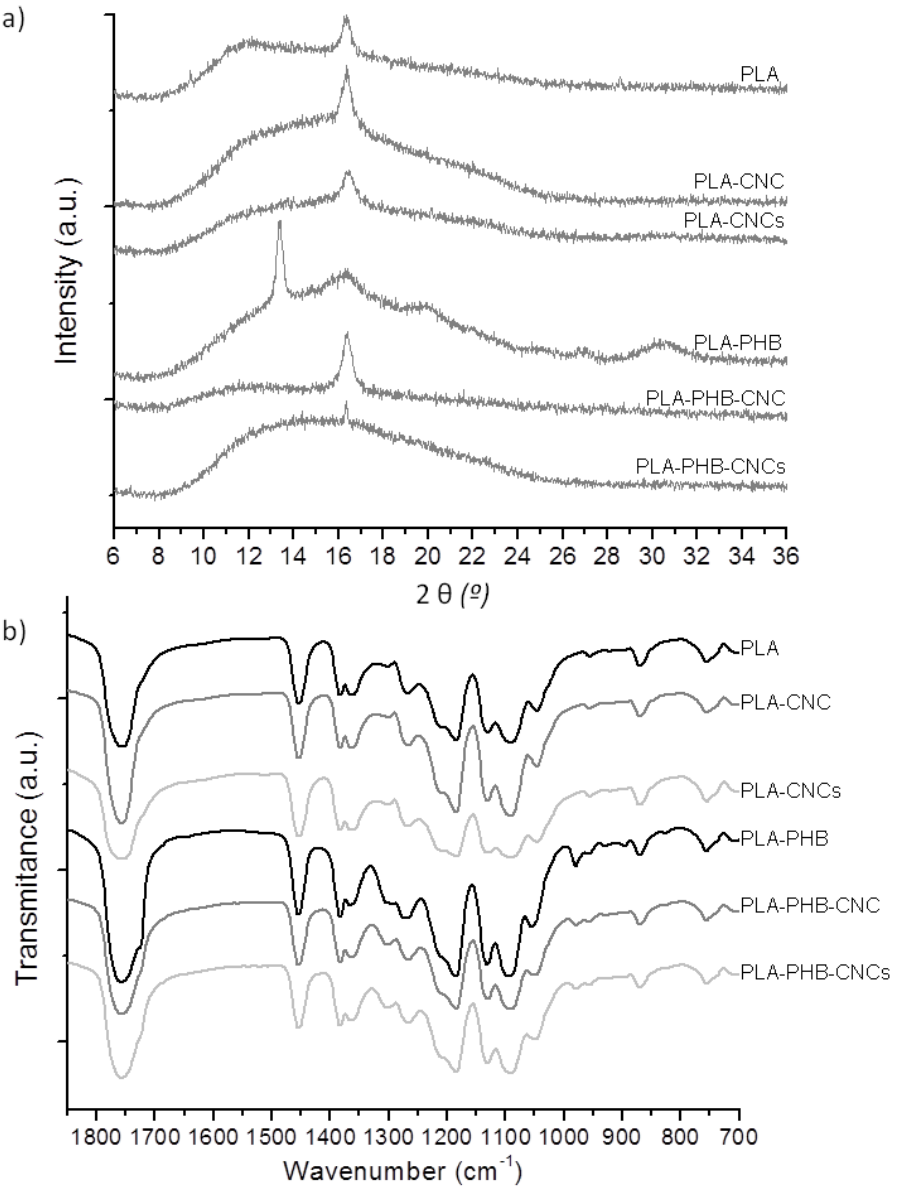


**Figure III.6.5. a)** X-ray diffraction patterns of PLA and PLA-PHB nanocomposite films **b)** Infrared spectra of PLA and PLA-PHB nanocomposite films

Figure III.6.5-b shows the FTIR spectra in the 1900–700 $cm^{-1}$ region. At 1750 $cm^{-1}$ the typical stretching of amorphous carbonyl group (C=O) assigned to lactides was present in all PLA [4] based formulations showing a particularly broad absorption in PLA-PHB blends attributed to the crystalline carbonyl stretching of PHB [8, 10, 36]. This broadening evidences the molecular interaction between both polymers at the selected proportion which has been ascribed to a transesterification reaction between PLA and PHB during melt processing [8]. Moreover, PLA-PHB blend shows a shoulder at 1720 $cm^{-1}$ that is replaced by broader bands in PLA-PHB-CNC and PLA-PHB-CNCs. This behaviour has been related to the hydrogen interactions between the C=O groups in PHB and -OH groups in CNC [26]. The CH deformation and asymmetric bands appear at 1382 $cm^{-1}$ and 1365 $cm^{-1}$, respectively [4]. The intensity of the peak at 1382 $cm^{-1}$ increased in PLA-PHB blends spectra due to the $CH_3$ symmetric deformation of PHB [17]. Moreover, the band at 980 $cm^{-1}$ assigned to the coupling of C-C backbone stretching with the $CH_3$ stretching vibration band decreases due to CNC and CNCs presence. FTIR spectra showed the miscibility between PLA, PHB and CNC or CNCs, particularly in the ternary systems confirming that CNC and CNCs improve the molecular interaction between PLA-PHB.

## 4. CONCLUSION

The study of the blend processing and characterization of the innovative combination of PLA, PHB and cellulose nanocrystals showed the potential of these nanocomposite films for the food packaging industry. Cellulose nanocrystals (CNC) and surfactant modified cellulose nanocrystals (CNCs) were synthesized from microcrystalline cellulose by acid hydrolysis. Synthesized nanocrystals were successfully incorporated in PLA and PLA-PHB blends by preparing a masterbatch prior to the film forming process. The use of a masterbatch improved the dispersion of CNC and CNCs in the final nanocomposite films and made easier the processability between PLA and PHB. CNC and CNCs improved the interfacial adhesion between PLA and PHB and consequently an enhancement of the thermal stability was achieved by shifting the initial degradation temperature of the ternary systems around 10°C to higher temperatures. This result indicates an improvement of the usually small processing window of the PHB. Thus, PLA, PHB and cellulose nanocrystals can be processed in the region from at least 160°C and below 200°C. Moreover, PHB increased the crystallinity of PLA due to its nucleation effect. However, the overall crystallinity was further increased in the PLA-PHB blend by the addition of CNC and this effect was more evident with the addition of modified CNCs, highlighting the positive effect of surfactant modification on the final nucleation process.

The incorporation of surfactant modified cellulose nanocrystals into PLA-PHB blends represents an effective procedure to improve the compatibility between both polymers processed by means of a simple melt-blending process. Moreover, synergic effects in the final properties of ternary nanocomposites are present such as enhanced crystallinity, improved thermal stability and better interfacial adhesion among PLA, PHB and cellulose nanocrystals; showing their suitability for film food packaging industry.

**Acknowledgments**

This research was supported by the Ministry of Science and Innovation of Spain (MAT2011-28468-C02-01 and MAT2011-28468-C02-02). M.P. Arrieta thanks Generalitat Valenciana (Spain) for Santiago Grisolía Fellowship (GRISOLIA/2011/007) and Universitat Politècnica de València for the Development Support Programme PAID-00-12 (SP20120120).

**REFERENCES**

[1] Fortunati E, Armentano I, Iannoni A, Kenny JM. Development and thermal behaviour of ternary PLA matrix composites. Polymer Degradation and Stability. 2010;95(11):2200-2206.

[2] Armentano I, Bitinis N, Fortunati E, Mattioli S, Rescignano N, Verdejo R, et al. Multifunctional nanostructured PLA materials for packaging and tissue engineering. Progress in Polymer Science. 2013.

[3] Arrieta MP, Parres F, López J, Jiménez A. Development of a novel pyrolysis-gas chromatography/mass spectrometry method for the analysis of poly(lactic acid) thermal degradation products. Journal of Analytical and Applied Pyrolysis. 2013;101:150-155.

[4] Auras R, Harte B, Selke S. An overview of polylactides as packaging materials. Macromolecular Bioscience. 2004;4(9):835-864.

[5] Arrieta MP, López J, Ferrándiz S, Peltzer MA. Characterization of PLA-limonene blends for food packaging applications. Polymer Testing. 2013;32(4):760-768.

[6] Kose R, Kondo T. Size effects of cellulose nanofibers for enhancing the crystallization of poly(lactic acid). Journal of Applied Polymer Science. 2013;128(2):1200-1205.

[7] Martino VP, Jiménez A, Ruseckaite RA, Avérous L. Structure and properties of clay nano-biocomposites based on poly(lactic acid) plasticized with polyadipates. Polymers for Advanced Technologies. 2011;22(12):2206-2213.

[8] Zhang M, Thomas NL. Blending polylactic acid with polyhydroxybutyrate: The effect on thermal, mechanical, and biodegradation properties. Advances in Polymer Technology. 2011;30(2):67-79.

[9] Calvão PS, Chenal JM, Gauthier C, Demarquette NR, Bogner A, Cavaille JY. Understanding the mechanical and biodegradation behaviour of poly(hydroxybutyrate)/rubber blends in relation to their morphology. Polymer International. 2012;61(3):434-441.

[10] Arrieta MP, López J, Hernández A, Rayón E. Ternary PLA-PHB-Limonene blends intended for biodegradable food packaging applications. European Polymer Journal. 2014;50(1):255-270.

[11] Malinová L, Brožek J. Mixtures poly((R)-3-hydroxybutyrate) and poly(l-lactic acid) subjected to DSC. Journal of Thermal Analysis and Calorimetry. 2011;103(2):653-660.

[12] Koller M, Salerno A, Dias M, Reiterer A, Braunegg G. Modern biotechnological polymer synthesis: A review. Food Technology and Biotechnology. 2010;48(3):255-269.

[13] Erceg M, Kovačić T, Klarić I. Thermal degradation of poly(3-hydroxybutyrate) plasticized with acetyl tributyl citrate. Polymer Degradation and Stability. 2005;90(2 SPEC. ISS.):313-318.

[14] Corre YM, Bruzaud S, Audic JL, Grohens Y. Morphology and functional properties of commercial polyhydroxyalkanoates: A comprehensive and comparative study. Polymer Testing. 2012;31(2):226-235.

[15] Bartczak Z, Galeski A, Kowalczuk M, Sobota M, Malinowski R. Tough blends of poly(lactide) and amorphous poly([R,S]-3-hydroxy butyrate) - morphology and properties. European Polymer Journal. 2013.

[16] Imre B, Pukánszky B. Compatibilization in bio-based and biodegradable polymer blends. European Polymer Journal. 2013;49(6):1215-1233.

[17] Furukawa T, Sato H, Murakami R, Zhang J, Duan YX, Noda I, et al. Structure, dispersibility, and crystallinity of poly(hydroxybutyrate)/ poly(L-lactic acid) blends studied by FT-IR microspectroscopy and differential scanning calorimetry. Macromolecules. 2005;38(15):6445-6454.

[18] Vogel C, Siesler HW. Thermal degradation of poly(ε-caprolactone), poly(L-lactic acid) and their blends with poly(3-hydroxy-butyrate) studied by TGA/FT-IR spectroscopy. Macromolecular Symposia. 2008;265(1):183-194.

[19] Abdelwahab MA, Flynn A, Chiou BS, Imam S, Orts W, Chiellini E. Thermal, mechanical and morphological characterization of plasticized PLA-PHB blends. Polymer Degradation and Stability. 2012;97(9):1822-1828.

[20] Fortunati E, Armentano I, Iannoni A, Barbale M, Zaccheo S, Scavone M, et al. New multifunctional poly(lactide acid) composites: Mechanical, antibacterial, and degradation properties. Journal of Applied Polymer Science. 2012;124(1):87-98.

[21] Brinchi L, Cotana F, Fortunati E, Kenny JM. Production of nanocrystalline cellulose from lignocellulosic biomass: Technology and applications. Carbohydrate Polymers. 2013;94(1):154-169.

[22] Rayón E, López J, Arrieta MP. Mechanical characterization microlaminar structures extracted from cellulosic materials using nanoindentation technique. Cellulose Chemistry and Technology. 2013;47(5-6):345-351.

[23] Bitinis N, Verdejo R, Bras J, Fortunati E, Kenny JM, Torre L, et al. Poly(lactic acid)/natural rubber/cellulose nanocrystal bionanocomposites Part I. Processing and morphology. Carbohydrate Polymers. 2013.

[24] Fortunati E, Puglia D, Monti M, Peponi L, Santulli C, Kenny JM, et al. Extraction of Cellulose Nanocrystals from Phormium tenax Fibres. Journal of Polymers and the Environment. 2013;21(2):319-328.

[25] Fortunati E, Puglia D, Monti M, Santulli C, Maniruzzaman M, Kenny JM. Cellulose nanocrystals extracted from okra fibers in PVA nanocomposites. Journal of Applied Polymer Science. 2013;128(5):3220-3230.

[26] Patrício PSDO, Pereira FV, Dos Santos MC, De Souza PP, Roa JPB, Orefice RL. Increasing the elongation at break of polyhydroxybutyrate biopolymer: Effect of cellulose nanowhiskers on mechanical and thermal properties. Journal of Applied Polymer Science. 2013;127(5):3613-3621.

[27] Fortunati E, Peltzer M, Armentano I, Torre L, Jiménez A, Kenny JM. Effects of modified cellulose nanocrystals on the barrier and migration properties of PLA nano-biocomposites. Carbohydrate Polymers. 2012;90(2):948-956.

[28] Bondeson D, Mathew A, Oksman K. Optimization of the isolation of nanocrystals from microcrystalline cellulose by acid hydrolysis. Cellulose. 2006;13(2):171-180.

[29] Fortunati E, Armentano I, Zhou Q, Iannoni A, Saino E, Visai L, et al. Multifunctional bionanocomposite films of poly(lactic acid), cellulose nanocrystals and silver nanoparticles. Carbohydrate Polymers. 2012;87(2):1596-1605.

[30] Martínez-Sanz M, Abdelwahab MA, Lopez-Rubio A, Lagaron JM, Chiellini E, Williams TG, et al. Incorporation of poly(glycidylmethacrylate) grafted bacterial cellulose nanowhiskers in poly(lactic acid) nanocomposites: Improved barrier and mechanical properties. European Polymer Journal. 2013.

[31] UNE-EN ISO. Paper, board and pulps - Determination of dry matter content - Oven-drying method. 2008.

[32] Turner II JF, Riga A, O'Connor A, Zhang J, Collis J. Characterization of drawn and undrawn poly-L-lactide films by differential scanning calorimetry. Journal of Thermal Analysis and Calorimetry. 2004;75(1):257-268.

[33] Fortunati E, Armentano I, Zhou Q, Puglia D, Terenzi A, Berglund LA, et al. Microstructure and nonisothermal cold crystallization of PLA composites based on silver nanoparticles and nanocrystalline cellulose. Polymer Degradation and Stability. 2012;97(10):2027-2036.

[34] Bitinis N, Fortunati E, Verdejo R, Bras J, Kenny JM, Torre L, et al. Poly(lactic acid)/natural rubber/cellulose nanocrystal bionanocomposites. Part II: Properties evaluation. Carbohydrate Polymers. 2013.

[35] Hossain KMZ, Ahmed I, Parsons AJ, Scotchford CA, Walker GS, Thielemans W, et al. Physico-chemical and mechanical properties of nanocomposites prepared using

cellulose nanowhiskers and poly(lactic acid). Journal of Materials Science. 2012;47(6):2675-2686.

[36] Phuong Nguyen T, Domenek S, Guinault A, Sollogoub C. Crystallization behavior of poly(lactide)/poly(beta-hydroxybutyrate)/talc composites. Journal of Applied Polymer Science. 2013;129(6):3355-3365.

## 7. Multifunctional PLA-PHB/cellulose nanocrystal films. Mechanical, barrier and disintegration properties

*Arrieta, M.P[a,e], Fortunati, E.[b], Dominici, F [b]., Rayón, E.[c], López, J.[a], Kenny, J.M.[b,d]*

[a]Instituto de Tecnología de Materiales. Universitat Politècnica de Valencia, 03801 Alcoy-Alicante, Spain.

[b]Materials Engineering Centre, UdR INSTM, NIPLAB, University of Perugia, 05100, Terni, Italy.

[c] Instituto de Tecnología de Materiales. Universitat Politècnica de Valencia, E-46022, Valencia, Spain.

[d]Institute of Polymer Science and Technology, CSIC, Juan de la Cierva 3, Madrid 28006, Spain.

[e]Analytical Chemistry, Nutrition and Food Sciences Department, University of Alicante, P.O. Box 99, E-03080 Alicante, Spain.

**Polymer Degradation and Stability**

**(Submitted)**

**Abstract**

Nanocomposite films based on poly(lactic acid)-poly(hydroxybutyrate) (PLA-PHB) blends and synthesized cellulose nanocrystals (CNC) or surfactant modified cellulose nanocrystals (CNC-s), as bio-based reinforcement, were prepared by melt extrusion followed by film forming. The obtained nanocomposites are intended for short-term food packaging. Thus, the mechanical, optical, barrier and wettability properties were studied. Functionalized CNC-s contributes to enhance the interfacial adhesion between PLA and PHB, leading to improved mechanical stiffness and increased film stretchability. The synergic effects of the PHB and CNC-s on the PLA barrier properties were confirmed by increases in oxygen barrier properties and reductions in surface wettability of the nanocomposites. The disintegration process in composting conditions of PLA was delayed by the addition of PHB, while CNC speeded it up. PLA-PHB-CNC-s formulations showed enhanced mechanical performance, improved water resistance, reduced oxygen and UV-light transmission, as well as appropriate disintegration in compost suggesting possible applications as packaging material.

**Keywords:** poly(lactic acid); poly(hydroxybutyrate); modified cellulose nanocrystals; nanocomposites; biodegradation; barrier properties.

## 1. INTRODUCTION

Many positive characteristics of PLA have situated it as the most used biopolyester for biodegradable food packaging industry. Among other properties, PLA compared to other biopolymers shows easy processability [1], superior transparency, availability in the market [2], excellent printability [3], high rate of disintegration in compost [4]. Conversely, the use of PLA films for food packaging has been strongly limited because of their poor mechanical and barrier properties [5]. Moreover, for large-scale industrial production PLA must guarantee adequate thermal stability or low thermal degradation during processing and use [6].

It is known that the crystalline phase has an important impact on mechanical and permeation properties; as a result, considerable academic and industrial research efforts have been focused to increase PLA crystallinity. In this sense, the addition of poly(hydroxybutirate) (PHB), a highly crystalline biopolymer, to the PLA matrix by melt blending has been considered as an easy way to increase PLA crystallinity and regulate its properties [7]. PHB, the most common representative of poly(hydroxyalkanoates) (PHA), with a high degree of crystallinity, has been also proposed for short-term food packaging applications [8]. PHB has a similar melting temperature to PLA, allowing blending both polymers in the melt state through a readily available processing technology. In a previous work, PLA was melt blended with 25wt% of PHB showing an improvement in oxygen barrier and water resistant, whilst reducing the inherent high transparency of PLA [9]. Transparency is an essential issue to be considered in the development of materials intended for food packaging since seeing through the packaging is one of the most important requirements for the consumers [2]. Moreover, to preserve food products until they reach the consumer, packagings sometimes require protecting food products from ultraviolet light [10]. It has been reported that PHB acts as better light barrier in the visible [8,9] and ultraviolet light regions [8] than PLA.

The use of nanocomposites to improve the inherent shortcomings of PLA based packaging materials has proven to be a promising technology. The ideal nanoparticle should be biobased and biodegradable. In this sense, bioresources obtained from agricultural-related industries have received significant attention, particularly focused on cellulosic materials and especially to its specific form of cellulose nanocrystals (CNC), which have been revealed to be an interesting model filler [11] for various biopolymer matrices including PLA [3, 12,13] and PHB [14], beside others biopolymers such as poly(vinyl alcohol) (PVA) [11] and poly(hydroxybutyrate-co-hydroxyvalerate) (PHBV) [15]. Cellulose nanocrystals have shown better mechanical properties than a majority of

the commonly used reinforcing materials and offer additional exceptional advantages such as biodegradability, high stiffness and low density [12] abundance in nature and low cost [16].

Although nanocelluloses have a great potential as mentioned above, the high amount of -OH on the surface of the crystals induces high attraction between them [17]. Thus, the high polarity of cellulose surface and the resultant low interfacial compatibility with hydrophobic polymer matrices make difficult the homogenous dispersion of nanocellulose in polymers [18]. For that reason, a surface modification of CNC by a surfactant (CNC-s) has been proposed and successful dispersion of CNC-s in the PLA matrix was achieved [3, 12]. This specific type of modification enhances the interfacial adhesion polymer/nanofiller and thus improves some final properties of the final nanocomposites such as mechanical performance [12], oxygen barrier and water resistance [19], which are particularly interesting for materials intended for food packaging.

In a previous work, the processing performance of PLA-PHB with CNC or CNC-s was optimized and it was verified that the functionalization of CNC-s favour+rs the dispersion into PLA-PHB blend matrix enhancing the interfacial adhesion by means increasing the thermal stability [20]. The main objective of this research is to propose this high performance nanocomposite films for biodegradable food packaging industry. For this purpose, the combination of ternary system based in PLA, PHB and cellulose nanocrystals blend was developed to enhanced PLA barrier and mechanical properties. Cellulose nanocrystals (CNC) were synthesized from microcrystalline cellulose (MCC) as well as further modified using a surfactant (CNC-s) to improve the dispersion in the biopolymer matrix. Then nanocrystals were melt-blended with a previous prepared PLA-PHB masterbatch and finally processed into films. The processing of these systems and their crystalline and thermal stability properties were reported previously [20]. The mechanical, optical and barrier properties were tested with the aim to evaluate their suitability for the food packaging sector are reported here. Additionally, the disintegrability under composting of the multifunctional materials was evaluated to get information about their post-use.

## 2. MATERIALS AND METHODS

### 2.1. Materials

Poly(lactic acid) (PLA 2002D, $M_n$ = 98,000 g·mol$^{-1}$, 4 wt% D-isomer) was supplied by NatureWorks (USA), Poly(hydroxybutyrate) (PHB, under the trade name PHI002) was acquired from NaturePlast (France) and microcrystalline cellulose (MCC, dimensions of 10-15 μm) was purchased from Sigma-Aldrich.

### 2.2. Nanocrystals synthesis and modification

Acid hydrolysis of micro crystalline cellulose (MCC) was carried out by using sulphuric acid 64% (w/w) at 45 °C for 30 min with continuous stirring [12]. The obtained cellulose nanocrystals (CNC) in an acid solution were washed with ultrapure water (1:200), centrifugated and dialyzed until neutral pH. An ion exchange resin was added to the cellulose suspension for 24 h and then was removed by filtration in order to ensure that all ionic materials were removed except the $H^+$ counter ions associated with the sulfate groups on the CNC surfaces. After that, nanocrystals suspensions were ultrasonicated (Vibracell 75043, 750 W, Bioblock Scien-tific) for 2 minutes in an ice bath. Surface modified cellulose nanocrystals (CNC-s) were also prepared by adding a surfactant (STEFAC TM 8170, Stepan Company Northfield) in 1/1 (w/w). Finally, cellulose nanocrystals in powder were obtained by a freeze-drying process of previously neutralized solutions (1.0% (w/w) of 0.25 mol l$^{-1}$ NaOH).

### 2.3. PLA-PHB-nanocomposites preparation

75 wt% of PLA was blended with 25wt% of PHB and reinforced with 5wt% of pristine (CNC) or surfactant modified (CNC-s) cellulose nanocrystals. Masterbatches were prepared by using a twin-screw microextruder (DSM explorer 5&15 CC Micro Compounder) by following the same processing conditions as described in a previous work [20]. Briefly, using a temperature profile of mixing process with a maximum temperature of 200°C with three-step temperature procedure of 180-190-200°C and a screw speed of 150 rpm for 2 minutes. Masterbatches were pelletized and mixed for one minute and directly processed in films with a head force of 3000N. Then, a film procedure was conducted to obtain six formulations, including the neat PLA and PLA-PHB blend. The

obtained formulations with a thickness ranged from 10 to 30μm were named as PLA, PLA-CNC, PLA-CNCs, PLA-PHB, PLA-PHB-CNC and PLA-PHB-CNCs.

### 2.4. Characterization techniques

The mechanical behaviour was investigated by tensile test in a digital Lloyd instrument LR 30K, performed on rectangular probes (100 mm x 10 mm) at room temperature by following the UNE-EN ISO 527-3 standard [21] with a crosshead speed of 5 mm/min, a load cell of 500N and an initial gauge length of 50 mm. Average tensile strength (*TS*), percentage elongation at break ($\varepsilon_B$ %) and Young's modulus (*E*) were calculated from the resulting stress-strain curves as the average of five measurements of each composition.

The absorption spectra of nanocomposites, obtained in the 700-250 nm region, were investigated by a Perkin-Elmer (Lambda 35, USA) UV-VIS spectrophotometer. Nanocomposite film colour properties were evaluated in the CIELAB colour space by using a KONICA CM-3600d COLORFLEX-DIFF2, HunterLab, Hunter Associates Laboratory, Inc, (Reston, Virginia, USA). The instrument was calibrated with a white standard tile. Yellowness index (*YI*) and colour coordinates, *L* (lightness), a* (red-green) and b* (yellow-blue) were measured at random positions over the film surface. Average values of five measurements were calculated. Total color difference ($\Delta E$) was calculated with respect to the control pure PLA film or PLA-PHB film as:

$$\Delta E = \sqrt{\Delta a^{*2} + \Delta b^{*2} + \Delta L^{*2}} \qquad \textbf{Equation III.7. 1}$$

The oxygen transmission rate (OTR) was measured to study the oxygen permeability of the nanocomposites by using a Systech Instruments 8500 oxygen permeation analyzer (Metrotec S.A, Spain) at room temperature and 2.5 atm. 14 cm diameter circle films were compressed between the upper and lower diffusion chamber. Pure oxygen (99.9% purity) was introduced into the upper half of the sample chamber while nitrogen was injected into the lower half. To prepare the appropriate samples for OTR measurements , masterbatch pellets were set in discs by using a DSM Xplore 10-ml injection molding machine at 175, 180 and 190 °C with a pressure profile in three steps: 6 bar for 4 min, 8 bar for 5 min and 8 bar for 3 min. Discs were then processed into films by compression moulding process at 180°C in a hot press (Mini C 3850, Caver, Inc., Wabash, IN, USA) with a pressure cycle of 3 MPa for 1 min, 5 MPa for 1 min, and 10 MPa for 2 min.

Nanocomposite films were then quenched to room temperature at atmospheric pressure. Their average thickness was between 180 and 250μm.

Surface wettability of films was studied through water contact angle measurements with a standard goniometer (EasyDrop-FM140, KRÜSS GmbH, Hamburg, Germany) equipped with a camera and Drop Shape Analysis SW21; DSA1 software was used to test the water contact angle ($\theta^{o}$) at room temperature. The contact angle was determined by randomly putting 5 drops of distilled water (≈ 2 μL) with a syringe onto the film surfaces and the average values of ten measurements for each drop were used.

## 2.5. Disintegrability under composting conditions

The disintegration under composting conditions of PLA and PLA-PHB nanocomposites was investigated on the basis of the ISO 20200 standard [22]. A solid synthetic waste was prepared by mixing 10% of compost supplied by Gesenu S.p.a. (Perugia, Italy), with 30% rabbit food, 10% starch, 5% sugar, 1% urea, 4% corn oil and 40% sawdust. The water content of the substrate was around 50 wt% and the aerobic conditions were guaranteed by mixing it softly [4]. Nanocomposite films (cut in 15 x 15 $mm^2$) were weighed and buried at 4-6 cm depth in perforated plastic boxes, containing the prepared mix, and incubated at 58°C. Each nanocomposite film was recovered at 1, 2, 3, 7, 10, 14 and 21 days of disintegration, cleaned with distilled water, dried in an oven at 37°C during 24 h and reweighed. The disintegration degree was calculated by normalizing the sample weight, at different days of incubation, to the initial weight. In order to determine the time at which 50% of each film was degraded, disintegrability degree values were then fitted using the Boltzmann equation (OriginPro 8.1.software) as follows:

$$m = \frac{(m_i - m_\infty)}{1 + e^{(1 - t_{50}/d_t)}} \qquad \textbf{Equation III.7. 2}$$

where $m_i$ and $m_\infty$ are the initial and final mass values measured respectively at the beginning of the exposition to compost and after the final asymptotes of the disintegrability test, and $t_{50}$ is the time at which materials disintegrability reaches the average value between $m_i$ and $m_\infty$, known as the half-maximal degradation, $d_t$ is a parameter that describes the shape of the curve between the upper and lower asymptotes [23].

Photographs of recovered samples were taken for visual comparison. Surface microstructure of PLA and PLA-PHB nanocomposites before and after 3 days of incubation

in composting were studied by optical microscopy using a LV-100 Nikon Eclipse equipped with a Nikon sight camera at 20x magnifications using the extended depth of field (EDF-z) imaging technique.

The relationship between *meso*-lactide and L,D-lactide form in the polymer after compost incubation was also studied by Pyrolysis-Gas Chromatography/ Mass Spectrometry (Py-GC/MS) by means of a Pyroprobe 1000 pyrolyzer (CDS Analytical, Oxford, Pennsylvania, USA) at 1000°C for 0.5s, coupled with a gas chromatograph (6890N, Agilent Technologies) and a mass selective detector (Agilent 5973N) on the basis of a previous developed method [23].

Fourier infrared spectra of the samples in the 400-4000 $cm^{-1}$ range were recorded by a Jasco FTIR 615 spectrometer, in transmission mode.

### 2.6. Statistical analysis

Significance in the mechanical, wettability and colour parameters differences were statistically by one-way analysis of variance (ANOVA) using OriginPro 8 software. To identify which groups were significantly different from other groups, means comparison were done employing a Tukey's test with a 95% confidence level.

## 3. RESULTS AND DISCUSSION

### 3.1. Mechanical properties

As it can be seen from tensile curves (Figure III.7.1-a), the neat PLA film showed a characteristic plastic deformation that it was reduced with both, PHB and CNC incorporation. CNC and PHB proved to be effective to increase PLA modulus (Figure III.7.1-b), but no significant differences were observed between the Young's modulus of PLA-CNCs and PLA films. While CNCs or PHB produced a decrease on the tensile strength (*TS*) of PLA, the combination of PHB and CNC-s produce a nanocomposite (PLA-PHB-CNCs) with comparable *TS* with respect to PLA. This behaviour can be related with the more efficient dispersion of functionalized cellulose nanocrystals (CNC-s) [3] resulting in an enhancement in the interfacial adhesion and therefore in a better interaction between PLA and PHB [20]. Moreover, the PLA-PHB-CNC-s film revealed the highest deformation at break, showing an increase of 175% with respect to the neat PLA film, while significant lower elongations at break respect to the PLA film were measured for the other nanocomposite formulations. Films for food packaging are required to maintain their

integrity in order to withstand the stress that occurs during shipping, handling and storage [24] andPLA-PHB-CNC-s is therefore far stretchable and stiff with comparable strength than PLA and could be defined as the best formulation for food packaging applications.

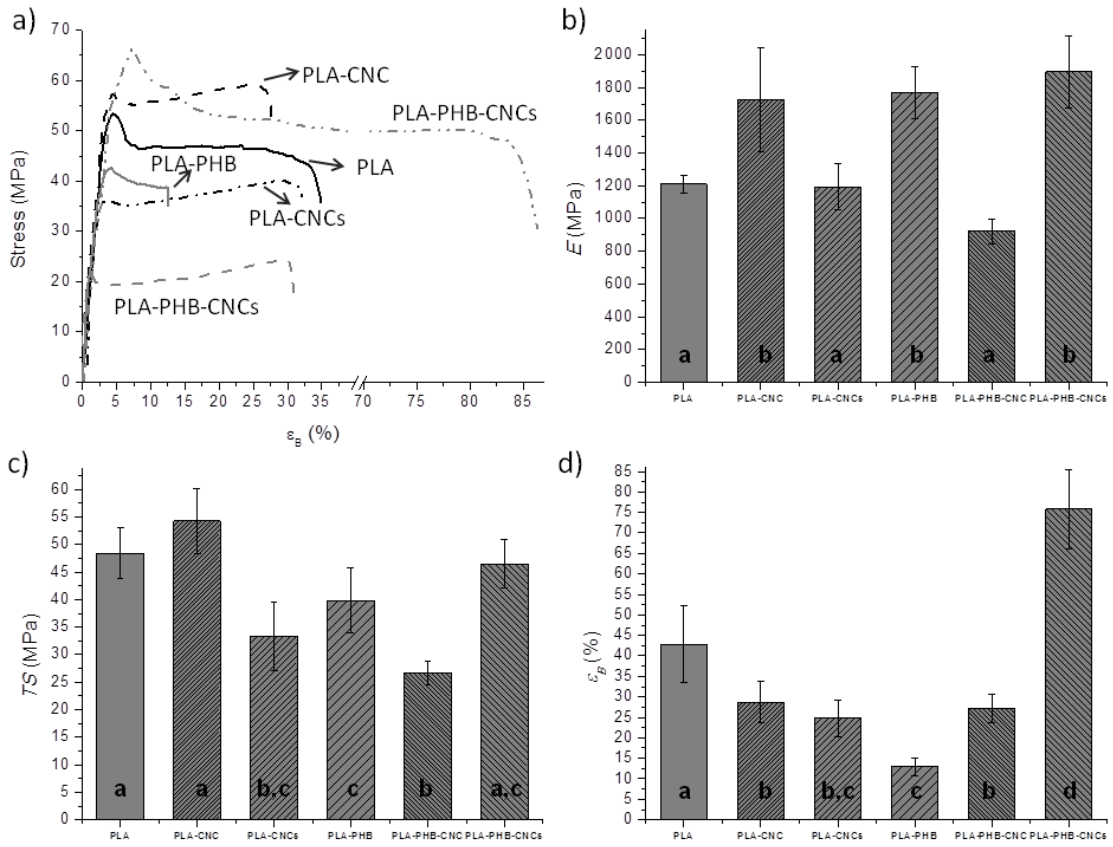


**Figure III.7.1.** Tensile test results of PLA, PLA-PHB and nanocomposite films: a) Stress-strain curves, b) Young's Modulus ($E$), c) Tensile strength ($TS$) and d) Elongation and break ($\varepsilon_B$). [a-d]Different letters on the bars within the same image indicate significant differences between formulations ($p < 0.05$).

### 3.2. Optical and colourimetric properties

The absorption spectra of PLA, PLA-PHB and nanocomposites are shown in Figure III.7.2-a while the visual appearances of the films are displayed in Figure III.7.2-b. Neat PLA film proved to be the most transparent showing the highest transmission in the visible region of the spectra (400-700 nm). No significant changes were observed due to the presence of CNC or CNC-s in the visible region of the spectra, thus PLA-CNC and PLA-CNC-s resulted in highly transparent films, referred to the light transmission in the range of 540–560 nm [10, 25], as it can be observed in Figure III.7.2-b. The good transparency of

PLA-CNC films has been related with the good dispersion of cellulose nanocrystals into PLA matrix [12, 25]. On the other hand, a 25wt% of PHB, provokes a reduction of the light transmission of the films. Both, PHB and cellulose nanocrystals show a blocking effect on the virtually transparent PLA matrix at the UV spectra region (250-400 nm). Cellulose nanocrystals reduced the UV light transmission with a maximum centered at 275 nm which corresponds to the UV-C region (280-100nm), generally created from artificial light sources [10]. This behaviour was more evident with surface modified nanocrystals (CNC-s). The PLA-PHB-CNCs film showed a blocking effect in the UV light spectra region with the lowest UV-C light transmission, while maintaining the high transparency in the visible spectra region.

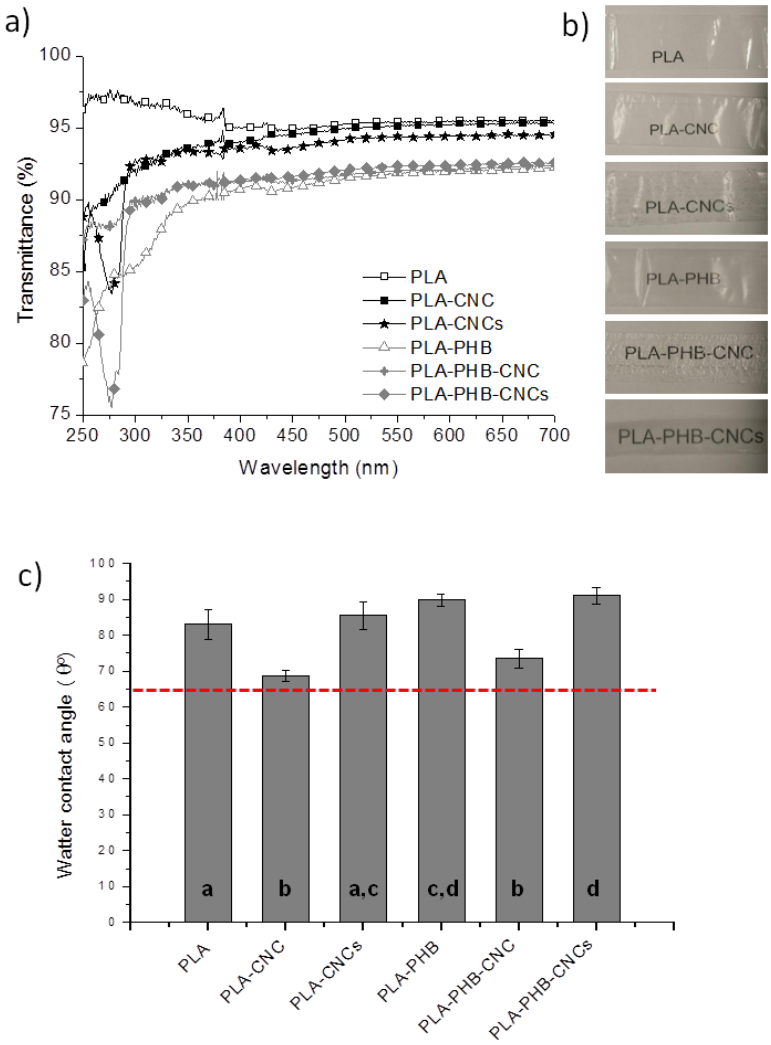


**Figure III.7.2.** PLA, PLA-PHB and nanocomposite films: **a)** UV-Vis spectra, **b)** Visual appearance, **c)** contact angle measurements.

[a-d]Different letters on the bars within the same image indicate significant differences between formulations ($p < 0.05$).

Table III.7.1 summarizes the colour parameters obtained for PLA, PLA-PHB and cellulose nanocrystal based nanocomposites. PLA showed the highest *L* value confirming it characteristic high brightness. *L* is significantly affected by CNC, CNC-s and PHB presence, although all film samples present still higher *L* values than commercial low density polyethylene (LDPE) and poly(ethylene terephthalate) (PET) films [10]. Negative values of the a* coordinate reveal a deviation towards green, while positive values for b* are indicative of a deviation towards yellow. As a consequence of the PHB presence, the highest deviations towards green and yellow colours were observed in the PLA-PHB blend, in accordance to previous studies [26]. As a result, the yellowness index (YI) showed the maximum value for the PLA-PHB film, followed by PLA-PHB-CNCs and PLA-PHB-CNC. The YI is used to describe the change in colour of a sample from clear toward yellow. It must be noticed, that the obtained YI values are significant lower than those previously reported for PLA [9, 10] and PLA-PHB (75:25) blends [9, 26]. The main reason for this important reduction in YI is due to the lower films thickness obtained by the processing film methodology used in the present work. Despite the total color differences obtained with respect to the neat PLA film were significant different in all cases, the total colour differences were in general smaller than 2.0, being this value the threshold of perceptible colour difference for the human eye [27], with the exception of the PLA-PHB film as can be confirmed in Figure III.7.2-b.

**Table III.7.1.** Colour parameters from CIELab space and *YI* of PLA, PLA-PHB and nanocomposite films.

| **Samples** | ***L*** | **a*** | **b*** | **ΔE** | **YI** |
|---|---|---|---|---|---|
| PLA | 94.64 ± 0.01$^{a}$ | -0.98 ± 0.01$^{a}$ | 0.76 ± 0.02$^{a}$ | - | 0.70 ± 0.03$^{a}$ |
| PLA-CNC | 93.57 ± 0.01$^{b}$ | -1.08 ± 0.02$^{b}$ | 0.62 ± 0.02$^{b}$ | 1.08 ± 0.01 | 0.52 ± 0.02$^{b}$ |
| PLA-CNCs | 94.28 ± 0.01$^{c}$ | -1.01 ± 0.01$^{c}$ | 0.83 ± 0.01$^{c}$ | 0.37 ± 0.01 | 0.82 ± 0.02$^{c}$ |
| PLA-PHB | 93.79 ± 0.01$^{d}$ | -1.07 ± 0.01$^{b}$ | 1.54 ± 0.01$^{d}$ | 1.15 ± 0.01 | 2.14 ± 0.02$^{d}$ |
| PLA-PHB-CNC | 93.55 ± 0.01$^{e}$ | -0.91 ± 0.01$^{d}$ | 1.03 ± 0.01$^{e}$ | 1.12 ± 0.01 | 1.29 ± 0.01$^{e}$ |
| PLA-PHB-CNCs | 93.69 ± 0.01$^{f}$ | -1.04 ± 0.01$^{c}$ | 1.48 ± 0.01$^{f}$ | 1.19 ± 0.01 | 2.07 ± 0.03$^{f}$ |

**ΔE** Calculated by using PLA film colour coordinates as reference.

$^{a\text{-}f}$ Different superscripts within the same column indicate significant differences between formulations ($p < 0.05$).

### 3.3. Oxygen transmission rate and wettability

In a previous reported work the incorporation of CNC and functionalized CNC-s had shown reductions in OTR values of neat PLA film (30.5 $cm^3 * mm * m^{-2} * day^{-1}$) of about 43% and 48%, respectively [19]. In this case, the addition of PHB reduced the oxygen permeation of PLA to 13.3 $cm^3 * mm * m^{-2} * day^{-1}$ (reduction of 56%) due to the increased crystallinity in the system [9, 20]. Nevertheless, from the OTR values obtained in ternary systems (15.3 $cm^3 * mm * m^{-2} * day^{-1}$ for PLA-PHB-CNC and 13 $cm^3 * mm * m^{-2} * day^{-1}$ for PLA-PHB-CNC-s), it can be noticed that the incorporation of CNC or CNC-s to PLA-PHB blend did not provoke major changes in OTR values. The low OTR values obtained for the PLA-PHB blend and ternary nanocomposites highlight the advantage of blending PLA with crystalline PHB. These films are therefore attractive for food packaging applications were barrier to oxygen is critical to avoid or reduce oxidative processes.

Additionally, films for food packaging are required to protect foodstuff from humidity during transport, handling and storage. Thus, water contact angle measurements were carried out to evaluate the hydrophilic/hydrophobic character of films and the results are shown in Figure III.7.2-c [27]. It should be noticed that all formulations showed values higher than 65º, being materials acceptable for the intended end-use applications. PHB has a hydrophobic character due to the poor affinity of the water to the non-polar polymer surface [28]. In this way, the PLA-PHB blend showed significant increased water resistance in comparison with neat PLA, in good accordance with a previous reported work [9]. The presence of CNC in PLA and PLA-PHB caused an increase in wettability, while functionalized CNC-s did not significantly change PLA or PLA-PHB wettability. The positive effect of cellulose nonocrystal chemical modification in the wettability of PLA and PLA-PHB films is mainly due to the presence of sulfate groups with low polarity on the surface that increase the surface hydrophobicity of the final material.

### 3.4. Disintegration under composting

Figure III.7.3-a shows the visual appearance of PLA, PLA-PHB and cellulose nanocrystal based nanocomposites after different time of disintegration in composting conditions where it is possible to confirm the biodegradable character of all the formulations studied. After only 1 day of incubation, films become smaller, with the exception of PLA-PHB blend, which started the film size reduction on the second day of incubation. After 7 days of incubation binary and ternary formulation films became breakable and small pieces of films were recovered. It also could be noticed that they

changed their color and became more opaque after 7 days. When the degradation process of the polymer matrices started, a change in the refraction index of the materials was observed as a result of water absorption and/or presence of products formed by the hydrolytic process [29].

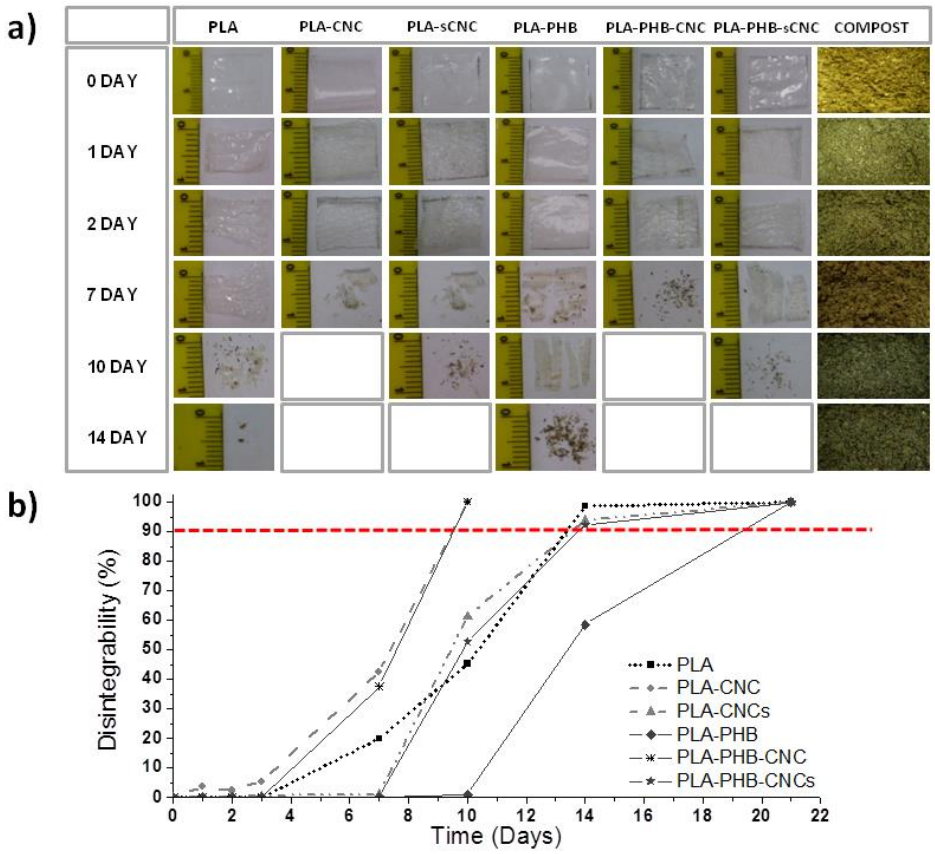


**Figure III.7.3. a)** Visual appearance of film samples before and after different incubation days under composting conditions. **b)** Degree of disintegration of films under composting conditions as a function of time.

Additionally, the films disintegrability was evaluated in terms of mass loss as a function of incubation time (Figure III.7.3-b), in which the line at 90% of disintegration represents the goal of disintegrability test [4]. Unmodified cellulose nanocrystals (CNC) speed up the disintegration of PLA and PLA-PHB blend from 14 days and 21 days, respectively, to 10 days. Comparable findings were previously reported for PLA nano-biocomposite films with functionalized cellulose nanocrystals and silver nanoparticles [30]. Accordingly, after 10 days CNC incorporated films were visibly disintegrated (Figure III.7.2-a), while CNC-s incorporated counterparts reached between 50-60% of disintegrability and need 14 days to reach the goal of the disintegrability test (Figure III.7.3-b). It is known that the PLA disintegration in compost starts by a hydrolysis process

[31], thus this different behaviour observed between the pristine and modified cellulose nanocrystals could be ascribed to the more hydrophobic character of functionalized cellulose nanocrystals that protect the polymer matrix from the water attack. In brief, PLA-CNC and PLA-PHB-CNC lost more than 90% of the initial matter in 10 days; PLA, PLA-PHB-CNC and PLA-PHB-CNC in 14 days and PLA-PHB in 21 days. These short degradation times have been related to the low thickness of tested samples [4]. Some changes in compost colour were observed (Figure III.7.3-a) due to the aerobic fermentation that results in dark humus soil.

However, all formulations showed different rate of disintegration and thus the Boltzmann function was used to correlate the sigmoidal behavior of the mass loss during the disintegrability in the composting process (Figure III.7.4). The estimated regression parameters of the fitted results of the non-linear model and $t_{50}$ were calculated, while $m_i$ and $m_\infty$ values were assigned as 0% and 100% of disintegrability, respectively. The correlation coefficients between theoretical and experimental data ($R^2$) were higher than 0.990 in all cases, indicating that only minor differences were observed in the fitting of the model to experimental values. The rate of disintegration under composting conditions was longer for PLA-PHB with a half-maximal degradation ($t_{50}$) at about 14 days, with respect to neat PLA that showed $t_{50}$ at about 10 days, due to the fact that the polymer disintegrability in composting starts in the amorphous phase of the polymers [32] and the increasing crystallinity in PLA-PHB blend due to the PHB presence delays the PLA degradation rate [9, 26].

Both cellulose nanocrystals speed up the rate of disintegration of PLA and PLA-PHB shifting half-maximal degradation to lower values. The $t_{50}$ of PLA was shifted from 10 days to 7 days in PLA-CNC and remains practically constant in PLA-CNCs, while the $t_{50}$ of PLA-PHB was shifted from 14 days to 7 days and to 10 days in PLA-PHB-CNC and PLA-PHB-CNC-s, respectively. As a result, PLA-PHB-CNC showed higher rate of disintegration than PLA-CNC-s, even when PLA-PHB-CNC ($\chi_c$ = 18.5 %) is more crystalline than PLA-CNC-s ($\chi_c$ = 11.0 %)[20]. This unexpected result could be explained with the fact that during disintegration in compost, PLA surface is firstly attacked by water where polymer chain are hydrolyzed [4] and as a result the smaller molecules become susceptible for enzymatic degradation mediated by microorganisms [31]. Meanwhile, PHB disintegration is firstly caused by polymer surface erosion mediated by microorganisms which then are able to spread gradually inside the polymer matrix [33]. PLA-PHB-CNC showed higher surface polarity than PLA-CNC-s. Thus, the water attack starts on the more susceptible component, CNC, with hydroxyl groups available on the surface, allowing the hydrolysis in PLA-PHB-CNC, which is followed by the microorganisms attack, while CNC-s is protecting PLA in

PLA-CNCs. In the meantime, available -OH are now able to attack he carbon of the ester group and produce intramolecular degradation, followed by the hydrolysis of the ester link [34]. As a consequence, the higher surface polarity of PLA-PHB-CNC and the -OH presence that catalyze the hydrolysis process, leading to a higher disintegration rate for PLA-PHB-CNC than PLA-CNC-s.

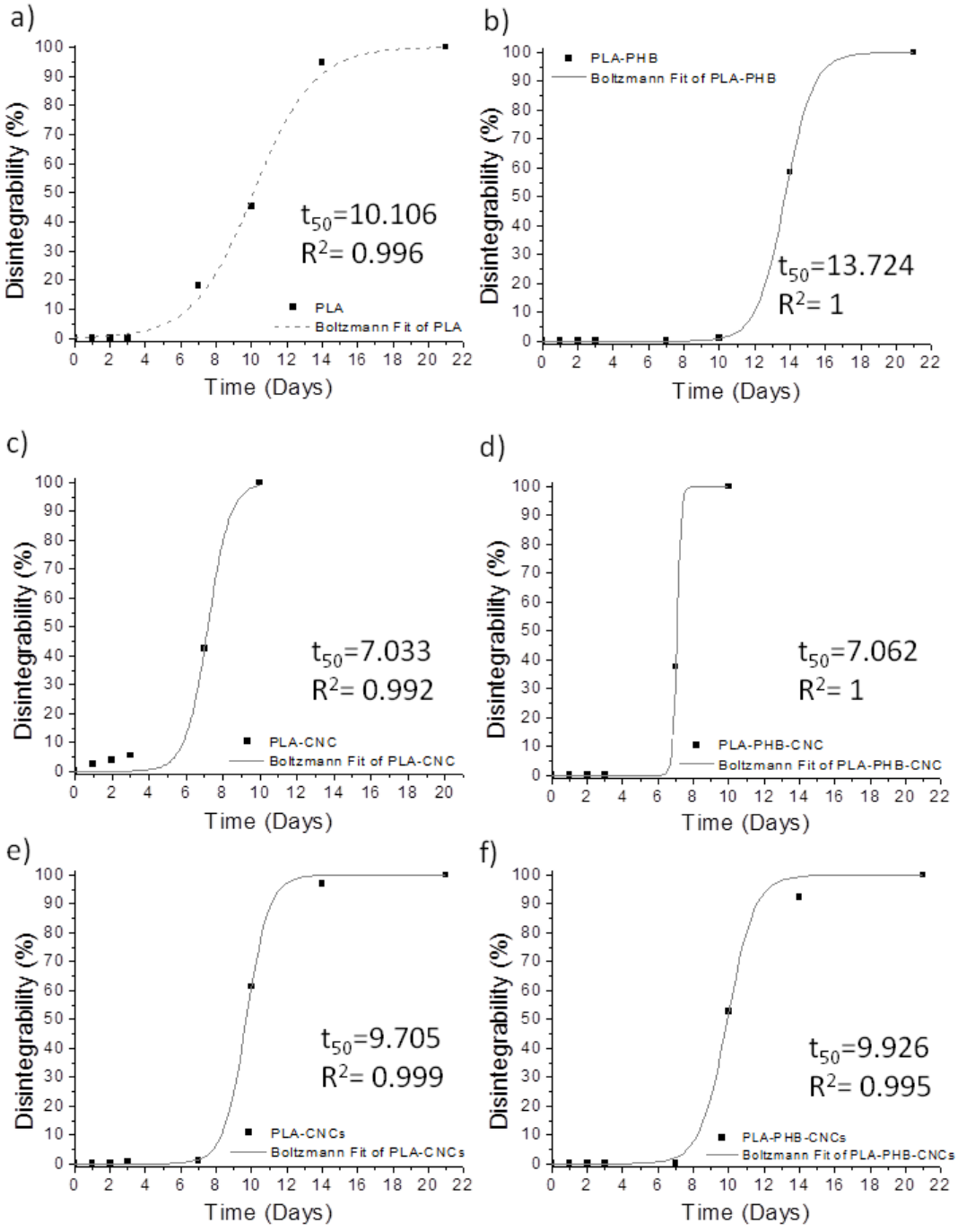


**Figure III.7.4.** Disintegrability of PLA, PLA-PHB and nanocomposite films as a function of time.

Micrograph observations of film surfaces before and after 3 days in composting, and their profiles measured by the EDF-z technique, are shown in Figure III.7.5 PLA and PLA nanocomposite films before composting showed smoother profile than PLA-PHB counterparts. Similar behaviour was observed in a previous work where neat PLA, neat PHB films roughness were investigated by means of confocal microscopy. The PLA film showed a smoother roughness profile than PHB [9]. In general, after 3 days in composting all formulations showed a more irregular EDF-z profile with respect to the same formulation before composting.

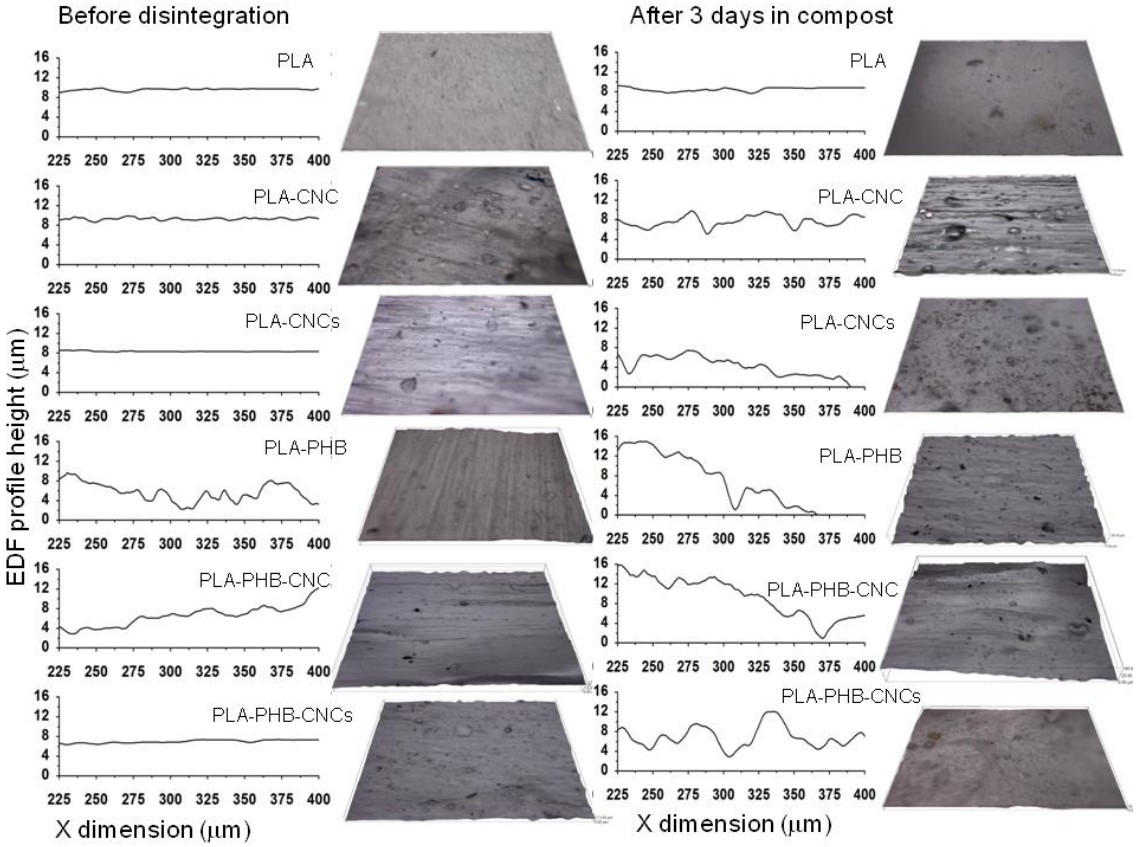


**Figure III.7.5.** Optical micrographs (20 X) of PLA, PLA-PHB and nanocomposite films and their EDF-z profiles.

The chemical changes of nanocomposite films before and after 1, 2 and 3 days in composting were followed by FTIR analysis. At higher time of disintegration, film samples could not be studied in the FTIR spectrometer due the small portions of films recovered. The main differences found were in the 2000-1200 $cm^{-1}$ region of the FTIR spectra as shown in Figure III.7.6. The typical asymmetric stretching of the carbonyl group (-C═O) of PLA centered at 1760 $cm^{-1}$ become broader during composting due to an increase in the number of carboxylic end groups in the polymer chain during the hydrolytic degradation

[29]. Moreover, a band at 1722 $cm^{-1}$ was also apparent (shown by gray arrows) that has been associated with crystalline C=O stretching vibration of PHB [35]. In some samples, this band appears as a shoulder due to its low intensity and the strong stretching vibration of carbonyl group.

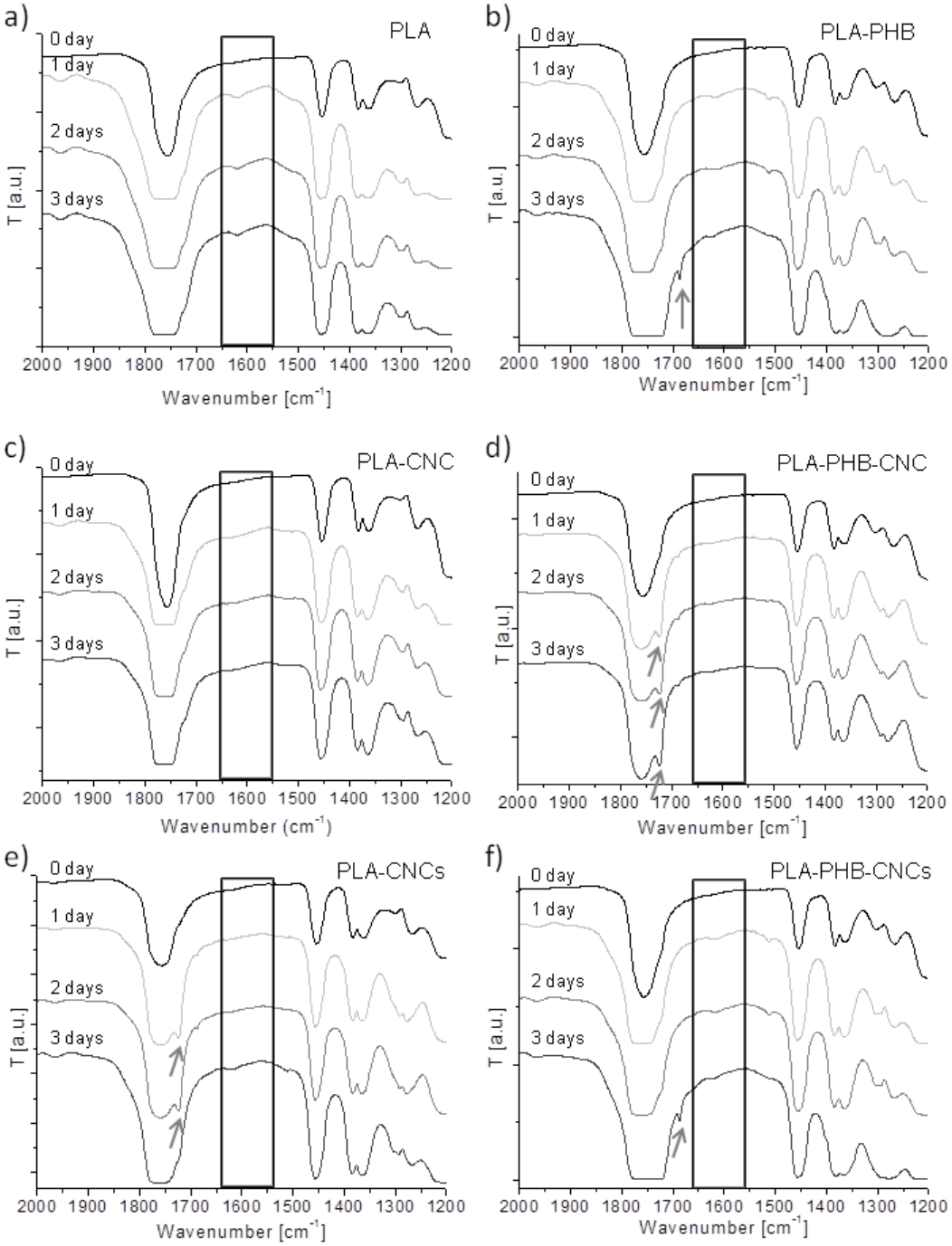


**Figure III.7.6.** Infrared spectra (2000-1200 $cm^{-1}$) of PLA, PLA-PHB and nanocomposite films before and after different time of incubation under composting conditions.

A small band at 1687 $cm^{-1}$ was apparent (shown by black arrows) in PLA-PHB and PLA-PHB-CNC-s after three days of composting. This band has been reported to be a crystalline band, although its spectral origin is not yet assigned [35, 36]. The clear appearance of this band in PLA-PHB and PLA-PHB-CNC-s is supported by the early degradation of the amorphous phase of the polymer blend while the crystalline PHB remains in the polymer matrix. Similar results indicating that PHB slow down the disintegration rate of PLA in PLA-PHB blends have been previously reported [26]. In the region between 1550-1650 $cm^{-1}$ the appearance of a broad band was observed for all formulations. The appearance of this band has been previously observed during the degradation of PLA-MCC based composites and was related to the presence of carboxylate ions in degraded PLA composites [4].

Figure III.7.7-a. shows the typical Py-GC/MS chromatogram of PLA-PHB-CNCs obtained by pyrolysing the film at 1000°C for 0.5s. The pyrolysis of all PLA based films is characterized by the presence of two peaks with very similar mass spectra (m/z = 32, 43, 45 and 56) in which the peak at 17 min corresponds to *meso*-lactide and the peak at 18 min with the highest signal intensity in all samples to (*L*) and/or (*D*)-lactide [23]. Films with PHB showed the broad peak of crotonic acid (6.7 min, m/z = 39, 41, 68, 69, and 86)[9, 26], while nanocomposte films showed a peak at 22.5 min assigned to thermal degradation products of the cellulose structure (m/z = 55, 69, 87 and 103 )[37]. The groups of small peaks appearing at retention times between 19 min and 22 min were assigned to the thermal degradation products of PLA with the characteristic series of signals at $m/z = 56 + (n \times 72)$ attributed to PLA degradation products such as dimers ($n$=2) and trimers ($n$=3) [23]. In general, the intensity of peaks decreased with composting time. However, the *meso*-lactide intensity showed a lower decrease with respect to the (D,L)-lactide equivalent. The ratio *meso*-lactide:lactide has been used as a semi-quantitative sign of the degradation of PLA [9, 23, 26, 38, 39]. Figure III.7.7-b shows the reduction of (*D*,*L*)-lactide with respect to *meso*-lactide after the pyrolysis of the recovered samples. No significant differences were observed between PLA and PLA-PHB blend until 7 days in composting, but after 10 days, the PLA relationship [lactide/*meso*-lactide$_{t=10\ days}$/ lactide/meso-lactide$_{t=0\ days}$] highly decreased. Nanocomposites showed similar reduction in 3 days of composting, but higher times revealed higher reduction for unfunctionalized nanocomposites (PLA-CNC and PLA-PHB-CNC). The estimated reduction of the (*D*,*L*)-lactide form with respect to the *meso*-lactide followed a similar tendency that the disintegrability test. In this sense, PLA-CNC and PLA-PHB-CNC showed the highest degradation rate suggestive of the polymer shortening by the hydrolysis resulted in a higher amount of lactic acid. It is known that microorganisms prefer the *L*-lactide form of

lactic acid rather than the D-form, thus there was a higher enzymatic degradation of *L*-lactide influencing the formation of a higher amount of *meso*-lactide form during the pyrolysis test [38].

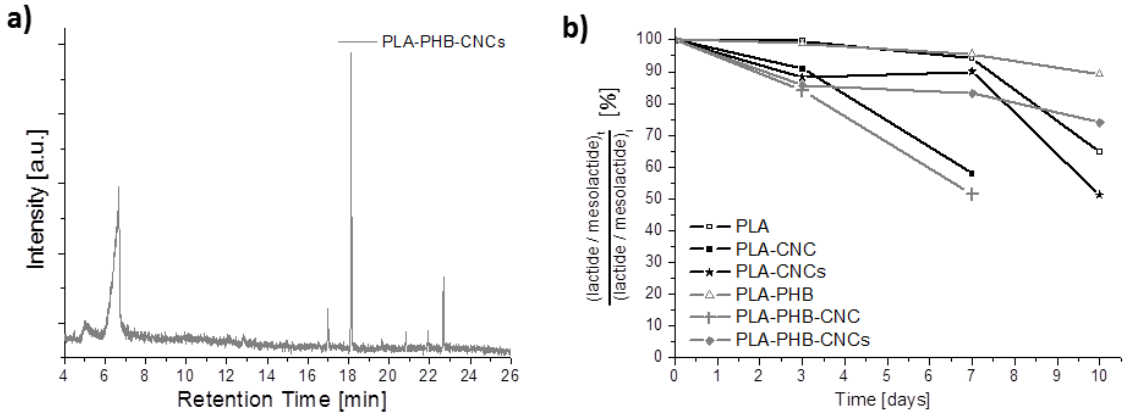


**Figure III.7.7. a)** Py- GC/MS chromatogram of PLA-PHB-CNCs nanocomposite film, **b)** mesolactide:lactide ratio loss of PLA, PLA-PHB and nanocomposite films.

## 4. CONCLUSION

PLA-PHB based nanocomposite films reinforced with synthetized CNC and functionalized CNC-s intended for food packaging were developed and characterized. The combination of PHB and the better dispersed CNC-s demonstrated the reinforcing effect increasing simultaneously the Young modulus and elongation at break, with comparable tensile strength to those of neat PLA. PHB and functionalized CNC-s showed a slight UV blocking effect on the virtually transparent PLA matrix. Although the addition of PHB led to a decrease in PLA high transparency, it did not compromise the ultimate optical properties due to the low film thickness achieved. The presence of PHB increased the cristallinity of PLA and its nucleation effect reduced the polymer chains mobility enhancing the oxygen barrier performance of final PLA-PHB blend films while the wettability was reduced. Moreover, functionalized CNC-s, which increases the polymer-nanoparticle interfacial adhesion, also reduced the oxygen transmission at the same time as it decreased the surface adhesive forces improving the water resistance. Finally, CNC based nanocomposites showed the highest rate of disintegration in compost, while the surface hydrolysis of functionalized CNC-s nanocomposite films started somewhat later and the presence of crystalline PHB delayed the disintegration process.

The results of this research suggest that the novel combination of PLA-PHB blends and functionalized CNC-s opens a new perspective for their industrial application for short term food packaging.

**Acknowledges**

This research was supported by the Ministry of Science and Innovation of Spain (MAT2011-2846-C02-01 and MAT2011-28468-C02-02). M.P. Arrieta thanks Generalitat Valenciana (Spain) for Santiago Grisolía Fellowship (GRISOLIA/2011/007) and Universitat Politècnica de València for the Development Support Programme PAID-00-12 (SP20120120). The Authors acknowledge Gesenu S.p.a. for compost supply. Authors gratefully thank Prof. Alfonso Jiménez (University of Alicante, Spain) for his assistance with OTR measurements.

**REFERENCES**

[1] Fortunati E, Armentano I, Iannoni A, Kenny JM. Development and thermal behaviour of ternary PLA matrix composites. Polymer Degradation and Stability. 2010;95(11):2200-2206.

[2] Arrieta MP, López J, Ferrándiz S, Peltzer MA. Characterization of PLA-limonene blends for food packaging applications. Polymer Testing. 2013;32(4):760-768.

[3] Fortunati E, Armentano I, Zhou Q, Puglia D, Terenzi A, Berglund LA, et al. Microstructure and nonisothermal cold crystallization of PLA composites based on silver nanoparticles and nanocrystalline cellulose. Polymer Degradation and Stability. 2012;97(10):2027-2036.

[4] Fortunati E, Armentano I, Iannoni A, Barbale M, Zaccheo S, Scavone M, et al. New multifunctional poly(lactide acid) composites: Mechanical, antibacterial, and degradation properties. Journal of Applied Polymer Science. 2012;124(1):87-98.

[5] Mattioli S, Peltzer M, Fortunati E, Armentano I, Jiménez A, Kenny JM. Structure, gas-barrier properties and overall migration of poly(lactic acid) films coated with hydrogenated amorphous carbon layers. Carbon. 2013;63:274-282.

[6] Carrasco F, Gámez-Pérez J, Santana OO, Maspoch ML. Processing of poly(lactic acid)/organomontmorillonite nanocomposites: Microstructure, thermal stability and kinetics of the thermal decomposition. Chemical Engineering Journal. 2011;178:451-460.

[7] Zhang M, Thomas NL. Blending polylactic acid with polyhydroxybutyrate: The effect on thermal, mechanical, and biodegradation properties. Advances in Polymer Technology. 2011;30(2):67-79.

[8] Bucci DZ, Tavares LBB, Sell I. Biodegradation and physical evaluation of PHB packaging. Polymer Testing. 2007;26(7):908-915.

[9] Arrieta MP, López J, Hernández A, Rayón E. Ternary PLA–PHB–Limonene blends intended for biodegradable food packaging applications. European Polymer Journal. 2014;50(0):255-270.

[10] Auras R, Harte B, Selke S. An overview of polylactides as packaging materials. Macromolecular Bioscience. 2004;4(9):835-864.

[11] Fortunati E, Luzi F, Puglia D, Terenzi A, Vercellino M, Visai L, et al. Ternary PVA nanocomposites containing cellulose nanocrystals from different sources and silver particles: Part II. Carbohydrate Polymers. 2013.

[12] Fortunati E, Armentano I, Zhou Q, Iannoni A, Saino E, Visai L, et al. Multifunctional bionanocomposite films of poly(lactic acid), cellulose nanocrystals and silver nanoparticles. Carbohydrate Polymers. 2012;87(2):1596-1605.

[13] Martínez-Sanz M, Lopez-Rubio A, Lagaron JM. High-barrier coated bacterial cellulose nanowhiskers films with reduced moisture sensitivity. Carbohydrate Polymers. 2013;98(1):1072-1082.

[14] Patrício PSDO, Pereira FV, Dos Santos MC, De Souza PP, Roa JPB, Orefice RL. Increasing the elongation at break of polyhydroxybutyrate biopolymer: Effect of cellulose nanowhiskers on mechanical and thermal properties. Journal of Applied Polymer Science. 2013;127(5):3613-3621.

[15] Martínez-Sanz M, Villano M, Oliveira C, Albuquerque MGE, Majone M, Reis M, et al. Characterization of polyhydroxyalkanoates synthesized from microbial mixed cultures and of their nanobiocomposites with bacterial cellulose nanowhiskers. New Biotechnology. 2013.

[16] Fortunati E, Peltzer M, Armentano I, Jiménez A, Kenny JM. Combined effects of cellulose nanocrystals and silver nanoparticles on the barrier and migration properties of PLA nano-biocomposites. Journal of Food Engineering. 2013.

[17] Aranguren MI, Marcovich NE, Salgueiro W, Somoza A. Effect of the nano-cellulose content on the properties of reinforced polyurethanes. A study using mechanical tests and positron anihilation spectroscopy. Polymer Testing. 2013;32(1):115-122.

[18] Jonoobi M, Mathew AP, Abdi MM, Makinejad MD, Oksman K. A Comparison of Modified and Unmodified Cellulose Nanofiber Reinforced Polylactic Acid (PLA) Prepared by Twin Screw Extrusion. Journal of Polymers and the Environment. 2012;20(4):991-997.

[19] Fortunati E, Peltzer M, Armentano I, Torre L, Jiménez A, Kenny JM. Effects of modified cellulose nanocrystals on the barrier and migration properties of PLA nano-biocomposites. Carbohydrate Polymers. 2012;90(2):948-956.

[20] Arrieta MP, Fortunati E, Dominici F, Rayón E, López J, Kenny JM. Multifunctional PLA-PHB/cellulose nanocrystal films: Processing, structural and thermal properties. Carbohydrate Polymers. 2014;0(0):0.

[21] UNE-EN ISO. 527-3. Plastics: Determination of Tensile Properties. Part 3: Test Conditions for Films and Sheets. 1995.

[22] UNE EN ISO 20200. Determination of the degree of disintegration of plastic materials under simulated composting conditions in a laboratory-scale test. . 2006.

[23] Arrieta MP, Parres F, López J, Jiménez A. Development of a novel pyrolysis-gas chromatography/mass spectrometry method for the analysis of poly(lactic acid)

thermal degradation products. Journal of Analytical and Applied Pyrolysis. 2013;101:150-155.

[24] Bonilla J, Fortunati E, Atarés L, Chiralt A, Kenny JM. Physical, structural and antimicrobial properties of poly vinyl alcohol-chitosan biodegradable films. Food Hydrocolloids. 2013.

[25] Armentano I, Bitinis N, Fortunati E, Mattioli S, Rescignano N, Verdejo R, et al. Multifunctional nanostructured PLA materials for packaging and tissue engineering. Progress in Polymer Science. 2013.

[26] Arrieta MP, López J, Rayón E, Jiménez A. Disintegrability under composting conditions of plasticized PLA-PHB blends. Polymer Degradation and Stability. 2014;0(0):0.

[27] Arrieta MP, Peltzer MA, López J, Garrigós MDC, Valente AJM, Jiménez A. Functional properties of sodium and calcium caseinate antimicrobial active films containing carvacrol. Journal of Food Engineering. 2014;121(1):94-101.

[28] Puglia D, Fortunati E, D'Amico DA, Manfredi LB, Cyras VP, Kenny JM. Influence of organically modified clays on the properties and disintegrability in compost of solution cast poly(3-hydroxybutyrate) films. Polymer Degradation and Stability. 2014;99(1):127-135.

[29] Fortunati E, Puglia D, Santulli C, Sarasini F, Kenny JM. Biodegradation of Phormium tenax/poly(lactic acid) composites. Journal of Applied Polymer Science. 2012;125(SUPPL. 2):E562-E572.

[30] Fortunati E, Rinaldi S, Peltzer M, Bloise N, Visai L, Armentano I, et al. Nano-biocomposite films with modified cellulose nanocrystals and synthesized silver nanoparticles. Carbohydrate Polymers. 2014;101(0):1122-1133.

[31] Kale G, Auras R, Singh SP. Comparison of the degradability of poly(lactide) packages in composting and ambient exposure conditions. Packaging Technology and Science. 2007;20(1):49-70.

[32] Calvão PS, Chenal JM, Gauthier C, Demarquette NR, Bogner A, Cavaille JY. Understanding the mechanical and biodegradation behaviour of poly(hydroxybutyrate)/rubber blends in relation to their morphology. Polymer International. 2012;61(3):434-441.

[33] Weng YX, Wang L, Zhang M, Wang XL, Wang YZ. Biodegradation behavior of P(3HB,4HB)/PLA blends in real soil environments. Polymer Testing. 2013;32(1):60-70.

[34] Lucas N, Bienaime C, Belloy C, Queneudec M, Silvestre F, Nava-Saucedo JE. Polymer biodegradation: Mechanisms and estimation techniques - A review. Chemosphere. 2008;73(4):429-442.

[35] Guo L, Sato H, Hashimoto T, Ozaki Y. FTIR study on hydrogen-bonding interactions in biodegradable polymer blends of poly(3-hydroxybutyrate) and poly(4-vinylphenol). Macromolecules. 2010;43(8):3897-3902.

[36] Mousavioun P, George GA, Doherty WOS. Environmental degradation of lignin/poly(hydroxybutyrate) blends. Polymer Degradation and Stability. 2012;97(7):1114-1122.

[37] Jiménez A, Ruseckaite RA. Binary mixtures based on polycaprolactone and cellulose derivatives : Thermal degradation and pyrolysis. Journal of Thermal Analysis and Calorimetry. 2007;88(3):851-856.

[38] Khabbaz F, Karlsson S, Albertsson AC. Py-GC/MS an effective technique to characterizing of degradation mechanism of poly (L-lactide) in the different environment. Journal of Applied Polymer Science. 2000;78(13):2369-2378.

[39] Westphal C, Perrot C, Karlsson S. Py-GC/MS as a means to predict degree of degradation by giving microstructural changes modelled on LDPE and PLA. Polymer Degradation and Stability. 2001;73(2):281-287.

## 8. PLA-PHB blends incorporated with chatechin intended for active food packaging applications

**Abstract**

Active biobased packaging materials based on poly(lactic acid)-poly(hydroxybutyrate) (PLA-PHB) blends were prepared by melt blending and full characterized. The incorporation of catechin, as antioxidant compound, improved the thermal stability, whereas its release was improved by the addition of acetyl(tributyl citrate) (ATBC) as plasticizer. While the addition of ATBC resulted in a reduction of elastic modulus and hardness, catechin incorporation produced more rigid materials due to hydrogen bonding interactions between catechin hydroxyl groups and carbonyl groups of PLA and PHB. Since the obtained blends are intended for fatty food packaging, the quantification of catechin released into fatty food simulant and the antioxidant effectiveness after the release process were also demonstrated. The effect of the materials exposition to food simulant was deeply investigated. PHB added materials maintained the structural and mechanical properties after 10 days in a test medium that represent the worst foreseeable conditions of the intended use. Thus, the developed plasticized PLA-PHB incorporated with catechin materials show their potential as biobased active packaging for fatty food.

**Keywords:** poly(lactic acid); poly(hydroxybutyrate); catechin, antioxidant, active packaging.

## 1. Introduction

An increasing attitude towards the reduction of the environmental impact produced for the plastic waste, in particular from the food packaging sector, has increased the research and industry attention in the developing of new biodegradable materials. In this sense, the most promising raw material for the production of biodegradable food packaging is poly(lactic acid) due to its high mechanical strength, superior transparency and easy processability [1]. However, PLA is high brittleness [2], it shows relatively high oxygen permeation [3] and lower water vapour permeability [4] limiting PLA uses in food packaging.

Thus, many research studies have been focused on PLA modification for extending its industrial applications in the food packaging sector; such as the addition of modifiers, copolymerization or blending. The modification of PLA by blending with other biobased and/or biodegradable polymer has many advantages, because it offers the opportunity to tuning the physical properties in a wide range through a relatively simple approach [5]. Nevertheless, only nontoxic substances approved for food contact can be considered as modifying agents for PLA. Moreover, the modifiers should be miscible with PLA and not be too volatile to avoid evaporation at the elevated temperatures used for PLA industrial processing [6].

It has been reported that PLA blended with 25wt% of PHB showed optimal miscibility between both polymers and improved mechanical properties compared with those of pure PLA [7] by enhancing the PLA crystallinity [8, 9]. In previous works, it was shown that PLA-PHB (75:25) blends showed improved properties of the final formulation [5] particularly significant in the packaging field, such as oxygen barrier and surface wettability [9, 10], while their disintegrability in composting conditions suggested a valuable end-life option for PLA-PHB packaging materials [9, 11].

Concerning the field of application, plasticizers are frequently incorporated into PLA matrix intended for food packaging to overcome some ductility [1, 12]. Particularly, PLA could be melt processed with PHB due to their similar melting temperatures [5] and their processability could be improved by the addition of plasticizers at the same time as resulting in more flexible materials [9, 10]. Acetil(tributyl citrate) (ATBC) has been suggested as one of the most efficient plasticizers for PLA accepted to be in contact with food products [13]. Moreover, it has been shown that PLA-PHB plasticized with ATBC offers good perspective for biodegradable food packaging industry by improving the polymer performance in films manufacturing and uses, better than other plasticizers such

as PEG [10] and D-Limonene [9], it also speeds up the disintegration under composting conditions [11] in relation to their environmentally friendly post-use.

On the other hand, current worldwide trends to reduce the use of food additives have given way to investigations of incorporating the additives, such as antimicrobial or antioxidant compounds, into the food packaging. These systems are known as active food packaging and offer the opportunity to provide continuous release of active compounds from packaging material to the foodstuffs, having an important effect on the shelf-life extension without the need of direct incorporation of additives onto the final food product. However, it is expected that an active agent shows higher affinity for the polymer matrix than the foodstuffs. Consequently, the design of active packaging system is aimed in the strategy to obtain an effective release capacity of active agent from the polymer matrix. It is known that the plasticizer presence increases the polymer chain mobility in PLA-PHB blends [9, 10] and for this reason it is expected that the mass transport of the active agent should be modified [15] resulting in an effective way to improve the release of the active substance from the polymer matrix [16]. One of the main drawbacks of polymer modifiers is the negative effect of the additives on the thermal stability. Thermal degradation is responsible for serious damage to many polymeric materials during processing [1]. In this sense, antioxidants are chosen not only as an active substance to protect food deterioration and extend its shelf life [16, 17], but also to protect the polymers matrices from thermo-oxidative degradation during processing [17, 18] because antioxidants are able to act with the free radicals formed during thermo-oxidation blocking further polymer degradation [19].

For food contact applications, synthetic additives are being replaced by natural preservatives due to safety [15] and environmental concern. Most of the common natural antioxidants are phenolic compounds derived from flavonoids [17, 19] which are sourced primarily from renewable resources and they have been in use for centuries. For instance, catechins are flavonoids with multiple biological effects [17] have gained considerable attention due to their potential benefits on human health [20] related to anti-mutagenic, anti-diabetic, anti-inflamatory, antibacterial and anti-viral qualities and prevention against several kinds of cancer [21].

Catechins have been suggested as effective natural antioxidants in many polyolefins for active food packaging applications [15, 17, 20]. Catechin is one of the major active constituents of green tea and is well known for its healthy properties having a positive acceptance from consumers. Moreover, concerning the polymers transformation, PLA and PHB should be processing in the region from at least 160ºC and below 200 ºC [5],

and catechin is nonvolatile compound being optimal for melt processing in order to avoid or reduce its loss during polymer processing [17].

The main objective of this work was to develop a biodegradable active packaging based on PLA-PHB blends added with catechin, as antioxidant agent, intended for fatty food packaging application. These systems were plasticized with ATBC with dual objective to overcome ductility required for film manufacturing and uses, but also to improve the kinetic of release of catechin from the polymer matrix to the foodstuff. The developed materials were characterized concerning their structure, nanomechanical and thermal properties. The release capacity of catechin into fatty food simulant after the release process was tested, as well as its antioxidant effectiveness. While the morphological, structural and nanomechanical properties were also followed during the material exposition to food simulant.

## 2. Materials and methods

### 2.1. Materials

Poly(lactic acid) (PLA 2003D, $M_n$ = 98,000 g·mol$^{-1}$, 4 wt% D-isomer) was supplied by NatureWorks (USA), Poly(hydroxybutyrate) (PHB, under the trade name PHI002) was acquired by NaturePlast (France). catechin dehydrate (CAT), (-)-epicatechin (EC), Irgafos 168 [tris(2,4-di-tert-butylphenil)phosphate] (I168), and acetyl tri-n-butyl citrate (ATBC) and 2,2-diphenyl-1-picrylhydrazyl (DPPH) 95% free radical, were purchased from Sigma-Aldrich (Madrid, Spain).

Methanol (MeOH) and Ethanol (EtOH) HPLC grade were supplied by Merck (Darmstadt, Germany). Water was purified by means a Milli-Q ultrapure water purification system (Millipore, Bedford, MA, USA).

### 2.2. Samples preparation

Samples were prepared by blending the materials in a microextruder equipped with twin conical co-rotating screws (MiniLab Haake Rheomex CTW5, Thermo Scientific) with a capacity of 7 cm$^3$. A screw rotation rate of 40 rpm, temperature of 190ºC and residence time of 1 minute were used. The concentration ratios of the obtained films are summarized in Table III.8.1.

**Table III.8.1.** Films formulations

| Formulations | PLA (wt%) | PHB (wt%) | ATBC (wt%) | I168 (wt%) | CAT (wt%) |
|---|---|---|---|---|---|
| PLA (control) | 99.8 | | | 0.2 | |
| PLA-ATBC | 84.8 | | 15 | 0.2 | |
| PLA-CAT | 94.8 | | | 0.2 | 5 |
| PLA-ATBC-CAT | 79.8 | | 15 | 0.2 | 5 |
| PLA-PHB | 74.85 | 24.95 | | 0.2 | |
| PLA-PHB-ATBC | 63.6 | 21.2 | 15 | 0.2 | |
| PLA-PHB-CAT | 71.1 | 23.7 | | 0.2 | 5 |
| PLA-PHB-ATBC-CAT | 59.85 | 19.95 | 15 | 0.2 | 5 |

### 2.3. Field emission scanning electron microscopy (FESEM)

The films cross-section performed in liquid nitrogen were coated with a thin palladium-gold layer to be observed by field emission scanning electron microscopy (FESEM, Supra 25-Zeiss).

### 2.4. Thermogravimetric analysis

Thermogravimetric analysis was performed with a thermogravimetric analyzer TGA/SDTA-851e Mettler Toledo (Schwarzenbach, Switzerland). Tests were run under dynamic mode from 30 to 600 ºC at 10 ºC $min^{-1}$ in air (50 mL $min^{-1}$). The initial degradation temperatures ($T_0$) were determined at 5% mass loss while temperatures at the maximum degradation rate ($T_{max}$) were calculated from the first derivative of the TG curves (DTG).

### 2.5. Differential Scanning Calorimetry (DSC)

Dynamic DSC experiments were performed in a Mettler Toledo calorimeter (Mettler Toledo, Schwerzenbach, Switzerland) by using two different atmospheres of air (250 ml/min) and nitrogen (50 ml/min) with sample weight about 4 mg in hermetic aluminum pans.

Samples analyzed under air conditions were heated from 30 to 350 ºC with a heating rate of 10ºC/min while samples analyzed under nitrogen conditions were subjected to a cycle program consisting in a first heating stage from 30 to 180ºC at a heating rate of 10ºC $min^{-1}$, followed by a cooling process up to 30ºC and subsequent

heating up to 250ºC in order to erase materials thermal history. The glass transition temperature ($T_g$) was taken at the mid-point of heat capacity changes. The melting temperature ($T_m$) and cold crystallization temperature ($T_{cc}$) were obtained from the second heating and the degree of crystallinity ($\chi_c$) was calculated through Equation III.8. 1:

$$\chi_c = 100\% \times \left[\frac{\Delta H_m - \Delta H_c}{\Delta H_m^c}\right] \times \frac{1}{W_{PLA}} \qquad \textbf{Equation III.8. 1}$$

where $\Delta H_m$ is the melting enthalpy, $\Delta H_{cc}$ is the cold crystallization enthalpy, $\Delta H_m^c$ is the melting heat associated to pure crystalline PLA (93J $g^{-1}$)

## 2.6. X-ray diffraction

The crystalline phases of the nanocomposite films were studied by X-ray diffraction (XRD) equipment (BRUKER AXS D5005, SCSIE Universitat de València). Scanning was performed on square film surfaces (15mm x 15mm) mounted in an appropriate sample holder. The patterns for profile fitting were obtained from a diffractometer using Cu $K_\alpha$ radiation with a scanning step of 0.02º between 2.5º and 40º in 2θ with a collection time of 10s per step and the voltage was held at 40kV.

## 2.7. Wettability

The surface wettability of films was evaluated by measuring the water contact angle with an Easy-Drop Standard goniometer FM140 (KRÜSS GmbH, Hamburg, Germany) equipped with a camera and analysis software (Drop Shape Analysis SW21; DSA1). Samples for wettability measurements were prepared as disc films with an average thickness between 180 and 230 μm) by compression moulding process at 180ºC in a hot press (Mini C 3850, Caver, Inc., Wabash, IN, USA). The contact angle was calculated randomly adding five drops of distilled water (2 μL) with a syringe onto the film surfaces at room temperature and the average values of ten measurements for each drop were used.

## 2.8. Release studies

Release studies of the antioxidant flavonoid catechin were conducted by the determination of the specific migration into a solution of 50% ethanol as fatty food simulant (Simulant D1) at 40ºC [22].

Release tests were performed by total immersion of pre-weighed rectangular strips film pieces (80 mm x 0.40 mm x 0.12 mm) in 10 ml of food simulant contained in glass-stoppered tubes with PTFE closures at 40 ºC. For fatty food that will be stored at ambient conditions (at temperatures between 20 and 40ºC) for not as much of 30 days, legislation orders that food packaging materials should be assayed at contact temperature in worst foreseeable use of 40ºC for 10 days. In this work, the migration test was conducted during 20 days. Thus, samples were taken at 1, 5, 10 and 20 days. Working standard catechin solution in the food simulant and pure simulant were run simultaneously with the migration test to check for interferences and all samples were performed in triplicate.

## 2.9. Measurement of released antioxidant

The released chatechin was measured after the contact period, an aliquot of each simulant was filtered through an Acrodisc PTFE CR 13mm, 0.2µm filter (Waters, Milford, MA, USA) and quantified by HPLC-PDA-FL. Waters 2695 (Waters, Mildford, MA, USA) HPLC system with a gradient pump and an automatic injector was used for HPLC analysis equipped with a stainless steel column packed with SunFireTM C18 (150 mm x 3.0 mm, 3.5 µm) (Waters) kept at 35 ºC following the methodology described by Castro López and colleagues [15]. The method consisted of a two solvent gradient elution at a flow rate of 0.5 ml min-1. Mobile phase was composed by water (A) and methanol (B).The following gradient elution profile was used: mobile phase composition started at 25% B and maintained for 0.5 min. Then, it was linearly increased to 40% B in 4.5 min, 60% B in 1 min and 100% B in 2 min. Finally, it was maintained for 3 min and brought back to recover the initial chromatographic conditions. Detection was performed on a fluorescence detector (FL, model 2475, Waters) with an excitation wavelength of 280 nm and an emission wavelength of 310 nm, and on a photodiode array detector (PDA, model 996 UV) set in the range of 200 to 400 nm while 277 nm output signal was selected as a quantification wavelength [20]. Output signals were monitored and processed with a personal computer operated under the EmpowerTM software (Waters). Catechin and epicatechin were identified by means of retention time and UV or FL spectrum comparison

with corresponding peaks in the standard solution and injection volume of 3µl. Release data was expressed as the percentage of catechin released into the food simulant after the contact period: amount of catechin released per kilogram of film with reference to the initial amount of catechin loaded per kilogram of film formulation.

The stability of catechin was also evaluated in the simulant under selected exposure conditions, by storing a solution of the additive in the simulant in parallel with the migration tests and quantified using the same procedure as for the samples [16].

The release process is normally described by the kinetics of the diffusion of the antioxidant in the film and is expressed by the diffusion coefficient (D). D is usually estimated using the Fickian diffusion law [15, 16]. When the release of antioxidant reached equilibrium, a rigorous model for describing the migration controlled by Fickian diffusion in a packaging film is used as explain Equation III.8. 2:

$$\frac{M_t}{M_{F,\infty}} = 1 - \sum_{n=0}^{\infty} \frac{8}{(2n+1)^2\pi^2} \, exp\left[\frac{-D\,(2n+1)^2\pi^2 t}{Lp^2}\right] \qquad \textbf{Equation III.8. 2}$$

where $M_t$ is the mass of the migrant in the food simulant at a particular time t (s), MF,∞ is the mass of the migrant in the food at equilibrium, LP is the film thickness (cm), D is the diffusion coefficient ($cm^2\ s^{-1}$), and t (s) is time.

Nevertheless, when release is slow and equilibrium is not reached at the end of the experiment, with the boundary condition of $M_t / M_P < 0.6$, the Equation III.8. 3 can be used:

$$\frac{M_t}{M_p} = \frac{4}{L_p}\left(\frac{Dt}{\pi}\right)^{1/2} \qquad \textbf{Equation III.8. 3}$$

$M_P$ is the initial loading of antioxidants in the film. *D* is estimated from the slope of the plot of $M_t$ / $M_P$ versus $t^{1/2}$ and the intersection with the x axis represents the time-lag.

## 2.10. Antioxidant activity

Antioxidant effectiveness of development materials was measured according DPPH-method by determining the absorbance of release medium at different times by means UV-Vis spectrophotometer at 517 nm. The antioxidant activity was obtained according to Equation III.8.4:

$$I\ (\%) = \left(\frac{Abs_{control} - Abs_{sample}}{Abs_{control}}\right) \times 100\% \qquad \textbf{Equation III.8. 4}$$

where $I$ (%) is the percentage of inhibition values. The results were calculated in % of inhibition as mean of three replicates and they were expressed as the equivalent gallic acid concentration (ppm) by using a calibrated curve of gallic acid concentration versus I (%).

## 2.11. Nanomechanical analysis

The mechanical hardness ($H$) and elastic modulus ($E$) properties of films before migration studies and after 10 days in contact with food simulant D1 were determined by a nanoindenter machine G-200 (Agilent Technologies, Santa Clara, CA, USA). All samples were indented in the same experiment. Indentations were performed at maximum 2000 nm constant depth using a Berkovich diamond tip. An array of 16 indentations was performed for each sample. The area function that is used to estimate the contact area at low depths was previously calibrated in fused silica. The stiffness required to calculate the contact area beyond indenter and elastic modulus was obtained by means of the Continuous Stiffness Measurement (CSM) technique [23]. CSM technique provides in-depth profiles of the stiffness response and subsequently, profiles of $H$ and $E$ in-depth.

## 2.12. Statistical analysis

Experimental data were statistically analyzed with OriginPro 8 software. One-way analysis of variance (ANOVA) was carried out and significant differences among formulations were recorded at 95% confidence level according to Tukey's post hoc test.

## 3. Results

### 3.1. Morphological characterization

Figure III.8.1 shows FESEM images of cryo-fractured surfaces of un-plasticized (left side) and plasticized films (right side). While un-plasticized films showed a smooth fracture, plasticized samples showed a clear plastic behaviour with no apparent phase separation. These results show that ATBC is well incorporated into the PLA and PLA-PHB matrix in agreement with previous observations [10]. The characteristic plastic behaviour was more evident in PLA-ATBC (Figure III.8.1-b) and PLA-ATBC-CAT (Figure III.8.1-d) than in plasticized PLA-PHB counterparts (Figure III.8.1-f and Figure III.8.1-h). The PLA and PLA-PHB films incorporated with CAT appear to be more porous without a plain smoothness (Figure III.8.1-c and Figure III.8.1-g).

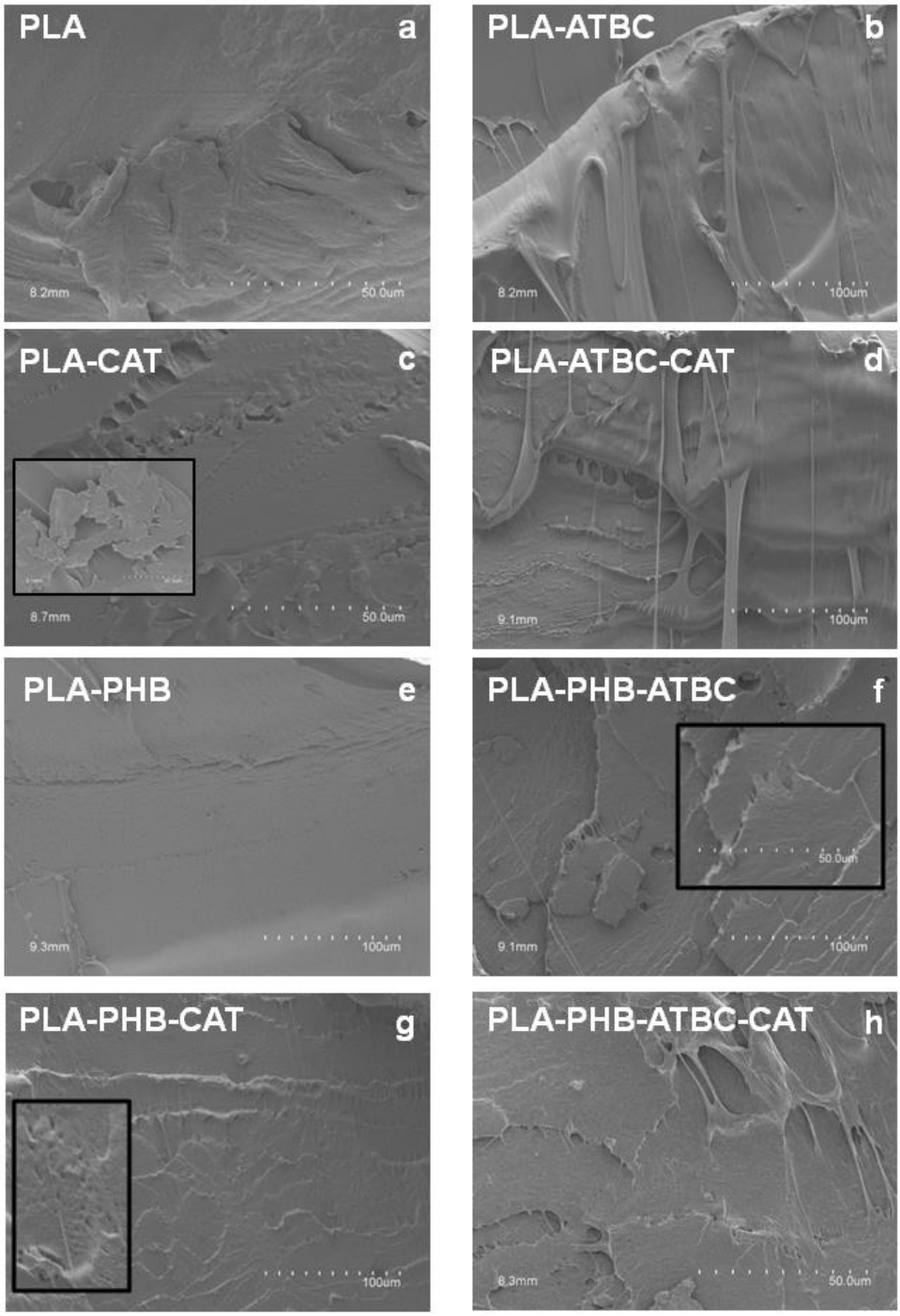


**Figure III.8.1.** Microstructure of fracture surface of un-plasticized (left side) and plasticized films (right side).

### 3.2. Thermogravimetric analysis (TGA)

The thermal decomposition was studied by TGA and DTG (Figure III.8.2). Stabilized with catechin and un-stabilized PLA and plasticized-PLA materials decomposed in one step process (Figure III.8.2-a) while PLA-PHB blends counterparts decomposition took

place in two well separated steps. In the first degradation process the total weight loss is close to 25% and corresponds to the degradation of PHB and the second stage is related with the degradation of PLA. Figure III.8.2-b shows that PHB decreases the thermal stability of the final formulation in accordance with previous results [9, 10].

Table III.8.2 also summarizes the main thermal parameters obtained by TGA and DTG. While ATBC shifted the $T_0$ to lower degradation temperatures, catechin led to an increment in $T_0$ delaying the beginning of the thermal decomposition process in all cases indicative of effective stabilizing effect. As well, catechin presence leads to a displacement of the $T_{max}$ of PLA towards slightly higher values in PLA and plasticized PLA samples (PLA-CAT and PLA-ATBC-CAT). However, in PLA-PHB blends as the same time as the $T_{max}$ corresponding to the degradation of PHB showed a considerable increment of about 10ºC with catechin addition, the $T_{max}$ of PLA was shifted to lower values and this behaviour was particularly noticeable in PLA-PHB-ATBC-CAT where the reduction was about 14ºC. Antioxidant capacity of catechin protects the polymer degradation at the first stage leading the $T_{max}$ of the blends to higher values while it could keep heat and then accelerate the degradation at higher temperatures.

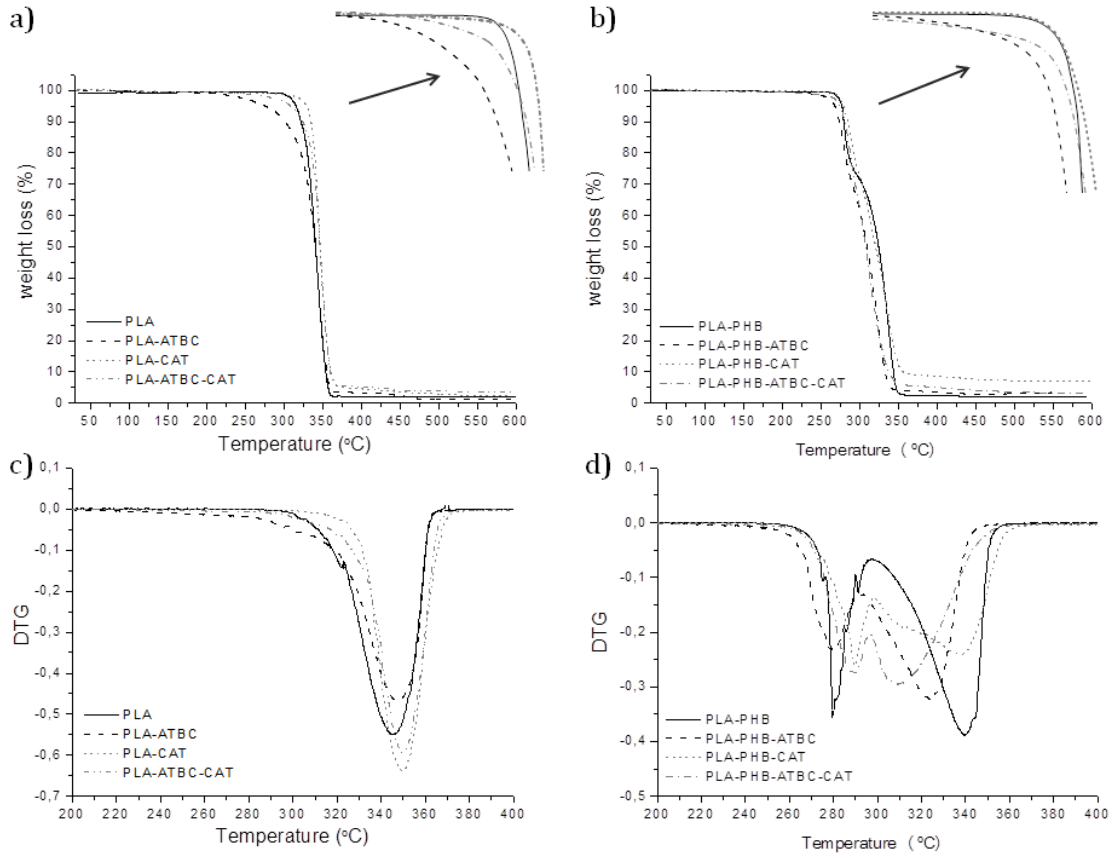


**Figure III.8.2**. TGA and DTG of PLA (a and c) and PLA-PHB (b and d) based films

### 3.3. Differential Scanning Calorimetry

The oxidation onset temperature (OOT) was used to evaluate the effectiveness of catechin to increase the polymer stability under oxidative atmosphere and results are summarized in Table III.8.2. OOT values clearly increased with the addition of catechin in all cases showing its effectiveness to protect PLA, PLA-PHB, plasticized PLA and plasticized PLA-PHB against oxidation, as it was already commented in TGA results. However, PLA and PLA-ATBC stabilized with catechin showed higher values of OOT than PLA-PHB counterparts. It must be noticed that while ATBC decreases the thermal stability of PLA it slightly increases the thermal stability of PLA-PHB blend due to the fact that ATBC improves the interaction between both polymers [10]. Consequently, catechin could be considered as a natural stabilizer for PLA, PLA-PHB and its plasticized systems.

**Table III.8.2**. TGA and DSC thermal parameters of PLA and PLA-PHB samples

| | $T_0$ (ºC) | $T_{max}$ PHB (ºC) | $T_{max}$ PLA (ºC) | OOT (ºC) | $T_g$ (ºC) | $T_{cc}$ (ºC) | $T_m$ (ºC) | $\Delta H_{cc}$ (J/g) | $\Delta H_m$ (J/g) | $\chi_c$ (%) |
|---|---|---|---|---|---|---|---|---|---|---|
| PLA | 315.7 | | 345.5 | 265.7 | 63.8 | 118.1 | 153.4 | 24.5 | 27.9 | 3.6 |
| PLA-ATBC | 276.0 | | 346.5 | 232.0 | 45.81 | 95.9 | 153.8 | 22.3 | 25.0 | 3.5 |
| PLA-CAT | 329.3 | | 349.6 | 320.2 | 64.7 | 129.6 | 154.1 | 12.6 | 15.3 | 3.1 |
| PLA-ATBC-CAT | 308.8 | | 350.1 | 299.3 | 54.4 | 115.8 | 145.0 | 24.5 | 27.1 | 3.4 |
| PLA-PHB | 275.0 | 279.3 | 339.7 | 267.7 | 63.2 | 130.0 | 158.6 | 8.5 | 11.9 | 4.8 |
| PLA-PHB-ATBC | 268.4 | 279.4 | 323.8 | 271.8 | 60.6 | 106.3 | 157.0 | 19.0 | 22.4 | 5.7 |
| PLA-PHB-CAT | 279.3 | 289.5 | 337.8 | 280.0 | 62.1 | 150.0 | 155.4 | 0.1 | 7.2 | 4.9 |
| PLA-PHB-ATBC-CAT | 275.1 | 289.5 | 309.6 | 281.2 | 57.7 | 126.0 | 152.5 | 5.3 | 8.1 | 5.1 |

Figure III.8.3-a and Figure III.8.3-b shows the thermograms for the DSC second heating where it is possible to observe the glass transition temperature (Tg), the cold crystallization exotherm ($T_{cc}$) and the melting endotherm ($T_m$) of the PLA (Figure III.8.3-a) and PLA-PHB (Figure III.8.3-b) based films. DSC thermal properties are also summarized in Table III.8.2. Polymer matrix, plasticizer and antioxidant seem to be compatible in view of the fact only one $T_g$ was observed for all formulations. ATBC induced the depression in $T_g$ of all samples confirming its plasticizing effect. Moreover, the lowest $T_g$ values was presented by PLA-ATBC followed by PLA-ATBC-CAT due to their higher plastic behaviour, in good accordance with FESEM micrographs. ATBC also shifted the Tcc to lower values, whereas catechin shifted the $T_{cc}$ to higher temperatures probably as a result of increased crystals nuclei density which requires more thermal energy to crystallise PLA. Catechin presence also promoted faster crystallization of PLA and PLA-PHB and the plasticized systems, most likely due to hydrogen bonding interactions between catechin hydroxyl groups and carbonyl groups of PLA and PHB. Similar findings were previously reported by López de Dicastillo et al (2013) who found an induction effect of catechin on the crystal nucleation of maleic anhydride modified poly(propylene) (MAPP) and also the formation of intermolecular hydrogen bonds between catechin and poly(propylene) (PP).

PHB slightly increased $T_m$ temperature respect to the neat PLA [9]. Neat PLA showed the $T_m$ corresponding to the melt of stable α homocrystals developed during the heating process. Meanwhile, plasticized PLA systems (PLA-ATBC and PLA-ATBC-CAT) showed a multimelting behaviour ascribed to the presence of different PLA crystals. Disordered α' crystals are formed when the $T_{cc}$ is below 110 ºC [24]. The crystallization rate of PLA is very high at temperatures between 100-118 ºC [25] where disorder-to-order phase transition (α' to α) takes place [24]. Similar findings were observed in PLA plasticized with oligomeric lactic acid (OLA) [26]. On the other hand, the presence of multimelting temperatures in PLA-PHB blends, after the PLA melting peak, at around 175ºC and 185ºC corresponds to the as-formed PHB crystals during blending process and re-crystallized PHB crystals formed during DSC heating, respectively [5, 7]. Different behaviour was observed in plasticized PLA-PHB blends (PLA-PHB-ATBC and PLA-PHB-ATBC-CAT). PLA-PHB-ATBC showed the $T_{cc}$ below 110ºC and as a consequence the multimelting PLA peak as well as the as-formed and recrystallized PHB crystals. Whereas, the multimelting behaviour was not detected for PLA-PHB-ATBC-CAT. The CAT presence considerably shifted the $T_{cc}$, from 106.3 ºC in PLA-PHB-ATBC to 126.0 ºC in PLA-PHB-ATBC-CAT, avoiding the formation of disordered PLA α' crystals. The nonappearance of as-formed and recrystallized PHB crystals could be related with an improvement in the interfacial adhesion between PLA, PHB and ATBC due to CAT presence.

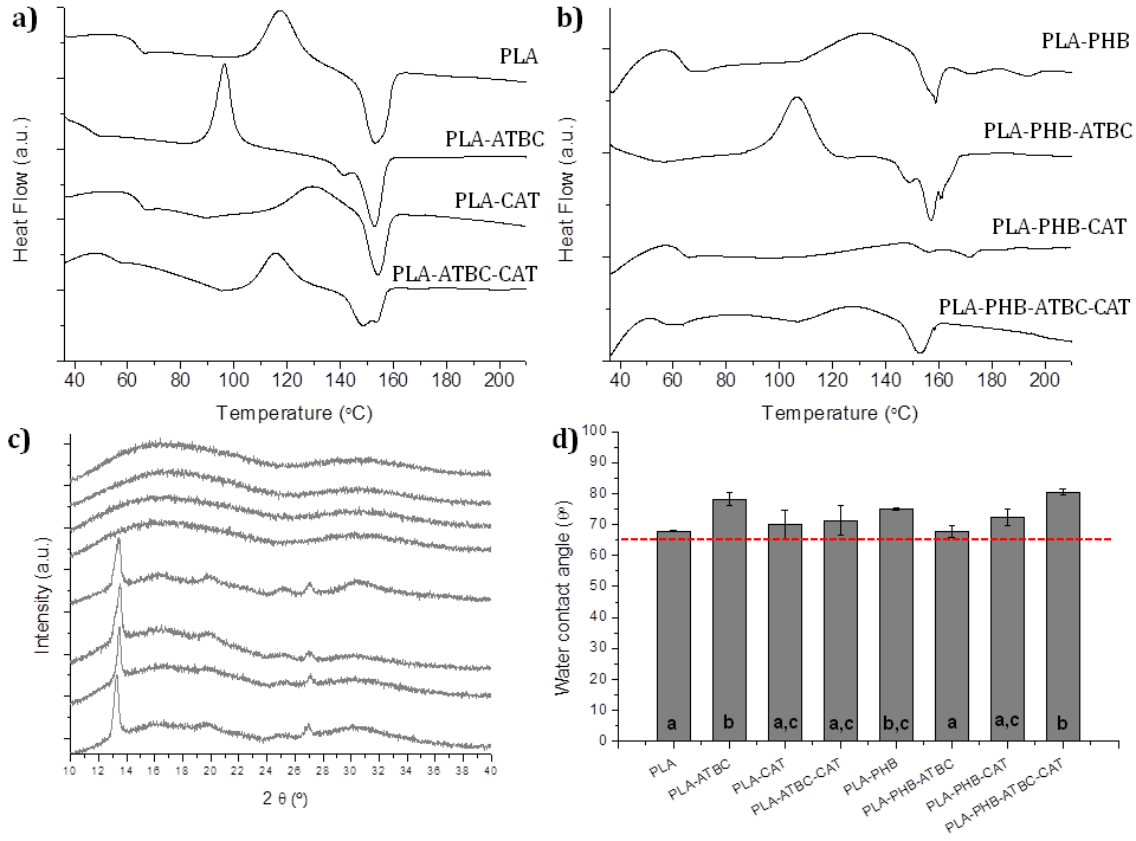


**Figure III.8.3.** DSC second heating scan of a) PLA based films and b) PLA-PHB based films.

**c)** X-ray diffraction patterns of PLA and PLA–PHB based films.

**d)** Contact angle measurements of PLA and PLA–PHB based films.

[a-d] Different letters on the bars indicate significant differences between formulations ($p < 0.05$).

Figure III.8.3-c shows a comparative plot of the crystalline profiles of films. PLA had one broad diffraction peak centered at 2θ = 15º and a smaller one centered at 2θ = 31º. The X-ray patterns of PLA-ATBC, PLA-CAT and PLA-ATBC-CAT are very similar to that of neat PLA. The presence of crystalline PHB showed an increase in the crystallinity of PLA in PLA-PHB blend, where the characteristic reflection peaks of PHB at 2θ =13.5º and 2θ = 16.9º, as well as the weak peaks at higher 2θ, are observed owing to the crystal growth rate of PHB is higher and faster than those of PLA [27].

The surface hydrophobicity is an important issue in materials intended for food packaging applications since they are required to protect foodstuff from humidity during transport, handling and storage. Thus, water contact angle measurements were conducted to study the water absorption of these material surfaces (Figure III.8.3-d). The line at 65 θº represents the limit value between hydrophilic surface (θº < 65º) and hydrophobic

surface (θº > 65º). All studied formulations showed values higher than 65º showing a poor affinity of the water to the material surfaces highlighting their potential use for packaging applications. The addition of 15 wt % ATBC and 25 wt % of PHB significantly increased the water resistance of PLA ($p < 0.05$). Meanwhile, the wettability of PLA and PLA-PHB remained practically unchanged ($p > 0.05$) with the addition of 5 wt % of catechin in PLA-CAT and PLA-PHB-CAT. PLA-PHB-ATBC-CAT film resulted in material with a surface increased ($p < 0.05$) hydrophobicity with respect to those of PLA-PHB-ATBC and PLA-PHB-CAT. One possible explanation for this behaviour could be that a strong interaction of catechin hydroxyl groups with PLA and PHB chains, which interaction is also improved by the ATBC presence, did not show surface orientation affecting the surface chemical properties leading to an increase on the surface hydrophobicity.

### 3.4. Catechin release

The migration of the catechin from PLA and PLA-PHB based developed materials expressed as the percentage of catechin and epicatechin released into the food simulant D1 per day and their diffusion kinetics obtained by HPLC-PDA are shown in Figure III.8.4-a and Figure III.8.4-b, respectively.

The incorporation of ATBC showed a significant increase of the release capacity from PLA and PLA-PHB matrices. After 10 contact days catechin released levels increased about 3 times in both PLA and PLA-PHB with respect to the corresponding films without plasticizer. Castro-Lopez et al (2013) also showed an improvement on the release of antioxidants from polypropylene matrix due to the use of plasticizers in the formulations with increased diffusion coefficients between 1 and 2 orders of magnitude [15].

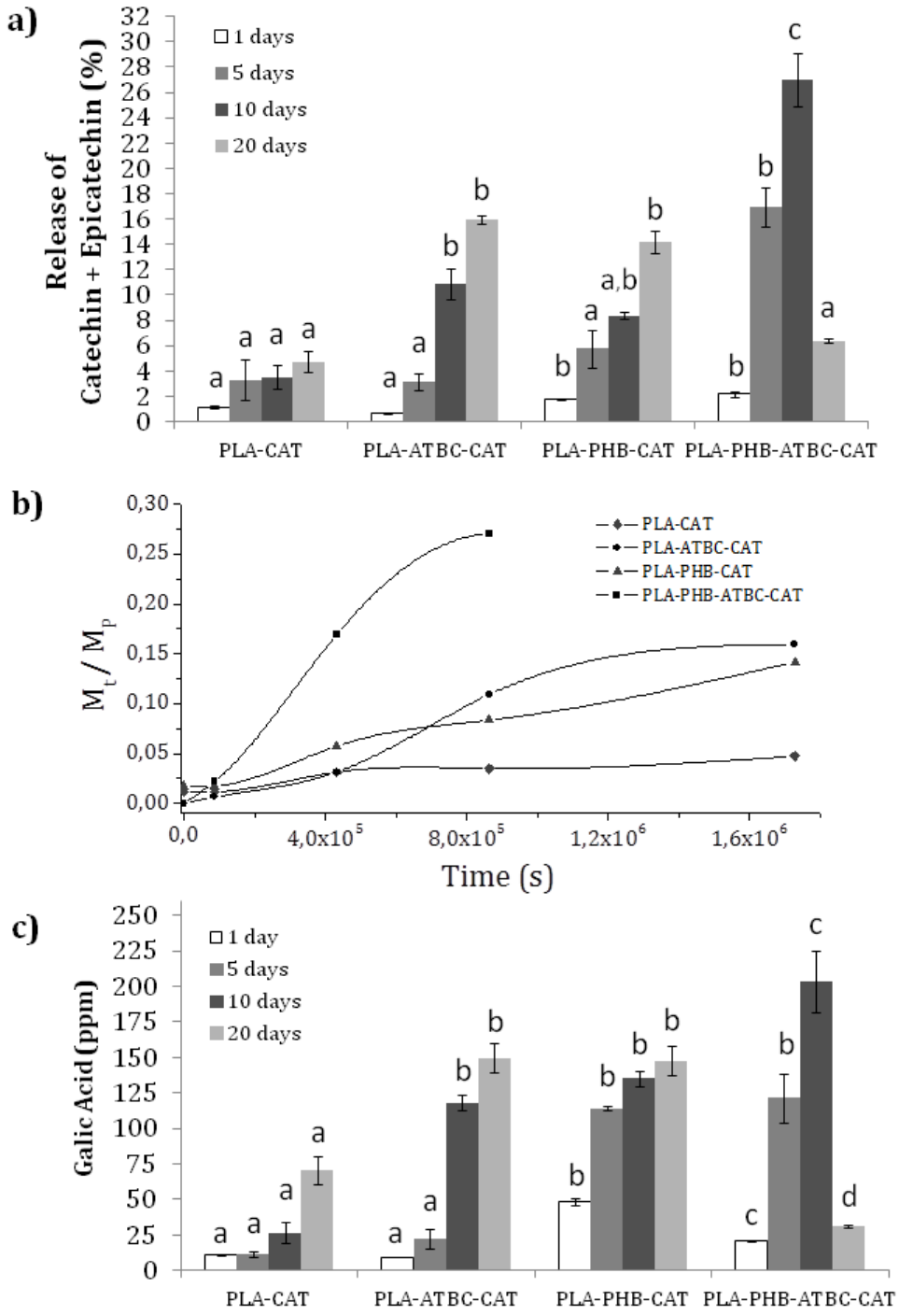


**Figure III.8.4**. a) catechin (%) released from PLA and PLA-PHB based materials calculated by means HPLC-PDA.

**b)** Diffusion kinetics of catechin from PLA and PLA-PHB based materials.

**c)** Antioxidant activity of catechin expressed as Galic Acid concentration (ppm) measured by DPPH radical scavengers.

[a-d]Different letters on the bars within the same day indicate significant differences between formulations ($p < 0.05$).

Diffusion coefficients were estimated from Figure III.8.4-b and from the slope of the curve obtained by Equation and they also showed the positive effect of the plasticizer presence on the release of catechin from PLA and PLA-PHB based materials. Increased values from 1.9 x $10^{-12}$ $cm^2$ $s^{-1}$ in PLA-CAT to 8.3 x $10^{-11}$ $cm^2$ $s^{-1}$ in PLA-CAT-ATBC and from 2.6 x $10^{-11}$ $cm^2$ $s^{-1}$ in PLA-PHB-CAT to 3.5 x $10^{-10}$ $cm^2$ $s^{-1}$ in PLA-PHB-CAT-ATBC were observed, due to the ability of plasticizer to increase the polymer chain mobility and thus the release of catechin.

It is expected that the higher amount of crystalline regions of PLA-PHB blends slowed the diffusion of catechin. However, the addition of PHB showed somewhat increment in the release of active compound in comparison with those formulations without PHB, particularly noticeable in PLA-PHB-ATBC-CAT film (Figure III.8.4-a). The incorporation of PHB only produced an induction period in the diffusion process, leading to an increase in time-lag from 30 s in PLA-CAT to 209 s and to 252 s in PLA-PHB-CAT and PLA-PHB-ATBC-CAT respectively, because of the limited polymer chain mobility in PLA-PHB based blends. However, once the diffusion process started, the migration of catechin got faster in PHB added samples as shown the increment in one order of magnitude of the diffusion coefficient with respect of PLA based materials counterparts. This behaviour could be ascribed to the higher affinity of the simulant D1 with less polar catechin added PLA-PHB blends in comparison with catechin added PLA equivalents, as it was already commented in wettability test. Thus, the higher penetration capacity of Simulant D1 in the PLA-PHB matrix than in PLA matrix, after the required time-lag, speeded up the catechin migration process as a function of time. Additionally, after the 10 contact days an enhance of crystallinity of all tested materials was observed by X-ray diffraction as it can be seen in Figure III.8.5. The diffraction patterns clearly show an increased intensity of the peak at 2θ = 16.5 º for all formulations, attributed to the typical α crystals form of the crystalline phase of PLA [26], showing the highest intensity in plasticized samples. Thus, the higher penetration capacity of Simulant D1 in PLA-PHB blends at the same time as the increase of crystallinity of amorphous PLA based materials led to comparable catechin migration profiles for PLA-ATBC-CAT and PLA-PHB-CAT at 5, 10 and 20 contact days in Simulant D1.

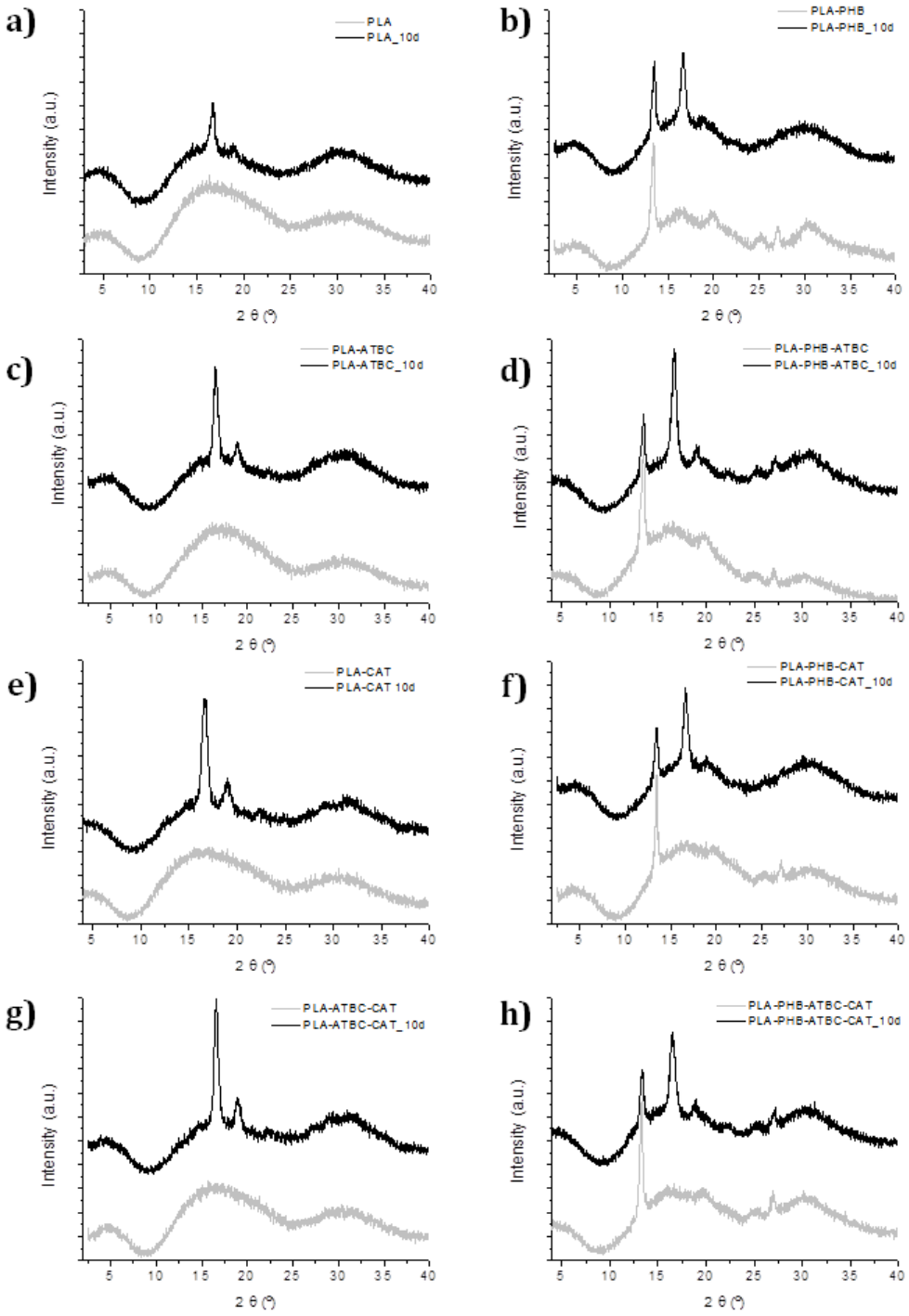


**Figure III.8.5.** X-ray diffraction patterns of PLA and PLA–PHB based films before and after 10 days in contact with Simulant D1.

The highest diffusion process was observed for PLA-PHB-ATBC-CAT samples between 0 and 10 days. However, at the highest period of contact time studied here, of 20 days, a reduction of catechin concentration occurred showing the not possible lower value than those obtained at 5 and 10 days. This unexpected result could be explained to the feasible interaction between the free catechin molecules in the food simulant, possibly

forming dimmers or oligomers, which cannot be quantified by the experimental methodology used here. In fact, in a food simulant the released compound is dispersed into the food simulant where no oxidation processes are happening as can occur in a real packed food environment. The molecules of catechin migrated from the packaging are expected to interact with food components jamming in oxidations processes.

It should be taken into account that the inherent biodegradability of PLA based materials could be a drawback in food packaging, where the material structure needs to be guaranteed at least during the food shelf life [31]. For this reason, the morphology of cross section of the films after 10 and 20 days exposed to simulant D1 was also studied by FESEM (Figure III.8.6). PLA and PLA-PHB based materials preserved their structure at 10 days of the migration test. Meanwhile, PLA, PLA-ATBC (Figure III.8.6-a) and PLA-PHB and PLA-PHB-ATBC (Figure III.8.6-b) showed increased plastic behaviour at 20 days caused by the plasticization effect produced by the simulant dispersion into the polymer matrix. In most cases, the materials become rougher with increasing migration time. As well, at 20 days some cavities were formed in PLA catechin incorporated samples (Figure III.8.6-a), whereas many cavities were observed in PLA-PHB catechin incorporated samples (Figure III.8.6-b) as a result of the higher loss of catechin in this sample. This observation supported our conclusion that higher levels of catechin than those obtained here should be released from PLA-PHB-ATBC-CAT sample after 20 days in contact with food simulant.

It should be noticed that all catechin incorporated materials showed an effective release of catechin in worst foreseeable use conditions between 0 and 10 days as indicates the current legislation for fatty food intended to be transported, handed and stored at ambient conditions.

### 3.5. Antioxidant activity

The effectiveness of the developed materials as antioxidant packaging systems was demonstrated by the reduction of stable free radical DPPH caused by catechin presence in food simulant and the obtained results are expressed as acid galic (AG) concentration (Figure III.8.4-c). As expected, the antioxidant activity shows comparative tendency to the catechin release. It is known that the solubility characteristics of the antioxidant can determine its effectiveness [28]. Catechin shows highly solubility in ethanol (50 g L-1) [17] and consequently catechin incorporated materials usually show high activity in ethanol containing simulants [15, 17, 21, 29, 30]. Thus, the high affinity of catechin for fatty food simulants and its high antioxidant activity give good reasons for its addition in plasticized PLA and PLA-PHB materials for fatty foodstuff.

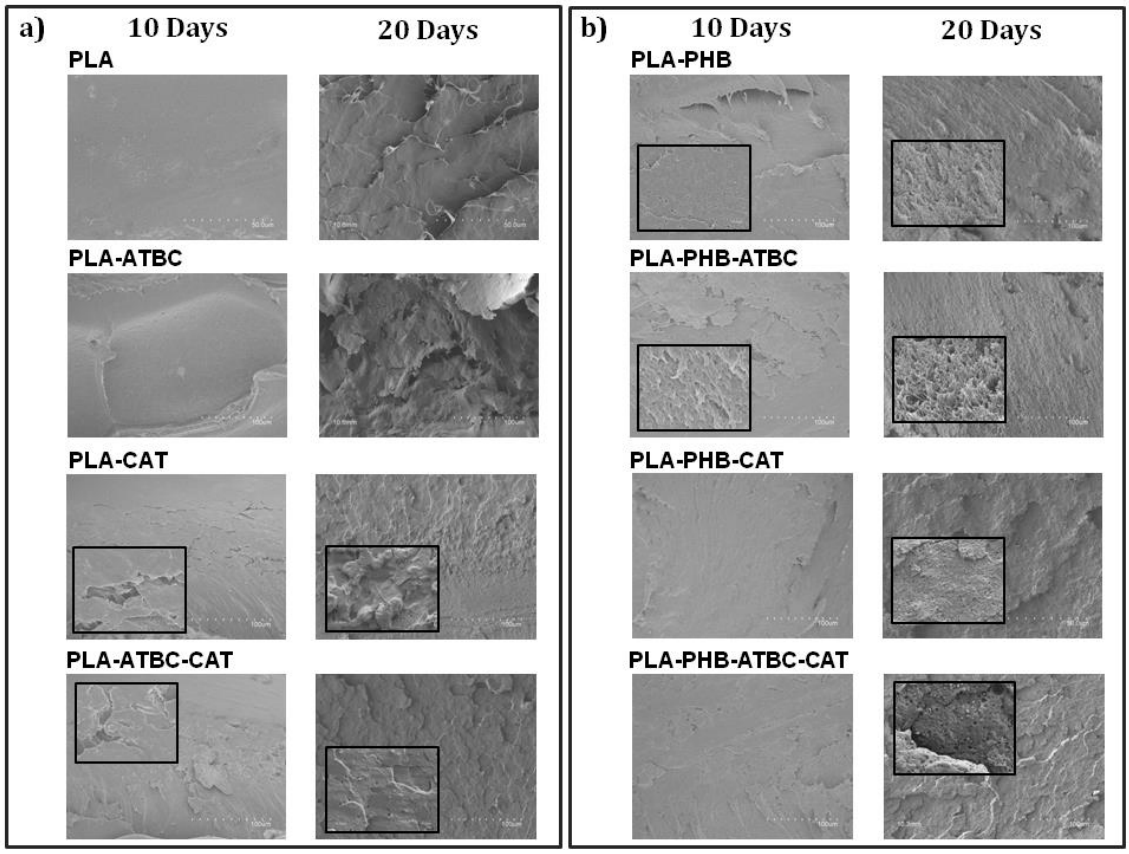


**Figure III.8.6**. FESEM images of a) PLA based materials and b) PLA-PHB based materials after 10 and 20 days exposed to simulant D1.

### 3.6. Mechanical features of the films

The mechanical behaviour of all samples was assayed before and after 10 days in contact with food simulant D1 by means of nanoindentetion test. The mean of elastic modulus (*E*) and hardness (*H*) values for each sample was calculated in the range from 500 nm to 1000 nm and the obtained values are showed in Figure III.8.7. As expected, plasticized samples before release studies showed lower *H* and *E* values than unplasticized ones showing the effectiveness of ATBC to plasticize PLA and PLA-PHB systems, in accordance with previous results [10, 11]. On the other hand, catechin added samples showed increased *H* and *E* values with respect to their counterparts without catechin. This result confirms that catechin produced somewhat reinforcing effect blocking the elastic and plastic deformation mechanisms owing to the enhancement of the materials interfacial adhesion, in accordance with DSC experiments.

The nanomechanical results of assayed samples after release studies showed scattered values, probably due to residues of Simulant D1 and/ or released components from the polymer matrices on their surfaces. This activated surface is able to affect the

short distance forces between the surface and nanoindenter tip. After 10 days in contact with simulant D1, catechin added materials revealed in general a drastically diminution of *E* and *H* values as a result of the release of catechin to the food simulant, with the exception of PLA-PHB-ATBC-CAT who mainly maintained the mechanical properties without significant changes. This result highlights an additional positive effect of catechin incorporation to plasticized PLA-PHB systems.

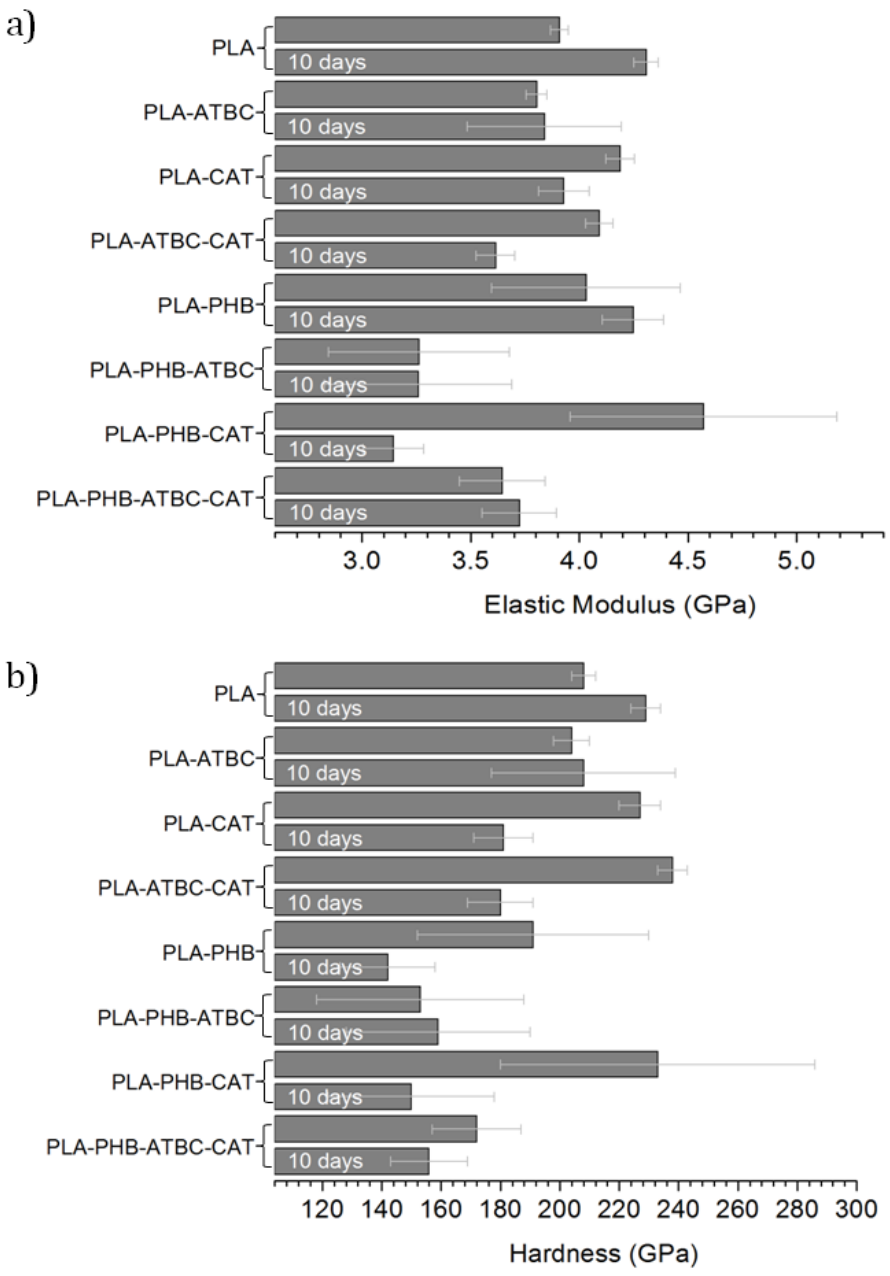


**Figure III.8.7.** Nanomechanical results of materials essayed before and after 10 days in contact with simulant D1. **(a)** Elastic modulus (*E*) and **(b)** Nanohardness (*H*).

## 4. Conclusions

Antioxidant active films based on plasticized PLA and PLA-PHB added with catechin were successfully prepared by melt blend process and fully characterized. Materials showed hydrophobic nature, homogeneity and good miscibility showing only one Tg.

Catechin presence delayed the initial degradation temperature improving the thermal stability of all materials and making broader the usually small processing window of PHB. Additionally, a reinforcing effect due to the positive interaction of catechin with the plasticized PLA and PLA-PHB matrices was observed by the shift of cold crystallization temperature to higher temperatures as well as the increment in elastic modulus values.

The addition of plasticizer increased the ductility of materials required for film manufacture and favoured the controlled release of catechin from polymer matrices. As well, the antioxidant activity was observed to be proportional to the antioxidant concentration in the food simulant.

Among all the tested materials, PLA-PHB-ATBC-CAT showed the best characteristics for its potential industrial use for fatty food preservation since this formulation showed the best kinetics behaviour and the greatest amount of catechin migration at 10 days in contact with fatty food simulant. As a consequence, PLA-PHB-ATBC-CAT also showed the uppermost antioxidant activity at the same time as the structural and mechanical properties were preserved without significant changes.

## Acknowledgments

This work has been supported by the Spanish Ministry of Economy and Competitiveness (MAT2011-28648-C02-01 and MAT2011-28468-C02-02) M.P. Arrieta thanks Generalitat Valenciana for Santiago Grisolía Fellowship (GRISOLIA/2011/007). Authors gratefully acknowledge Prof. Mª Dolores Salvador (Polytechnic University of Valencia) for her assistance with nanomechanical analysis.

## References

[1] Arrieta MP, López J, Ferrándiz S, Peltzer MA. Characterization of PLA-limonene blends for food packaging applications. Polymer Testing. 2013;32(4):760-768.

[2] Auras R, Harte B, Selke S. An overview of polylactides as packaging materials. Macromolecular Bioscience. 2004;4(9):835-864.

[3] Hwang SW, Shim JK, Selke S, Soto-Valdez H, Matuana L, Rubino M, et al. Migration of α-tocopherol and resveratrol from poly(L-lactic acid)/starch blends films into ethanol. Journal of Food Engineering. 2013;116(4):814-828.

[4] Fortunati E, Armentano I, Iannoni A, Barbale M, Zaccheo S, Scavone M, et al. New multifunctional poly(lactide acid) composites: Mechanical, antibacterial, and degradation properties. Journal of Applied Polymer Science. 2012;124(1):87-98.

[5] Arrieta MP, Fortunati E, Dominici F, Rayón E, López J, Kenny JM. Multifunctional PLA–PHB/cellulose nanocrystal films: Processing, structural and thermal properties. Carbohydrate Polymers. 2014;107(0):16-24.

[6] Jamshidian M, Arab Tehrany E, Cleymand F, Leconte S, Falher T, Desobry S. Effects of synthetic phenolic antioxidants on physical, structural, mechanical and barrier properties of poly lactic acid film. Carbohydrate Polymers. 2012;87(2):1763-1773.

[7] Zhang M, Thomas NL. Blending polylactic acid with polyhydroxybutyrate: The effect on thermal, mechanical, and biodegradation properties. Advances in Polymer Technology. 2011;30(2):67-79.

[8] Ni C, Luo R, Xu K, Chen GQ. Thermal and crystallinity property studies of poly (L-lactic acid) Blended with oligomers of 3-hydroxybutyrate or dendrimers of hydroxyalkanoic acids. Journal of Applied Polymer Science. 2009;111(4):1720-1727.

[9] Arrieta MP, López J, Hernández A, Rayón E. Ternary PLA–PHB–Limonene blends intended for biodegradable food packaging applications. European Polymer Journal. 2014;50(0):255-270.

[10] Arrieta MP, Samper MD, López J, Jiménez A. Combined Effect of Poly(hydroxybutyrate) and Plasticizers on Polylactic Acid Properties for Film Intended for Food Packaging. Journal of Polymers and the Environment. 2014.

[11] Arrieta MP, López J, Rayón E, Jiménez A. Disintegrability under composting conditions of plasticized PLA-PHB blends. Polymer Degradation and Stability. 2014(0).

[12] Martino VP, Jiménez A, Ruseckaite RA, Avérous L. Structure and properties of clay nano-biocomposites based on poly(lactic acid) plasticized with polyadipates. Polymers for Advanced Technologies. 2011;22(12):2206-2213.

[13] Courgneau C, Domenek S, Guinault A, Avérous L, Ducruet V. Analysis of the Structure-Properties Relationships of Different Multiphase Systems Based on Plasticized Poly(Lactic Acid). Journal of Polymers and the Environment. 2011;19(2):362-371.

[14] Arrieta MP, Peltzer MA, López J, Garrigós MDC, Valente AJM, Jiménez A. Functional properties of sodium and calcium caseinate antimicrobial active films containing carvacrol. Journal of Food Engineering. 2014;121(1):94-101.

[15] Castro López MDM, De Dicastillo CL, Vilariño JML, Rodríguez MVG. Improving the capacity of polypropylene to be used in antioxidant active films: Incorporation of plasticizer and natural antioxidants. Journal of Agricultural and Food Chemistry. 2013;61(35):8462-8470.

[16] Castro López MDM, Dopico García S, Ares Pernas A, López Vilariño JM, González Rodríguez MV. Effect of PPG-PEG-PPG on the tocopherol-controlled release from films intended for food-packaging applications. Journal of Agricultural and Food Chemistry. 2012;60(33):8163-8170.

[17] López De Dicastillo C, Castro-López MDM, Lasagabaster A, López-Vilariño JM, González-Rodríguez MV. Interaction and release of catechin from anhydride maleic-grafted polypropylene films. ACS Applied Materials and Interfaces. 2013;5(8):3281-3289.

[18] Peltzer M, Navarro R, López J, Jiménez A. Evaluation of the melt stabilization performance of hydroxytyrosol (3,4-dihydroxy-phenylethanol) in polypropylene. Polymer Degradation and Stability. 2010;95(9):1636-1641.

[19] Samper MD, Fages E, Fenollar O, Boronat T, Balart R. The potential of flavonoids as natural antioxidants and UV light stabilizers for polypropylene. Journal of Applied Polymer Science. 2013;129(4):1707-1716.

[20] Lopez de Dicastillo C, del Mar Castro-Lopez M, Manuel Lopez-Vilarino J, Victoria Gonzalez-Rodriguez M. Immobilization of green tea extract on polypropylene films to control the antioxidant activity in food packaging. Food Research International. 2013;53(1):522-528.

[21] Castro-López MDM, López-Vilariño JM, González-Rodríguez MV. Analytical determination of flavonoids aimed to analysis of natural samples and active packaging applications. Food Chemistry. 2014;150:119-127.

[22] Regulation E. No 1935/2004 of the European Parliament and of the Council of 27 October 2004 on materials and articles intended to come into contact with food. Off. J. Eur. Union, L. Legis. (Engl. Ed.) 2004, 338 (Nov. 13),. 2004/ 2011. p. 4-17.

[23] Rayón E, López J, Arrieta MP. Mechanical characterization of microlaminar structures extracted from cellulosic materials using nanoindentation technique. Cellulose Chemistry and Technology. 2013;47(5-6):345-351.

[24] Zhang J, Tashiro K, Tsuji H, Domb AJ. Disorder-to-order phase transition and multiple melting behavior of poly(L-lactide) investigated by simultaneous measurements of WAXD and DSC. Macromolecules. 2008;41(4):1352-1357.

[25] Jamshidian M, Tehrany EA, Imran M, Jacquot M, Desobry S. Poly-Lactic Acid: Production, applications, nanocomposites, and release studies. Comprehensive Reviews in Food Science and Food Safety. 2010;9(5):552-571.

[26] Burgos N, Martino VP, Jiménez A. Characterization and ageing study of poly(lactic acid) films plasticized with oligomeric lactic acid. Polymer Degradation and Stability. 2013;98(2):651-658.

[27] Abdelwahab MA, Flynn A, Chiou BS, Imam S, Orts W, Chiellini E. Thermal, mechanical and morphological characterization of plasticized PLA-PHB blends. Polymer Degradation and Stability. 2012;97(9):1822-1828.

[28] Gómez-Estaca J, López-de-Dicastillo C, Hernández-Muñoz P, Catalá R, Gavara R. Advances in antioxidant active food packaging. Trends in Food Science and Technology. 2014;35(1):42-51.

[29] López-De-Dicastillo C, Alonso JM, Catalá R, Gavara R, Hernández-Munoz P. Improving the antioxidant protection of packaged food by incorporating natural flavonoids into ethylene-vinyl alcohol copolymer (EVOH) films. Journal of Agricultural and Food Chemistry. 2010;58(20):10958-10964.

[30] López De Dicastillo C, Nerín C, Alfaro P, Catalá R, Gavara R, Hernández-Muñoz P. Development of new antioxidant active packaging films based on ethylene vinyl alcohol copolymer (EVOH) and green tea extract. Journal of Agricultural and Food Chemistry. 2011;59(14):7832-7840.

[31] Dopico-García MS, Ares-Pernas A, González-Rodríguez MV, López-Vilariño JM, Abad-López MJ. Commercial biodegradable material for food contact: Methodology for assessment of service life. Polymer International. 2012;61(11):1648-1654.

# IV. CONCLUSIONES

De a cuerdo con los objetivos planteados las principales conclusiones obtenidas de la presente tesis doctoral se resumen de la siguiente manera:

- Se desarrolló y validó un método analítico para la identificación y cuantificación de los principales productos de degradación térmica de PLA mediante pirólisis acoplada a cromatografía de gases y espectrometría de masas.

- La adición de D-Limoneno a la matriz de PLA aumentó la flexibilidad de los films sin afectar la transparencia ni las propiedades colorimétricas. Sin embargo, no mejoró la estabilidad térmica del PLA y se produjeron pérdidas de D-limoneno durante el proceso de producción de los films. Se redujo La humectabilidad mientras que las propiedades barrera al oxigeno se vieron afectadas negativamente por el efecto de plastificación.

- La incorporación de PHB incrementó la cristalinidad de PLA mejorando las propiedades de barrera al oxígeno y reduciendo la humectabilidad. Sin embargo, el PHB redujo la transparencia dándole una coloración ámbar al material.

- La adición de plastificantes a las mezclas de PLA-PHB mejoró la interacción entre los dos polímeros y generó un aumento de la ductilidad y transparencia de los films. La estabilidad térmica y las propiedades de barrera al oxígeno se vieron afectadas. La degradación en condiciones de compostaje fue favorecida por la presencia de plastificante. El plastificante ATBC resultó el más eficaz de los tres plastificantes estudiados, dado que produjo el mayor aumento de la ductilidad sin afectar demasiado las propiedades barreras.

- Se sintetizaron nanocristales de celulosa satisfactoriamente a partir de celulosa microcristalina. Los nanocristales obtenidos se modificaron superficialmente con un surfactante lo que permitió una mayor compatibilidad con las matrices poliméricas de PLA y PHB.

- La preparación de un masterbatch de PLA-PHB previo a la incorporación de los nanocristales optimizó la dispersión de los mismos en la matriz polimérica mejorando la estabilidad térmica de los materiales debido al efecto de nucleación. Este efecto fue más notorio en el caso de los nanocristales modificados superficialmente.

- La óptima dispersión de los nanocristales de celulosa modificados superficialmente y su efecto reforzante sobre la matriz polimérica de PLA-PHB generó un aumento de las propiedades barrera al oxígeno y del módulo elástico. La funcionalización de los nanocristales produjo una reducción de la transmisión de la luz UV, un efecto de plastificación aumentando la elongación a la rotura de los films favoreciendo también su degradación en condiciones de compostaje.

- La adición de (+)-catequina produjo un incremento de la estabilidad térmica y un efecto reforzante de la matriz de PLA-PHB, mostrando un aumento de la temperatura de cristalización y del módulo elástico. La adición de ATBC favoreció la liberación del antioxidante de la matriz polimérica hacia el simulante de alimentos grasos en el cual demostró una elevada capacidad antioxidante. Los films de PLA-PHB-ATBC-CAT conservaron sus propiedades estructurales y mecánicas durante la exposición al simulante alimentario (10 días a 40ºC).

Como conclusión global del presente trabajo, se puede indicar que la modificación de mezclas de PLA-PHB mediante la adición de plastificantes, nanocristales de celulosa y/o catequina demostraron su potencial como materiales destinados al envasado de alimentos. Siendo materiales provenientes de recursos naturales y biodegradables.

# VI. ANEXOS

Journal of Analytical and Applied Pyrolysis 101 (2013) 150–155

Contents lists available at SciVerse ScienceDirect

Journal of Analytical and Applied Pyrolysis

journal homepage: www.elsevier.com/locate/jaap

# Development of a novel pyrolysis-gas chromatography/mass spectrometry method for the analysis of poly(lactic acid) thermal degradation products

Marina Patricia Arrieta[a,b,*], Francisco Parres[a], Juan López[a], Alfonso Jiménez[b]

[a] Instituto de Tecnología de Materiales, Universitat Politècnica de València, Plaza Ferrándiz y Carbonell 1, 03801 Alcoy, Alicante, Spain
[b] Analytical Chemistry, Nutrition and Food Sciences Department, University of Alicante, P.O. Box 99, E-03080 Alicante, Spain

ARTICLE INFO

*Article history:*
Received 22 May 2012
Accepted 27 January 2013
Available online 4 February 2013

*Keywords:*
Poly(lactic acid)
Thermal degradation
Pyrolysis
Py-GC/MS
Logistic model
Boltzmann model

ABSTRACT

Thermal degradation of PLA is a complex process since it comprises many simultaneous reactions. The use of analytical techniques, such as differential scanning calorimetry (DSC) and thermogravimetry (TGA), yields useful information but a more sensitive analytical technique would be necessary to identify and quantify the PLA degradation products. In this work the thermal degradation of PLA at high temperatures was studied by using a pyrolyzer coupled to a gas chromatograph with mass spectrometry detection (Py-GC/MS). Pyrolysis conditions (temperature and time) were optimized in order to obtain an adequate chromatographic separation of the compounds formed during heating. The best resolution of chromatographic peaks was obtained by pyrolyzing the material from room temperature to 600 °C during 0.5 s. These conditions allowed identifying and quantifying the major compounds produced during the PLA thermal degradation in inert atmosphere. The strategy followed to select these operation parameters was by using sequential pyrolysis based on the adaptation of mathematical models. By application of this strategy it was demonstrated that PLA is degraded at high temperatures by following a non-linear behaviour. The application of logistic and Boltzmann models leads to good fittings to the experimental results, despite the Boltzmann model provided the best approach to calculate the time at which 50% of PLA was degraded. In conclusion, the Boltzmann method can be applied as a tool for simulating the PLA thermal degradation.



## 1. Introduction

Biopolymers are becoming more and more interesting for many industrial sectors, such as packaging, automotive and many others since they are obtained from renewable resources and they are intrinsically biodegradable. Several biopolymers have been investigated as alternatives to non-degradable commodities to produce materials with similar properties to those of the common polymers [1].

Among all commercial biopolymers, poly(lactic acid) (PLA) is one of the most attractive and mainly used in many applications, being biocompatible and biodegradable [2]. Currently, PLA is used in food packaging industry for short shelf life products [3,4]. Although the inherent biodegradable and compostable characteristics of PLA, the high growth on its production in the last years and application in the packaging market represents an upcoming new main source of polymer waste and new strategies for PLA waste management should be proposed [5]. Therefore, the fact that biodegradable polymers, and particularly PLA, should be considered as waste suggests that pyrolysis may offer an alternative option for waste treatment of biomass and biopolymers [6]. In this sense, PLA has a high potential energy content making it suitable for thermal processes with energy recovery. It has been reported that PLA waste is suitable to be used in pyrolysis facilities due to the high conversion efficiency of the polymer [7]. Therefore, pyrolysis of PLA may offer an alternative to this polymer waste management, while being economically and environmentally attractive [2]. The application of thermo-chemical operations to PLA must be carefully tackled, taking into account healthy and environmental issues and guaranteeing the right management of emitted gases [7]. Although some research work has been published on the PLA pyrolysis [8], only semi-quantitative results of the PLA degradation products were reported [8–10].

The study of polymers thermal degradation is especially important because it is relevant for their processing, characterization, potential applications and thermal recycling [9] as well as to guarantee their complete life cycle. The obtained products during thermal degradation depend on the selected conditions. Furthermore, degradation mechanisms of a particular polymer are dependent on its structure and they can follow different paths

* Corresponding author at: Instituto de Tecnología de Materiales, Universitat Politècnica de València, Plaza Ferrándiz y Carbonell 1, 03801 Alcoy, Alicante, Spain. Tel.: +34 966528433; fax: +34 966528433.
*E-mail addresses:* marrieta@itm.upv.es, marina.arrieta@ua.es (M.P. Arrieta).

0165-2370/$ – see front matter © 2013 Elsevier B.V. All rights reserved.
http://dx.doi.org/10.1016/j.jaap.2013.01.017

Polymer Testing 32 (2013) 760–768

Contents lists available at SciVerse ScienceDirect

Polymer Testing

journal homepage: www.elsevier.com/locate/polytest

Material properties

# Characterization of PLA-limonene blends for food packaging applications

Marina P. Arrieta [a,*], Juan López [a], Santiago Ferrándiz [a], Mercedes A. Peltzer [b]

[a] Instituto de Tecnología de Materiales, Universitat Politècnica de València, Plaza Fernandiz y Carbonell Nº 1, 03801 Alcoy, Alicante, Spain
[b] Analytical Chemistry, Nutrition and Food Sciences Department, University of Alicante, P.O. Box 99, E-03080 Alicante, Spain

ARTICLE INFO

*Article history:*
Received 14 February 2013
Accepted 22 March 2013

*Keywords:*
PLA
Limonene
Plasticizer
Packaging

ABSTRACT

Polymers derived from renewable resources are now considered as promising alternatives to traditional petro-polymers as they mitigate current environmental concerns (raw renewable materials/biodegradability). D-limonene can be found in a variety of citrus, indeed is the main component of citrus oils and one of most important contributors to citrus flavor. The incorporation of limonene in PLA matrix was evaluated and quantified by Pyrolysis Gas Chromatography Mass Spectrometry (Py-GC/MS). Transparent films were obtained after the addition of the natural compound. Mechanical properties were evaluated by tensile tests. The effect of limonene on mechanical properties of PLA films was characterized by an increase in the elongation at break and a decrease in the elastic modulus. The fracture surface structure of films was evaluated by scanning electron microscopy (SEM), and homogeneous surfaces were observed in all cases. Barrier properties were reduced due to the increase of the chain mobility produced by the D-limonene.



## 1. Introduction

Polymers derived from renewable resources are now considered as promising alternatives to traditional petro-polymers as they mitigate current environmental concerns (raw renewable materials/biodegradability). It is widely accepted that the use of long-lasting polymers for short-term and disposable applications, such as packaging, is not entirely satisfactory [1]. As a result, the biopolymer industry is growing rapidly since biodegradables polymers made from renewable resources have a less negative effect on the environment compared to the conventional petroleum based materials largely used in commodities [2].

Polylactide (PLA) is one of the most promising bio-based polyesters for food packaging [1,2] because of its good mechanical, superior transparency, ease of processing and availability in the market [3]. In this sense, poly(lactic acid) (PLA) is one of the most attractive biopolymers with many short-term or disposable applications, such as disposable cutlery (plates, cups, lids and drinking straws), bags and film packaging [4,5]. PLA is also widely used in rigid and flexible food packaging applications [6] since it has been approved by the US Food and Drug Administration (FDA) as a food contact substance [7,8]. However, the use of PLA for food packaging is somewhat limited because of its poor ductility, thermal and oxygen barrier properties [3].

Recent studies have been conducted on the use of limonene as a new novel monomer to obtain polyterpenes [9]. D-limonene can be found in a variety of citrus, indeed is the main component of citrus oils and one of most important contributors to citrus flavor [10,11]. Is the most abundant monocyclic monoterpene in nature and represents more than 90% of orange peel oil, being the most important residue in the citrus industry [12]. The limonene diffusion through packaging has been widely studied in different food contact materials such as polyethylene (PE) [13], low density polyethylene (LDPE) [14], high density polyethylene (HDPE), polystyrene (PS) [15] and PLA [15,16].

* Corresponding author. Tel./fax: +34 966528433.
*E-mail addresses:* marrieta@fcm.upv.es, marina.arrieta@ua.es (M.P. Arrieta).

0142-9418/$ – see front matter © 2013 Elsevier Ltd. All rights reserved.
http://dx.doi.org/10.1016/j.polymertesting.2013.03.016

European Polymer Journal 50 (2014) 255–270

Contents lists available at ScienceDirect

European Polymer Journal

journal homepage: www.elsevier.com/locate/europolj

# Ternary PLA–PHB–Limonene blends intended for biodegradable food packaging applications

Marina P. Arrieta[a,d,*], Juan López[a], Alberto Hernández[b], Emilio Rayón[c]

[a] Instituto de Tecnología de Materiales, Universitat Politècnica de València, Plaza Ferrandiz y Carbonell 1, 03801 Alcoy, Alicante, Spain
[b] Servicio de Microscopía Óptica y Confocal, Centro de Investigación Príncipe Felipe, Eduardo Primo Yúfera 3, E46012 Valencia, Spain
[c] Instituto de Tecnología de Materiales, Universitat Politècnica de València, Camí de Vera s/n, E46022 Valencia, Spain
[d] Analytical Chemistry, Nutrition and Food Sciences Department, University of Alicante (UA), P.O. Box 99, E-03080 Alicante, Spain

ARTICLE INFO

*Article history:*
Received 24 September 2013
Received in revised form 7 November 2013
Accepted 9 November 2013
Available online 20 November 2013

*Keywords:*
Poly(lactic acid) PLA
Poly(hydroxybutyrate) PHB
Limonene
Food packaging
Biodegradable

ABSTRACT

In this work poly(lactic acid) PLA and poly(hydroxybutyrate) PHB, were blended and plasticized with a natural terpene D-limonene (LIM) with the dual objective to increase PLA crystallinity and to obtain flexible films intended for food packaging applications. Materials were melt-blended and processed in transparent films. Structural and surfaces properties were evaluated. Moreover, functional properties were studied by means colorimetric parameters, oxygen permeation and water resistant measurements. In addition, thermal stability, crystallization behavior, mechanical as well as nanomechanical properties were investigated. FTIR spectra showed the characteristic bands corresponding to PLA and PHB and their rather molecular interaction. Py-GC/MS showed the characteristics peak of D-limonene as well as the thermal degradation products of PLA and PHB. D-limonene amount after processing was higher in PHB incorporated samples. PHB produced a reinforcing effect in PLA matrix and therefore an improvement in the oxygen barrier properties and the surface water resistance. Moreover, Scanning Confocal Microscopy surface images showed the dispersion of PHB crystal in PLA matrix. The influences of plasticization process on the mechanical properties showed that D-limonene provoked an increase in elongation at break. Disintegrability under composting conditions was also investigated and it was observed that PHB delays the PLA disintegrability under composting while D-limonene speed it up. In brief, the best results regarding structural, thermal, barrier and mechanical properties were found for the ternary PLA–PHB–LIM film.



## 1. Introduction

Increasing ecological concern towards a reduction on the environmental impact produced by plastics is contributing to the growth of the biodegradable polymer industry. During the last two decades, the great interest in the reduction of environmental impact caused by food packaging and their indiscriminate use, have increasingly received the scientist attention specially focused in the development of new biodegradable materials as a way to reduce the petroleum-based plastic residue. In this sense, poly(lactic acid) (PLA) is becoming increasingly popular as a biodegradable plastic owing to its high mechanical strength, superior transparency and easy processability compared to other biodegradables polymers [1]. Nowadays, PLA is an economically feasible material [2] derived from renewable resources [3], in particular from sugar and starch [4], chemically synthesized, commercially available with good performance characteristics as a packaging material [5] that is currently being used for many short-term applications, such as disposable cutlery (plates, cups, lids and drinking straws), bags and film packages [6].

* Corresponding author at: Instituto de Tecnología de Materiales, Universitat Politècnica de València, Plaza Ferrandiz y Carbonell 1, 03801 Alcoy, Alicante, Spain. Tel./fax: +34 966528433.
*E-mail address:* marrieta@itm.upv.es (M.P. Arrieta).

0014-3057/$ - see front matter © 2013 Elsevier Ltd. All rights reserved.
http://dx.doi.org/10.1016/j.eurpolymj.2013.11.009

**Journal of Polymers and the Environment (JOOE)**
<stephen_mccarthy2@uml.edu>
Para: Marina Patricia Arrieta <marrieta@itm.upv.es>

5 de marzo de 2014, 15:45

Dear Dr. Marina Patricia Arrieta:

We are pleased to inform you that your revised manuscript, "Combined effect of poly(hydroxybutyrate) and plasticizers on polylactic properties for film intended for food packaging" has been accepted for publication in the Journal of Polymers and the Environment.

For queries regarding your accepted paper, please contact Poongulazhali Jayaraj at poongulazhali.jayaraj@springer.com.

If you are using the track changes feature to revise your manuscript please do disable this feature before uploading your revised manuscript.

Please remember to always include your manuscript number, JOOE-D-13-00031R2, whenever inquiring about your manuscript. Thank you.

Best regards,

Stephen McCarthy
Editor-in-Chief
Journal of Polymers and the Environment

ARTICLE IN PRESS

Polymer Degradation and Stability xxx (2014) 1–12

Contents lists available at ScienceDirect

Polymer Degradation and Stability

journal homepage: www.elsevier.com/locate/polydegstab

# Disintegrability under composting conditions of plasticized PLA–PHB blends

M.P. Arrieta [a,b,*], J. López [a], E. Rayón [c], A. Jiménez [d]

[a] Instituto de Tecnología de Materiales, Universitat Politècnica de Valencia, E-03801 Alcoy, Alicante, Spain
[b] Catholic University of Córdoba, Camino a Alta Gracia Km 716, 5017 Córdoba, Argentina
[c] Instituto de Tecnología de Materiales, Universitat Politècnica de Valencia, E-46022 Valencia, Spain
[d] Analytical Chemistry, Nutrition and Food Sciences Department, University of Alicante, E-03080 Alicante, Spain

ARTICLE INFO

*Article history:*
Received 26 November 2013
Received in revised form
20 January 2014
Accepted 26 January 2014
Available online xxx

*Keywords:*
Poly(lactic acid)
Poly(hydroxybutyrate)
Blend
Biodegradable
Plasticizers

ABSTRACT

The disintegration under composting conditions of films based on poly(lactic acid)–poly(hydroxybutyrate) (PLA–PHB) blends and intended for food packaging was studied. Two different plasticizers, poly(ethylene glycol) (PEG) and acetyl-tri-n-butyl citrate (ATBC), were used to limit the inherent brittleness of both biopolymers. Neat PLA, plasticized PLA and PLA–PHB films were processed by melt-blending and compression molding and they were further treated under composting conditions in a laboratory-scale test at 58 ± 2 °C. Disintegration levels were evaluated by monitoring their weight loss at different times: 0, 7, 14, 21 and 28 days. Morphological changes in all formulations were followed by optical and scanning electron microscopy (SEM). The influence of plasticizers on the disintegration of PLA and PLA–PHB blends was studied by evaluating their thermal and nanomechanical properties by thermogravimetric analysis (TGA) and the nanoindentation technique, respectively. Meanwhile, structural changes were followed by Fourier transformed infrared spectroscopy (FTIR). The ability of PHB to act as nucleating agent in PLA–PHB blends slowed down the PLA disintegration, while plasticizers speeded it up. The relationship between the meso-lactide to lactide forms of PLA was calculated with a Pyrolysis–Gas Chromatography–Mass Spectrometry device (Py–GC/MS), revealing that the meso-lactide form increased during composting.



## 1. Introduction

Poly(lactic acid), PLA, and poly-hydroxybutyrate (PHB) are two of the bio-based and biodegradable polymers which have focused some attention by their possibilities as environmentally-friendly food packaging materials. In this sense, PLA is currently the most used biopolymer in the food packaging sector for short shelf-life products [1–4], owing to its high mechanical strength, easy processability, superior transparency, availability and low cost. Poly(-hydroxybutyrate) (PHB) is the most common representative of poly(hydroxyalkanoates) (PHA) [5], and it has been also proposed for short-term food packaging applications [6]. Conversely, there are not many commercial products of PHB by its narrow processing window, high brittleness, [5] and price [7].

A considerable number of research work has been reported on the miscibility between PLA and PHB and possible applications in food packaging [8–11] It is known that PLA shows limited or partial miscibility with low molar mass PHB [10,12]. The temperature used during the blend preparation has also significant influence in the miscibility between both polymers. In this sense Zhang et al. (1996) reported that PLA–PHB blends prepared at high temperature exhibited greater miscibility than those prepared by solvent casting at room temperature [13] since PLA–PHB systems are fully miscible in the melt state [11,14]. This effect could be due to the trans-esterification reaction between PLA and PHB chains [13]. In addition, the miscibility between PLA and PHB is strongly dependent on their ratio in the blend. For instance, Furukawa et al. (2005) studied PLA/PHB films prepared by solvent casting in chloroform with blending ratios (w/w) 20/80, 40/60, 60/40, and 80/20 (PLA/PHB). They reported that PHB crystallized as very small spherulites that may act as nucleation sites of PLA in the 20/80 blend [8]. Similarly, Zhang and Thomas (2011) studied PLA/PHB blends in different proportions (100/0, 75/25, 50/50, 25/75 and 0/100, w/w) prepared by melt blending followed by compression molding [9]. They found

* Corresponding author. Instituto de Tecnología de Materiales, Universitat Politècnica de Valencia, E-03801 Alcoy, Alicante, Spain. Tel./fax: +34 965528413.
*E-mail addresses:* marrieta@itm.upv.es, marrieta@ua.es (M.P. Arrieta).

http://dx.doi.org/10.1016/j.polymdegradstab.2014.01.034
0141-3910/

Carbohydrate Polymers 107 (2014) 16–24

Contents lists available at ScienceDirect

Carbohydrate Polymers

journal homepage: www.elsevier.com/locate/carbpol

# Multifunctional PLA–PHB/cellulose nanocrystal films: Processing, structural and thermal properties

M.P. Arrieta[a,e], E. Fortunati[b,*], F. Dominici[b], E. Rayón[c], J. López[a], J.M. Kenny[b,d]

[a] Instituto de Tecnología de Materiales, Universitat Politècnica de Valencia, 03801 Alcoy-Alicante, Spain
[b] Materials Engineering Centre, UdR INSTM, NIPLAB, University of Perugia, 05100 Terni, Italy
[c] Instituto de Tecnología de Materiales, Universitat Politècnica de Valencia, E-46022 Valencia, Spain
[d] Institute of Polymer Science and Technology, CSIC, Juan de la Cierva 3, Madrid 28006, Spain
[e] Analytical Chemistry, Nutrition and Food Sciences Department, University of Alicante, P.O. Box 99, E-03080 Alicante, Spain

ARTICLE INFO

*Article history:*
Received 28 December 2013
Received in revised form 6 February 2014
Accepted 8 February 2014

*Keywords:*
Poly(lactic acid)
Poly(hydroxybutyrate)
Cellulose nanocrystals
Blends
Nanocomposites
Film processing
Thermal properties

ABSTRACT

Cellulose nanocrystals (CNCs) synthesized from microcrystalline cellulose by acid hydrolysis were added into poly(lactic acid)–poly(hydroxybutyrate) (PLA–PHB) blends to improve the final properties of the multifunctional systems. CNC were also modified with a surfactant (CNCs) to increase the interfacial adhesion in the systems maintaining the thermal stability. Firstly, masterbatch pellets were obtained for each formulation to improve the dispersion of the cellulose structures in the PLA–PHB and then nanocomposite films were processed. The thermal stability as well as the morphological and structural properties of nanocomposites was investigated. While PHB increased the PLA crystallinity due to its nucleation effect, well dispersed CNC and CNCs not only increased the crystallinity but also improved the processability, the thermal stability and the interaction between both polymers especially in the case of the modified CNCs based PLA–PHB formulation. Likewise, CNCs were better dispersed in PLA–CNCs and PLA–PHB–CNCs, than CNC.



## 1. Introduction

Several biodegradable polymers have been investigated during the last few decades as alternatives to non-degradable polymers currently used in film production with particular attention to the food packaging sector (Armentano et al., 2013; Fortunati, Armentano, Iannoni, & Kenny, 2010). In this sense, poly(lactic acid) (PLA) is one of the most attractive biodegradable polymers used in short-term food commodities (Arrieta, Parres, López, & Jiménez, 2013). PLA can be processed by usual thermoplastic technologies such as extrusion, injection molding, sheet extrusion, blow molding, thermoforming and film forming) (Auras, Harte, & Selke, 2004). PLA is a semicrystalline polymer with low softening temperature and therefore it shows glasslike appearance at room temperature. It is being used in the food industry since seeing through the packaging is one of the most important requirements for consumers (Arrieta, López, Ferrándiz, & Peltzer, 2013) and PLA shows high transparency. Unfortunately, so far the use of PLA as film for food packaging is limited because PLA shows high brittleness (Auras, Harte, & Selke, 2004), low heat resistance (Kose & Kondo, 2013) and poor barrier properties (Martino, Jiménez, Ruseckaite, & Avérous, 2011). Interest in reducing PLA inherent brittleness and improving gas barrier properties has led researchers and industries to develop new PLA matrices with increased crystallinity.

Poly(hydroxybutyrate) (PHB) is the best known poly(hydroxyalcanoate) (PHA) synthesized by controlled bacterial fermentation (Zhang & Thomas, 2011). It presents high crystallinity (Calvão et al., 2012); nevertheless, the main drawback of PHB is that it has the melting temperature at about 170–180 °C (Arrieta, López, Hernández, & Rayón, 2014; Malinová & Brožek, 2011), close to the degradation temperature (typically around 270 °C) (Koller, Salerno, Dias, Reiterer, & Braunegg, 2010), showing a small processing window for melt extrusion (Koller, Salerno, Dias, Reiterer, & Braunegg, 2010; Malinová & Brožek, 2011). Thus, PHB processing temperature should be at least 180–190 °C but its thermal degradation takes place very quickly at these temperatures (Erceg, Kovačić, & Klarić, 2005). Nevertheless, the melting temperature of PHB can be lowered far below the thermal decomposition temperature to make this material much easier to process (Corre, Bruzaud, Audic, & Grohens, 2012) through chemical

* Corresponding author. Tel.: +39 0744492921; fax: +39 0744492950.
*E-mail address:* elena.fortunati@unipg.it (E. Fortunati).

http://dx.doi.org/10.1016/j.carbpol.2014.02.044
0144-8617/

**Polymer Degradation and Stability** <pdst@elsevier.com> 11 de febrero de 2014, 18:16
Para: marrieta@itm.upv.es

Dear Dr. Marina Arrieta,

You have been listed as a Co-Author of the following submission:

Journal: Polymer Degradation and Stability
Title: PLA-PHB/cellulose based films: Mechanical, barrier and disintegration properties
Corresponding Author: Elena Fortunati
Co-Authors: Marina P Arrieta, PhD Student; Franco Dominici; Emilio Rayòn, PhD; Juan Lopez, Prof; Josè M Kenny, Prof

We would like to invite you to link your ORCID to this submission. If the submission is accepted, then your ORCID will be transferred to ScienceDirect and CrossRef and will be updated on your ORCID account.

To go to a dedicated page in EES where you can link an existing ORCID, or sign-up for an ORCID, please click the following link:
http://ees.elsevier.com/pdst/l.asp?i=30341&l=I7Q8XAQX

Please note: If you did not co-author this submission, please do not follow the above link but instead contact the Corresponding Author of this submission at elena.fortunati@unipg.it.

What is ORCID?
"ORCID is an open, non-profit, community-based effort to create and maintain a registry of unique researcher identifiers and a transparent method of linking research activities and outputs to these identifiers."
http://www.ORCID.org

More information on ORCID can be found on the ORCID website, http://www.ORCID.org, or on our ORCID help page:
http://help.elsevier.com/app/answers/detail/a_id/2210/p/7923

Thank you,

Polymer Degradation and Stability